Contents

The effect of Air Flow Rate on Smoke Stratification in Longitudinal Tunnel Ventilation

***Jiří Pokorný*[1], *Lenka Brumarová*[1], *Petr Kučera*[1], *Jozef Martinka*[2], *Adam Thomitzek*[1] *and* *Pavel Zapletal*[3]**

The construction of tunnels is associated with mining. For safety and suitable working conditions, it is necessary to ensure that there is suitable ventilation during construction.

During operation, tunnels form the infrastructure of the area, which has a number of characteristics. Tunnel ventilation is designed with regards to many different factors. Longitudinal ventilation is especially used in one-way, extra-urban tunnels but in some cases also in urban or two-way tunnels.

The article describes the purpose and types of tunnel ventilation, focusing on longitudinal ventilation and ventilation design strategy. Longitudinal tunnel ventilation is the cause of significant turbulence that affects the smoke stratification. The article compares different tunnel ventilation options in terms of selected strategies and the different values of applied airflow rates.

A case study was conducted on the Klimkovice road tunnel in the Czech Republic using the fire model from the Fire Dynamics Simulator. The study compares the effect of airflow rate on smoke stratification. The study was conducted with air flow rate values of 0 to 5 $m.s^{-1}$.

The results of the study show that even with lower airflow rates, the smoke build-up is so significant that the safety of individuals in the tunnel cannot be ensured. The dynamicity of fire is also an important factor. Opting for a lower airflow rate strategy because of higher expected congestion or other factors is a questionable practice. Greater airflow rates, however, create better conditions for evacuating individuals, although it is also necessary to combine smoke stratification options with the selected ventilation strategy.

Keywords: *safety, tunnel, fire, longitudinal ventilation, smoke stratification*

Introduction

Tunnel construction must go hand in hand with safety. In the case of tunnelling, there is a necessity to supply fresh air to the exposed face of tunnel tubes. The design requirements for ventilating tunnels aren't as specific as in, for example, gassy or non-gassy mines; however, there is always the necessity to supply fresh air to the workplace.

The most limiting factors in ventilating tunnels are the gases carbon dioxide, monoxide, nitrogen oxides and hydrogen sulphide.

The actual ventilation of the mined tunnels depends on the profile and length of the excavation work. For example, short tunnelling activity can be ventilated by natural ventilation or by diffusion, provided the limit concentrations of the above gases are not exceeded.

In other cases, it is necessary to use artificial ventilation (separate), which is provided by fans usually located in front of the excavation portal and lutes, which bring fresh air to the face, or vice versa used air from the face. In such cases, it is blow or suction ventilation, the most commonly used type of ventilation being the blow type, especially with respect to the purchase costs of lutes, which may not have reinforcements, as in the case of the suction type of ventilation. In exceptional cases, for example, when using tunnelling platforms, or when performing small-profile underground works or extrusions where separate ventilation cannot be established, it can be ventilated by compressed air.

Generally, in tunnelling, there are two basic factors to consider when designing the type of ventilation, namely blasting and the associated exhaust ventilation after blasting operations, and the use of diesel engines, which, apart from electric motors, are the only kind that can work and operate in underground workspaces.

During operation, road tunnels are a complex structure, equipped with a number of construction elements and facilities that enable it to operate, and in many cases contribute to ensuring safety. It stipulates the technical and maintenance requirements for tunnels longer than 500 m (European Parliament Directive 2004/54/ES).

The safety requirements for building road tunnels are given by national regulations of each individual country. Examples are Road Tunnel Ventilation, Design, Dimensioning and Equipment, ASTRA 13001 from Switzerland (ASTRA 13001, 2008), RABT 2006 Tunnel Equipment and Operation Guidelines from Germany (RABT, 2006), Tunnel Ventilation - Basic Principles Austrian Research Association for Roads, Rail and Transport from Austria (RVS 09.02.31 2008) Manual 021 Norwegian Public Roads Administration Standard

[1] *Jiří Pokorný, Lenka Brumarová, Petr Kučera, Adam Thomitzek,* VSB – Technical University of Ostrava, Faculty of Safety Engineering, Lumírova 630/13, 700 30 Ostrava – Výškovice, Czech Republic, *jiri.pokorny@vsb.cz, lenka.brumarova@vsb.cz, petr.kucera@vsb.cz, adam.thomitzek@vsb.cz*

[2] *Jozef Martinka,* Slovak University of Technology in Bratislava, Faculty of Materials Science and Technology in Trnava, Jána Bottu 2781/25, 917 24 Trnava, Slovak Republic, *jozef.martinka@stuba.sk*

[3] *Pavel Zapletal, VSB* - Technical University of Ostrava, Faculty of Mining and Geology, 17. listopadu 2172/15, 708 00 Ostrava – Poruba, Czech Republic, *pavel.zapletal@vsb.cz*

Road Tunnels 03.04 from Norway (Manual 021, 2004)DMRB Volume 2 Section 2 Part 9 (BD 78/99) Design (substructures and special structures). Special structures. Design of road tunnels from Great Britain (DMRB, 1999) or NFPA 502 Standard for Road Tunnels, Bridges, and Other Limited Access Highways from the United States (NFPA 502, 2017).

In the Czech Republic and Slovakia, these requirements are governed by government decrees (Government decree no. 269/2009; Government decree no. 344/2006), technical standards ČSN 737507, 2013; STN 737507, 2008) and methodical instructions issued by ministries (Marasová et al., 2010).

Under the European Parliament Directive (EU) no. 305/2011 (which stipulates the harmonized conditions for introducing construction products on the market and repeals EU directive 89/106/EHS), one of the conditions road tunnels must also comply with are fire safety requirements (Regulation (EU) No 305, 2011). The requirements include securing the load-bearing property of the structure, limiting the spread of fire inside and outside the structure, ensuring the evacuation and the safety of individuals and securing the safety of rescue units. Safety standards for tunnels are also given by the World Road Association (World Road Association PIARC, 2019).

Operating road tunnels is historically associated with various emergency situations. One of the most dangerous situations is fire, significant examples being the incident in 1982 at the tunnel in Salang, Afghanistan, where 176 people died, the fire in the Montblanc tunnel in France in 1999, which killed 39 people, and the Gotthard tunnel in Switzerland in 2001, where more than 100 people lost their lives. Other notable examples include the fire in the tunnel on the highway between Florence and Bologna in 1993, which killed four people, the fire in the Pfänder tunnel near Bregenz in Austria in 1995, also killing four people, and the fire in the tunnel near Palermo in 1996, which killed five people. The causes of these fires were either road accidents or car fires. (World Road Association PIARC, 2019)

From 2013 to 2018, the Czech Republic experienced five road tunnel fires (Pokorny et al., 2018). Compared to the average total number of fires in the Czech Republic, which is around 20,000, this figure is negligible (Fire Rescue Service, Czech Republic, 2019). Despite this and no significant loss of life or damage to property and the environment, historical events demonstrate that the consequences of fires in tunnels can be devastating. (Kročová, 2015)

In order to mitigate emergency situations, tunnels must be prepared structurally, technically and organisationally (Yang, 2016) by the engineering architect, construction company, tunnel operator and rescue units (especially the fire rescue services and police). One of the most important requirements for securing the safety of underground structures is ventilation. The requirements for tunnel ventilation are similar to the requirements for general aboveground structures (Pokorny and Gondek, 2016).

It is possible to classify road tunnel ventilation into standard operating ventilation, emergency ventilation (fires), and environmentally friendly ventilation. In particular, standard operational requirements can be understood as those ensuring a suitable environment for persons who may be present. Emergency operation means creating conditions that ensure the safe evacuation of persons and effective intervention of rescue units. Environmental ventilation should ensure a minimal impact of the tunnel operation on the environment. (ASTRA 13001, 2008; Ministry of Transport, Department of Roads, 2013; Tomašková and Vargová, 2018).

The aim of this study was to determine the effect of longitudinal tunnel ventilation on the safety of individuals and the effectiveness of fire services under a given strategy and therefore also the different airflow rate values. The article investigates whether some stratification of smoke remained using low airflow rates.

Material and Methods

Tunnel fire ventilation

Tunnel fire ventilation is a supporting measure for the evacuation and rescue of individuals and also supports rescue units.

For the design of fire ventilation in tunnels, the essentials are the following (ASTRA 13001, 2008; NFPA 502, 2017):

- traffic intensity and mode,
- tunnel length,
- operating mode (one-way or two-way).

Based on the above criteria, tunnels can be divided into the following categories for ventilation purposes (ASTRA 13001, 2008; Ministry of Transport, Department of Roads, 2013):

- tunnels with unidirectional traffic and low probability of congestion (cat. T1, usually highway tunnels),
- tunnels with unidirectional traffic and a high probability of congestion (cat. T2, usually highway tunnels),
- tunnels with two-way traffic (cat. T3).

The following concepts (strategies) are applied in designing fire ventilation (Ministry of Transport, Road Department, 2013):

- natural (longitudinal) ventilation (suitable for short tunnels or T1 tunnels),
- longitudinal ventilation, fixed installation (suitable for tunnels or T1 tunnels),
- longitudinal ventilation with airflow regulation at defined values (suitable for T2 and T3 tunnels),
- transverse ventilation (suitable for T2 and T3 tunnels).

The given classification was put in place in the Czech Republic. In principle, however, it is also used for many foreign countries where the classification may be modified.

For longitudinal ventilation in tunnels, the required airflow rate is essential. Airflow velocity requirements vary somewhat in the design guidelines and are listed in Table 1 for clarity.

Table 1. Airflow velocity setpoints for longitudinal ventilation

Country	**Character** (category) **tunnel**	**Required flow rate for longitudinal ventilation** ($m.s^{-1}$)	**Note**
France (Annexe n° 2, 2000)	one-way extra-urban tunnels	3	
	one-way urban tunnels	3	recommended for tunnels up to 500 m long
		1 - 2 (Phase 1) 3 (Phase 2)	Phase 1 - the evacuation of persons 2nd phase - support of rescue units
	bidirectional	3	
Czech Republic (Ministry of Transport, Department of Roads, 2013)	unidirectional tunnels with a lower incidence of congestion (T1)	critical air velocity up to 10	the critical speed is generally about 3 $m.s^{-1}$
	unidirectional tunnels with a higher incidence of congestion (T2)	1.2	
	bidirectional tunnels (T3)	1.2	
Germany (RABT, 2006)	unidirectional tunnels with a lower incidence of congestion	2.3 – 3.6	depends on tunnel slope, tunnel tube shape (rectangular, hipped) and fire intensity
	unidirectional tunnels with a higher incidence of congestion	1.5	
	bidirectional tunnels (T3)	1.5	
Netherlands (Huijben et al. (2006)	Not dependent on tunnel characteristics	2.5	
Norway (Manual 021, 2004)	tunnels longer than 500 m and inclined ≥ 2 °	min. 2	fire ventilation is specified by calculation
	other tunnels with inclination < 2 °	2	fire intensity 5 MW
		3.5	fire intensity 20 MW
Austria (RVS 09.02.31 (2008)	Not dependent on tunnel characteristics	2	or air volume flow in the tunnel 120 $m^3.s^{-1}$
Switzerland (ASTRA 13001, 2008)	unidirectional tunnels with a lower incidence of congestion (RV 1)	3	
	unidirectional tunnels with a higher incidence of congestion (RV 2)	1.5 - 3	depending on the tunnel gradient and direction of ventilation
	bidirectional (GV)	1.5	
Slovakia (TP 049, 2018)	one-way traffic with a low probability of congestion (common highway tunnels) (A)	1.5 - 2 (1 – 1.5 for exceptional bidirectional traffic)	phase 1 - the evacuation of persons
	one-way traffic with a high probability of congestion (common highway tunnels) (B)	1 – 1.5	in the case of smoke extraction with longitudinal ventilation 1.5 - 2 $m.s^{-1}$ from both sides to the extraction point
	two-way traffic tunnels (C)	1 – 1.5	
	all variants	critical air velocity up	2nd phase - support of

		to 10	rescue units initiation upon the demand of rescue units
United States of America (NFPA 502, 2017)	Not dependent on tunnel characteristics	critical air velocity up to 10	
		2.54 – 2.95	large-scale tests
Great Britain (DMRB 1999)	Not dependent on tunnel characteristics	1.3	fire output 3 MW
		3	fire output 25 MW
		7	fire output 25 MW

Table 1 shows that in unidirectional tunnels with a lower incidence of congestion, critical speeds are generally required. In unidirectional tunnels with a higher incidence of congestion, it is usually required to reduce the airflow rate below the critical speed (the flow rate reduction is in the range of 1.2 – 1.5 m.s^{-1}).

Conversely, higher airflow rates will cause a more intense influx of smoke to the tunnel (smoke stratification will be quickly interrupted, and the smoke will be channelled in one direction).

The fire ventilation design is strongly linked to risk analysis. Risk analysis determines the choice of type and strategy of the ventilation system. The general techniques for risk analysis are applied to evaluate risk in road tunnels (for example, ČSN EN 31010, 2011; ČSN ISO 31000, 2018).

Fire design

An important factor in designing tunnel ventilation is the fire scenario most likely to develop fire (Haukur Ingason et al., 2015; ISO 16733-1, 2015; KUČERA et al., 2009). The heat output of the fire scenario in relation to the number of heavy truck vehicles per unit of time (typically a day) and the length of the tunnel is 5, 30 and 50 MW. Different heat outputs can be determined in the risk analysis. (Ministry of Transport, Roads Department, 2013). A heat output value of 30 MW is typically considered in a fire ventilation design.

Fire ventilation design and strategy in tunnels

Just as in other buildings and structures, the movement of smoke created during a tunnel fire is affected by several factors that range from low to high importance. The main factors affecting the movement of smoke in tunnel structures are as follows (Pokorny and Gondek, 2016):

- the tunnel's geometry,
- chimney effect,
- effect of stationary vehicles,
- wind,
- buoyancy effect created by the fire,
- increased gas volume,
- ventilation equipment.

When fire ventilation is designed for tunnel structures, these are important factors that must be considered.

Suitable strategies are applied to ventilate road tunnels. The strategy for longitudinal tunnel ventilation depends on the characteristics of the tunnel in terms of traffic direction (one-way or two-way) and the probability of congestion occurring (low or high). Fire ventilation should fulfil its given function in the selected strategy.

The aim of longitudinal ventilation in tunnels operating with one-way traffic and a low probability of congestion (T1) is to channel (expel) the smoke in the direction of vehicle traffic and prevent it spreading towards stationary vehicles. The critical air flow rate is typically between 2.5 to 3 m.s^{-1}. (ČSN 737507, 2013)

The aim of longitudinal ventilation in tunnels with one-way traffic and a high probability of congestion (T2) or in two-way traffic tunnels (T3) is to channel the smoke and limit its spread, or else decrease its flow rate and create the conditions for smoke stratification for a certain period of time. Generally, the airflow rate used is 1.2 m.s^{-1}. (ČSN 737507, 2013)

The critical gas flow rate is defined as the rate that ensures the smoke is channelled in the direction of vehicle traffic and limits its spread towards stationary vehicles. The critical gas flow rate and average smoke temperature can be determined by Kennedy's model and calculated with the following equations (NFPA 502, 2017):

$$V_c = K_1 \cdot K_g \cdot \left(\frac{g \cdot H \cdot Q}{\rho \cdot c_p \cdot A \cdot T_f}\right)^{\frac{1}{3}} \quad (1)$$

$$T_f = T + \left(\frac{Q}{\rho \cdot c_p \cdot A \cdot V_c}\right) \quad (2)$$

where

V_c critical flow rate [m.s^{-1}]

K_1 Froude number, $Fr^{-1/3}$ (0.606) [-]
K_g slope/gradient factor [-]
g acceleration due to gravity [$m.s^{-2}$]
H height of the tunnel at the location of the fire [m]
Q convective ratio of released heat flux [kW]
ρ average density of introduced air [$kg.m^{-3}$]
c_p specific heat capacity of smoke [$kJ.(kg.K)^{-1}$]
An area perpendicular to the airflow [m^2]
T_f average smoke temperature [K]
T average introduced air temperature [K]

Case study

Aim of the study

The frequently selected strategies, and therefore also different airflow rates for longitudinal fire ventilation in road tunnels, were evaluated in the case study.

The Klimkovice tunnel located in the Moravia-Silesian region near the city of Ostrava in the Czech Republic was selected for the case study. The Klimkovice tunnel is part of the D47 highway along the Bílovec – Ostrava, Rudná section. The tunnel is designed for one-way traffic with two tunnel tubes. The length of the tunnel is approximately 1000 m. The width of the road is 9.5 m, and the width of the two-way sidewalks is 1 and 1.2 m, the height of the tunnel is 4.8 m. The tunnel tubes have a longitudinal gradient of 0.6 %. The tunnel tubes are connected with five jumpers. Longitudinal ventilation is installed in the tunnel and consists of eight pairs of ventilators. The ventilators comply with the standard requirements of the Czech Republic to remain operational in temperatures of 400 °C for 90 minutes. The ventilators always become operational after five seconds. The tunnel commenced operation in 2008.

Fire model

The mathematical fire model used for the case study is the Fire Dynamics Simulator (FDS). The FDS model is a CFD model developed by NIST (National Institute of Standards and Technology, Maryland, USA) and allows numerous parameters associated with fire development to be set, including the 'enclosure volume' factor. The model applies Navier–Stokes equations, which are useful for evaluating the flux of smoke movement and also take heat into account. This fire model uses the Smokeview software to visualise the numerical calculations. (Fire Dynamics Simulator, 2019)

A computing grid with cell dimensions of 0.5 x 0.5 x 0.5 m was used for calculation. The initial temperature was set to 15 °C, relative air humidity at 70 %. The environmental conditions were determined primarily by the technical properties of the concrete linings and the airflow rate into the computing zone.

The input assumptions of the study

For the purposes of the study, the tunnel was evaluated as an isolated system without considering external effects on the portal (such as wind). The point of origin of the fire was set at a distance of 256 m from the more elevated portal in the direction of traffic (approximately one-third of the tunnel length). The main channel of longitudinal ventilation was therefore expected to be against the gradient of the tunnel. The heat output of the fire was simulated at two design levels: 5 MW (personal vehicle fire) and 30 MW (small truck or freight vehicle fire). The airflow rate of the tunnel was set for when ventilation was not in operation, these being 0.5 $m.s^{-1}$, 1 $m.s^{-1}$, 1.5 $m.s^{-1}$, 2 $m.s^{-1}$, 2.5 $m.s^{-1}$, 3 $m.s^{-1}$, 3.5 $m.s^{-1}$ and 5 $m.s^{-1}$.

The geometry of the tunnel and the location of the fire origin are shown in Fig. 1.

Evaluation method of the study

The study evaluated the effect of airflow rate on retaining smoke stratification in the tunnel. Environment visibility was selected as a limiting criterion. Visibility was evaluated at 20 evenly spaced measurement points along the axis of the tunnel (one point every 50 m of the tunnel's length) at a height of 2.5 m above the road's surface (the conventional limit value for evaluating the safety of individuals in respect of smoke from a fire) (ČSN P CEN/TR 12101-5, 2008). The moment of interruption of smoke stratification was defined as the moment when visibility decreased to 15 m. This is the conventional limit value when panic and a significant increase in the difficulty of evacuation is anticipated (Folwarczny and Pokorný, 2006; Hurley, 2015). Generally, the time for the safe evacuation of individuals via an unprotected emergency exit is expected at 2.5 min (HOSSER, 2013). The rate of movement of individuals towards an unprotected emergency exit is typically given as 30 $m.min^{-1}$ (ČSN 73 0804, 2010). On the basis of these assumptions, the distance of moving individuals to a safe distance was approximately 75 m.

Tunnel geometry

Location of fire in the tunnel

Fig. 1. The geometry of the tunnel and the location of the fire origin

Simulation results

The following figures show the results of the fire simulation model. Fig. 2 shows the temperature profile at 180 s during fire thermal power 30 MW and the movement of smoke near the fire origin point without ventilation at 600 s and during the fire thermal power at 5 MW.

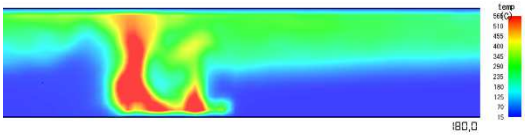

Temperature profile at fire thermal power of 30 MW

Smoke movement without ventilation and fire power of 5 MW

Fig. 2. Representation of temperature profile and smoke movement in the enclosed space

The movement of smoke near the fire origin at 5 MW and 30 MW at 600 s and various smoke velocities are shown in Fig. 3.

Thermal power of fire

5 MW

30 MW

Smoke movement at a flow rate of 0.5 m.s^{-1} and output of 5 MW

Smoke movement at a flow rate of 0.5 m.s^{-1} and output of 30 MW

Smoke movement at a flow rate of 1.0 m.s^{-1} and output of 5 MW

Smoke movement at a flow rate of 1.0 m.s^{-1} and output of 30 MW

Smoke movement at a flow rate of 3.5 m.s^{-1} and output of 5 MW

Smoke movement at a flow rate of 3.5 m.s^{-1} and output of 30 MW

Fig. 3. Demonstration of smoke movement near the fire origin at a thermal output of 5 MW and 30 MW

Visibility was evaluated after 100 seconds, 200 seconds, 300 seconds, 400 seconds, 500 seconds, and 600 seconds after the fire's development. The decrease in visibility for a fire heat output of 5 MW in relation to the simulated time and tunnel position is shown in Figures 4 to 12 (the source of fire is indicated by the red dashed line).

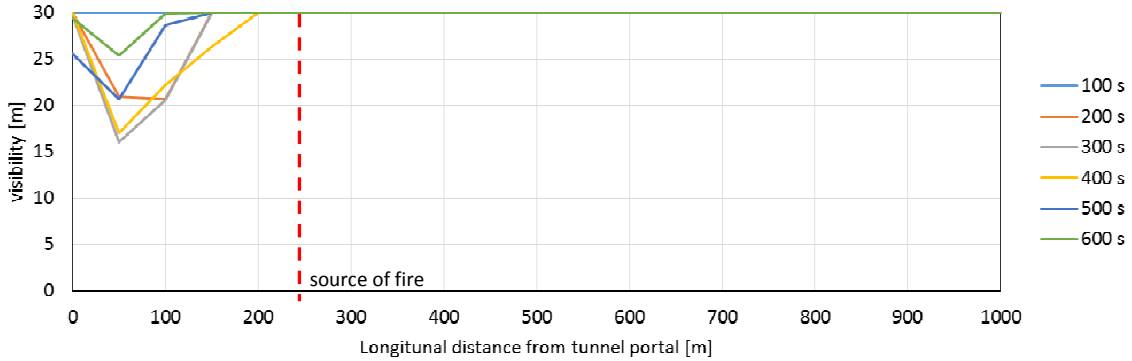

Fig. 4. Visibility without ventilation in relation to simulated time and position in the tunnel

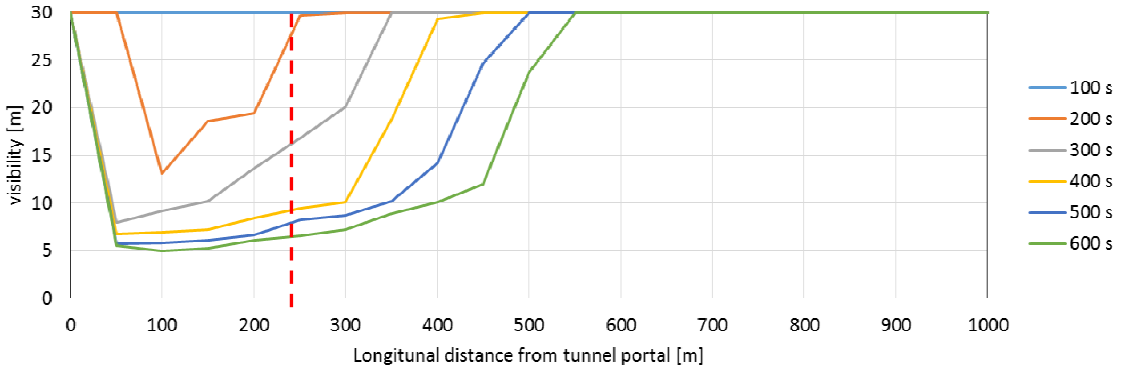

Fig. 5. Visibility for the flow rate of 0.5 m.s^{-1} in relation to simulated time and position in the tunnel

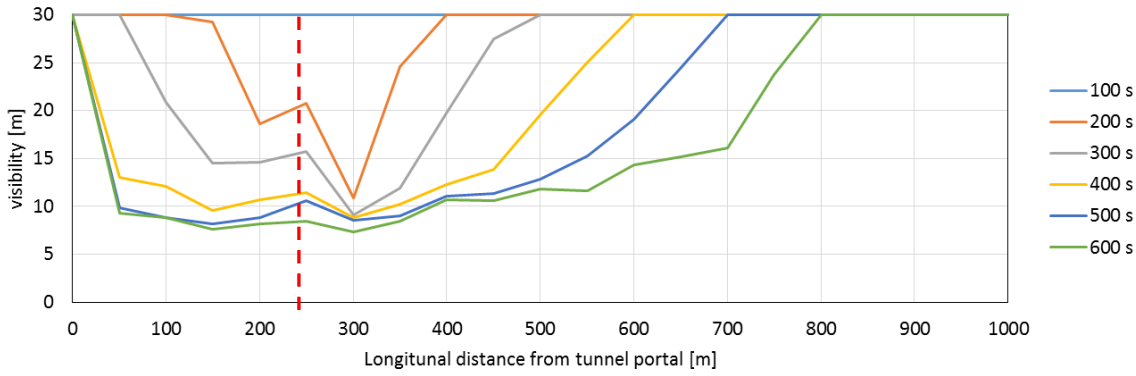

Fig. 6. Visibility for the flow rate of 1.0 m.s^{-1} in relation to simulated time and position in the tunnel

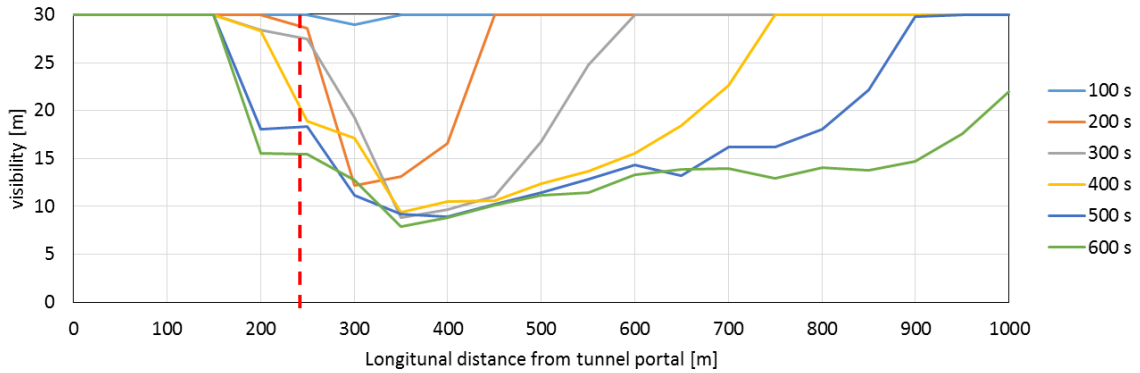

Fig. 7. Visibility for the flow rate of 1.5 m.s^{-1} in relation to simulated time and position in the tunnel

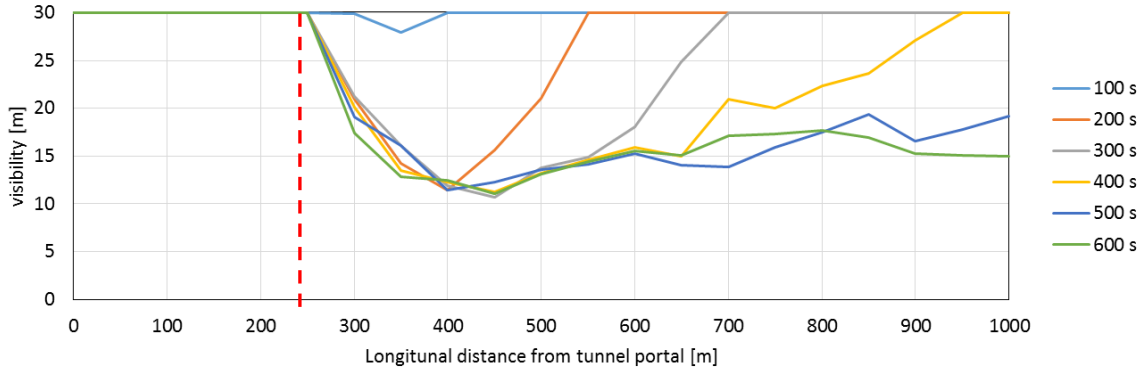

Fig. 8. Visibility for the flow rate of 2.0 m.s^{-1} in relation to simulated time and position in the tunnel

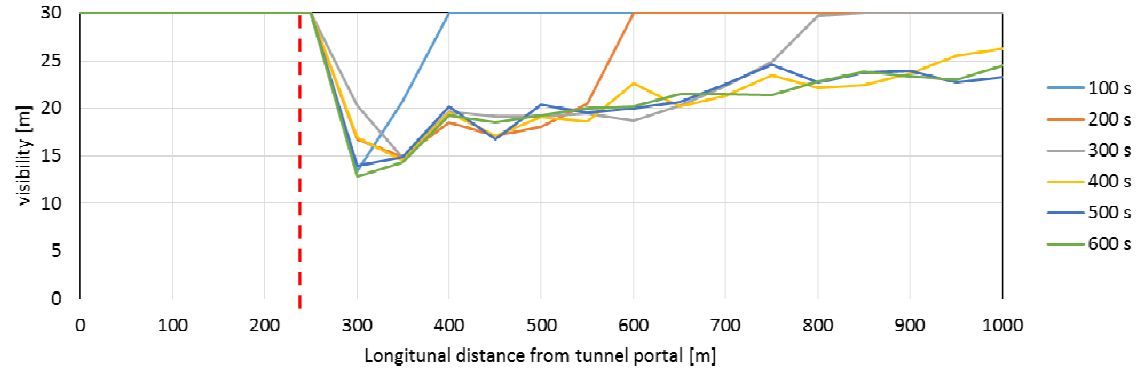

Fig. 9. Visibility for the flow rate of 2.5 m.s^{-1} in relation to simulated time and position in the tunnel

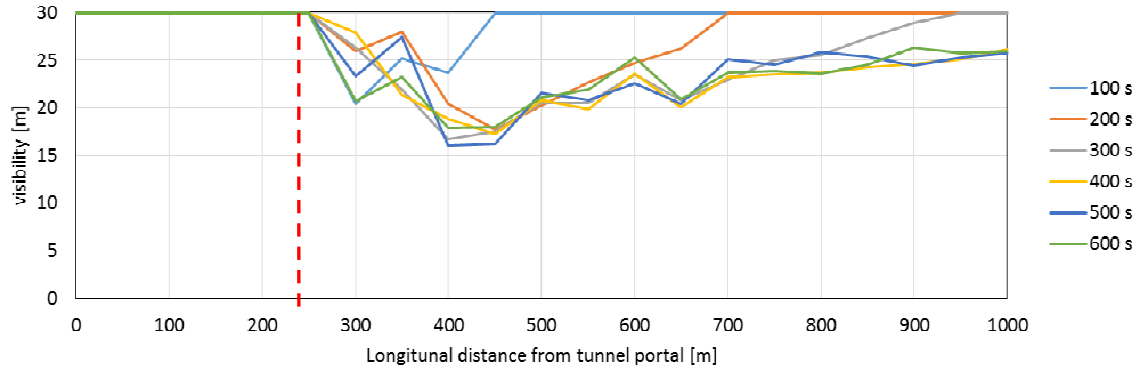

Fig. 10. Visibility for the flow rate of 3.0 m.s^{-1} in relation to simulated time and position in the tunnel

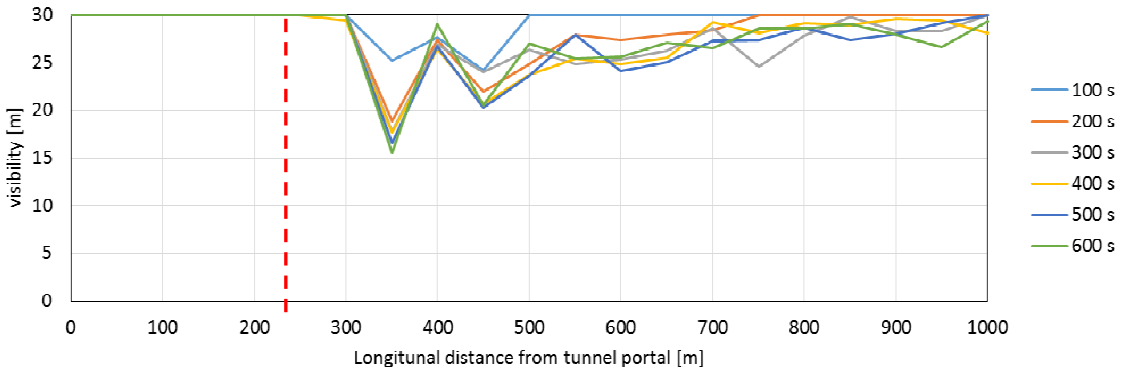

Fig. 11. Visibility for the flow rate of 3.5 m.s^{-1} in relation to simulated time and position in the tunnel

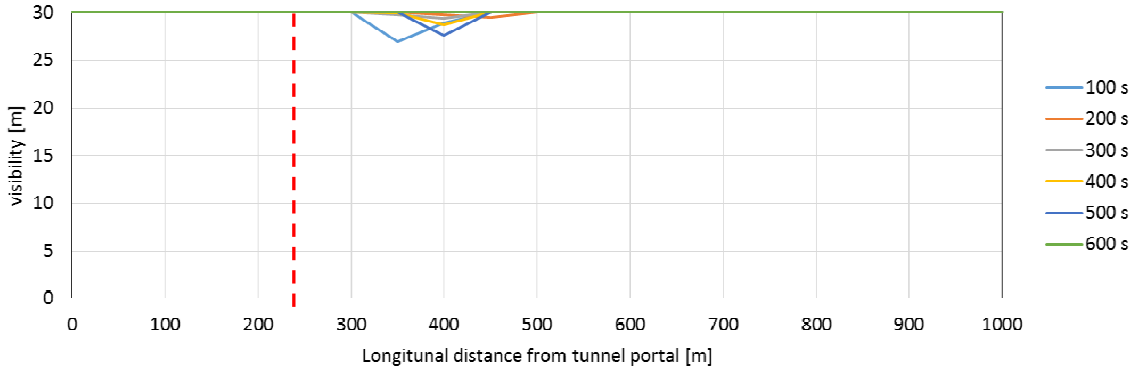

Fig. 12. Visibility for the flow rate of 5.0 m.s^{-1} in relation to simulated time and position in the tunnel

The decrease in visibility present during a fire heat output of 30 MW in relation to simulated time and position inside the tunnel is shown on Figure 13 to 21 (the source of fire is indicated by the red dashed line).

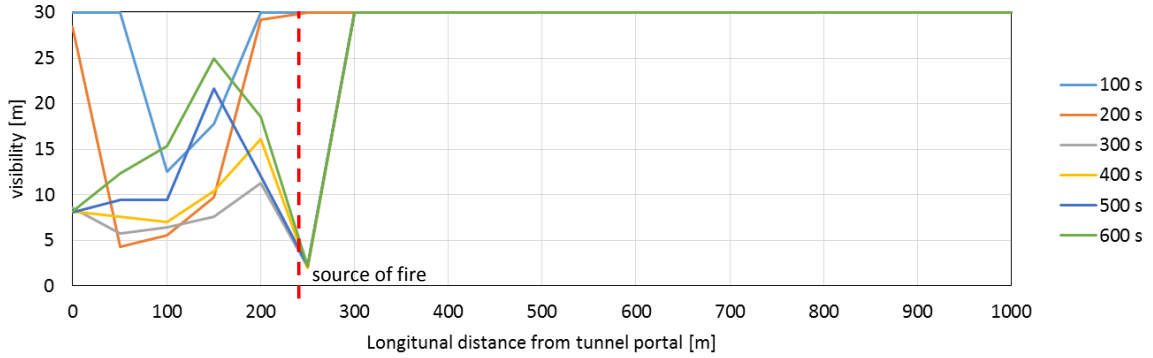

Fig. 13. Visibility without ventilation in relation to simulated time and position in the tunnel

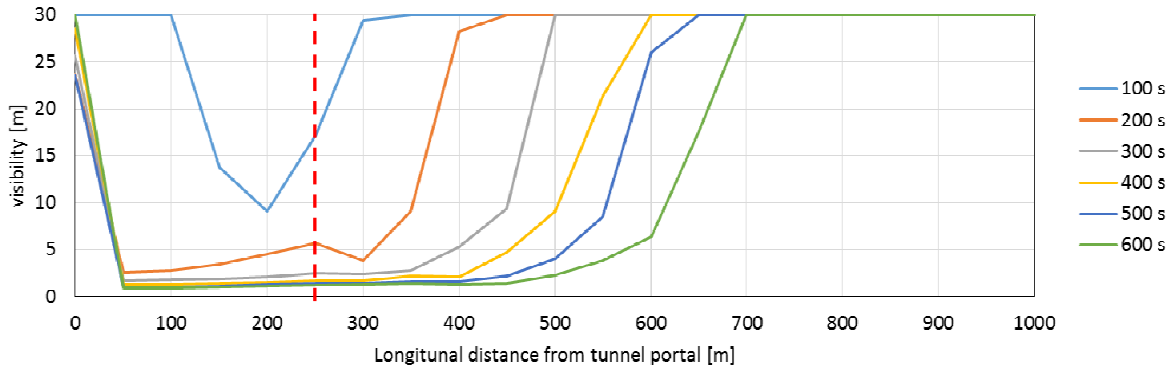

Fig. 14. Visibility for the flow rate of 0.5 m.s^{-1} in relation to simulated time and position in the tunnel

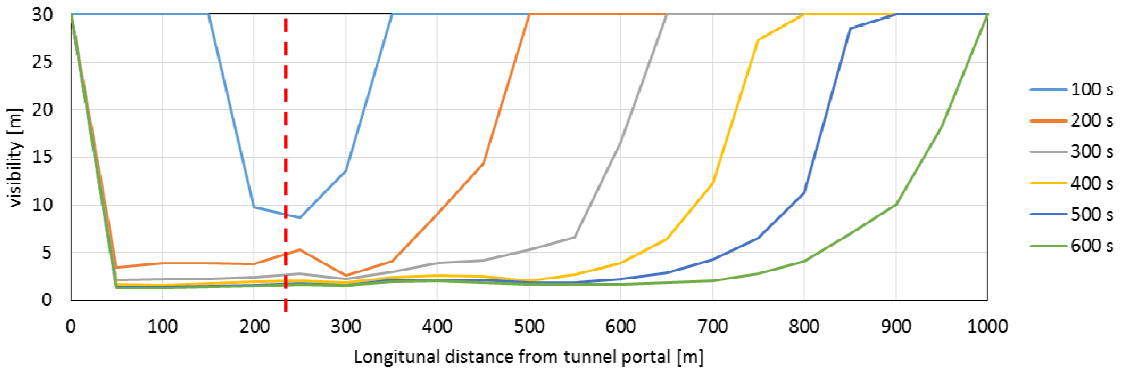

Fig. 15. Visibility for the flow rate of 1.0 m.s^{-1} in relation to simulated time and position in the tunnel

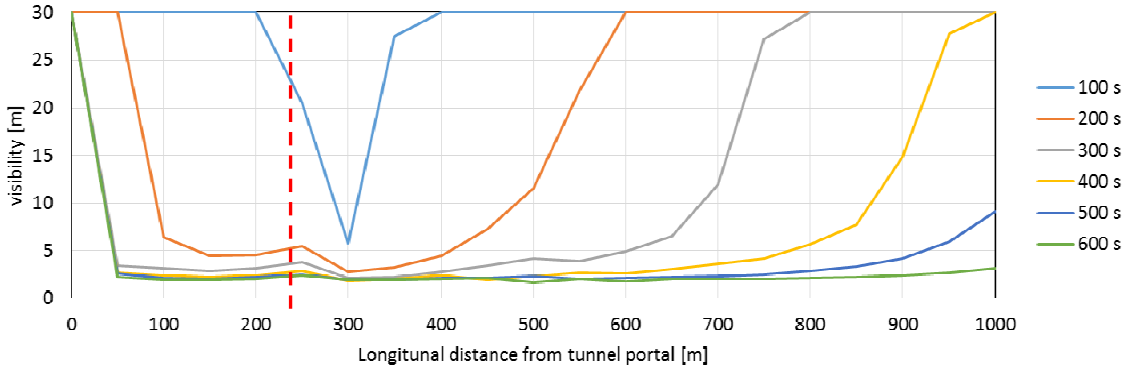

Fig. 16. Visibility for the flow rate of 1.5 m.s^{-1} in relation to simulated time and position in the tunnel

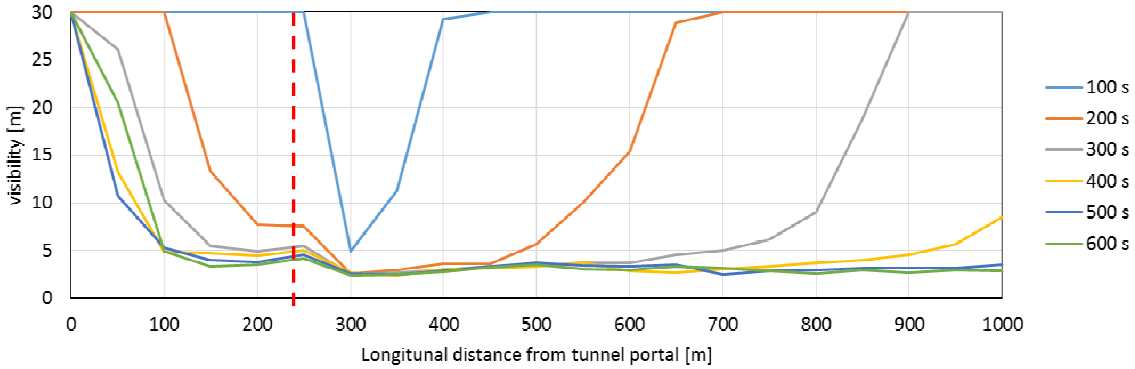

Fig. 17. Visibility for the flow rate of 2.0 m.s^{-1} in relation to simulated time and position in the tunnel

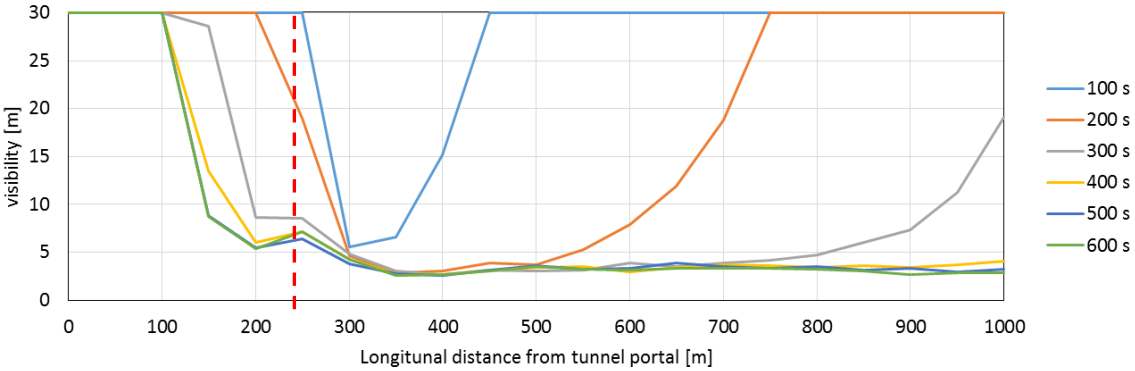

Fig. 18. Visibility for the flow rate of 2.5 m.s^{-1} in relation to simulated time and position in the tunnel

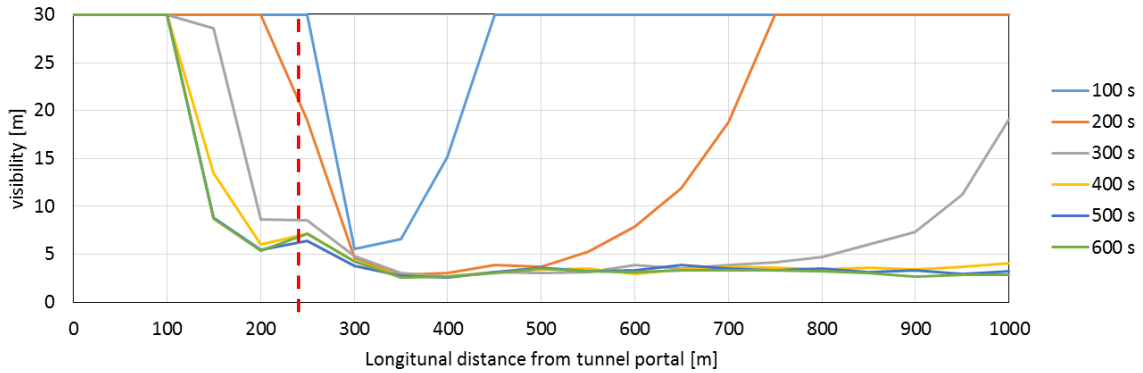

Fig. 19. Visibility for the flow rate of 3.0 m.s^{-1} in relation to simulated time and position in the tunnel

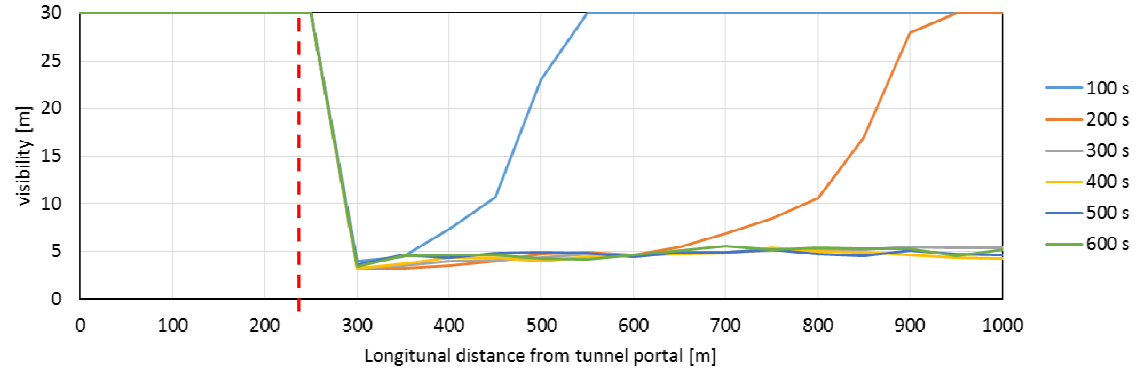

Fig. 20. Visibility for the flow rate of 3.5 m.s^{-1} in relation to simulated time and position in the tunnel

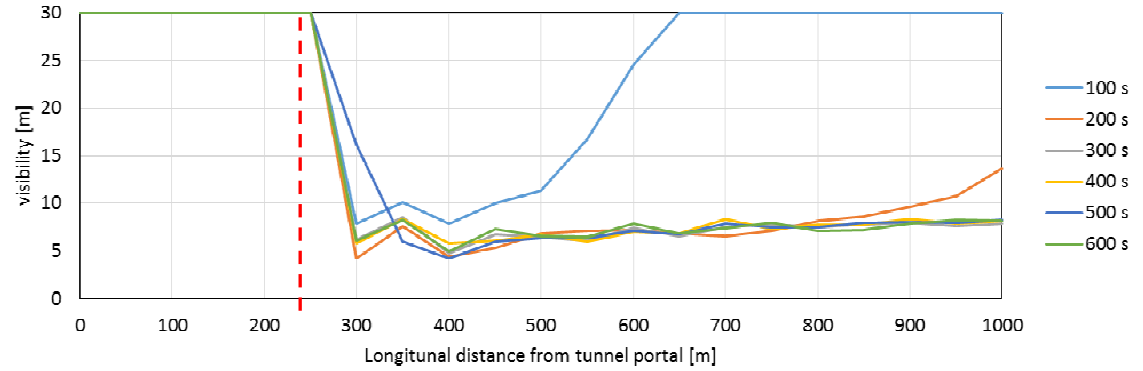

Fig. 21. Visibility for the flow rate of 5.0 m.s^{-1} in relation to simulated time and position in the tunnel

Results and Discussion

The Fire Dynamics Simulator model is a perspective model that has had a long development and been tested on real fires. It is used in a wide range of fire situations and considered suitable for tunnels (Mozer, 2013).

In the case study, the point of origin of the fire at a distance of 256 m from the more elevated portal in the direction of the flow of longitudinal ventilation (the first third of the tunnel) correlated strongly with smoke stratification observed along significant sections of the tunnel's tube (the remaining approximate two-thirds of the tunnel).

Heat outputs of 5 MW and 30 MW were considered for the case study. Although the heat output selected for the tunnel's fire ventilation design could be higher, the most common design value is 30 MW. The lower heat output value for evaluating smoke stratification in a tunnel represents an auxiliary situation in the context of the case study. A discussion on the variability and uncertainty of fire designs is given by (Kadlic and Mozer, 2017).

From Table 1, which describes the required air velocity values for longitudinal ventilation, it is apparent that in unidirectional tunnels with higher congestion rates and in bidirectionally operating tunnels, it is generally

required to reduce the air velocity (below the critical velocity 1.2 - 1.5 m.s^{-1}). In unidirectional tunnels with a lower incidence of congestion, it is usually required to reach critical rates (usually in the range of 2.5 - 3.5 m.s^{-1}).

In order to provide complete information, the simulation was also run for an airflow rate of 5 m.s^{-1}.

Smoke stratification was evaluated according to visibility, the limit criterion being the decrease of visibility to 15 m. On the basis of the given assumptions, the distance of moving individuals to a safe distance was approximately 75 m.

Table 2 shows the distance in relation to heat output, during which the airflow rate and time of fire development saw a decrease in visibility in the tunnel to 15 m or less (critical visibility level). The distances are given for time periods of 300 s and 600 s. These were representative periods that clearly showed the measured results.

Table 2. Comparison of the distance of smoke spread along the tunnel to heat output

Airflow rate [m.s^{-1}]	**Distance in the tunnel with visibility less than 15 m** [m]			
	Fire heat output 5 MW		Fire heat output 30 MW	
	Time of fire development [s]		**Time of fire development** [s]	
	300	600	300	600
0.0	0	0	250	435
0.5	195	460	435	615
1.0	300	610	585	980
1.5	220	650	700	975
2.0	305	275	745	925
2.5	5	60	790	870
3.0	0	0	725	735
3.5	0	0	720	720
5.0	0	0	720	720

The distances of the decrease to critical visibility shown in Table 2 are charted in Figure 22.

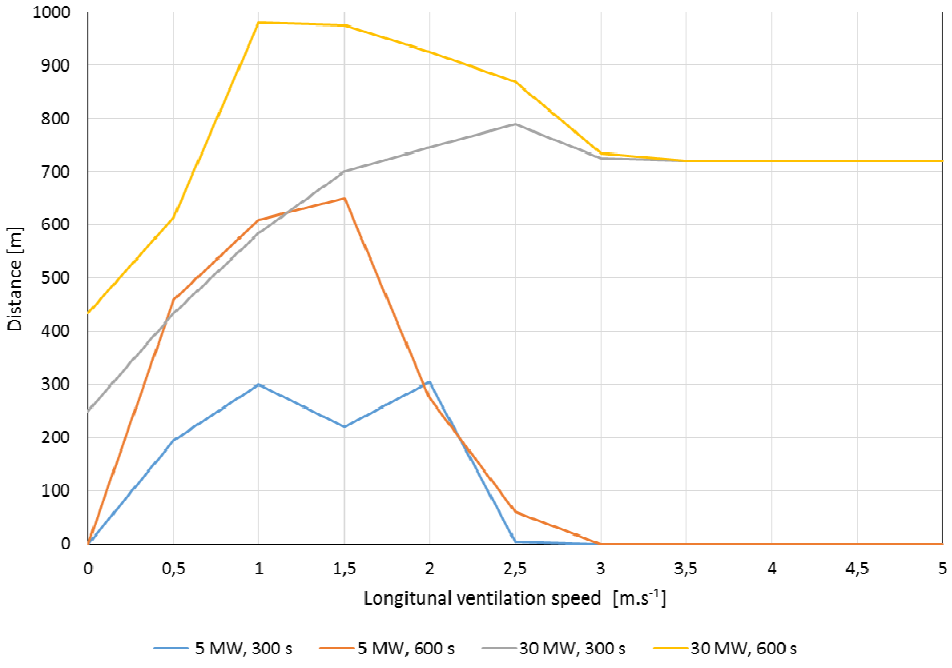

Fig. 22. Distance in the tunnel with visibility less than 15 m

Tables 2 and Figure 22 show that with a heat output of the fire of 5 MW, the distance of tunnel with a decrease to the level of critical visibility attained for a distance greater than 75 m for the airflow rate 0.5 to 2 m.s^{-1}. It is, therefore, a lower airflow rate. When the ventilation was not operating (air velocity is 0.0 m.s^{-1}) and with higher airflow rates, the visibility in the tunnel was satisfactory.

A different situation arose with a heat output of 30 MW. For all airflow rates, the threshold of critical visibility was crossed at a distance greater than 75 m. However, the results partially varied between the 300 s and 600 s periods. In the 300 s period, critical visibility distances were less when ventilation was not used and during

very low airflow rates (up to 1 $m.s^{-1}$). In the 600 s period, the shortest critical visibility distances were achieved when ventilation was not used and during very low airflow rates (up to 0.5 $m.s^{-1}$) and during high flow rates.

The results of the simulation show that airflow rates less than the critical rates did not lead to improving the conditions for evacuating people. In this way, it is debatable, whether the strategy of longitudinal ventilation, which is used in unidirectional tunnels with high congestion probability and bidirectional tunnels, where there are lower airflow rates designed than is the critical rate, is justifiable.

This is mainly caused by the gradient of the tunnel and the ongoing fire. With a heat output of 30 MW, smoke was channelled in the main direction of the flow of the ventilators during flow rates of up to 3.5 $m.s^{-1}$. This is a predictable phenomenon characteristic for airflow rates less than the critical air flow rate.

Figures 4 to 21 also show that over the course of the simulation (i.e., an uninterrupted development of fire), visibility inside the tunnel decreased and therefore deteriorated the conditions for evacuating and rescuing people. Therefore, it is important to decrease the time for evacuating and rescuing people as much as possible.

The results achieved by the case study were partly affected by the tunnel's design (e.g., dimensions, and gradient) and choice of point of fire origin (e.g. location, size, heat output). The Klimkovice tunnel examined in this case study can, however, be considered a typical tunnel in terms of design and technical equipment.

Conclusion

Road tunnel safety is currently a widely discussed issue. One of the most significant items of safety equipment is ventilation, which also ensures safety during a fire. One type of ventilation is longitudinal tunnel ventilation. The strategy of longitudinal tunnel ventilation depends on the characteristics of the tunnel according to its direction of traffic (one-way or two-way) and the probability of congestion. In one-way operated tunnels with a high probability of congestion and two-way tunnels, the selected airflow rates are less than the critical air flow rate.

The case study, however, illustrates that with low fire heat output, smoke stratification is interrupted along a significant length of the tunnel. With higher airflow rates, the results are more favourable. Higher values of heat flux show similar results in terms of smoke stratification.

The positive effect of lowering airflow rate below the critical value in terms of retaining smoke stratification is therefore debatable.

Acknowledgements: *This work was supported by the Ministry of the Interior of the Czech Republic Project No. VH20182020042 Population Protection in a Spatial Planning and within Setting Technical Conditions for Building Engineering.*

References

Annexe n° 2 (2000). Annexe n° 2 à la circulaire interministérielle n° 2000- 63 du 25 août 2000 relative à la sécurité dans les tunnels du réseau routier national - Instruction technique relative aux dispositions de sécurité dans les nouveaux tunnels routiers (conception et exploitation).

ASTRA 13001 (2008). Tunnel ventilation, Design, design and equipment, ASTRA 13001 [online]. Bundesamt für Strassen Astra. 2.03 vyd. Bern, 2008. Available from: www.astra.admin.ch.

ČSN 73 0804 (2010). Fire Protection of Buildings – Industrial Buildings. Prague: Czech Office for Standards, Metrology and Testing.

ČSN 737507 (2013). Design of Road Tunnels. Prague: Czech Office for Standards, Metrology and Testing.

ČSN EN 31010 (2011). Risk Management – Risk Assessment Techniques. Prague: Czech Office for Standards, Metrology and Testing.

ČSN ISO 31000 (2018). Risk Management – Principles and Guidelines. Prague: Czech Office for Standards, Metrology and Testing.

ČSN P CEN/TR 12101-5 (2008). Smoke and Heat Control Systems - Part 5: Guidelines on Functional Recommendations and Calculation Methods for Smoke and Heat Exhaust Ventilation Systems. Prague: Czech Office for Standards, Metrology and Testing.

DMRB (1999). Design manual for road and bridges. Design of road tunnels. Highway structures: Design (substructures and special structures) material. Special structures. Volume 2 Section 2 Part 9 (BD 78/99). London: The Highways Agency.

European Parliament Directive 54/ES. (2004). On minimum safety requirements for tunnels in the Trans-European Road Network [WWW Document], n.d. EUR-Lex. URL https://eur-lex.europa.eu/legal-content/CS/TXT/PDF/?uri=CELEX:32004L0054&from=CS (accessed 4.19.19).

Fire Dynamics Simulator (2019). FDS-SMV [WWW Document]. URL https://pages.nist.gov/fds-smv/ (accessed 3.22.19).

Folwarczny, L., Pokorný, J. (2006). Evacuation of People. Ostrava: Association of Fire and Safety Engineering. ISBN 978-80-86634-92-0.

Government Regulation No. 264/2009 Coll., on Safety Requirements for Road Tunnels Longer than 500 Meters [WWW Document], n.d. Laws for people. URL https://www.zakonyprolidi.cz/cs/2009-264/zneni-20090901 (accessed 7.2.17).

Government Regulation No. 344/2006 Coll., on Minimum Safety Requirements for Road Network Tunnels [WWW Document], n.d. URL https://www.slov-lex.sk/pravne-predpisy/SK/ZZ/2006/344/20060601 (accessed 4.19.19).

Haukur Ingason, Li, Y.Z., Lönnermark, A. (2015). Tunnel Fire Dynamics. Springer, New York. 504 s. ISBN 978-1-4939-2198-0.

Hosser, D. (2013). Guidelines for Fire Protection Engineering, Technical Report TB 04/01., 3rd revised and amended edition. Technical-Scientific Advisory Board (TWB) of the Association for the Promotion of German Fire Protection e.V. (vfdb), Braunschweig. 419 p. Available from: http://www.kd-brandschutz.de/files/downloads/Leitfaden2013.pdf.

Huijben, J.W., Fournier, P., Rigter, B.P. (2006). Aanbevelingen ventilatie van verkeerstunnels. Ministerie van Verkeer en Waterstaat, Rijkswaterstaat, Bouwdienst (RWS, BD), Utrecht.

Hurley, M. (2015). SFPE handbook of fire protection engineering. Springer Science+Business Media, New York, NY. 2015. ISBN 978-1-4939-2564-3.

ISO 16733-1 (2015). Fire safety engineering - Selection of design fire scenarios and design fires - Part 1 Selection of design fire scenarios. Geneva: International Organization for Standardization, Geneva, p. 31.

Kadlic, M., Mozer, V. (2017). Uncertainties Associated with Tunnel Design Fire Scenarios. Procedia Engineering [online]. Dostupné z: doi:10.1016/j.proeng.2017.06.067.

Kročova, Š. (2015). Protection of aquatic ecosystems against accidents in the Czech Republic. Inžynieria Mineralna. 2015, vol. 36, n. 2, pp. 225-230. ISSN 1640-4920.

Kučera, P., Kaiser, R., Pavlík, T., Pokorný, J. (2009). Fire Engineering: Fire Dynamics. Ostrava: Association of Fire and Safety Engineering. 152 p. ISBN 978-80-7385-074-6.

Manual 021 (2004). Road Tunnels 03.04. Norwegian Public Roads Administration.

Marasová, D., Taraba, V., Grendel, P. (2010). Legislation and its Requirements for Tunnel Safety. Acta Montanistica Slovaca. Košice: Technical University of Košice. 15, p. 9–13.

Ministry of Transport, Department of Roads (2013). Methodological Instruction. Ventilation of Road Tunnels. Choice of System, Design, Operation and Quality Assurance of Road Tunnel Ventilation Systems. Ministry of Transport, Department of Roads. [WWW Document]. URL http://www.pjpk.cz/data/USR_001_2_11_METODICKE_POKYNY/MP_vetrani_20132.pdf (accessed 7.2.17).

Mozer, V. (2013). Modelling fire severity and evacuation in tunnels. Communications: scientific letters of the University of Žilina. 15(4), 85–90. ISSN 1335-4205.

NFPA 502 (2017). Standard for Road Tunnels, Bridges, and Other Limited Access Highways, n.d. National Fire Protection Association, p. 72.

Pokorny, J., Gondek, H. (2016). Comparison of theoretical method of the gas flow in corridors with experimental measurement in real scale. Acta Montanistica Slovaca. 21, 146–153. ISSN 1335-1788.

Pokorny, J., Malerova, L., Wojnarova, J., Tomaskova, M., Gondek, H. (2018). Perspective of the use of road asphalt surfaces in tunnel construction, in: 22nd International Scientific on Conference Transport Means 2018. Presented at the Transport Means - Proceedings of the International Conference, Lithuania, ISSN 1822296X, pp. 290–296.

RABT, 2006. Guidelines for equipment and operation of road tunnels. Köln: Forschungsgesellschaft für Straßen- und Verkehrswesen e.V.

Regulation (EU) No 305. (2011). Laying down harmonised conditions for the marketing of construction products and repealing Council Directive 89/106/EEC Text with EEA relevance, 2011. URL https://eur-lex.europa.eu/legal-content/CS/TXT/PDF/?uri=CELEX:32011R0305&from=CS.

RVS 09.02.31, 2008. Tunnel Ventilation - Basic Principles. Austrian Research Association for Roads, Rail and Transport.

STN 737507 (2008). Design of Road Tunnels. Bratislava: Slovak Office for Standards, Metrology and Testing.

Tomašková, M., Vargová, M. (2018) Risk analysis of firefighting lifts and safety rules. In: New Trends in Process Control and Production Management. London: Taylor and Francis Group, 2018 S. 555-560. ISBN 978-1-138-05885-9.

TP 049, 2018. Technicke podmienky větranie cestnych tunelov TP 049. Bratislava: Ministry of Transport and Construction of the Slovak Republic Section of Road Transport and Roads.

Yang, X. (2016). Design Environmental Protection, Energy Saving and Safety Ventilation System of Long Highway Immersed Tunnel. Procedia Engineering 166, 32–36. https://doi.org/10.1016/j.proeng.2016.11.533.

World Road Association | PIARC [WWW Document] (2019) URL https://www.piarc.org/en/ (accessed 4.21.19).

Hydrocyclone separation as a tool for reduction of the amount of heavy metals in municipal solid waste incinerator (MSWI) residues

Silvie Koval[1], Helena Raclavska[2], Hana Skrobankova[1], Dalibor Matysek[2], Lukas Koval[3] *and* ***Franz Winter[4]***

Municipal solid waste incineration residues such as fly ash and air pollution control residues are classified as hazardous waste and disposed of, although they contain potential resources. The most problematic elements in municipal solid waste incineration residues are leachable heavy metals and salts. Therefore, these residues usually do not meet the criteria for recycling as construction material or for landscaping, as they possess an environmental risk (and are classified as an H15 hazard material - waste capable by any means, after disposal, of yielding another substance, for example, leachate). Thus, an efficient treatment method should comprise a washing step to remove soluble chlorides, combined with an elimination step aiming to remove the heavy metals. As a consequence, it was proposed to use a cyclosizer device (hydrocyclone principle) for the separation of the incineration residues in order to prove the statement that the highest concentration of heavy metals can be found within the finest particles. Chemical and physical properties of two air pollution control residue samples and one fly ash sample were examined prior to sorting the samples into five size fractions by the cyclosizer. The results show that chloride salts can be removed from the residues during the cyclosizer separation process, and heavy metals were concentrated in the fine particle size fraction after the process. On the basis of these findings it can be assumed that removing the finest size fraction from the municipal solid waste incineration residues (fractions <12 µm and <14 µm respectively), will decrease the heavy metal content by ***Hg*** *51* **ï** *60%;* ***Ag*** *32* **ï** *36%;* ***Cd*** *37* **ï** *46%;* ***Co*** *23* **ï** *27%;* ***Cr*** *30* **ï** *40%;* ***Cu*** *27* **ï** *37%;* ***Ni*** *21* **ï** *26%;* ***Pb*** *34* **ï** *42%;* ***Sb*** *44* **ï** *50%;* ***Zn*** *33* **ï** *40%. Concentrations of the heavy metals in the coarse fraction of these residues are below the regulatory limit, and therefore this study suggests that they can be used for recycling and reuse.*

Keywords: *cyclosizer, waste incineration, MSWI residues, heavy metal, fly ash, APC*

Introduction

The last two decades have seen a growing trend towards municipal solid waste incineration (MSWI) due to its unique benefits of mass and volume reduction of waste (Liu et al., 2016; Mikulį iÍ, 2016). There are several types of MSWI residues, though the finer fraction, referred to as fly ash (FA) and air pollution control (APC) residue, pose serious environmental problems (Yao et al., 2015; Raclavská et al., 2017).

Fly ash and APC residue consist of fine particles that contain significant amounts of leachable toxic elements, including heavy metals, chloride salts and sulphates (Saqib and Bäckström, 2016; Nowak et al., 2013).
The concentrations of metals in APC from combustion of municipal waste decrease in the following series: Zn > Cu > Pb > Sb > Cr > As > Cd (Saqib and Bäckström, 2016) or Zn > Pb > Cu > Cr > Ni > Cd, and the concentrations of Zn and Pb are higher by one order or more than those of other metals (Pan et al., 2013). Metals which are present in ion-exchangeable form are leached in the following order: Cd > Cu > Sb > Zn> As > Pb > Cr (Saqib and Bäckström, 2016). In addition, highly toxic organic substances and organic pollutants such as dioxins (PCDD), furans (PCDF) and PAHs are also present making the utilization of MSWI residues even more problematic (Saikia et al. 2007). Therefore, they usually do not meet the criteria for recycling as construction material or for possessing an environmental risk (and are classified as an H15 hazard material - waste capable by any means, after disposal, of yielding another substance, for example, leachate) (Aguiar et al., 2009). Several researchers have developed different treatment methods to decrease the leachability of the MSWI residues. These methods are generally classified as separation, stabilization/solidification and thermal techniques (Quina and Bordado, 2009). A limited number of studies mentioned fly ash and APC residue treatment using a hydrocyclone for their separation (Ko et al., 2013). Several studies recommended water washing the residues to remove soluble chlorides before applying another treatment (Mangialardi, 2003; Wang et al., 2010; Chen et al., 2017). A single washing, followed by washing of the filtration cake removes up to 99% of soluble chlorides according to a previous study (Hartmann, 2015). Recently authors have published the link between particle size and chemical composition of fly ash and they conclude that with decreasing particle size, the concentration of heavy metals increases (Wang et al., 2002; De Boom and Degrez, 2012). The distribution of major elements in different particle size fractions is less predictable (Fedje et al., 2010). The release of heavy metals into flue gas is related to chloride content in MSWI fly ash. Evaporation

[1] *Silvie Koval, Hana Skrobankova,* Centre ENET - Energy Units for Utilization of Non-Traditional, VSB - Technical University of Ostrava, 17. listopadu 15/2172, 708 33 Ostrava-Poruba, Czech Republic, *silvie.koval@vsb.cz, hana.skrobankova@vsb.cz*
[2] *Helena Raclavska, Dalibor Matysek,* Department of Geological Engineering, Faculty of Mining and Geology, VSB ï Technical University of Ostrava, 17. listopadu 15/2172, 708 33 Ostrava-Poruba, Czech Republic, *helena.raclavska@vsb.cz, dalibor.matysek@vsb.cz*
[3] *Lukas Koval,* CSIRO Mineral Resources, Technology Court 1, 4069 Pullenvale, QLD, Australia, *lukas.koval@csiro.au,*
[4] *Franz Winter,* Institute of Chemical Engineering, Vienna University of Technology, Getreidemarkt 9, 1060 Vienna, Austria, *franz.winter@tuwien.ac.at*

of Cd, Pb and Zn increases proportionally to increasing concentrations of chlorides in waste from MSWI (Chen et al., 2017).

Thus, an efficient treatment method should comprise a washing step to remove soluble chlorides, combined with an elimination step aiming to remove the heavy metals. As a consequence, it was proposed to use a cyclosizer device (hydrocyclone principle) for MSWI residue treatment. Apart from (Ko et al., 2013; Wang et al., 2002), there is a general lack of research in MSWI residue treatment by using a hydrocyclone or cyclosizer device. In addition to chlorides and heavy metals decrease, the question of high organic compound levels could be raised. However, the present study was limited to inorganic contaminants.

The objective of this study was to investigate the treatment of different MSWI residue samples to eliminate the hazard property H15 (reducing the chloride content) and mitigation of problematic elements (heavy metals, above all Hg and Pb). Three different residue samples were treated by using the cyclosizer device for separation. Chemical and physical properties of residue size classes were examined. The statement that the highest concentration of heavy metals can be found within the finest particles is to be investigated. Using these mineral processing methods for MSWI residue treatment could make it possible to eliminate the classification of the MSWI residues as an H15 hazard property material and re-categorize it from hazardous waste to non-hazardous waste. Therefore, treated MSWI residue is a promising material which can save the use of non-renewable natural resources and it is also cost-effective when there is no need to handle it as a hazardous material.

Materials and methods

Materials

The MSWI residue samples (two APC residues and one FA sample) used for measurements are referred to as APC 1, APC 2 and FA 3. MSWI residues samples were collected during the years 2013 and 2014. A detailed description of the samplesô origin is confidential. However, a description of the technologies used in the incineration plants is shown below:

APC 1 ï The incineration plant consists of 3 lines of grate furnaces, a dry flue gas cleaning system with the addition of crushed activated coke into the flue gas stream before the baghouse filter, utilizing municipal solid waste (188,000 t/y). The main reason for the injection of activated coke is the removal of mercury and other pollutants. The annual solid residue amount is 47,500 t of slag, 3,700 t of APC residue and 190 t of filter cake with a water content of approximately 40 per cent.

APC 2 ï The incineration plant consists of two lines of grate furnaces, a dry flue gas cleaning system and electrostatic precipitators, utilizing 203,000 t of municipal solid waste per year. The remaining dust (filter fly ash) is subtracted, followed by a wet chemical two-stage scrubber system. In the first stage, in an acidic environment, hydrochloric acid and mercury, as well as other substances, are extracted. After this, a fixed bed activated carbon absorber is installed. The remarkable differences are: the boiler ash and the filter ash are collected together, and a fixed bed carbon absorber is omitted. The annual solid residues amount is 44,000 t of slag, 3,300 t of APC residue and 270 t of filter cake with a water content of approximately 40 per cent.

FA 3 ï The incineration plant uses a fluidised combustion technology, electrostatic precipitators and utilises almost exclusively refuse-derived fuel (RDF), with a capacity of 110,000 t/y. Boiler ash and filter ash are collected together. Annually 10,100 t of bottom ash and 11,200 t of fly ash emerge as a solid residue.

Colour of the samples varied from light grey to light brown (colour was influenced by the incineration technology and combusted materials). All the residue samples were alkaline with **pH** values from **12.2** to **12.4** and **density**: **APC 1 = 2.97 g/cm^3, APC 2 = 2.85 g/cm^3, FA 3 = 2.49 g/cm^3**. Good wettability was typical for all samples. The raw residue samples obtained from the MSWI plants were homogenised for further analysis and treatment.

Methods

Chemical analysis. The chemical composition of the MSWI residues was determined by X-ray fluorescence (XEPOS III HE, Spectro) according to (CSN EN 15309, 2007). The analysis was conducted in the accredited laboratory Public Health Institute Ostrava, Czech Republic (ZUOVA). The MSWI samples (both raw and treated) were homogenised. The dry mass and the loss of ignition were established. The dry samples were ground to the size < 60 µm, and for the pellet preparation, the wax was added. The fluorescence analyses were conducted on the pelletised samples.

Mineralogical analysis. The phase composition of samples in the original state, after the removal of chlorides by washing, and after separation in hydrocyclone (APC1) were analysed using X-ray diffraction analysis. The verification of qualitative evaluation and also a semi-quantitative estimation of the composition of samples were determined by Rietveld analysis of diffraction data (software RayfleX Autoquan). Measurements were performed at the diffractometer Bruker AXS D8 Advance with 2ẽ /ẽ geometry, with Goebel mirror in the primary beam and with the energy dispersive detector SOL-XE. The results are presented together with estimates of statistical errors (statistical level 99%, i.e. 3ů).

Microanalysis of particles was performed by scanning electron microscope SEM, FEI Quanta 650 FEG equipped by analyzers EDX ï EDAX Apollo X, WDA ï LEXS, EBSD ï EDAX TSL, CL ï Gatan Mono 4. Polished sections were prepared for chemical analysis of particles. Chemical analysis of particles in separated grain size classes was focused on the identification of particles with the content of metals. The number of analysed particles in each class was 25.

MSWI residue separation. The separation was performed by using a cyclosizer (Metcon Laboratories, VSB-TUO). The cyclosizer is a precise laboratory apparatus for the rapid and accurate determination of particle size distribution within the sub-sieve range (Figure 1). Particles were separated according to their Stokesian settling characteristics by a principle based on the well-known hydraulic cyclone principle. The samples were sized at 100 µm before cyclosizing to achieve better separation results. Only the undersize fraction (< 100 µm) was used for the cyclosizer sorting. Separation size fraction boundaries were established according to the MSWI residue density (APC 1 = 2.97 g/cm^3, APC 2 = 2.85 g/cm^3, APC 3 = 2.49 g/cm^3), water temperature (10.1 °C) and flow speed (11.6 l/min). Approximately 180 L of water was used for the separation of 1.5kg of the sample. The S/L ratio was approximately 1:100.

The samples were sorted into five size fractions by the cyclosizer. The sixth size fraction was obtained by filtering the process water passing the No. 5 cyclone. Alternately, solids passing the No. 5 cyclone were determined by difference. The separated solids were settled, filtered, dried in ambient temperature and weighed to determine the size distribution.

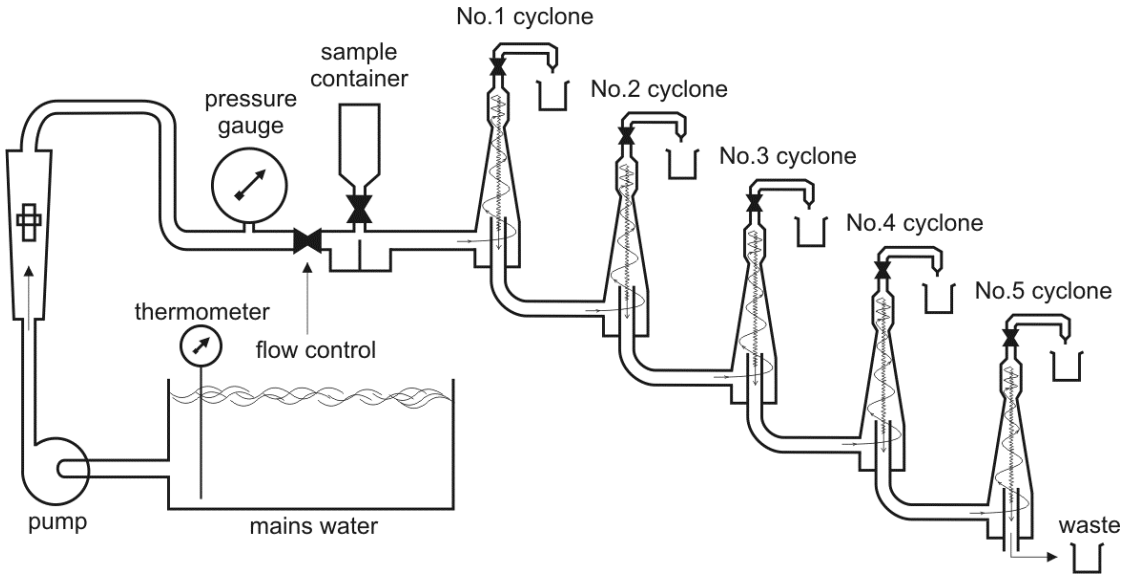

Fig. 1. The diagrammatic arrangement of the cyclosizer device

Size fractions

APC 1 and **APC 2:** 1 (49 ï 100 µm); 2 (34 ï 49 µm); 3 (23 ï 34 µm); 4 (16 ï 23 µm); 5 (12 ï 16 µm); 6 (< 12 µm)

FA 3: 1 (55 ï 100 µm); 2 (39 ï 55 µm); 3 (26 ï 39 µm); 4 (19 ï 26 µm); 5 (14 ï 19 µm); 6 (< 14 µm)

Results and discussion

Untreated MSWI residue characteristics

Chemical and physical analyses of untreated samples were performed to obtain essential characteristics. The chemical composition of MSWI residues is strongly influenced by the flue gas cleaning technology and by the material that is combusted. Concentrations of major components, especially chlorides, can significantly influence APC and FA behaviour for further treatment. The amount of the major components expressed in wt.%

was calculated in terms of oxides. Concentrations of the major components can be found in Table 1. The concentrations of heavy metals in unprocessed MSWI residues are presented in Table 2.

Generally, calcium had the highest representation within all of the MSWI residue samples (13.5 ï 21 wt.% present as CaO), which may be associated with the lime injected during the flue gas cleaning process. Furthermore, high chloride concentrations can be considered as a significant characteristic of MSWI solid residues (APC 1 ~ 14.1 wt.% and APC 2 ~ 9.7 wt.%). Lower chloride concentrations for FA 3 (2.6 wt.%) is in relation to the combusted material, as waste-derived fuel is primarily combusted in this incineration plant. However, FA 3 sample showed high concentrations of Al, Fe, Mg, P and Si.

Tab. 1. Major fly ash components concentrations in wt.%

Major MSWI residues components [wt.%]			
	APC 1	APC 2	FA 3
SiO_2	10.17	13.65	31.52
Al_2O_3	13.05	14.70	25.37
Fe_2O_3	2.18	3.88	7.60
CaO	18.84	21.10	13.57
MgO	0.77	0.86	2.43
Na_2O	14.39	10.97	4.05
K_2O	6.32	4.69	1.60
sulphates	8.13	4.92	2.53
chlorides	14.10	9.73	2.62
heavy metals	2.14	1.95	0.77
LOI	9.80	13.49	7.91

Heavy metals: the sum of Ag, As, Cd, Co, Cr, Cu, Hg, Ni, Pb, Sb, and Zn
LOI: loss on ignition

Tab. 2. The content of heavy metals (mg/kg) in unprocessed MSWI residues

Heavy metal content [mg/kg]			
	APC 1	APC 2	FA 3
Hg	37.1	16.8	1.9
Ag	18.2	11.4	3.1
Cd	237	181	12.2
Co	26	26	36.7
Cr	656	558	254
Cu	820	908	1550
Ni	51.9	60.4	56.9
Pb	2800	2580	1370
Sb	773	719	128
Zn	15900	14400	4210

MSWI residue obtained from the plant using baghouse filter technology for flue gas cleaning (APC 1) generally had the highest concentrations of heavy metals among the samples. Baghouse filters are usually located at the end of the flue gas cleaning process. Furthermore, in the case of APC 1, crushed activated coke is injected into the flue gas stream before the baghouse filter, which absorbs heavy metals, especially mercury, and other pollutants. The highest concentration of Hg (37.1 mg/kg) was found for APC 1. This concentration considerably exceeds the limit for Hg in a non-hazardous waste landfill (limit value of 20 mg/kg) (Purgar et al., 2014). In addition, Cd, Cr, Pb and Zn concentrations were highest in APC 1 sample.

Mineralogical phase analysis

The main mineral phases in fly ashes from MSWI form anhydrite, calcite, halite, and sylvite, calcium silicate, mayenite, and calcium aluminium silicate (Zhou et al., 2015). Mineralogical phase analysis of fly ashes is important from the point of view of determination of their puzzolan properties when utilised in the construction industry and also for determination of the form of chlorides occurrence that is important information for their removal because they represent the limiting factor for utilization of fly ashes (replacement of Portland cement in concrete). Chlorides form an important mineral phase of fly ashes from MSWI. They are present most often as halite (NaCl) and sylvite (KCl). Halite occurs in fly ashes in amounts from 2.4% (APC 3) to 12% (APC 1), sylvite is present in amounts from 4.3% (APC 2) to 7% (APC 1). Other crystalline phases in fly ashes from MSWI include anhydrite ($CaSO_4$) 2.61 ţ 5.74%, calcite ($CaCO_3$), quartz (SiO_2), periclase (MgO), hematite (Fe_2O_3) and silicate phase. The samples APC 1 and 2 have larnite (Ca_2SiO_4) 12% and alumosilicate: gehlenite ($Ca_2Al[AlSiO_7]$) 6.58 ï 8.06%. The sample APC 3 contains muscovite ($KAl_2[AlSi_3O_{10}](F,OH)_2$) and sanidine ($K[AlSi_3O_8]$). Amorphous component forms 37 ï 48% in APC 1 and 2, in fly ash APC 3 it is up to 64%. After removal of chlorides by washing, there appeared in fly ashes: tricalcium aluminate ($3CaO{\cdot}Al_2O_3$) in amounts of 3 ţ 6% and ettringite ($Ca_6Al_2(SO_4)_3(OH)_{12}{\cdot}26H_2O$) in concentrations up to 3%, formed during washing

of fly ash as a result of reaction of calcium aluminate with calcium sulphate (Chindaprasirt et al., 2013). The content of calcite in APC1 and APC2 increased after washing from 11 to 15%.

The sample APC1 separated in the cyclosizer proved that the amount of amorphous component increased (up to 55%) in comparison with APC1 in the original state (37.1%). The highest amount of amorphous component was found in the particle size class over 63 µm (59.1%), and the lowest amount was found in the particle size class from 12 to 28 µm. The content of the amorphous component increases again in particles of the size below 12 µm. In a relationship with the content of the amorphous component in individual particle size classes, it was determined the highest amount of gehlenite (9%), larnite (14%), anhydrite (6%) and halite (1.3%) in the particle size class from 12 to 28 µm. The highest amount of quartz was determined in the class over 63 µm. The highest content of calcite and periclase was determined in the class below 12 µm. Separation of APC1 in cyslosizer did not cause a significant enrichment of phases with puzzolan properties. The concentrations of halite varied in the range from 0.25 to 1.31%, and the lowest amounts were found in the class over 63 µm (0.52%) and below 13 µm (0.25%).

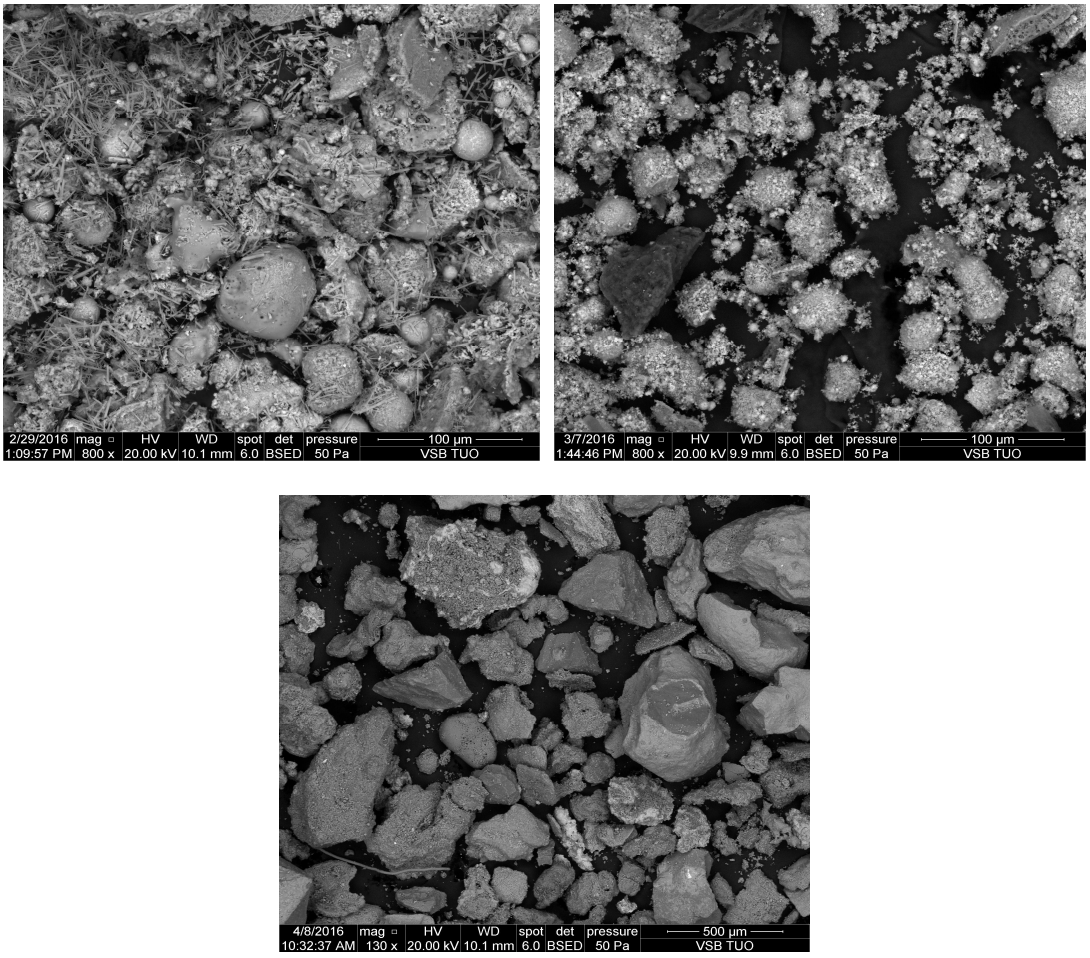

Fig. 2. Scanning electron microphotographs: APC1 – original sample (upper left), APC1 after separation in cyclosizer, particle size class 25 – 45 µm (upper right), sample after washing – extraction by water, removal of 98% water-soluble chlorides (below).

Nature of metal occurrence in particles of fly ash before the beginning of chloride removal by washing or separation in cyclosizer was studied by chemical analysis of particles. It was found that metals are present prevalently in the form of native metals (Pb), oxides: CuO, SnO, ZnO, FeO_x, PbO, or mixed phases: Pb-Al-O, Pb-Ca-O, Cr-Fe-O, Cr-Fe-Ca, Cr-Zn-O_x, Sn-Fe, Fe-Ca-O, and Fe-Cr. The analysis of particles after separation in cyclosizer proved that even when particles are separated according to the size, they are covered by particles of chloride of size from 1 to 2 µm. The same trend appears in all particle size classes from cyclosizer. The highest concentrations of chloride (17-21%) were determined in particles of size over 63 µm. The highest number of particles containing Zn was found in the particle size class from 63 µm to 1 mm (91%) and in the finest class below 25 µm (73%). The number of particles containing Zn in other particle size classes was 45%. The highest average concentration of Zn was determined in particles over 1 mm (9.15%). The particles with the highest average concentrations of Si (8.02%) and Al (3.92%) occur in the particle size class < 25 µm.

After the separation in cyclosizer, the microanalysis identified the particles containing Cu, Co and V, while particles containing Pb were not identified. Water-soluble salts of Pb were probably formed in the environment of the saturated chloride solution (Ye et al., 2017). From the results of microanalysis it follows that during the separation in cyclosizer, chlorides were not sufficiently effectively removed, which was caused by the short time of contact between water and particles (approximately 20 minutes). Hartmann et al. (2015) determined that leaching after one hour had the efficiency of 72% for the chloride removal, and only after 24 hours, it reaches 94%. Pan et al. (2008) report recovery of 86% after two hours of leaching. During the direct washing (24 hours), the efficiency of 98% was achieved at the ratio L/S=10:1 (Figure 2).

Water leachate

Landfill criteria and acceptance limits are not uniform within the European Union. Valid European legislation was used for the MSWI residue waste category evaluation (European Council Decision 2003/33/EC). Water leachate was prepared according to (CSN EN 12457-2, 2003) and compared to the limits according to (European Council Decision 2003/33/EC) in Table 3.

The total leachable fraction was by far largest for the APC 1 and was dominated by chlorides of Ca, Na and K, APC 2 was very similar. The APC 1 and APC 2 sample contained soluble forms of Pb in significant amounts. A comparison of the amounts of elements dissolved in the leachate revealed that the main sources of metal ions are likely to be chlorides. However, in the high pH range, Pb, as well as many other metals, show amphoteric behaviour and thus dissolve as oxo-anions. Such processes may also take place during a leaching test (Abbas et al., 2001). According to Takaoka et al. (2005), Pb and Zn mainly exist as water-soluble $PbCl_2$ and $ZnCl_2$ in MSWI residues. Furthermore, Ko et al. (2013) reported that only a small amount of Pb and Zn from MSWI fly ash could be transferred to the liquid phase, but Cr and Cu mostly remain in the solid phase (Hsiao et al., 2002). Higher concentrations of Pb found in the leachate from APC 1, and APC 2 in this study are in agreement with Ko et al. (2013). Nevertheless, a higher amount of Cr was found in a liquid phase in this study. Cr(VI) may have been dissolved and then transformed into a less soluble form in a secondary reaction such as reduction to Cr(III) in MSWI residue leachate (Abbas et al., 2001).

Tab. 3. Water leachate results of untreated MSWI residue samples, compared with European waste landfill limits (values exceeding the non-hazardous limits are highlighted)

Parameter	Unit	MSWI residues			Limits (2003/33/EC)		
		APC 1	APC 2	FA 3	I	NH	H
pH	[-]	10.64	11.63	9.43	-	-	-
D.S.	[mg/kg]	30925	19495	4055	4000	60000	100000
DOC	[mg/kg]	42.7	46.2	51.5	500	800	1000
Cl^-	[mg/kg]	**101046**	**89653**	14927	800	15000	25000
SO_4^{2-}	[mg/kg]	**23200**	11500	6680	1000	20000	50000
F-	[mg/kg]	46.5	49.4	5.1	10	150	500
As	[mg/kg]	0.9	0.1	0.3	0.5	2	25
Ba	[mg/kg]	6.1	5.8	5.0	20	100	300
Cd	[mg/kg]	0.005	0.331	0.015	0.04	1	5
Cr	[mg/kg]	**12.4**	2.0	9.8	0.5	10	70
Cu	[mg/kg]	0.2	0.2	0.2	2	50	100
Hg	[mg/kg]	0.022	0.009	0.005	0.01	0.2	2
Mo	[mg/kg]	**33.7**	4.5	4.4	0.5	10	30
Ni	[mg/kg]	0.2	0.2	0.2	0.4	10	40
Pb	[mg/kg]	**59.9**	**39.7**	0.3	0.5	10	50
Sb	[mg/kg]	**4.10**	0.419	0.050	0.06	0.7	5
Se	[mg/kg]	0.1	0.1	0.1	0.1	0.5	7
Zn	[mg/kg]	17.4	22.0	0.5	4	50	200
Phenol index	[mg/kg]	15.8	0.2	0.1	1	-	-

D.S.: dissolved solids; I = Inert; NH = Non-Hazardous; H = Hazardous

Generally, it was found that the concentrations of heavy metals in the solid phase were higher than those in the liquid phase, which is in agreement with (Ko et al., 2013). These findings support the premise that the hydrocyclone separation process can transfer water-soluble salts from MSWI residues to liquid phases while preserving most of the heavy metals in solid phases.

Cyclosizer separation

Quantitative analysis of sample yield was calculated using an initial weight of 80 g of sample. Results of the quantitative analysis (recovery rate) are shown in Table 4, and heavy metal yield results are shown in Figure 3.

Tab. 4. Recovery rates of MSWI residue samples after separation using a cyclosizer

Particle size range [µm]		APC 1	APC 2	FA 3	APC 1	APC 2	FA 3
APC 1 & APC 2	FA 3	[g]	[g]	[g]	[%]	[%]	[%]
49-100	55 ï 100	4.1	6.5	4.6	5.1	8.1	5.7
34-49	39 ï 55	6.5	9.0	8.8	8.2	11.3	11.0
23-34	26 ï 39	11.0	12.7	13.9	13.7	15.9	17.4
16-23	19 ï 26	9.0	9.1	11.1	11.2	11.3	13.9
12-16	14 ï 19	5.7	5.2	7.3	7.2	6.6	9.1
< 12	< 14	19.7	22.2	31.2	24.6	27.8	39.0
Dissolved solids		24.0	15.2	3.2	30.0	19.0	4.0
Sum		80	80	80	100	100	100

Elemental concentration in the size fractions was determined by using X-ray fluorescence analysis. The yield of the heavy metals chosen (Hg, Ag, Cd, Co, Cr, Cu, Ni, Pb, Sb a Zn) was calculated from the recovery rate of that size fraction (Table 4) and heavy metal concentrations in that size fraction. It can be concluded that the heavy metals tended to distribute into the size fractions in the same way for all fly ash samples, with the highest concentrations observed in two specific size fractions ï the oversize fraction (> 100 µm) and in the smallest size fraction (< 12 µm and < 14 µm respectively). Rönkkömäki et al. (2008), and Lanzerstorfer (2015) reported the same trend in the heavy metal distribution in the oversize and sub-sieve fraction for Cd and Zn. Moreover, according to Lanzerstorfer (2015), Pb is concentrated in the finest fraction of MSWI fly ash. Barbosa et al. (2013) examined fly ash samples from biomass incineration and showed an increasing concentration of all elements (except Hg) with decreasing particle size. Dahl et al. (2009) reported the tendency of increasing concentration with decreasing particle size for Zn but found no such consistent trend for Cd and Co.

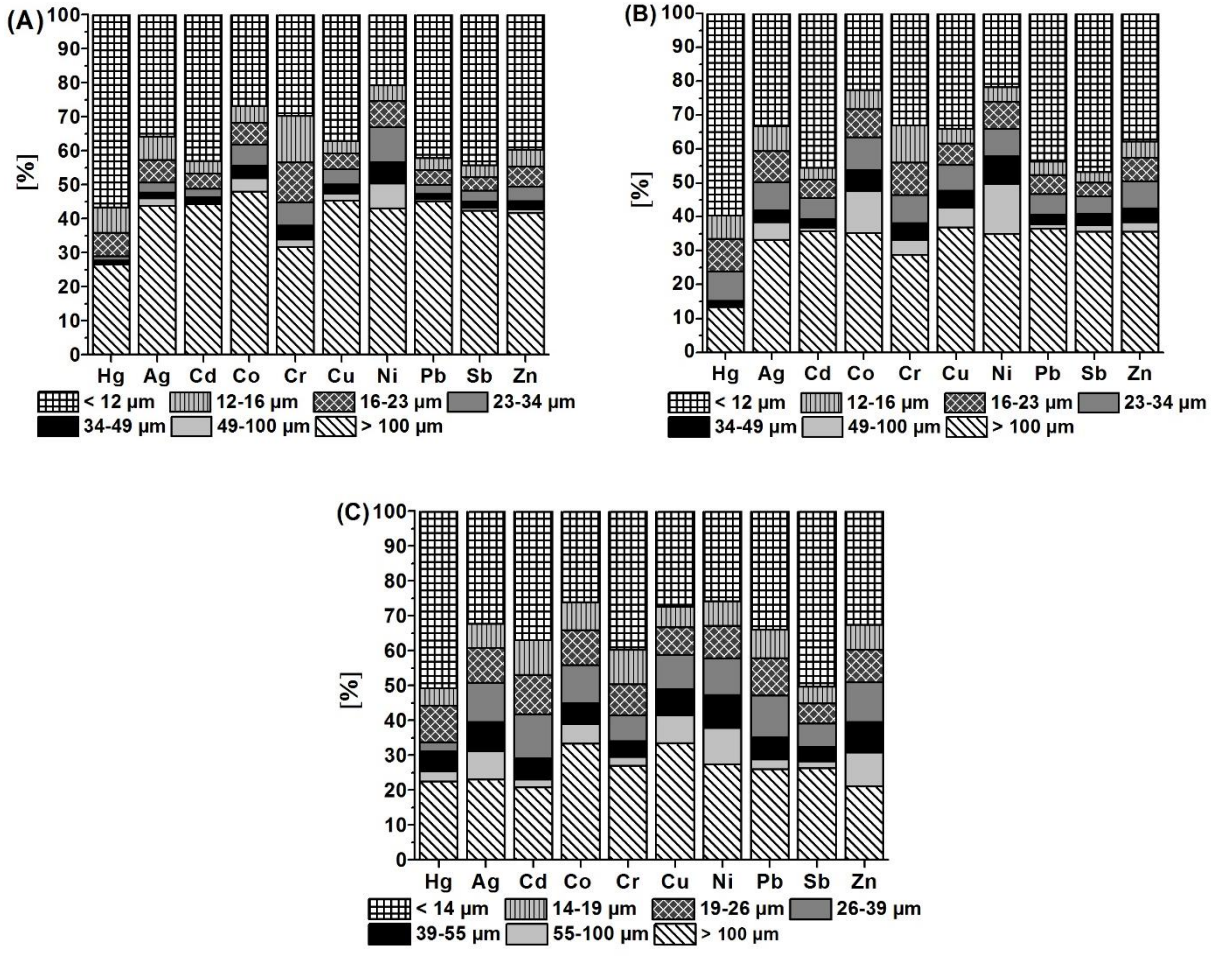

Fig. 3. Heavy metal yield after sieving and separation using a cyclosizer: (A) APC 1, (B) APC 2, (C) FA 3

On the basis of these results it can be assumed that after removal of the finest particles (fractions < 12 µm and < 14 µm respectively), the heavy metal content would be decreased by: ***Hg*** 51 ï 60%; ***Ag*** 32 ï 36%; ***Cd*** 37 ï 46%; ***Co*** 23 ï 27%; ***Cr*** 30 ï 40%; ***Cu*** 27 ï 37%; ***Ni*** 21 ï 26%; ***Pb*** 34 ï 42%; ***Sb*** 44 ï 50%; ***Zn*** 33 ï 40%. Theoretical mercury concentration for APC 1 would then be 16.32 mg/kg and for APC 2

13.72 mg/kg. These concentrations are within the Austrian landfill limit for mercury disposal (20 mg/kg), according to the Austrian Landfill statutory body (BGBl. II Nr. 104/2014).

Hydrocyclone separation is not a zero-waste technology. At the end of the process, wastewater containing high concentrations of salts (especially chlorides) and some heavy metals are generated; thus, it is essential to carry out wastewater treatment and recycling. However, high chloride-containing wastewater can be used for salt recovery or can be treated by adding sodium aluminate ($NaAlO_2$) to form insoluble Friedelôs salt at high pH conditions (Abdel-Wahab, 2002). The treated water can then be reused in the hydrocyclone separation process.

The above results demonstrate that hydrocyclone separation technology is promising for MSWI residue treatment and the heavy metal content reduction. However, the optimal separation boundary and separation efficiency should be investigated further. Therefore, it is proposed to build a pilot-scale hydrocyclone device for separating MSWI residues to confirm or deny the results stated in this paper.

Conclusion

Three MSWI residue samples from different incineration plants were examined within this study. Chemical and physical properties of two APC residue samples and one fly ash sample were examined. Higher content of heavy metals was found in the samples, ranging from 0.77 (FA 3) to 2.14 wt.% (APC 1). Therefore, a unique separation process was applied to reduce the heavy metals content. The separation into six size fractions was performed by using a cyclosizer. The results show that chloride salts can be removed from the MSWI residues during the cyclosizer separation process by simple water extraction process, when the value of ratio S:L = 1:10 is reached and the time of contact with water is sufficient, i.e. more than one hour. Furthermore, heavy metals were concentrated in the fine particle size fraction after the process. On the basis of these findings, it can be assumed that removing the finest size fraction from the MSWI residues (fractions < 12 µm and < 14 µm respectively), will decrease the heavy metal content by up to 60% for Hg (APC 2). In addition a significant decrease of other heavy metals was observed as well (namely Sb > Cd > Pb > Zn > Cr > Cu > Ag > Co > Ni). Hydrocyclone separation seems to be a very promising method that could be used for the reduction of heavy metal content in the MSWI residues. The coarse particles of the MSWI residues had Hg concentrations below the regulatory limit. Therefore, it can be suggested that they may be used for recycling and reuse. However, use of this process on an industrial scale and its economic value needs to be further investigated, which was not a part of this study.

Acknowledgements: *This paper was supported by the research projects of the Ministry of Education, Youth and Sport of the Czech Republic: The National Programme for Sustainability LO1404 ï TUCENET. The Christian Doppler Laboratory for Anthropogenic Resources is kindly thanked for scientific exchanges. The project of research and development MSMT-15304/2017-1, INTER-EXCELLENCE LTC17051 ñEuropean Anthroposhere as a Source of Mineral Raw Materialsò.*

References

Abbas, Z., Steenari, B.M. and Lindqvist, O. (2001). A study of Cr(VI) in ashes from fluidized bed combustion of municipal solid waste: leaching, secondary reactions and the applicability of some speciation methods. *Waste Management*, 21(8), pp. 725-739.

Abdel-Wahab, A. and Batchelor, B. (2002). Chloride removal from recycled cooling water using ultra-high lime with aluminium process. *Water Environmental Research*, 74, 2002, pp. 256-263.

Aguiar Del Toro, M., Calmano, W. and Ecke, H. (2009). Wet extraction of heavy metals and chloride from MSWI and straw combustion fly ashes. *Waste Management*, 29(9), pp. 2494-2499.

Austrian Landfill Statutory Body, Deponieverordnung (2008). *BGBl. II Nr. 104/2014 ï Nr. 39.* Verordnung des Bundesministers für Land- und Forstwirtschaft, Umwelt und Wasserwirtschaft über Deponien.

Barbosa, R., Dias, D., Lapa, N., Lopes, H. and Mendes, B. (2013). Chemical and ecotoxicological properties of size-fractionated biomass ashes. *Fuel Processing Technology*, 109, pp. 124-132.

Chen, W., Kirkelund, G.M., Jensen, P.E. and Ottosen, L.M. (2017). Comparison of different MSWI fly ash treatment processes on the thermal behavior of As, Cr, Pb and Zn in the ash. *Waste Management*, 68, pp. 240-251.

Chindaprasirt, P., Thaiwitcharoen, S., Kaewpirom, S. and Rattanasak, U. (2013). Controlling ettringite formation in FBC fly ash geopolymer concrete. *Cement and Concrete Composites*, 2013, 41, pp. 24-28.

Dahl, O., Nurmesniemi, H., Pöykiö, R. and Watkins, G. (2009). Comparison of the characteristics of bottom ash and fly ash from a medium-size (32 MW) municipal district heating plant incinerating forest residues and peat in a fluidized-bed boiler. *Fuel Processing Technology*, 90 (7-8), pp. 871-878.

De Boom, A and Degrez, M. (2012). Belgian MSWI fly ashes and APC residues: A characterisation study. *Waste Management*, 32(6), pp. 1163-1170.

European Council Decision (2003). *European Council Decision 2003/33/EC - Establishing criteria and procedures for the acceptance of waste at landfills pursuant to Article 16 of Annex II* to Directive 1999/31/EC.

Fedje, K.K., Rauch, S., Cho, P. and Steenari, B.M. (2010). Element associations in ash from waste combustion in fluidized bed. *Waste Management*, 30, pp. 1273-1279.

Hartmann, S., Koval, L., Ġkrobánková, H., Matýsek, D., Winter, F. and Purgar, A. (2015). Possibilities of municipal solid waste incinerator fly ash utilisation. *Waste Management and Research*, 33(8), pp. 740-747.

Hartmann, S., Matysek, D., Stary, M. and Skrobankova, H. (2015). Removal of Chlorides from Waste Incineration Residues. *InŨynieria Mineralna-Journal of the Polish Mineral Engineering Society*, 16(1), pp. 145-150.

Hsiao, M.C, Wang, H.P., Wei, Y.L, Chang, J-E. and Jou, C.J. (2002). Speciation of copper in the incineration fly ash of a municipal solid waste. *Journal of Hazardous Materials*, 91(1-3), pp. 301-307.

Ko, M.-S., Chen, Y.-L. and Wei, P.-S. (2013). Recycling of municipal solid waste incinerator fly ash by using hydrocyclone separation. *Waste Management*, 33(3), pp. 615-620.

Lanzerstorfer, Ch. (2015). Cyclone fly ash from a grate-fired biomass combustion plant: Dependence of the concentration of various components on the particle size. *Fuel Processing Technology*, 131, pp. 382-388.

Liu, S-J., Guo, Y.-P., Yang, H.-Y., Wang, S., Ding, H. and Qi, Y. (2016). Synthesis of a water-soluble thiourea-formaldehyde (WTF) resin and its application to immobilize the heavy metal in MSWI fly ash. *Journal of Environmental Management*, 182, pp. 328-334.

Mangialardi, T. (2003). Disposal of MSWI fly ash through a combined washing-immobilisation process. *Journal of Hazardous Materials*, 98(1-3), pp. 225-240.

Mikulļiĺ, H., von Berg, E., Vujanoviĺ, M., Wang, X., Tan, H. and Duiĺ, N. (2016). Numerical evaluation of different pulverized coal and solid recovered fuel co-firing modes inside a large-scale cement calciner. *Applied Energy*, 184, pp. 1292-1305.

Nowak, B., Aschenbrenner, P. and Winter, F. (2013). Heavy metal removal from sewage sludge ash and municipal solid waste fly ash - A comparison. *Fuel Processing Technology*, 105, pp. 195-201.

Pan, J.R., Huang, Ch., Kuo, J.J. and Lin, S.H. (2008). Recycling MSWI bottom and fly ash as raw materials for Portland cement. *Waste Management*, 28, pp. 1113-1118.

Pan, Y., Wu, Z., Zhou, J., Zhao, J., Ruan, X.,Liu J. and Qian, G. (2013). Chemical characteristics and risk assessment of typical municipal solid waste incineration (MSWI) fly ash in China. *Journal of Hazardous Materials*, 261, pp. 269-276.

Purgar, A., Fellner, J., Hahn, M., Hartmann, S., Lederer, J., Rechberger, H. and Winter, F. (2014). Mercury in Vienna´s waste incineration cluster and related problems for fly ash disposal. In *Proceedings Venice 2014, Fifth International Symposium on Energy from Biomass and Waste*, Venice, Italy.

Quina, M. J. and Bordado, J. C.M. (2009). Quinta-Ferreira, R. M., The influence of pH on the leaching behaviour of inorganic components from municipal solid waste APC residues. *Waste Management*, 29(9), 2009, pp. 2483-2493.

Raclavská, H., Corsaro, A., Hartmann-Koval, S. and Juchelková, D. (2017). Enrichment and distribution of 24 elements within the sub-sieve particle size distribution ranges of fly ash from wastes incinerator plants. *Journal of Environmental Management*, 203, pp. 1169-1177.

Rönkkömäki, H., Pöykiö, R., Nurmesniemi, H., Popov, K., Merisalu, E., Tuomi, T. and Välimäki, I. (2008). Particle size distribution and dissolution properties of metals in cyclone fly ash. *International Journal of Environmental Science*, 5(4), pp. 485-494.

Saikia, N., Kato, S. and Kojima, T. (2007). Production of cement clinkers from municipal solid waste incineration (MSWI) fly ash. *Waste Management*, 27(9), pp. 1178-1189.

Saqib, N. and Bäckström, M. (2016). Chemical association and mobility of trace elements in 13 different fuel incineration fly ashes. *Fue*l, 165, pp. 193-204.

Standards Czech (2003). *Characterisation of waste - Leaching - Compliance test for leaching of granular waste materials and sludges - Part 2: One stage batch test at a liquid to solid ratio of 10 I/kg for materials with particle size below 4 mm (without or with size reduction)*, CSN EN 12457-2:2003 (83 8005), Czech Standard.

Standards Czech (2007). *Characterization of waste and soil - Determination of elemental composition by X-ray fluorescence*, CSN EN 15309, Czech Standard.

Takaoka, M., Yamamoto, T., Tanaka, T., Takeda, N., Oshita, K. and Uruga, T. (2005). Direct Speciation of Lead, Zinc and Antimony in Fly Ash from Waste Treatment Facilities by XAFS spectroscopy. *Physica Scripta*, T115, pp. 943-954.

Wang, K.-S., Sun, C.-J. and Yeh, C.-C. (2002). The thermotreatment of MSW incinerator fly ash for use as an aggregate: a study of the characteristics of size-fractioning. *Resources, Conservation and Recycling*, 35(3), pp. 177-190.

Wang, L., Jin, Y., Nie, Y. and Li, R. (2010). Recycling of municipal solid waste incineration fly ash for ordinary Portland cement production: A real-scale test. *Resources, Conservation and Recycling*, 54, (12), pp. 1428-1435.

Yao, Z.T., Ji, X.S., Sarker, P.K., Tang, J.H., Ge, L.Q., Xia, M.S. and Xi, Y.Q. (2015). A comprehensive review on the applications of coal fly ash. *Earth-Science Reviews*, 141, pp. 105-121.

Ye, M., Li, G., Yan, P., Zheng, L., Sun, S., Huang, S., Li, H., Chen, Y., Yang, L. and Huang, J. (2017). Production of lead concentrate from bioleached residue tailings by brine leaching followed by sulfide precipitation. *Separation and Purification Technology*, 183, pp. 366-372.

Zhou, J., Wu, S., Pan, Y., Zhang, L., Cao, Z., Zhang, X., Yonemochi, S., Hosono, S., Wang, Y., Oh, K. and Qian, G. (2015). Enrichment of heavy metals in fine particles of municipal solid waste incinerator (MSWI) fly ash and associated health risk. *Waste Management*, 43, pp. 239-246.

Evaluation quality parameters of DEM generated with low-cost UAV photogrammetry and Structure-from-Motion (SfM) approach for topographic surveying of small areas

***Peter Blistan*[1], *Ľudovít Kovanič*[1], *Matej Patera*[1] *and* *Tomáš Hurčík*[1]**

Conventional geodetic methods and instruments such as total station, or GNSS, are commonly used for geodetic surveying of the ground surface. In recent years, with the development of drones - light Unmanned Aerial Vehicles (UAV) and their combination with a digital camera, opens new opportunities in the field of Earth's surface documentation. This combination of technologies made it possible to use digital photogrammetry to quickly and operatively document the Earth's surface. Using UAV photogrammetry, we can create an accurate and detailed surface model. The surface model can be created as GRID, TIN, respectively as a cloud of points, generated by processing aerial survey images in some processing software, for example, Agisoft Photoscan®. Its accuracy depends essentially on two sets of factors. One group are factors that depend on camera parameters, image flight and LMS processing. The second group consists of factors that influence the accuracy of the model - they depend on the modelling method used and the number of points used to create the terrain model. The research presented in this paper aims to analyze the accuracy of digital elevation models (DEM) created from a various dense cloud of points, obtained using low-cost UAV photogrammetry. The aim was to define - determine the relationship between the number of points entering the modelling and the accuracy of the terrain model obtained from the gradually diluted point-clouds. Quarry Jastrabá in the Slovak Republic was chosen as a representative tested area. The terrain in the quarry has a morphologically indented surface and is thus suitable for verifying the functional dependence between the number of points and the quality - the accuracy of the resulting model. The results show that it is possible to identify the relationship between the number of points used to create a terrain model and the accuracy of the model. This article aims to present the UAV utility for surface documentation and DEM creation. This article addresses the accuracy of the DEM and the optimum amount of points needed to generate it.

Keywords: *UAV, photogrammetry, structure from motion, DEM, point-cloud, GCP, regression analysis, RMSE.*

1. Introduction

During geodetic activities, we often encounter a requirement for surface landscape documentation to create a digital model (DEM). The documentation of the terrain is usually acquired by classical geodetic methods and instruments like GNSS or total stations (TS). In large areas, this process is laborious and slow. As a product of geodetic measurements carried out for documentation of the terrain, a file with X, Y, Z coordinates is obtained (Kovanic et al., 2013). As a result, DEM is usually created and evaluated. Its quality depends directly on the accuracy of the devices and methods used and mainly on the number of measured points. To achieve a precise and detailed surface model, it is necessary to survey more points on the terrain. This process is time-consuming, and nevertheless, we will not achieve the detail and quality of the surface model obtained, for example, terrestrial laser scanning (TLS), LIDAR (Moudry et al., 2019) or photogrammetry approach. Mentioned methods are known as non-selective. Their primary product is the dense point-cloud, which is subsequently processed. For the large ground mapping, mainly the aerial photogrammetry is particularly relevant.

With regard to the obtained results, it is likely the most appropriate equivalent of laser scanning. The current trend in photogrammetry is the use of unmanned aerial vehicles - UAV (Zhang and Elaksher, 2011). UAV photogrammetry is a cheap and in specific conditions accurate method of the surface documentation to create topographic maps and DEM (Colomina and Molina, 2014, Remondino et al., 2011, Neitzel and Klonowski, 2011).

UAV utilization and use of SfM brings benefits in several geosciences. E.g. in mining (Xiang et al., 2018), (Kovanic et al., 2017), (Blistan et al., 2016), (Fraštia et al. 2019), (Frastia, 2005), (Pukanska et al. 2014), (Vegsoova et al. 2019a), (Vegsoova et al. 2019b), potholing (Pukanska et al. 2017), structural geology (Fleming Zachariah et al., 2018), The use of UAVs for steep slope documentation is presented in this work (Agüera-Vega et al., 2018), Monitoring and stability of slopes and landslides (Yu et al., 2018), (Ardi et al., 2018), (Rossi et al., 2018), The accuracy and evaluation of DEM is addressed (Goetz et al., 2018), (Kršák et al., 2016), (Mali et al., 2018), (Polat et al., 2018) or 3D reconstruction techniques and SfM – (Carrivick et al., 2016), (Bartos et al., 2017) etc.

[1] *Peter Blišťan, Ľudovít Kovanič, Matej Patera, Tomáš Hurčík,* Institute of Geodesy, Cartography and GIS, BERG Faculty, Technical University of Kosice, Park Komenského 19, 04384, Kosice, Slovak Republic, *peter.blistan@tuke.sk*

UAVs (Fig. 2) offer simple control using special software - control software (Siebert and Teizer, 2014). It includes the UAV itself, as well as the control centre on the ground (Mozas-Calvache et al., 2012). Working with the UAV, apart from the flight itself, involves many activities (Shahbazi et al., 2015). The mapping workflow consists of the definition of the preparatory phase, the flight planning, the autonomous flight, the quality check of the data and the data processing. It is appropriate to use the GCP for the georeferencing of the model. Determination of coordinates on GCP can be done from the optimized coordinate network (Štroner et al., 2017), where the systematic errors are maximally suppressed (Braun et al., 2015). The final data products are elevation models, orthoimages, 3D models (Eisenbeiss, 2011; Nex and Remondino, 2013). The general workflow for UAV data acquisition and processing is in Figure 3.

Inexpensive UAV carriers are currently available. In terms of price-performance ratio, they are an interesting solution for reducing the incurred costs. Their main drawbacks are inferior quality compact cameras, which are used due to their low weight mainly with cheap and smaller UAV´s. In our research, we focus on verifying the quality of the DEM surface of the quarry obtained by photogrammetry using a low-cost UAV. This problem deals with many works (Fritz et al., 2013; Niranjan et al., 2007; Moudry et al., 2019; Urban et al., 2018). The benefit of this article is the analysis of the quality of the model in terms of the minimum (or optimal) amount of points needed to its generation. We can prove that the precision of the surface model created by low-cost UAVphotogrammetry meets the required accuracy criterion and the models thus obtained should be considerably cheaper, reliable and more detailed than DEM created from points using GNSS or LIDAR.

2. Material and Methods

2.1. Study area

As the area of interest for testing and evaluation of the quality of the DEM obtained by UAV photogrammetry, the quarry site Jastrabá near Žiar nad Hronom in Slovakia was chosen (Figure 1). In this quarry, the excavation of perlite is starting at present. The terrain relief in the quarry is unstable and morphologically rugged. Therefore the standard geodetic measurements are complicated. In the direction of the slope of the terrain, there are numerous furrows formed by flowing water during heavy rainfalls. These furrows are on average 15-20cm deep, but some reach a depth of 50 cm (Figure 1). This terrain is interesting for its complexity and its difficulty documentation using GNSS or TS. The detailed surveying of the entire surface of the quarry with the focus at least the deepest furrows would be time-consuming, and the resulting model would not be able to its true shape capture in necessary detail. Surveying all the smaller terrain features (about 15cm deep) is practically not possible. This quarry was chosen due to the occurrence of different surface types – flat (smooth) and rough.

Fig. 1. Area of interest – quarry Jastrabá

2.2. Methods and equipment

The low-cost UAV DJI Phantom 4 (Fig. 2 and Table 1) was used for the photogrammetric measurement. The flight was conducted in 6 airstrips in height 30 m above the average terrain level (Figure 4). During the flight, 178 images were taken. Longitudinal and lateral image overlap was set to 80%. For the transformation of the frame block into the S-JTSK coordinate system used in the Slovak republic, ten ground control points (GCP) were used. Their coordinates were determined terrestrially by the total station Leica TS 02 using the spatial polar method. Local coordinates were transformed by congruent transformation on connecting points determined by GNSS method. Leica GPS 900 instrument with differential RTN corrections was used. Consequently, the absolute horizontal and vertical RMSE were up to ± 20mm and ±40mm. Relative (inner) spatial RMSE of the GCPs was up to ± 5mm.

Tab. 1. DJI Phantom 4 – technical parameters.

Aircraft	
Weight (Battery & Propellers included):	1380g
Max Ascent / Descent Speed:	6m/s / 4m/s
Max Flight Speed:	20m/s
Max. flight time:	28 min.
Camera	
Operating Environment Temperature:	0℃-40℃
Sensor size:	1/2.3"
Effective Pixels:	12 Megapixels
Focal length	20mm
FOV	94°
Resolution:	4000×3000
Gimbal pitch	-90° to +30°
Remote Control	
Communication Distance (open area):	CE Compliant: 3,5km; FCC Compliant: 5km

Fig. 2. UAV – DJI Phantom 4

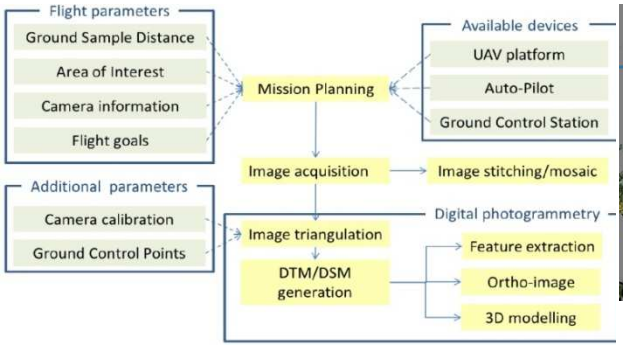

Fig. 3. Workflow for UAV data acquisition and processing (Nex and Remondino, 2013).

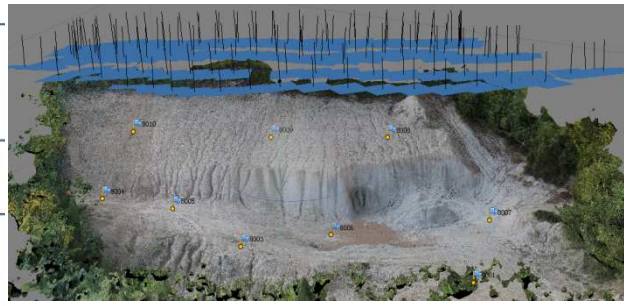

Fig. 4. Terrain model with the position of images and GCP

Processing of the images was performed by the photogrammetric software Agisoft PhotoScan® using the Structure from Motion method. Parameters of image alignment were set to highest with generic preselection of the images. Key point limit value was set to 40000. RMSE value on GCP´s before optimization was 55mm and 33 after the optimization. Value of residuals on control points was 45mm. GSD is 10mm / pixel. Dense cloud generation parameters were set to high quality with mild depth filtering to maintain high detail. In whole locality, 22 million points were generated. While processing, the ground extraction was performed to maintain surface details and the sufficient number of morphology points on the terrain.

Digital elevation model (DEM)

The Digital Elevation Model (DEM) is most often formed by a triangular network generated between directly or indirectly surveyed points, for example, photogrammetric measurement (Chen and Yue, 2010). DEM created from geodetic measurements is usually presented in the form of a wire model with a triangular structure,

and in the case of DEM created from photogrammetric measurements, this wire model is complemented by a photorealistic texture. Using photorealistic texture creates almost perfect digital copies of the real world.

The quality of DEM depends on the density of the input data, the accuracy of the geodetic method used to collect the data, and the selection of the interpolation method used to generate it (Song and Nan, 2009; Hurst, 2014).

Several methods are used to generate DEM. Delaunay triangulation belongs to the simplest ones. Delaunay triangulation as a duality to the Voronoi diagram is based on the definition that each cell of the Voronoi diagram contains one point from the set. The sides of the cell located exactly halfway between the Pi and Pj points of the two adjacent cells represent the axis perpendicular to the triangulation edge, can be seen in Figure 5. In other words, by joining two neighbouring Voronoi cells, we get the Delaunay triangulation edge. In each dimension, intertwined orthogonality applies (George and Borouchaki, 1998).

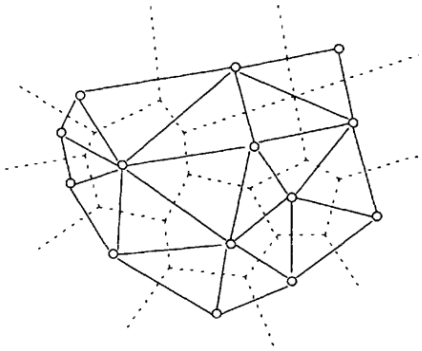

Fig.5. Delaunay triangulation(George and Borouchaki, 1998).

Point clouds preparation

Images obtained by aerial photogrammetry were fully processed by Agisoft PhotoScan®. Obtained dense point-cloud was exported. 3D model of the area of the whole quarry and the nearest surroundings was obtained (Fig. 4). Objects such as vegetation and air points were filtered using ground extraction in Trimble RealWorks® software. Subsequently, the area of interest was cropped by the polygonal fence to create a final selection for further processing. The whole cut out was named as General surface - 1500m^2 with dimensions of approximately 50 x 25m. This area was divided into two smaller parts having different morphometric characteristics. One part was less rugged, flat and was named as Flat (smooth) surface - 700m^2. The second, more rugged area was named Rough surface 350m^2 (Fig. 6). The preparatory work thus resulted in three point-clouds in separated files.

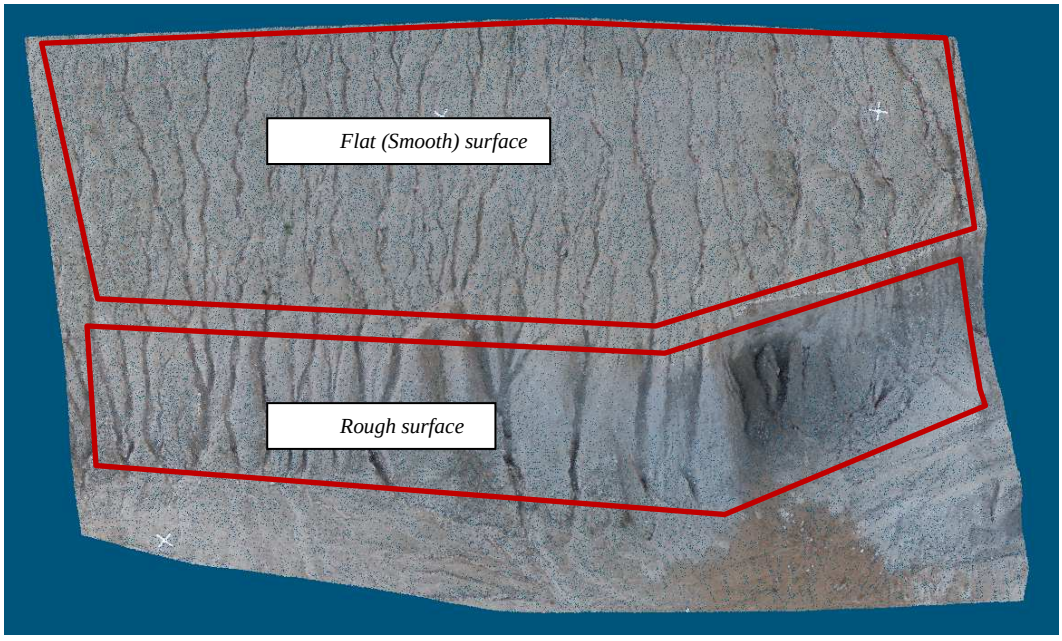

Fig.6. Dividing of the surfaces

The next step was the gradual dilution of point-clouds. The original dense point-clouds were spatially filtered using Trimble RealWorks®. The density of the points was gradually decreased over a range density from 5cm to 100cm. In this range, separate sets were created. Point-clouds with an interval of density dilution of 5 cm were obtained. For a distance between points from 1 m to 5 m, the interval of density dilution was 1 m. Examples of point-clouds are shown in fig. 7. Statistical parameters of generated point-clouds as the number of points per $1m^2$ area for individual areas are shown in Table 2.

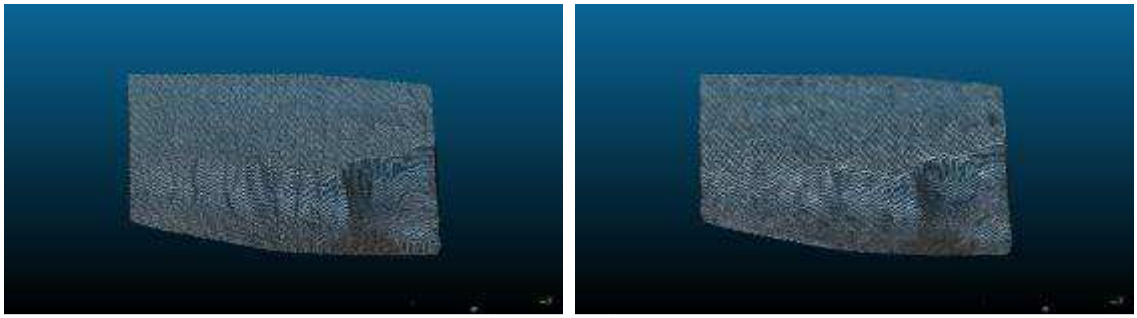

Fig.7. Examples of the spatially filtered point-clouds

The original cloud without spatial filtration was chosen as the reference. Mesh surfaces for these point-clouds were generated. The created models contained 1 218 667 points for the General area, 333 857 points for the Flat part and 473 212 points for the Rough part.

Comparing each set of points with the corresponding reference surface, their distances were determined. The CloudCompare v. 2.10.2 software was used. The shortest distances of each point of the compared set to the local mesh model of the reference surface were determined. The total RMSE of the individual files from the reference model is expressed in Tab. 2.

On fig. 8 (a) to (j), the calculated surface differences for the General area are shown graphically. Because of a large number of files, only selected files corresponding to the distance between points are listed. On fig. a) – 5 cm, b) – 20 cm, c) – 40 cm, d) – 60 cm, e) – 80 cm, f) – 100 cm, g) – 200 cm, h) – 300 cm, i) – 400 cm, j) – 500 cm. Similarly, fig. 9 and fig. 10 shows differences for Flat and Rough surfaces. They are displayed according to the same colour scale. The highest differences are approaching to the red colour.

Tab. 2: Statistics of the point-clouds and calculated parameters

	General surface			*Flat surface*			*Rough surface*		
Distance between points (m)	*Number of points*	*Number of points per 1m²*	*RMSE (m)*	*Number of points*	*Number of points per 1m²*	*RMSE (m)*	*Number of points*	*Number of points per 1m²*	*RMSE (m)*
Dense point-cloud	*1 218 667*	*870*	-	*333 857*	*742*	-	*473 212*	*1121*	-
0,05	*374 587*	*268*	*0,009*	*110 021*	*245*	*0,008*	*136 700*	*324*	*0,011*
0,1	*114 924*	*83*	*0,010*	*34 305*	*77*	*0,008*	*41 353*	*100*	*0,013*
0,15	*55 548*	*40*	*0,012*	*16 951*	*38*	*0,008*	*20 051*	*48*	*0,014*
0,2	*33 138*	*24*	*0,014*	*9 786*	*22*	*0,008*	*11 761*	*28*	*0,014*
0,25	*21 468*	*16*	*0,013*	*6 529*	*15*	*0,009*	*7 691*	*19*	*0,014*
0,3	*15 117*	*11*	*0,013*	*4 663*	*11*	*0,009*	*5 479*	*13*	*0,017*
0,35	*11 381*	*9*	*0,013*	*3 509*	*8*	*0,010*	*4 162*	*10*	*0,018*
0,4	*8 920*	*7*	*0,014*	*2 637*	*6*	*0,010*	*3 154*	*8*	*0,018*
0,45	*7 195*	*6*	*0,016*	*2 118*	*5*	*0,011*	*2 490*	*6*	*0,020*
0,5	*5 700*	*5*	*0,017*	*1 740*	*4*	*0,012*	*2 040*	*5*	*0,023*
0,55	*4 714*	*4*	*0,020*	*1 448*	*4*	*0,013*	*1 687*	*4*	*0,024*
0,6	*3 990*	*3*	*0,021*	*1 239*	*3*	*0,013*	*1 442*	*4*	*0,025*
0,65	*3 442*	*3*	*0,022*	*1 087*	*3*	*0,014*	*1 235*	*3*	*0,028*
0,7	*2 981*	*3*	*0,022*	*949*	*3*	*0,015*	*1 090*	*3*	*0,031*
0,75	*2 607*	*2*	*0,025*	*802*	*2*	*0,015*	*954*	*3*	*0,033*
0,8	*2 320*	*2*	*0,027*	*692*	*2*	*0,016*	*834*	*2*	*0,032*
0,85	*2 089*	*2*	*0,027*	*618*	*2*	*0,018*	*734*	*2*	*0,034*
0,9	*1 903*	*2*	*0,028*	*564*	*2*	*0,018*	*654*	*2*	*0,037*
0,95	*1 669*	*2*	*0,030*	*502*	*2*	*0,019*	*578*	*2*	*0,039*
1	*1 492*	*2*	*0,031*	*464*	*2*	*0,019*	*523*	*2*	*0,044*
2	*383*	*1*	*0,063*	*123*	*1*	*0,023*	*145*	*1*	*0,074*
3	*175*	*1*	*0,112*	*58*	*1*	*0,033*	*69*	*1*	*0,126*
4	*102*	*1*	*0,140*	*35*	*1*	*0,045*	*36*	*1*	*0,168*
5	*66*	*1*	*0,192*	*23*	*1*	*0,058*	*26*	*1*	*0,225*

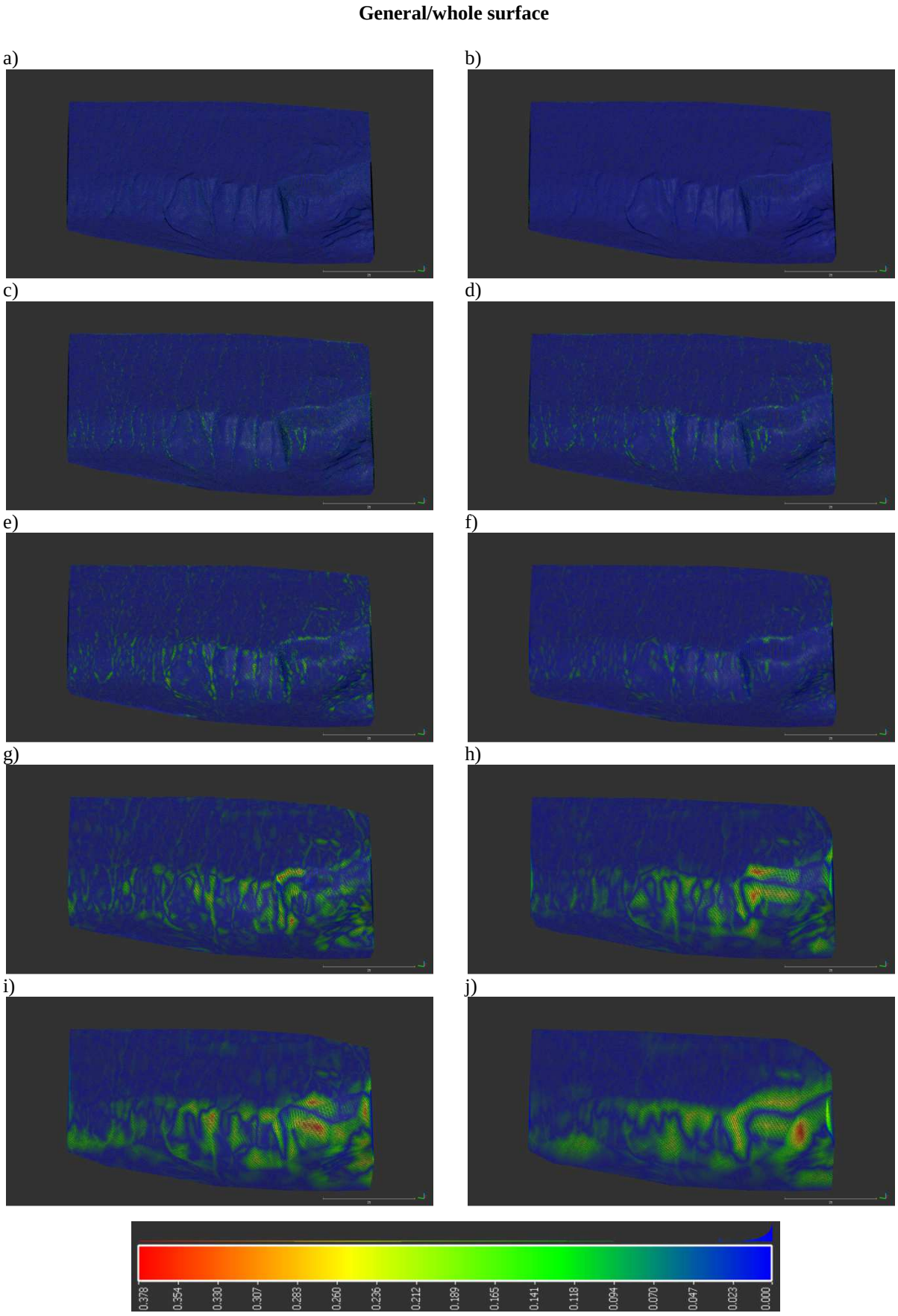

Fig. 8: Differences of the compared point-cloud to the reference model – General surface

Flat/smooth surface

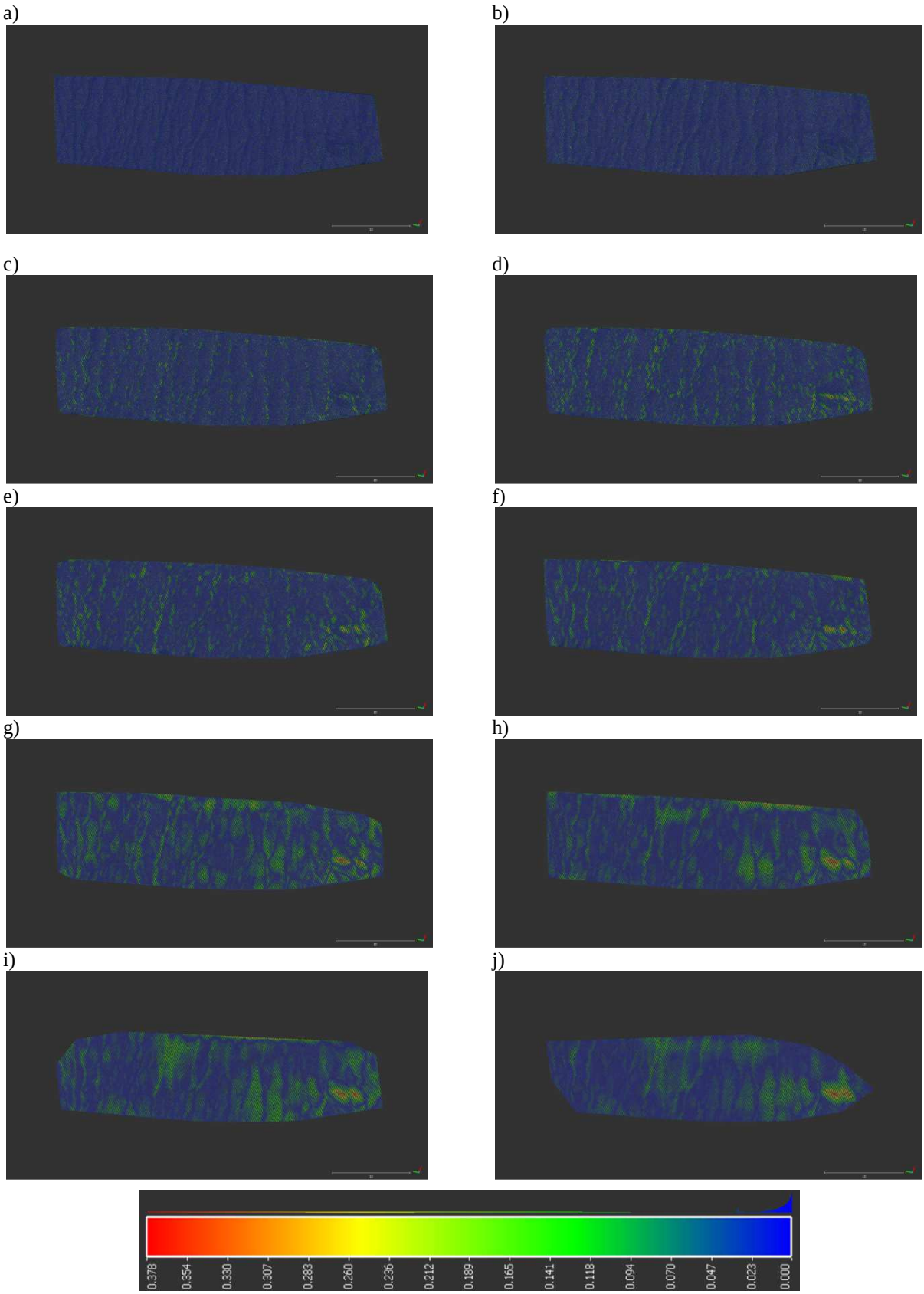

Fig. 9: Differences of the compared point-cloud to the reference model – Flat surface

Rough surface

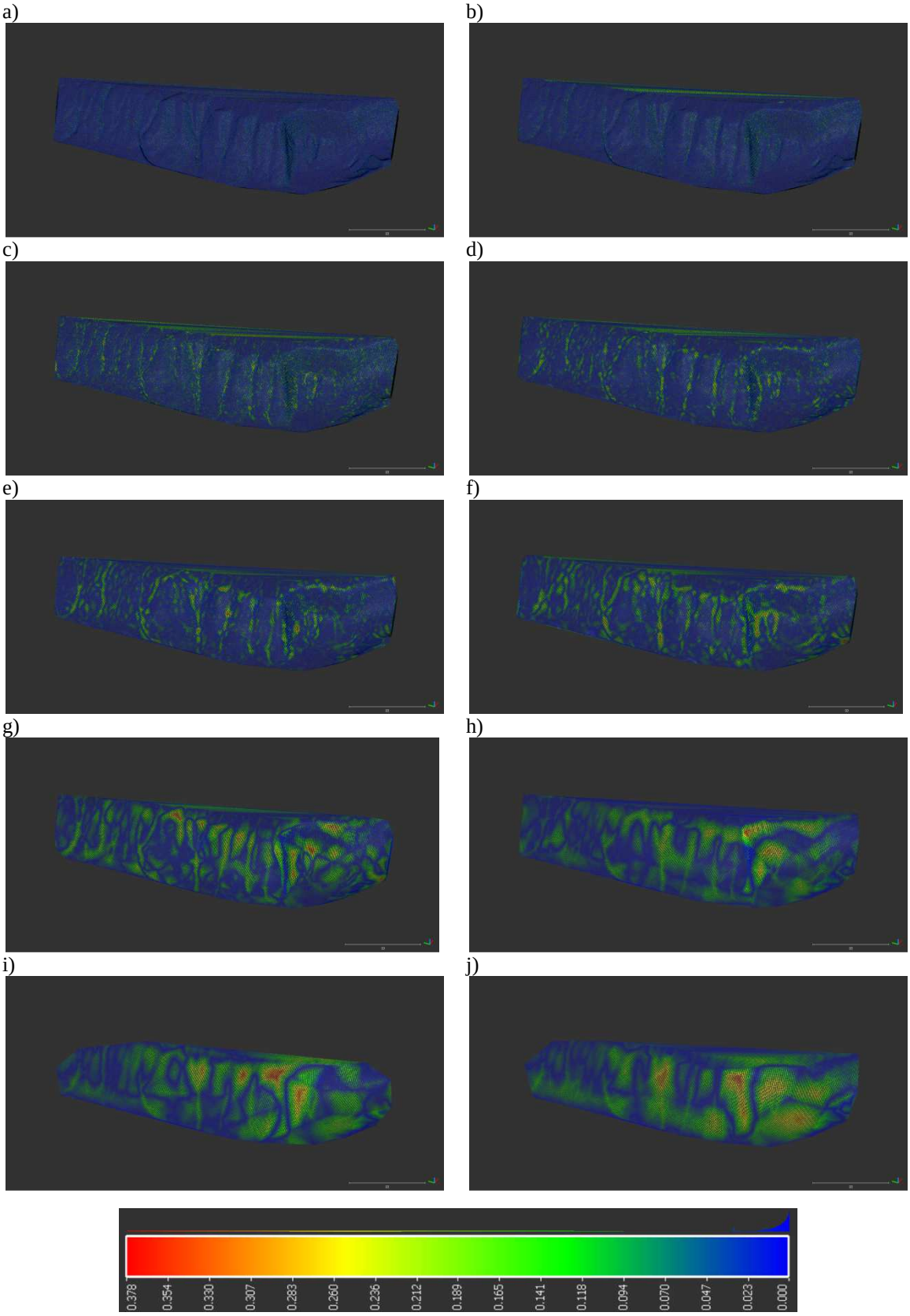

Fig. 10: Differences of the compared point-cloud to the reference model – Rough surface

Results and discussion

Regression and correlation analysis

Several mathematical functions were used during processing. However, polynomial functions have proved to be most suitable for the dependence of point distance and standard deviation and the power function for the point distance and number of points per unit area.

Polynomial function: $f(x) = \alpha + \beta.x + \gamma.y^2 + \delta.x^3 + ...$
Power function: $f(x) = n.x^{-a}$

Functional dependence and the degree of functional dependence for individual surface types were calculated using regression and correlation analysis. A polynomial function preferably approximates the dependency between variables. The regression model equations describe the investigated relationship between point distance (point density) and RMSE. The degree of dependence between the analyzed parameters and the modelled function is described by the Pearson coefficient. Based on the polynomial function, an increasing dependence is described where, with increasing distance between points (gradual dilution of points in the cloud, according to Table 2), the value of the RMSE increases. The RMSE results from the result of comparing two clouds against each other, the original with all points and the gradually diluted clouds. As the distance between the points increases, the standard deviation also increases, and thus the accuracy of the modelled object decreases. The values are shown in Tab. 2.

The correlation coefficient R^2 compares the estimated and actual values and reaches values ranging from 0 to 1. In the case of a value of 1, there is a strong correlation (100%) between the estimated and actual values and vice versa. Concerning the results of the regression and correlation analysis, functions describing the dependence between the above parameters, which were burdened with measurement errors, processing errors and random factors, were determined during measurement and processing. Using the computed values with modelling of the determined functions, the resulting graph can be used to determine the number of points per surface area regarding the required accuracy and character of the measured area. Tab. 3 shows the regression curve equations and calculated correlation coefficients separately for all surfaces and the selected maximum distance between points up to 5m and up to 1m. The graphs also show the values determined in the tab. 2. In the graphs on fig. 11 and 12, these dependencies are indicated as follows (values rise from zero values from left to right):
- General/whole: blue
- Smooth/flat: orange
- Rough/rugged: grey.

Tab. 3: Coefficients of polynomial functions and correlation coefficients obtained by regression and correlation analysis of individual surfaces.

- Distance between points: $x \leq 5$**m**:

Surface	**Regression model**	**Adjusted R^2**
General/whole	$y = 0{,}0026x^2 + 0{,}0241x + 0{,}0058$	$R^2 = 0{,}9964$
Flat/smooth	$y = 0{,}0028x^2 + 0{,}0293x + 0{,}008$	$R^2 = 0{,}9988$
Rough	$y = 0{,}0002x^2 + 0{,}0087x + 0{,}0079$	$R^2 = 0{,}9836$

- Distance between points: $x \leq 1$**m**:

Surface	**Regression model**	**Adjusted R^2**
General/whole	$y = 0{,}0098x^2 + 0{,}0131x + 0{,}0088$	$R^2 = 0{,}9810$
Flat/smooth	$y = 0{,}016x^2 + 0{,}0158x + 0{,}0104$	$R^2 = 0{,}9873$
Rough	$y = 0{,}0053x^2 + 0{,}0075x + 0{,}0069$	$R^2 = 0{,}9905$

Using the same method, the functional relations between the point distance (point density) and the number of points per unit area were determined. The power function best approximates this curve. Results are shown in the tab. 4 and on the graphs on fig. 11 and 12 are shown by the black curve.

Tab. 4: Coefficients of power functions and correlation coefficients obtained by regression and correlation analysis for General surface.

- Distance between points: $x \leq 5$**m**:

Surface	**Regression model**	**Adjusted R^2**
General/whole	$y = 1{,}0425x^{-1{,}869}$	$R^2 = 0{,}9996$

- Distance between points: $x \leq 1$**m**:

Surface	**Regression model**	**Adjusted R^2**
General/whole	$y = 1{,}1129x^{-1{,}865}$	$R^2 = 0{,}9994.$

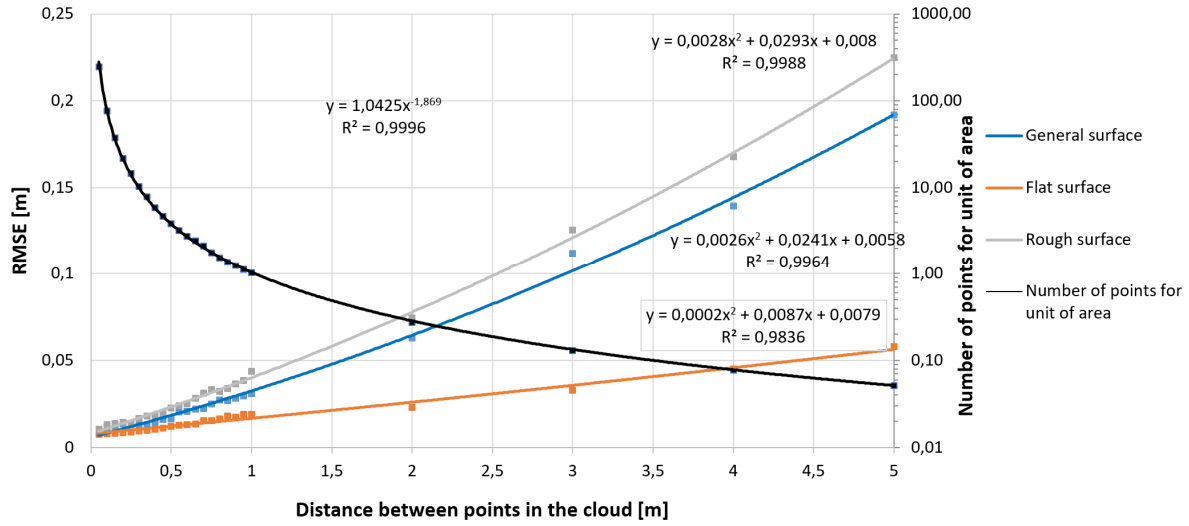

Fig. 11: Graphical representation of regression functions for individual terrain models - a distance of points up to 5m

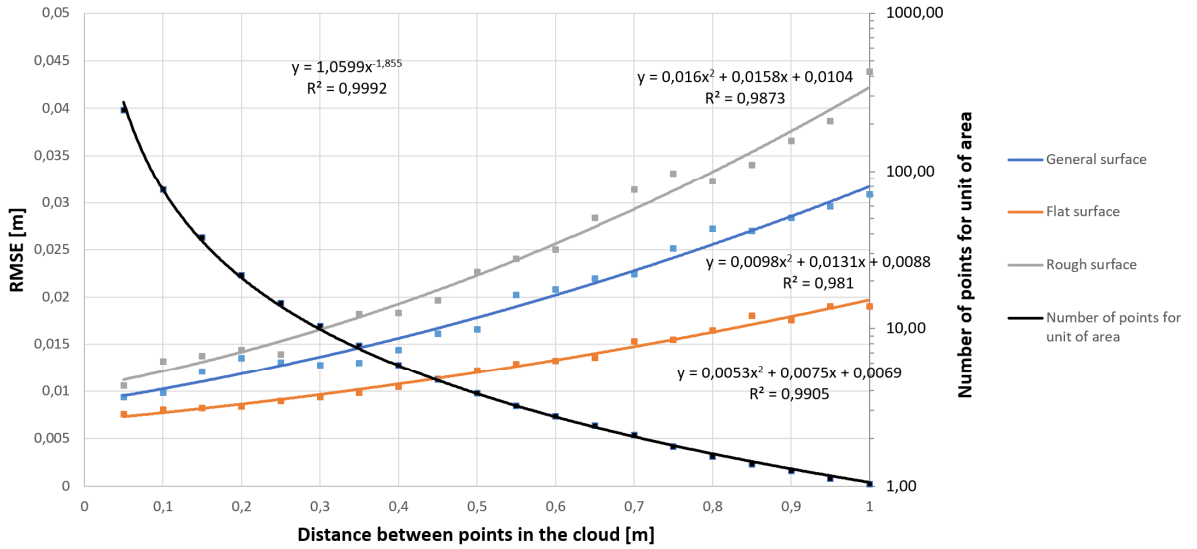

Fig. 12: Graphical representation of regression functions for individual terrain models - a distance of points up to 1m

Based on measured and processed data in the form of evaluation of their functional dependencies, we can obtain two types of functions between three variables (accuracy, the distance between points, number of points per area unit), which are connected by functional links. When solving the accuracy of a model we can determine before measuring how exactly, in terms of the number of points and their distance from each other, we have to survey

the given surface to achieve the necessary modelling accuracy. Such a procedure can be used in practice, for example, in aerial photogrammetry, laser scanning, classical geodetic measurement, where the required density of points in mapping will be determined based on our results.

Analytical solution of the dependence of model quality on the number of points

Fig. 11 and 12 are graphical representations of regression functions expressing the quality of the terrain model as a function of the number of points used to their modelling. The nomograms in Fig. 13 and 14 express the dependence of the accuracy of the terrain model on the amount of input data. In practice, nomograms can be used for:

- determining the minimum number of points per unit area for required model accuracy
- determination of the minimum mutual distance of points for required model accuracy and vice versa
- determination of the standard deviation of the model at a known number of measured points per unit area
- determination of the standard deviation of the model at a known distance between the measured points

Figures 13 and 14 show examples of the use of the nomogram for each model. The colours of the arrows correspond to the colours of the surfaces. Based on the predetermined maximum value of the standard deviation for the design and modelling, we draw a horizontal line from the RMSE scale to the curve of the area under consideration (for example, grey – rough surface). When intersecting the approximation curve of a given surface, the line from the intersection point runs vertically to the scale "Distance between points in the cloud (m)". Finally, we place the horizontal line again from the point of intersection of the power curve (black) to the scale "Points per unit area". In this way, we get an indication of the number of points needed to achieve a given accuracy. Reciprocally, if we know the number of points per unit area in an existing cloud and we assume the type of surface we can determine the expected RMSE. The third way of using the nomogram is if we know the distance of points in the existing cloud as an input parameter. Then it is possible to derive RMSE from the nomogram.

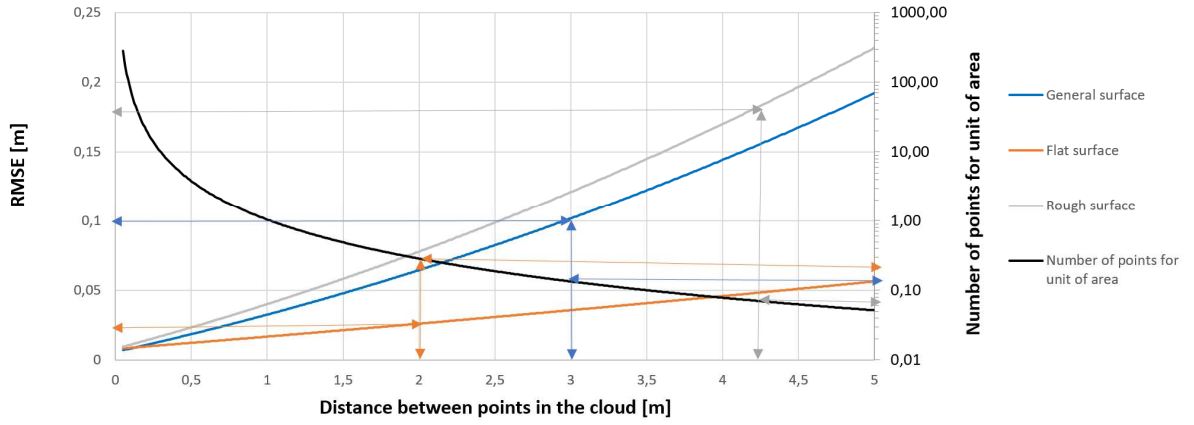

Fig.13: Functional dependence between model quality and number of points used for its creation - a distance of points up to 5m

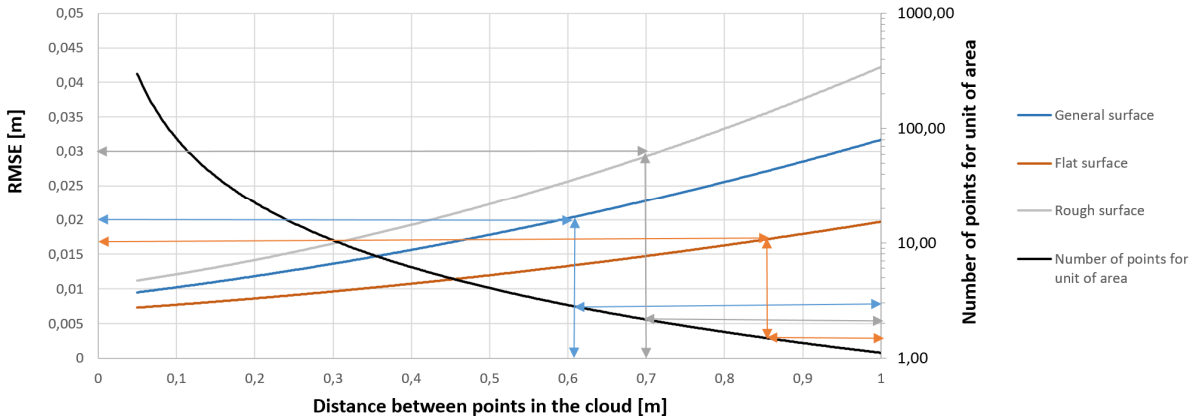

Fig.14: Functional dependence between model quality and number of points used for its creation - a distance of points up to 1m

Conclusion

Using the regression and correlation analysis, the most suitable regression functions for describing the quality of the terrain model at the representative locality Jastrabá estimated. The locality is specific in that it was possible to allocate two types of surfaces - rough and flat. The correlation and regression analysis determines the dependence between the distance of points and the standard deviation expressing the quality of the resulting model. The dependence between the number of points per unit area and the standard deviation expressing the quality of the resulting model was also determined.

Nomograms were created from regression models expressing the functional dependence between the quality of the model and the number of points used for its creation. Nomograms were created for three types of surfaces - rough, flat and general. A nomogram with a mutual distance of points up to 5m can be used for common geodetic measurements using TS or GNSS. The nomogram with the mutual distance of points to 1m can be used for terrestrial or UAV laser scanning or UAV photogrammetry.

Acknowledgement: *This work was supported by project SKHU/1601/4.1/187, by the Scientific Grant Agency of the Slovak Republic (VEGA – MŠVVaŠ SR) through the project. No. 1/0844/18 and the Cultural and Educational Grant Agency of the Slovak Republic (KEGA – MŠVVaŠ SR) through the project. No. 004TUKE-4/2019.*

References

Agüera-Vega, F., Carvajal-Ramírez, F., Martínez-Carricondo, P., Sánchez-Hermosilla López, J., Mesas-Carrascosa, F. J., García-Ferrer, A., & Pérez-Porras, F. J. (2018). Reconstruction of extreme topography from UAV structure from motion photogrammetry. *Measurement: Journal of the International Measurement Confederation, 121*, 127-138. doi:10.1016/j.measurement.2018.02.062

Ardi, N. D., Iryanti, M., Asmoro, C. P., Nurhayati, N., & Agustine, E. (2018). Mapping landslide potential area using fault fracture density analysis on unmanned aerial vehicle (UAV) image. Paper presented at the *IOP Conference Series: Earth and Environmental Science, , 145*(1) doi:10.1088/1755-1315/145/1/012010

Bartos, K., Pukanska, K., Repan, P., Ksenak, L., Sabova, J. (2019) Modelling the Surface of Racing Vessel's Hull by Laser Scanning and Digital Photogrammetry. *REMOTE SENSING*, Vol. 11 (13), DOI: 10.3390/rs11131526

Blistan, P., Kovanič, Ľ., Zelizňaková, V., & Palková, J. (2016). Using UAV photogrammetry to document rock outcrops. *Acta Montanistica Slovaca, 21*(2), 154-161

Braun, J., Štroner, M., Urban, R., & Dvořáček, F. (2015). Suppression of systematic errors of electronic distance meters for measurement of short distances. *Sensors (Switzerland), 15*(8), 19264-19301. doi:10.3390/s150819264

Colomina, I. and Molina, P. (2014) Unmanned aerial systems for photogrammetry and remote sensing: A review, *ISPRS Journal of Photogrammetry and Remote Sensing, Volume 92, Pages 79–97, 2014*.

Eisenbeiss, H. (2011) The Potential of Unmanned Aerial Vehicles for Mapping, Photogrammetrische Woche 2011, Dieter Fritsch (Ed.), Wichmann Verlag, Heidelberg, pp. 135-145

Fraštia, Marek - Liščák, Pavel - Žilka, Andrej - Pauditš, Peter - Bobáľ, Peter - Hronček, Stano - Sipina, Slavomír - Ihring, Pavol - Marčiš, Marián. Mapping of debris flows by the morphometric analysis of DTM: a case study of the Vrátna dolina Valley, Slovakia. In Geografický časopis. Vol. 71, no. 2 (2019), s. 101-120. ISSN 0016-7193

Fraštia, Marek. Possibilities of using inexpensive digital cameras in applications of close-range photogrammetry. In Slovak Journal of Civil Engineering. Vol. 13, No. 2 (2005), s.20-28. ISSN 1210-3896.

Fleming Zachariah, D., & Pavlis Terry, L. (2018). An orientation based correction method for SfM-MVS point clouds—Implications for field geology. *Journal of Structural Geology, 113*, 76-89. doi:10.1016/j.jsg.2018.05.014

Fritz, A., Kattenborn, T. and Koch, B. (2013) UAV-based photogrammetric point clouds - tree stem mapping in open stands in comparison to terrestrial laser scanner point clouds, International Archives of the Photogrammetry, Remote Sensing and Spatial Information Sciences, Volume XL-1/W2, 2013, UAV-g 2013, 4 – 6 September 2013, Rostock, Germany

George, P. and Borouchaki, H. (1998) Delaunay Triangulation and Meshing. Application to Finite Elements. Editions Hermes, Paris, 1998

Goetz, J., Brenning, A., Marcer, M., & Bodin, X. (2018). Modeling the precision of structure-from-motion multi-view stereo digital elevation models from repeated close-range aerial surveys. *Remote Sensing of Environment, 210*, 208-216. doi:10.1016/j.rse.2018.03.013

Hurst, P.J. (2014) A Comparison of Interpolation Methods for Estimating Mountaintop Removal, (2014), Directed by Dr. Rick L. Bunch, pp 86

Chen, C. and Yue, T. (2010) A method of DEM construction and related error analysis. Computers & Geosciences , 36, (2010), pp 717-725

Kovanič, L. (2013). Possibilities of terrestrial laser scanning method in monitoring of shape deformation in mining plants. [Mozliwości wykorzystania naziemnego skaningu laserowego w monitorowaniu deformacji w zakładach górniczych] *Inzynieria Mineralna, 14*(1), 29-41

Kovanič, Ľ., Blišťan, P., Zelizňaková, V., & Palková, J. (2017). *Surveying of open pit mine using low-cost aerial photogrammetry* doi:10.1007/978-3-319-45123-7_9

Kršák, B., Blišťan, P., Pauliková, A., Puškárová, P., Kovanič, L., Palková, J., & Zelizňaková, V. (2016). Use of low-cost UAV photogrammetry to analyze the accuracy of a digital elevation model in a case study. *Measurement: Journal of the International Measurement Confederation, 91*, 276-287. doi:10.1016/j.measurement.2016.05.028

Mali, V. K., & Kuiry, S. N. (2018). Assessing the accuracy of high-resolution topographic data generated using freely available packages based on SfM-MVS approach. *Measurement: Journal of the International Measurement Confederation, 124*, 338-350. doi:10.1016/j.measurement.2018.04.04

Moudry, V., Gdulova, K., Fogl, M., Klapste, P., Urban, R., Komarek, J., Moudra, L., Štroner, M., Bartak, V., Solsky, M. (2019). Comparison of leaf-off and leaf-on combined UAV imagery and airborne LiDAR for assessment of a post-mining site terrain and vegetation structure: Prospects for monitoring hazards and restoration success, *APPLIED GEOGRAPHY*, Vol. 104, 32-41 DOI: 10.1016/j.apgeog.2019.02.002

Moudry, V., Urban, R., Stroner, M., Komarek, J., Broucek, J., Prosek, J. (2019). Comparison of a commercial and home-assembled fixed-wing UAV for terrain mapping of a post-mining site under leaf-off conditions, *INTERNATIONAL JOURNAL OF REMOTE SENSING*,Vol. 40 (2), 555-572, DOI:10.1080/01431161.2018.1516311

Mozas-Calvache, A.T., Pérez-García, J.L., Cardenal-Escarcena, F.J., Mata-Castro, E. and Delgado-García, J. (2012) Method for photogrammetric surveying of archaeological sites with light aerial platforms, Journal of Archaeological Science, Volume 39, Issue 2, February 2012, Pages 521–530

Neitzel, F. and Klonowski, J. (2011) Mobile 3D mapping with a low-cost UAV system.Int. Arch.Photogramm. Remote. Sens. *Spat. Inf. Sci. 38 , 2011, pp. 1–6.*

Nex, F. and Remondino, R. (2013) UAV for 3D mapping applications: A review. Applied Geomatics 6 (1) March 2013, pp.1-15. DOI: 10.1007/s12518-013-0120-x

Niranjan, S., Gupta, G., Sharma, N., Mangal, M. and Singh, V. (2007) Initial efforts toward mission-specific imaging surveys from aerial exploring platforms: UAV, in: Map World Forum, Hyderabad, India, 2007

Polat, N., & Uysal, M. (2018). An experimental analysis of digital elevation models generated with lidar data and UAV photogrammetry. *Journal of the Indian Society of Remote Sensing*, , 1-8. doi:10.1007/s12524-018-0760-8

Pukanská, K., Bartoš, K., & Sabová, J. (2014). Comparison of survey results of the surface quarry spišské tomášovce by the use of photogrammetry and terrestrial laser scanning. *Inzynieria Mineralna, 15*(1), 47-54

Pukanská, K., Bartoš, K., Bella, P., Rákay ml, Š., & Sabová, J. (2017). Comparison of non-contact surveying technologies for modelling underground morphological structures. *Acta Montanistica Slovaca, 22*(3), 246-256

Rossi, G., Tanteri, L., Tofani, V., Vannocci, P., Moretti, S., & Casagli, N. (2018). Multitemporal UAV surveys for landslide mapping and characterization. *Landslides, 15*(5), 1045-1052. doi:10.1007/s10346-018-0978-0–129.

Rusnák, M., Sládek, J., Kidova, A., Lehotský, M. (2018) Template for high-resolution river landscape mapping using UAV technology. *Measurement* 2018, 115.

Rusnak, M., Sladek, J., Pacina, J. and Kidova, A (2019) Monitoring of avulsion channel evolution and river morphology changes using UAV photogrammetry: Case study of the gravel bed Ondava River in Outer Western Carpathians. *AREA*, Volume: 51, Issue: 3, Pages: 549-560

Remondino, F., Barazzetti, L., Nex, F., Scaioni, M. and Sarazzi, D.: UAV photogrammetry for mapping and 3D modeling–current status and future perspectives, in: H. Eisenbeiss, M. Kunz, H. Ingensand (Eds.), Proceedings of the International Conference on Unmanned Aerial Vehicle in Geomatics (UAV-g) *2011, Zurich, Switzerland*.

Siebert, S. and Teizer, J. (2014) Mobile 3D mapping for surveying earthwork projects using an Unmanned Aerial Vehicle (UAV) system, Automation in Construction 41 (2014) 1-14

Shahbazi, M., Sohn, G., Théau, J. and Menard P. (2015) Development and evaluation of a UAV-photogrammetry system for precise 3D environmental modeling; Sensors (Switzerland),Volume 15, Issue 11, 30 October 2015, Pages 27493-27524

Song, R. and Nan, J. (2009) Interactive modeling and visualization of 3D geological bodies, ICCIT 2009 - 4th International Conference on Computer Sciences and Convergence Information Technology, 2009, Article number 5367910, Pages 447-450

Štroner, M., Michal, O., & Urban, R. (2017). Maximal precision increment method utilization for underground geodetic height network optimization. *Acta Montanistica Slovaca, 22*(1), 32-42

Urban, R., Štroner, M., Kremen, T., Braun, J., Moser, M. (2018). A novel approach to estimate systematic and random error of terrain derived from UAVs: a case study from a post-mining site *ACTA MONTANISTICA SLOVACA*, Vol. 23 (3), 325-336

Urban, R., Štroner, M., Blistan, P., Kovanič, Ľ., Patera, M., Jacko, S., Ďuriška, I., Kelemen, M. and Szabo, S.: The Suitability of UAS for Mass Movement Monitoring Caused by Torrential Rainfall-A Study on the Talus Cones in the Alpine Terrain in High Tatras, Slovakia. In: *ISPRS International journal of geo-information*. Nr. 8, vol. 8 (2019), pp. 317-317

Vegsoova, O., Straka, M. and Sulovec, M. (2019 a) Global Assessment of Industrial Expansion for Minimizing Environmental Impacts Utilizing the Principles of Mining and Logistics, *Rocznik Ochrona Środowiska*, 21, pp. 14- 28,

Vegsoova, O., Straka, M. and Rosova, A. (2019 b): Protecting and securing an environment affected by industrial activity for future utilization, *Rocznik Ochrona Środowiska*, 21, pp. 98- 111,

Xiang, J., Chen, J., Sofia, G., Tian, Y., & Tarolli, P. (2018). Open-pit mine geomorphic changes analysis using multi-temporal UAV survey. *Environmental Earth Sciences, 77*(6) doi:10.1007/s12665-018-7383-9

Yu, J., Gan, Z., Zhong, L., & Deng, L. (2018). Research and practice of UAV remote sensing in the monitoring and management of construction projects in riparian areas. Paper presented at the *International Archives of the Photogrammetry, Remote Sensing and Spatial Information Sciences - ISPRS Archives, , 42*(3) 2161-2165. doi:10.5194/isprs-archives-XLII-3-2161-2018

Zhang, C. and Elaksher, A. (2011) An unmanned aerial vehicle-based imaging system for 3D measurement of unpaved road surface distresses, J. Comput. Aided Civ.Infrastruct. Eng. 27 (2) (2011) 118

Parametric Studies of Total Load-Bearing Capacity of Steel Arch Supports

***Petr Horyl*[1], *Richard Šňupárek*[2], *Pavel Maršálek*[1], *Zdeněk Poruba*[3] *and* *Krzysztof Pacześniowski*[4]**

The supports in roadways are dimensioned to the amount of the load applied during the roadway's life. Roadways are exposed to the effect of rock pressure associated with the roadway drivage and with subsequent operations that extract coal, which significantly affect the original stability of rock mass. This induced secondary stress leads to the disturbance of sedimentary rocks, which are mostly of slight and medium strength, and to the significant deformations in roadways. The gate-roads are mainly supported with yielding steel arch support (TH profiles). The load-bearing capacity of the steel arch supports is a key parameter in the design of roadways support. Determination of this parameter can be done using large testing frames in experimental laboratories. Another essentially cheaper way is to create a computer model which exhibits a good correlation with respect to the existing data from equivalent laboratory conditions. In this paper, we present the validated computer model of the steel arch supports through which the influences of important factors, namely different materials, number of the clamps in the yielding friction joints, and different values of tightening torque on the total load-bearing capacity, were determined. This parametrical study was created based on the practical requirements from industry, and the obtained results will be reflected in the design of new types of steel arch supports.

Keywords: *steel arch support, yielding, friction, bolted connection, clamp, joint, mining, FEM*

Introduction

The predominant amount of Europian coal deposits exploited underground are extracted by the longwall method with controlled caving. Experience shows that roadways, which ensure all transport and ventilation in coalfaces, restrict both output and safety as well as the economy in coal production (Becker, 1984). Roadways are exposed to the effect of rock pressure associated with the drivage of roadways and with subsequent operations that extract coal, which significantly affect the original stability of rock mass (Hood and Brown, 1999). This induced secondary stress leads to the disturbance of sedimentary rocks, which are mostly of slight and medium strength, and to the significant deformations in roadways. With the occurrence of very firm rock layers, the dynamic phenomena of rock pressure-rock bursts are induced, which again primarily affect roadways (Brauner, 1981). Therefore, the research of the most efficient methods for supporting and ensuring the roadways in coal mines presents a fundamental problem for mining as well as geomechanical engineers (Šňupárek and Konečný, 2010). From the geomechanical point of view, the shape and size of the underground workings are essential. The gateways are driven in the seam, often with some stripping in the floor or in the roof, and their full-size cross-section is 15–20 m^2 in average, with the mean advance of machine-driven openings about 8 to 10 m per day. The gate-roads are mainly supported with yielding steel arch support (TH profiles). For these roadways, it is necessary to design an optimal support system respecting the loads to which the roadway will be exposed during its life (Hoek and Brown, 2002).

The plan of monitoring in roadways and determination of stabilization measures are usually part of monitoring procedures in order to avoid exceeding critical values of loading. The supports in roadways are dimensioned to the amount of the load applied during the roadway's life. In the first period of drivage of a mine working, the minimum bearing capacity of the supports must correspond to the load of the loosened rock in its vicinity or, as the case may be, to a portion of this load. Moreover, the supports must comply with the yield function with respect to a certain coherence of the loosened rock (Brady and Brown, 2004). According to the arch theory, a natural arch is formed above the roadway, and along this natural arch, the rocks separate from the rock mass. The rocks inside the arch are disturbed, and, therefore, these rocks have to be supported with the supports in the roadway. The necessary spacing of arches of the conventional support can be determined on the basis of comparison of the calculated standard load with the load-bearing capacity of supporting (Jacobi, 1961).

[1] *Petr Horyl , Pavel Maršálek,* IT4Innovations, VŠB – Technical University of Ostrava, 17. listopadu 15/2172, 708 33 Ostrava-Poruba, Czech Republic, VŠB-Technical University of Ostrava, Department of Applied Mechanics, 17. listopadu 15/2172, 708 33 Ostrava-Poruba, Czech Republic, *petr.horyl@vsb.cz, pavel.marsalek@vsb.cz,*

[2] *Richard Šňupárek,* Institute of Geonics ASCR, Institute of Clean Technologies for Mining and Utilization of Raw Materials for Energy Use, Studentska 1768, 708 00 Ostrava, Czech Republic, *richard.snuparek@ugn.cas.cz*

[3] *Zdeněk Poruba,* VŠB-Technical University of Ostrava, Department of Applied Mechanics, 17. listopadu 15/2172, 708 33 Ostrava-Poruba, Czech Republic, *zdenek.poruba@vsb.cz*

[4] *Krzysztof Pacześniowski,* Glowny Instytut Gornictwa, Department of Mechanical Devices Testing, Plac Gwarków 1, 40-166 Katowice, Poland, *paczes@life.home.pl*

The total load-bearing capacity F_E of arch frames plays an important role in the design of steel arch supports. Under the laboratory conditions, this capacity F_E is defined as the scalar sum of the external forces actively produced by hydraulic cylinders No. 4-6 (red arrows in Figures 1 and 2). This value of capacity of the steel arch supports is affected not only by their structure and material but also by the method of load application (Brodny, 2010). It is necessary to obtain the values of the total load-bearing capacity for different constructions under the agreed scheme of loading corresponding to the real mining conditions. The total load-bearing capacity of arch frames in mining practice is currently being approximately assessed. The exact values can be verified in laboratories with large frames (in Europe, for instance, in DMT Essen or GIG Katowice).

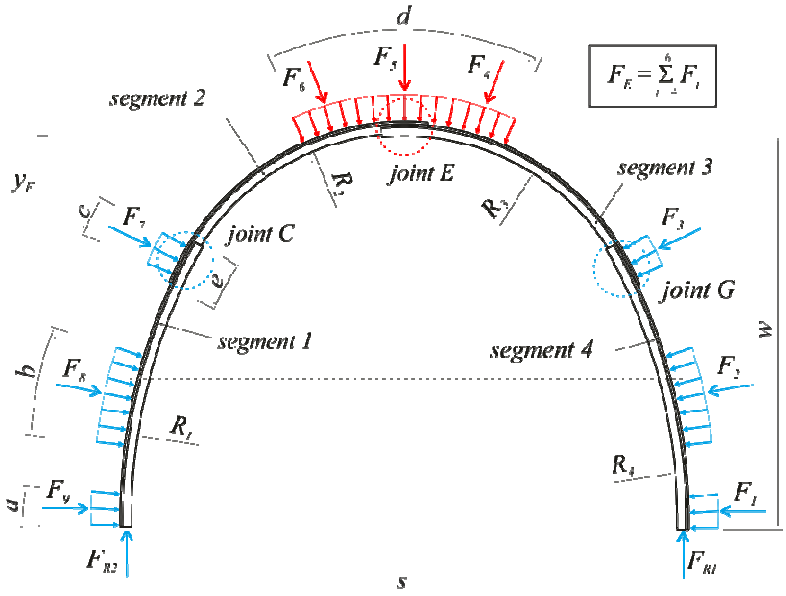

Fig. 1. Testing scheme, front view

The experimental research for verification of the computer modelling method was realized in the Laboratory of Mechanical Devices Testing GIG Katowice (Poland). The tests of the steel arch supports comply with the requests of the standard (Standard PN-G-15000-05, 1992). The external loading is excited by movable hydraulic force elements $F_4 – F_6$, see Figure 1. Other hydraulic force elements $F_1 – F_3$ and $F_7 – F_9$ are immobile, and they serve as supports. The subject of laboratory testing is the SP16 steel arch supports used in Ostrava Karvina mines with basic dimensions, width s = 5 920 mm and height w = 4 240 mm. This support frame consists of four segments (the TH29 profile) connected by the clamps realized by the bolted connections. The overlap length of segments is e = 500 mm. All geometrical properties are shown in Table 1. Testing of the steel arch supports was performed in the two following modes: as the rigid (welded) support - unyielding segments are fixed by welding of double segments - and as the yielding support with standard clamps - friction joints.

Table 1. Geometry of steel arch support

Parameter	[mm]	**Parameter**	[mm]
s	5 920	a	170
w	4 240	b	1 000
e	500	c	220
$R_1 = R_4$	5 950	d	3 000
$R_2 = R_3$	2 620		

Material and Methods

The history of computer modelling of steel arch mining supports, presented first in the crucial paper by authors Horyl and Šňupárek (Horyl and Šňupárek, 1992), began even before 1992. The calculations were performed using their own Finite element method-based software, and supports (segments) were modelled

by a planar beam element. The joints between the segments were simplified – they were modelled without a yielding function. The results in that paper indicated that steel arch supports combined with rock-bolts are most resistant against the instantaneous dynamic loading. The computer models were further refined using a shell finite element. The bolted connections with the pre-loading effect were firstly included in this model of friction joints (Horyl et al., 1997). It caused intense numerical modelling of the support response on the rock bursts (Horyl and Šňupárek 2005). Later on, the bolting fixation impact on that response was modelled (Horyl, Šňupárek, 2007, 2009 and Horyl, Vicherek, 2007). On a global scale, these calculations were unique. Only later, computer models were consistently created by spatial finite element – solid type (Horyl et al., 2012, 2013, and 2014). The aim of the calculations was to determine how much energy of external load causes plastic deformation of the supports. Energy values, which have a damaging effect on the bolt body and cause loose stability of the whole support frame after that situation, were observed.

The methodology of Computer Modelling. On the basis of this long-term experience with modelling and analysis of main parts of the support, a complete spatial finite element (FE) model of SP16 steel arch support was designed. The problem was solved as a static structural analysis with neglecting of inertia effects. All parts of this support (segments, clamps) were created and assembled according to drawings without any shape simplification. The scheme of the FE model is depicted in Figure 2.

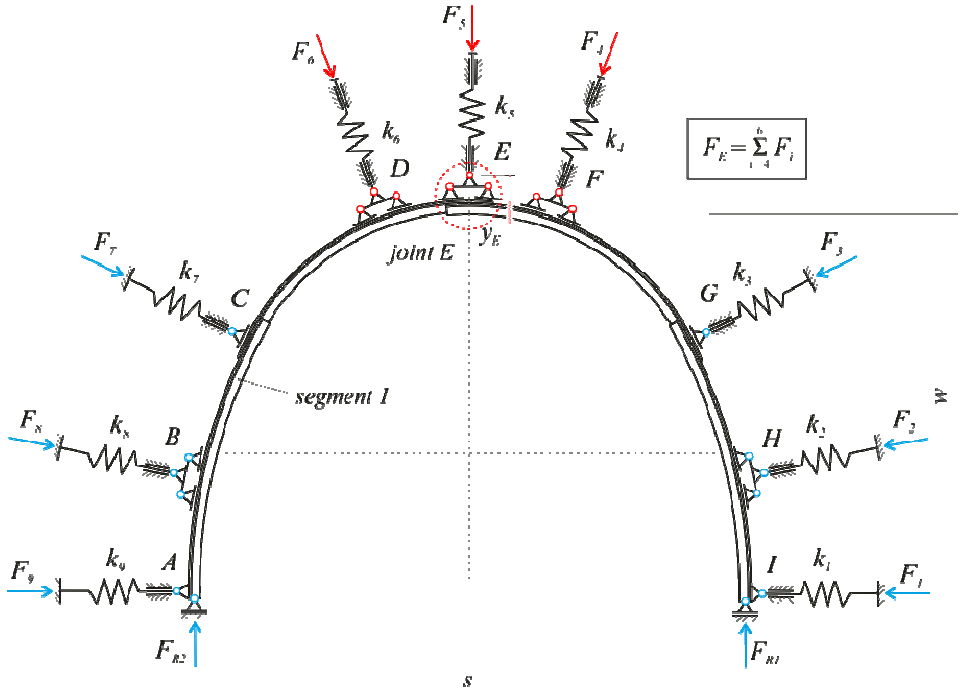

Fig. 2. Boundary condition of the FE model, front view

The boundary conditions correspond to those described above in the standard (Standard PN-G-15000-05, 1992). Hydraulic cylinders were replaced by spring elements with equivalent stiffness $k_1 – k_9$ = 9 kN/mm (without considering these flexible members, the values of vertical deformations y_E will be significantly distorted in comparison with the testing data). The supporting mechanism of the hydraulic cylinders pushing on the segments was realised by the multi-point constraints (MPC) elements connecting one layer of solid elements with a joint mechanism (detail in Figure 5). The bolted connections used for clamp preloading were modelled by a specific method. The bolt body represents two beam elements which are attached using the MPC elements to the upper and lower yokes, see Figure 5. The whole task of the total load-bearing capacity of the steel arch support containing 1.1 mil degrees of freedom (DOF) was solved using MSC MARC 2013 solver. The time for solving one task on the computer station with 16 central processing units (CPU) corresponded to 15 hours. The summary of used finite elements is shown in Table 2.

Table 2. Finite elements used for welded / yielding support model

Type of element	MARC description	Number of elements
Solid elements	Hex8 (SOLID7), Penta6 (SOLID136)	242,000 / 260,000
Spring elements	-	9 / 9
Bolt body d_b = 22.05 mm	Line2, (Beam98)	12 / 18
Multi-point constraints	RBE2	33 / 39

The FE models of both support types (welded and yielding) were compared with the experimental results from the tests (Horyl et al., 2016). The evaluated results show considerable correlation with the existing experimental testing data from laboratory, see Figure 3, 4 (Horyl et al., 2017). This validated FE model of the steel arch supports was used for the following parametric studies.

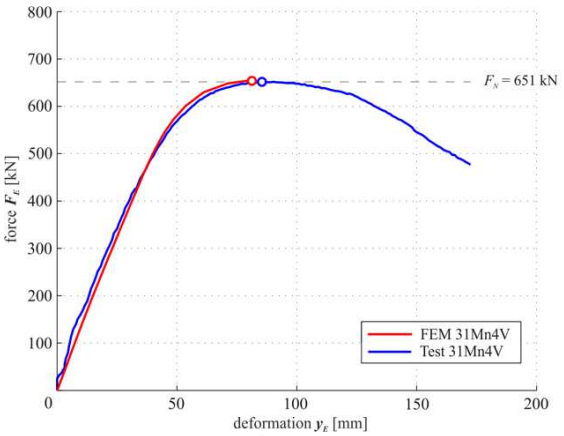

Fig. 3. Comparison of the welded support testing and FE simulation (Horyl et al., 2017)

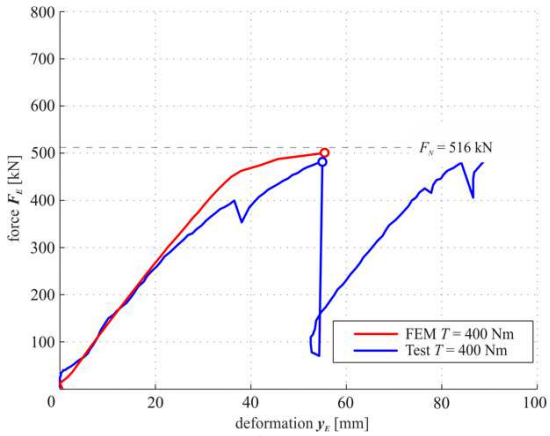

Fig. 4. Comparison of the yielding support testing and FE simulation, tightening torque T = 400 Nm (Horyl et al., 2017)

Material Variations (welded support). The scheme of the welded support was used for investigation of the material variations, i.e. three common steel types for segments (Table 3) – because in this scheme the friction between segments does not affect the total load-bearing capacity in this test. The way of welding of the unyielding joint E (see Figure 2) and discretization of the FE model is described in Figure 5. The supporting mechanism E represents the pressure plates of hydraulic segment E, which carries a part of external loading on the arch support.

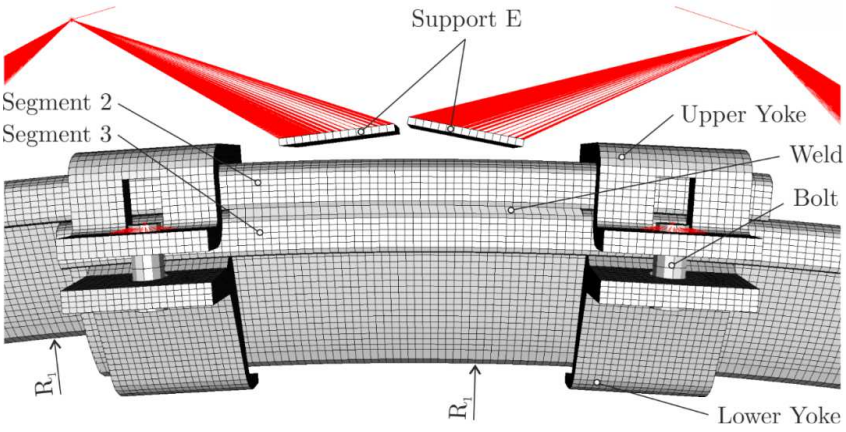

Fig. 5. FE model of welded support – detail of the joint E

The material properties of all FE model parts are listed in Table 3. Young's modulus of elasticity E, yielding stress σ_y, ultimate stress σ_u, and elongation A were determined from the manufacturer data sheets (Steel Qualities, 2015). For describing the plasticity effects, the bilinear material model with isotropic hardening was used.

Table 3. Material properties of structure parts

Structure part	Material properties			
	Young's Modulus of Elasticity E [MPa]	Yielding Stress σ_y [MPa]	Ultimate Stress σ_u [MPa]	Elongation A [%]
Steel support 31Mn4U	200 000	350	520	18
Steel support 31Mn4V		520	650	19
Steel support H500M		480	650	18
Weld 31Mn4U		245	364	18
Weld 31Mn4V		364	455	19
Weld H500M		336	455	18
Upper / lower yoke (S295)		295	470	20
High strength screw M24 (class 8.8)		640	800	12
Stiffness of hydraulic cylinders		$k_1 - k_9 = 9$ [kN/mm]		

The total load-bearing capacity F_E is determined at the end of the simulation due to excessive displacement. This excessive displacement is caused by a small increase in loading forces. The calculation did not converge at this time, producing extremely large deflection in the form of the rigid body motion. The relationships between the load-bearing capacity F_E and vertical deformation y_E for different steel types (31Mn4U/V and H500M) used for the welded support are shown in Figure 6 and Table 4.

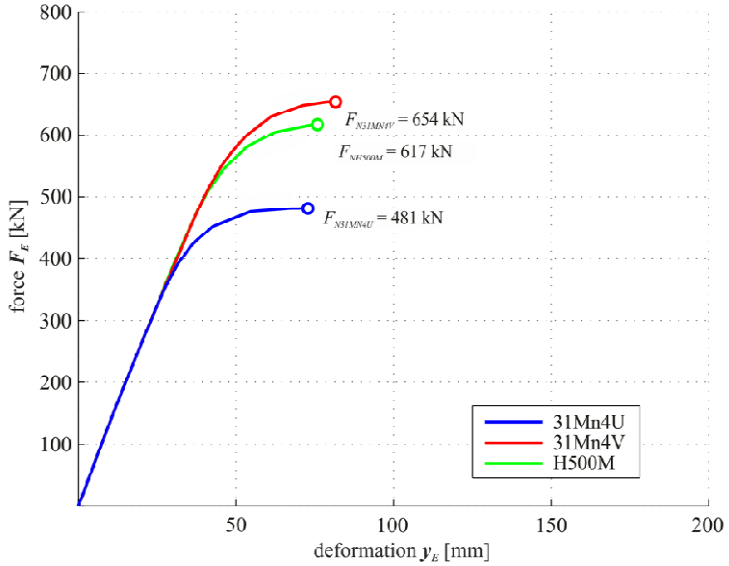

Fig. 6. Relationship between the total load-bearing capacity F_E [kN] and vertical deflection y_E [mm] for different steel types used for welded support

Table 4. Total load-bearing capacity of the welded supports

Steel type used for the welded support	Maximal deflection y_E [mm]	Total load-bearing capacity F_E [kN]
31Mn4U	73	481
H500M	76	617
31Mn4V	82	654

Variations of Friction (yielding support). The total load-bearing capacity of the friction joints (maximal value of normal forces being capable of bearing the connection without a slip of the segments) plays an important role in the static design of the steel arch supports (Hoek and Brown, 2002). Construction of the friction joint with respect to the strength of its different parts and the tightening torque applied to the bolted connection represent meaningful technical aspects regarding the function of the yielding supports. The constructions of the yielding joints have to meet two requirements. The clamping force has to be strong enough to provide a safe total load-bearing capacity of the steel arch support but not too strong to eliminate the yielding effect (Brodny, 2014). While the current design of the friction joints is unified, there is no general consensus regarding the values of the applied tightening torque T on the bolted connections with two or three clamps per friction joint.

The 31Mn4V standard steel type was chosen as the preferred material. The support frame consists of four segments connected by friction joints. The Coulomb friction was prescribed for the friction between parts in the model. The coefficients of friction were taken from (Horyl et al., 2014). The coefficients of friction used for all structure parts are presented in Table 5. The computer modelling was focused on the comparison of supports with two or three clamps per joint and different values of the tightening torque applied to the bolted connection T = 300-450 Nm used in practice (Maršálek and Horyl, 2016). However, especially the higher values of the tightening torque cause the creation of plastic hinges in parts of the connection and the very segments.

Tab. 5. Coefficient of friction and preloading of the bolted connection

Structure part	Coefficient of friction f [-]
Bolt thread	0.13
Under nut	0.17
Between segments/yokes	0.27

Tightening torque T [Nm]	Axial force in the bolt body F_0 [kN]
300	63.3
350	73.9
400	84.4
450	95.0

Three clamps per connection (yielding support). The yielding joint was realised by a uniform distribution of three clamps per connection, as is shown in Figure 7.

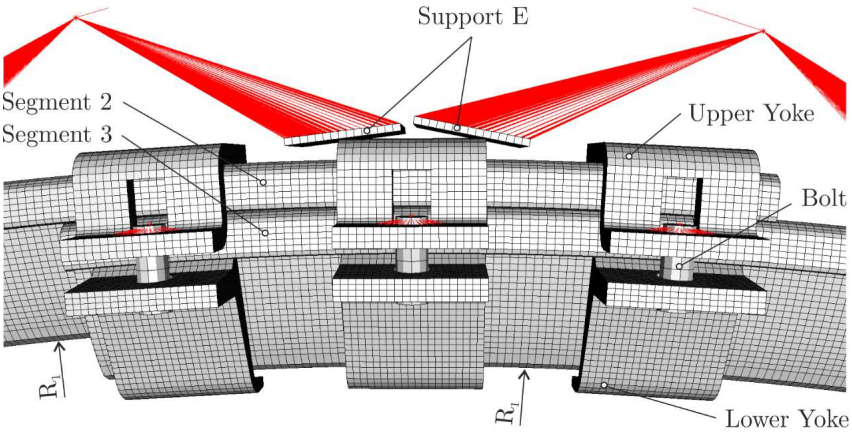

Fig. 7. FE model of yielding support with three clamps per connection – detail of friction joint E

The results of computer simulations show the lowest total load-bearing capacity F_E = 408 kN for the tightening torque T = 300 Nm and highest total load-bearing capacity F_E = 552 kN for the tightening torque of T = 450 Nm, see Figure 8 and Table 6. These values cause a significant uncontrolled slip of the upper friction joints E and the end of the calculation.

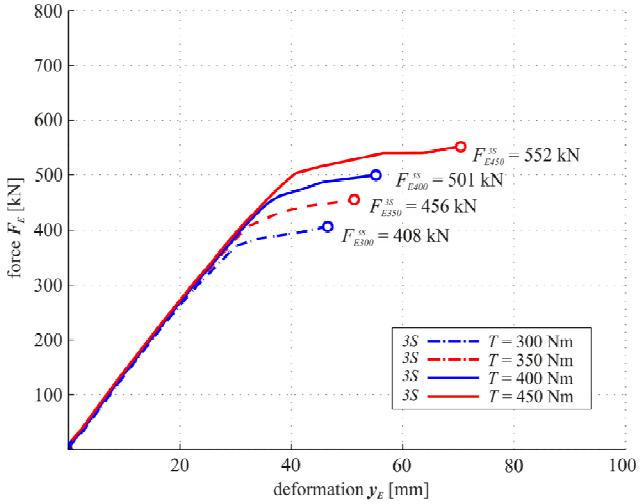

Fig. 8. Relationship between total load-bearing capacity F_E [kN] and vertical deformation y_E [mm] for different torque T at the yielding support with three clamps per connection obtained by the FE model

Table 6. Total load-bearing capacity of the yielding support with three clamps per connection obtained by the FE model

Tightening torque	Deflection at the first slip y_1 [mm]	Total load-bearing capacity F_E [kN]
T = 300 Nm	47	408
T = 350 Nm	52	456
T = 400 Nm	56	501
T = 450 Nm	71	552

The field of equivalent stress (von Misses hypothesis) in the most important part of the structure is depicted in Figure 9. It is the ultimate condition identified for minimum tightening torque T = 300 Nm. As is apparent from Figure 9, in the location of the contact of two different radii of the segments significant increase of plastic hinges are formed.

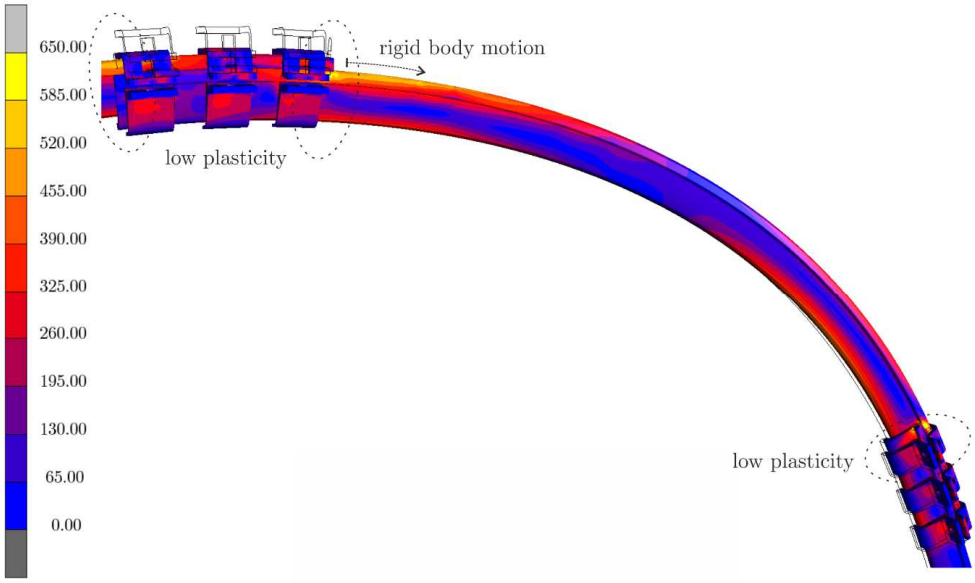

Fig. 9. Field of equivalent stress σ [MPa] – von Mises – in the yielding support with 3 clamps per connection, tightening torque T = 300 Nm, state before the rigid body motion (load F_E = 408 kN)

Two clamps per connection (yielding support). This modification of the yielding joint is performed by removing the middle clamp in each joint (Figure 10).

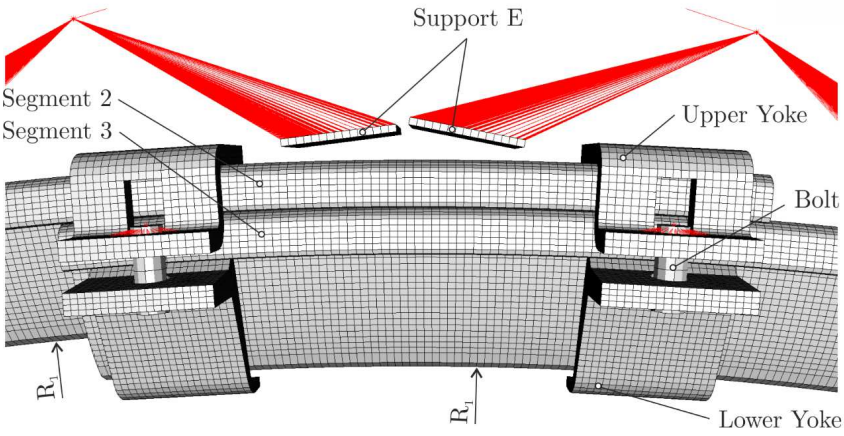

Fig. 10. FE model of the yielding support with two clamps per connection - detail of friction joint E

The results of computer simulations show the lowest total load-bearing capacity F_E = 268 kN for tightening torque T = 300 Nm and the highest total load-bearing capacity F_E = 399 kN for tightening torque T = 450 Nm, see Figure 11 and Table 7.

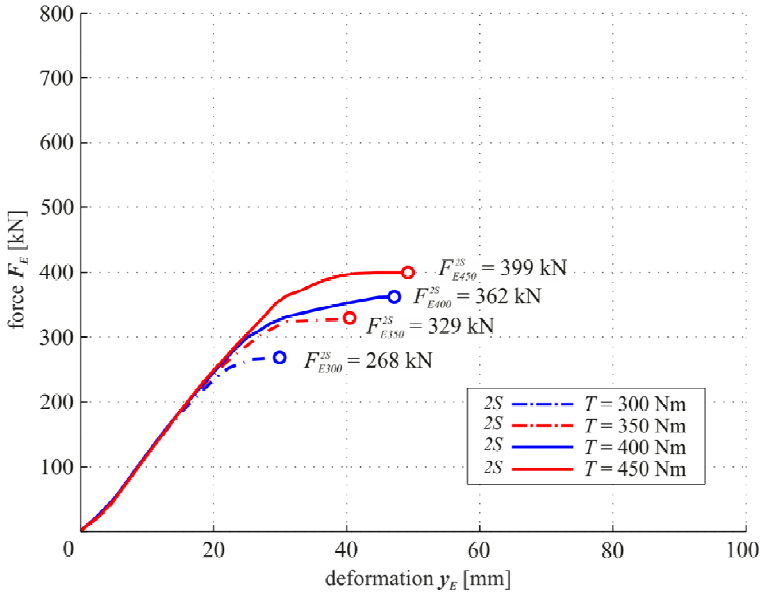

Fig. 11. Relationship between total load-bearing capacity F_E [kN] and vertical deflection y_E [mm] for different torque of bolts at the yielding support with two clamps per connection obtained by the FE model

Table 7. Load-bearing capacity of the yielding support with two clamps per connection obtained by the FE model

Tightening torque	Deformation at the first slip y_1 [mm]	Total load-bearing capacity F_E [kN]
T = 300 Nm	30	268
T = 350 Nm	40	329
T = 400 Nm	47	362
T = 450 Nm	49	399

Figure 12 presents the field of equivalent stress (von Misses hypothesis) for maximum tightening torque T = 450 Nm in the last state before the uncontrolled slip. It is apparent that each clamp transfers a higher load, but the value of the load-bearing capacity is similar to the yielding joint realized by tree clamps tightened by torque T = 300 Nm.

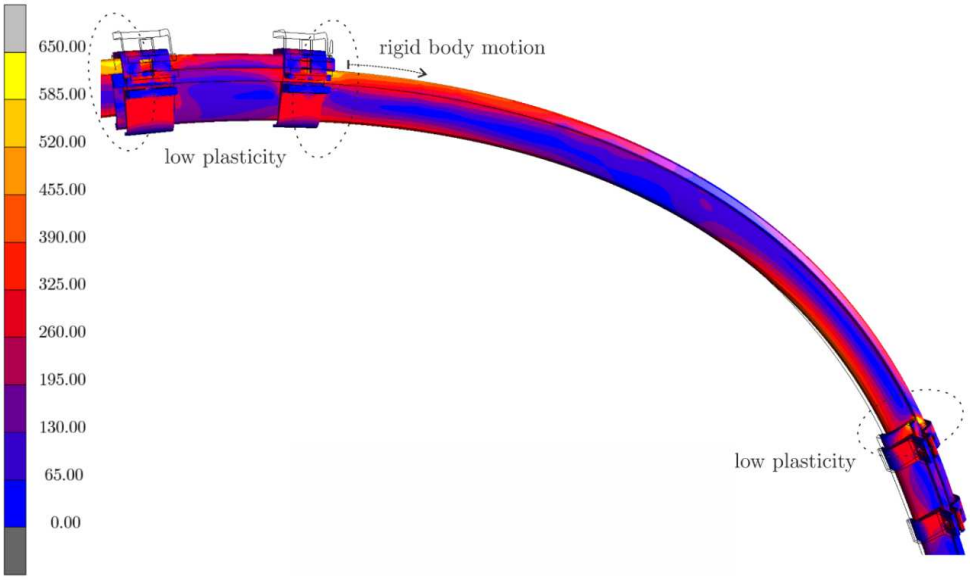

Fig. 12. Field of equivalent stress σ [MPa] – von Mises – in yielding support with two clamps per connection, tightening torque T = 450 Nm, state before the rigid body motion (load F_E = 399 kN)

Results

Material variations were performed on the model of the welded support. The total load-bearing capacity of the supports is more or less directly proportional to yielding stress values of used steel type (Figure 6). The comparison of the computer modelling results of the total load-bearing capacity of the yielding steel arch supports is described in Figure 13.

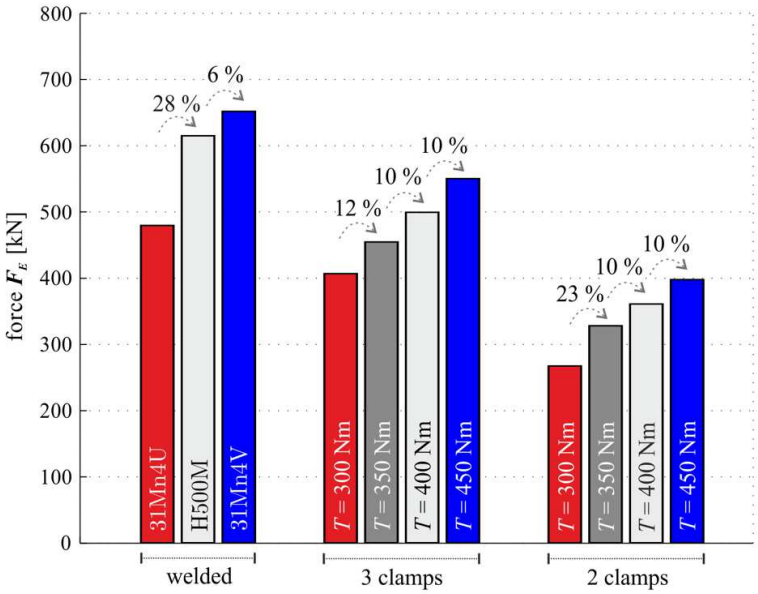

Fig. 13. Comparison of the total load-bearing capacity of the steel arch supports

The effects of the friction joints on the total load-bearing capacity of the yielding steel arch supports were investigated on different types of connections (two or three clamps per friction joint) and different values of the tightening torque on the bolted connection. Using three clamps per connection brings approx. 40 % increase in the value of the total load-bearing capacity of the support in comparison with two clamps. Increase in the tightening torque applied on the bolted connection in the range of 300-450 Nm brings 35-40 % increase in the value of the total load-bearing capacity of the yielding support (with steps approx. 10-12 % per tightening torque T = 50 Nm). The load-bearing capacity of the yielding support with two clamps tightened by maximum torque T = 450 Nm is almost the same as the total load-bearing capacity of the support with three clamps tightened by minimal torque T = 300 Nm (Figure 8 and Figure 11). Increasing resistance against the slipping effect in frictional connections due to a number of clamps and due to torque of bolts also causes the higher total load-bearing capacity of the whole steel arch.

Discussion

The total load-bearing capacity of steel arch support presents an important parameter for support design. This value is affected not only by their construction and material but also by the scheme of load application. In some cases (point loads, high lateral loading) even yielding arch support behaves like rigid welded construction. In our paper, we deal with the scheme of loading with major vertical weight corresponding with loading in the experimental laboratory (Figure 1). A serious problem of computer modelling of yielding arch supports consists in the course of deformation in yielding joints. The slips occur in jumps, and after every slip, the geometry of the whole arch is changed. Moreover, the jumps causing successive slips are caused by the slow velocity of the displacement of the hydraulic cylinders and by the non-linear behaviour of the frictional forces between the contact pairs. The coefficient of friction is dependent not only on the degree of corrosion between the arches but also on their relative velocities. For a detailed description of this behaviour, it would be necessary to consider the inertia of the system and to solve the task as a dynamic with a nonlinear description of the friction effect.

However, by the study of data from laboratory tests of yielding arches, we found that the load-bearing capacity at the first slip in yielding joint represents with sufficient accuracy the total load-bearing capacity of steel arch support (Horyl et al., 2017) (Figure 4). To determine the total load-bearing capacity, the presented static model described in this work is sufficiently accurate and can be used to predict laboratory tests.

Acknowledgements: *This work was supported by The Ministry of Education, Youth and Sports from the National Programme of Sustainability (NPU II) project „IT4Innovations excellence in science - LQ1602“, by the IT4Innovations infrastructure which is supported from the Large Infrastructures for Research, Experimental Development and Innovations project „IT4Innovations National Supercomputing Center – LM2015070“ and by project from Institute of Clean Technologies for Mining and Utilisation of Raw Materials for Energy Use - Sustainability Program, Reg. No. L01406.*

References

Becker, H. (1984). Schneidtechnische Entwicklung beim Strackenvortrieb. Gluckauf, 120.

Brady, H. G. and Brown, E. T. (2004). Rock mechanics for underground mining. Kluwer Academic Publishers. Dordrecht.

Brauner, G. (1981). Gebirgsdruck und Gebirgsschlage. Essen Verlag Gluckauf.

Brodny, J. (2010). Determining the working characteristic of a friction joint in a yielding support. Archives of Mining Sciences, 55(4).

Brodny, J. (2014). Modeling yielding joint of metal arch support in underground roadways. Gornyi Zhurnal, 4.

Hoek, E. and Brown, E. T. (2002). Practical estimates of rock mass strength. Int. J. Rock Mech. Min. Sci., 34.

Hood, M. and Brown, E. (1999). Mining Rock Mechanics yesterday, today and tomorrow. Proc. 9th Congr. ISRM, Paris.

Horyl, P. and Šnupárek, R. (2012). Reinforcing measures of steel roadway support in rockburst prone areas. Archives of Mining Sciences, 57(1).

Horyl, P. and Maršálek, P. and Šňupárek, R. and Pacześniowski, K. (2016). Total load-bearing capacity of yielding steel arch supports. Rock Mechanics and Rock Engineering: From the Past to the Future, Cappadocia.

Horyl, P. and Šňupárek R. (1992). Parametrical study of roadway support under dynamic loading due to rock bursts. In Proceedings of the International Symposium on Rock Support, Rotterdam.

Horyl, P. and Šňupárek, R. (2005). Modelling of effects of rockburtsts on steel arch roadway support underground. 6th International Symposium on Rockburst and Seismicity in Mines Proceedings, Perth.

Horyl, P. and Šňupárek, R. (2007). Behaviour of steel arch supports under dynamic effects of rockbursts. Transactions of the Institutions of Mining and Metallurgy, 116(3).

Horyl, P. and Šňupárek, R. (2009). Rockbolts as reinforcing elements under dynamic impact of rockbursts. Proceedings of the ISRM-Sponsored International Symposium on Rock Mechanics, Hong Kong.

Horyl, P. and Šňupárek, R. and Hlaváčková, M. (2013). Loading capacity of yielding connections used in steel arch roadway supports. Proceedings of the Seventh International Symposium on Ground Support in Mining and Underground Construction, Perth.

Horyl, P. and Šňupárek, R. and Maršálek, P. (2014). Behaviour of frictional joints in steel arch yielding supports. Archives of Mining Sciences, 59(3).

Horyl, P. and Šňupárek, R and Maršálek, P. and Pacześniowski, K. (2017). Simulation of laboratory tests of steel arch support. Archives of Mining Sciences, 62(1).

Horyl, P. and Šňupárková, J. and Šňupárek R. (1997). The rise and propagation of plastic zones in the steel arch tunnel support due to large deformations. Proceedings International Symposium on Rock Support, Oslo.

Horyl, P. and Vicherek, A. (2007). Computer modeling of bolting fixation into rock. 15. Ansys Conference & 25. CADFEM Users' Meeting, Dresden.

Jacobi, P. (1961). Praxis der Gebirgbeherrschung. Essen Verlag Gluckauf.

Maršálek, P. and Horyl, P. (2016). Modelling of bolted connection with flexible yokes used in mining industry. International Conference of Numerical Analysis and Applied Mathematics 2016, Rhodes.

Šňupárek, R. and Konečný, P. (2010). Stability of Roadways in Coalmines alias Rock Mechanics in Practice. Journal of Rock Mechanics and Geotechnival Engineering.

Standard PN-G-15000-05 (1992). Obudowa chodników odrzwiami podatnymi z kształtowników korytkowych - Odrzwia łukowe otwarte - Badania stanowiskowe (in Polish).

Steel Qualities (2015). Special Sections. ArcelorMittal Rodange and Schifflange", <http://www.ares.lu/4_mining.htm>.

Metals Recovery: Study of the Kinetic Aspects of Copper Acidic Leaching Waste Printed Circuit Boards from Discarded Mobile Phones

Martina Laubertová[1], Bora Derin[2], Jarmila Trpčevská[1], Klaudia Šándorová[3] *and* ***Emília Sminčáková[1]***

This study was performed to investigate the possibility of copper recovery from the waste printed circuit boards (WPCBs) of waste mobile phones using a hydrometallurgical route as cleaner technology for environmental protection. In recycling, elements such as copper and aluminium are recovered, as well as the precious metals gold, silver, platinum and palladium, which can be recouped profitably from electronic waste and make this waste very valuable for recycling. In the experiments, the conventional agitated acid leaching method was used for mechanically pre-treated WPCBs with a mean Cu content of 19.09 wt % in a sulphuric acid medium with the presence of Fe^{3+} as an oxidant. The effects of $Fe_2(SO_4)_3$ concentration, leaching time, temperature and the ratio of liquid to solid phase on the recovery of copper from the solutions were studied. The highest Cu extraction was achieved at 363 K after 15 min of leaching, and a liquid to solid ratio (L/S) of 20. The value of activation energy (Ea), which was found to be ~14.87 kJ.mol^{-1}, indicates that this process is diffusion controlled. The apparent order of reaction with regard to the initial $Fe_2(SO_4)_3$ concentration at 313 K was calculated as 0.55. The proposed scheme of copper recovery from WPCBs of mobile phones was designed.

Keywords: *copper, metallurgy, leaching, discarded mobile phones*

Introduction

Nowadays, "waste of electrical and electronic equipment" (WEEE) such as discarded mobile phones (MP), computers or TV sets is one of the world's fastest-growing problems and needs to be tackled immediately. In the European Union (EU) alone, the amount of WEEE is expected to grow to 12 million tonnes by 2020 ("Waste Electrical & Electronic Equipment (WEEE)," 2018). Statistics also indicate that in 2019 the number of mobile phone users will reach 4.68 billion in the world ("Number of mobile phone users worldwide from 2013 to 2019 (in billions)," 2018). WEEE, which consists of very complex materials and components, may cause major environmental and health problems, if not properly managed. Besides, the production of modern electronics needs the use of scarce and expensive resources such as gold, silver and rare earth elements. A mobile phone consists of several parts, including the display unit, battery, front and back cases and printed circuit boards (WPCBs). WPCBs in mobile phones contain many base, precious and rare metals, such as Au, Ag, Pd, Ta, Nd, Al, Cu, Sn, Co, Fe, and Pb. These elements or their alloys are found inside or on the surface of WPCBs. (Palmieri et al., 2014; Sarath et al., 2015). The most attention to the treatment of discarded mobile phones is focused on copper, due to its high content in phones and its current world consumption. The total world production of refined copper was reached 23.4 million tonnes in 2016 (Brown, 2018) ("Secondary copper production up 6% in the first quarter of 2018," 2018). Future global copper demand is expected to keep increasing due to copper's absolutely necessary role in modern technologies. Due to the above-mentioned concerns, these WPCBs have to be removed from discarded mobile phones and selectively treated (European Parliament & The Council Of The European Union, 2012). In general, there are three basic ways to recover valuable metals from secondary resources: pyrometallurgical, hydrometallurgical and a combined method (Moskalyk and Alfantazi, 2003; Behnamfard et al, 2013; Kasper et al., 2018; Rudnik et al., 2015; Birloaga et al., 2013; Havlik et al., 2011). In the EU, the biggest companies use pyrometallurgical treatment methods based on smelting for metal recovery from WEEEs on an industrial scale (Rocchetti et al., 2018). For example, tin, lead, zinc, nickel and precious metals are recovered from electronic scraps, e.g. printed circuit boards, using the Kayser Recycling System (KRS) in Aurubis, Lumen in Germany (Maurell-Lopez et al., 2011; Laubertová et al., 2017). Another example is the Kaldo Furnace process practised at Boliden, Ronnskar in Sweden (Cui and Zhang, 2008) ("Boliden," 2018). The electronic scraps are first smelted in an IsaSmelt furnace to recover precious metals along with Cu in the form of Cu-bullion in Umicore's integrated metal smelter and refinery (Hagelüken, 2006). These smelters can treat more than 200,000 ton/year of precious metal-bearing materials such as by-products from non-ferrous companies and electronic scraps. The hydrometallurgical processes are an alternative to pyrometallurgical treatments of WEEE due to some characteristic advantages such as the possibility of treating heterogeneous materials, lower environmental impact including low gas emission, and

[1] *Martina Laubertová, Jarmila Trpčevská, Emília Sminčáková,* Technical University of Kosice, Faculty of Materials, Metallurgy and Recycling, Institute of Recycling Technologies, Letna 9, 042 00, Kosice, Slovakia; *martina.laubertova@tuke.sk (corresponding author), jarmila.trpcevska@tuke.sk, emilia.smincakova@tuke.sk*

[2] *Bora Derin,* University, Metallurgical and Materials Eng. Dept., 34469, Istanbul, Turkey, *bderin@itu.edu.tr*

[3] *Klaudia Šándorová,* Technical University of Kosice, Faculty of Mining, Ecology, Process Control and Geotechnologies, Institute of Earth Resources, Department of Land Management, Letna 9, 042 00, Kosice, Slovakia, *klaudia.sandorova@tuke.sk*

selective recovery of elements (Laubertova et al., 2011). Some studies exist which focus on treating WPCBs with hydrometallurgical methods (Jing-ying et al., 2012; Zazycki et al., 2017). For example, Kim et al. (2011) leached small pieces of WPCBs (2-3 mm) from discarded MPs in a two-stage leaching process. They selective dissolved copper and gold using electro-generated chlorine as an oxidant. They then leached the crushed WPCBs in an H_2SO_4 acid solution with the addition of H_2O_2 as an oxidant for copper recovery (Camelino et al., 2015; Yang et al., 2011) used combinations of supercritical water and diluted hydrochloric acid leaching methods to recover copper from WPCBs (Xiu and Zhang, 2015). Laubertova et al. (2012) leached the different fractions of WPCBs in either ferric sulfate or a mixture of $FeCl_3$ and $Fe_2(SO_4)_3$ solutions (Laubertova and Sandorova, 2013; Yang et al., 2011). Bioleaching has also been used to leach out gold and copper from waste mobile phone WPCBs (Chi et al., 2011). As seen in the literature, the different fraction of WPCBs of MPs and different acid leaching media were used for the leaching process. A kinetic investigation was also carried out to evaluate the kinetic constants during the leaching processes in different acid leaching media (Dutta at al., 2018; Ha et al., 2014; Kim et al., 2011). According to the literature (Havlik, 2008), a thermodynamic study of the leaching process of copper indicates that it is possible to use an acid oxidizing medium for leaching. However, these studies did not describe the kinetic aspects of leaching of WPCBs in ferric sulphate as a solvent medium. The present research attempts to develop an alternative process for the leaching of copper from mechanically pre-treated WPCBs of MPs using ferric sulphate as a leaching solution. Thermodynamic data were determined using Outotec HSC Chemistry Software from Outotec Research with Oy modelling package 8.0 (Roine, 2002).

The leaching of WPCBs in $Fe_2(SO_4)_3$ solutions is described by chemical reaction Eq. 1:

$$Cu + 2Fe^{3+} + SO_4^{2-} = 2Fe^{2+} + CuSO_4 \qquad \Delta G^0_{293} = -64.54\ kJ \qquad (1)$$

The negative value of the standard Gibbs energy suggests that this reaction is thermodynamically feasible and spontaneous. The objectives of this study are listed as follows:

1) Determination of the chemical composition of Cu-containing wastes (WPCBs from waste button mobile phones).

2) Cu recovery by means of agitated leaching of WPCBs from MPs with different parameters such as liquid to solid ratio, reaction temperature, leaching times and $Fe_2(SO_4)_3$ concentrations.

3) Based on kinetics measurements, obtaining values of the apparent activation energy Ea and the apparent reaction order n, with regard to the initial $Fe_2(SO_4)_3$ concentration in the leaching solution.

Materials and methods

Sample characterization

Discarded MPs collected in a recycling facility in Slovakia were used in these experiments. The sampling procedure of WPCBs shown in Fig. 1 was used for preparing a representative sample for chemical analysis (Laubertova et al., 2018; Mickova, 2018).

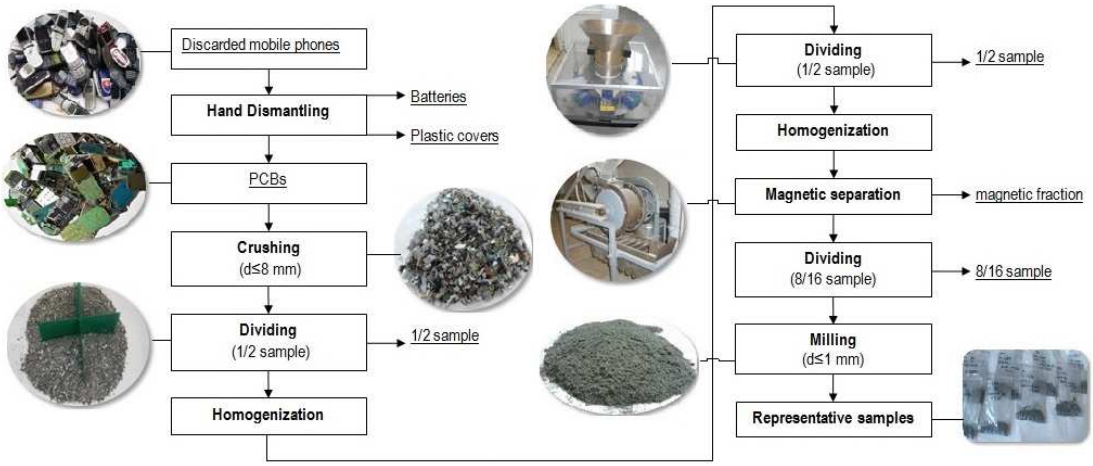

Fig. 1. Methodology for printed circuit boards sampling from discarded mobile phones

After manual dismantling and sorting of MPs, the non-magnetic fraction of WPCBs was mechanically milled and then sieved to less than 1.25 mm. In order to evaluate the size distribution of the treated sample, 100 g of the selected sample obtained by quartering was sieved with a vibration sieve shaker using 1.25; 0.71; 0.65;

0.40; 0.25; 0.08 mm openings. The size distribution of WPCB samples used for the experiments is shown in Fig.2.

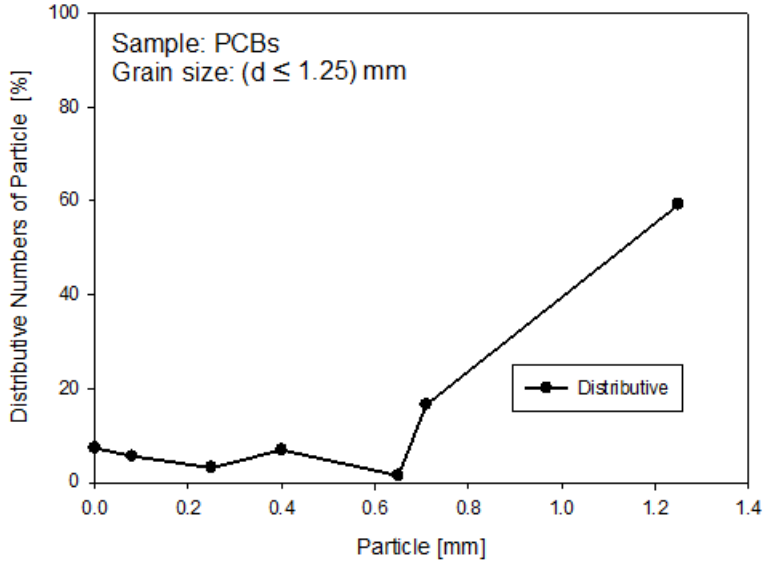

Fig. 2. Particle distribution of the treated sample WPCBs (d ≤ 1.25 mm)

X-ray diffractometer Phillips PW 1710 X´Pert PRO MRD (Co-Kα) was used for qualitative phase analysis. Sample evaluation was performed using software RIFRAN. Due to the fact that it is not possible to obtain an objective diffractogram from such large particles, the samples were milled on a vibratory mill to obtain a fine-grained homogeneous fraction suitable for X-ray diffraction qualitative analysis. Diffraction pattern of the sample is shown in Fig. 3. The results of the phase analysis show that all samples contain metals and / or Cu, Sn, Pb, Zn, Fe alloys. The proportion of plastics represented by the high background of the diffractogram in the region around 25 ° Bragg angle 2Theta is significantly represented. This fact makes the identification more difficult.

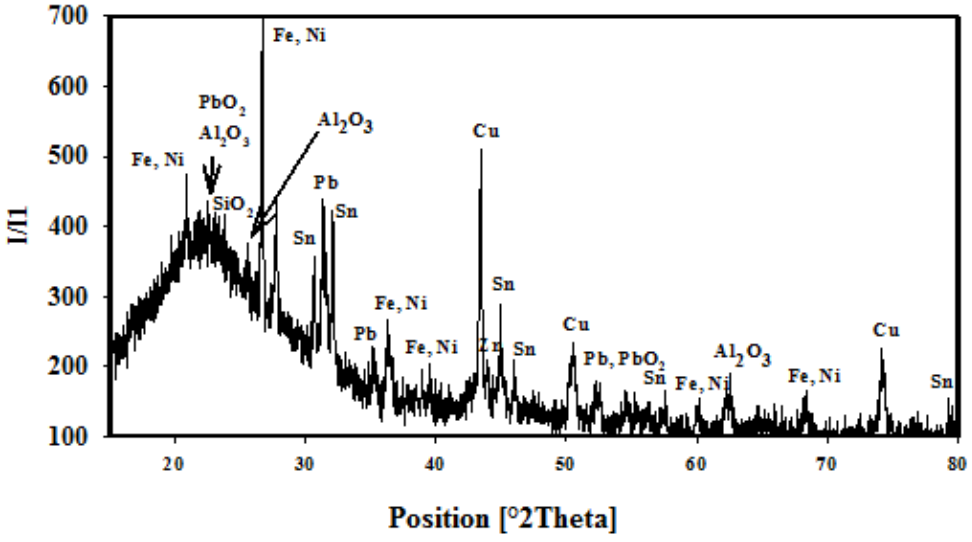

Fig. 3. XRD pattern of the fine-grained fraction of the WPCBs

Five representative samples (1g each) taken from treated WPCBs (d ≤ 1.25 mm) were subjected to atomic absorption spectroscopy (AAS) (Varian Spectrometer AA 20+) analysis to determine the concentrations of the selected metals. The average results of the elemental analysis of the WPCB samples are shown in Table 1.

Table.1. Average results of elemental analysis of five representative WPCBs samples using the AAS technique

Element	**Cu**	**Ni**	**Sn**	**Zn**	**Pb**	**Al**	**Fe**	**Au**	**Ag**
Content (wt %)	19.09	1.26	1.286	1.776	0.403	0.826	1.956	0.036	0.093
Standard deviation „s"	6.304	0.341	0.629	1.21	0.202	0.249	1.405	0.005	0.021
Coefficient of variation „C_V"	0.33	0.26	0.48	0.68	0.5	0.30	0.718	0.157	0.223

Experimental procedure

$Fe_2(SO_4)_3$ and H_2SO_4 were used for leaching representative WPCB samples in an aqueous medium. The leaching experiments were conducted in a conventional reactor with a stirrer at 400 RPM. The effect the concentration of the solution on the leaching rate was investigated in the concentration range from 0.1 mol dm^{-3} to 1 mol dm^{-3} $Fe_2(SO_4)_3$ at 0.5 mol dm^{-3} H_2SO_4. The used liquid to solid (L/S) ratios were 10, 20 and 30 (200 mL solution/20-10-6.6 g solids). The effect of temperature on the leaching rate was also investigated at temperatures between 314 K and 363 K in the solution containing 1 $Fe_2(SO_4)_3$+0.5 mol dm^{-3} H_2SO_4. The schematic representation of the experimental set-up is shown in Fig. 4. A solution mixture of sulphuric acid and Fe^{3+} as an oxidizing agent were used for leaching. For all experiments, 0.5 mol dm^{-3} H_2SO_4 was oxidized with 1 mol dm^{-3} $Fe_2(SO_4)_3$. The leaching time for each experiment was 60 minutes. Every 5, 10, 15, 30 and 60 minutes a 5 ml sample was taken for chemical analysis. The samples were subjected to atomic absorption spectroscopy for determination of Cu content.

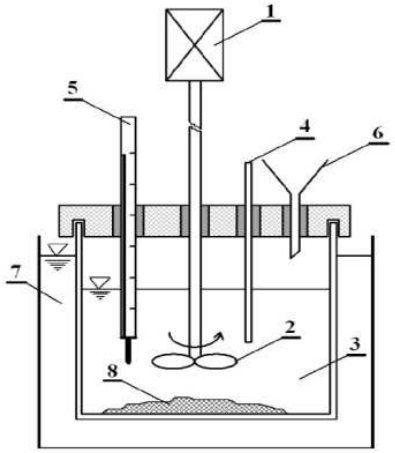

Fig. 4. Schematic diagram of the conventional agitated leaching system (Trung et al., 2011)
1- a drive of the mixer with constantly adjustable stirring, 2 – mixer, 3 – leaching agent, 4 – liquid sample collection, 5 – thermometer, 6 – material input, 7- thermostat, 8 – sample

Results and discussion

Before the experimental investigation, a computational thermochemical study was carried out to predict the possible phases of the system depending on changing parameters. The classical Eh-pH (Pourbaix) diagrams are known for being similar to "predominance diagrams" which show the regions where various aqueous ions or solid compounds predominate (Bale et al., 2016). In this study, a new type of aqueous phase diagram named FactSage 7.2 was used to separate the aqueous species from the solid phases by real phase boundaries. The diagram was calculated at constant molalities of Cu, Fe, Zn, and Ni as used in the experiments. In the calculations, the Pitzer database for concentrated solutions was used, and the temperature and total pressure of the system were selected as 80 °C and 1 atm respectively. The aqueous phase diagram of our H_2O-$Fe_2(SO_4)_3$-H_2SO_4-Cu-Zn-Ni system calculated with the FactSage phase diagram module is shown in Fig. 5. The y-axis shows the oxidation potential, log $P(O_2)$, which is related to Eh, while the x-axis is the $Fe_2(SO_4)_3$ concentration

given as the molality (mol/kg H_2O) in the solution. As seen in the figure, when the molality of H_2SO_4 was fixed at 0.5 in the system, there was a stable aqueous region throughout the system for a certain oxygen partial pressure range (i.e. $\log_{10}PO_2$, between -35 and -50 atm). When the oxygen amount increased in the system, Fe_2O_3 precipitated out from the solution. In reducing conditions, in addition to gas, solid Cu, ferrous sulphate, and iron oxides started precipitating out. For example, when the oxidation potential and the molality of $Fe_2(SO_4)_3$ were selected as -40 atm and 1 respectively, all metallic elements (i.e. Cu, Zn, Ni, and Fe) in the aqueous solution were calculated to be almost entirely in the (2+) oxidation states.

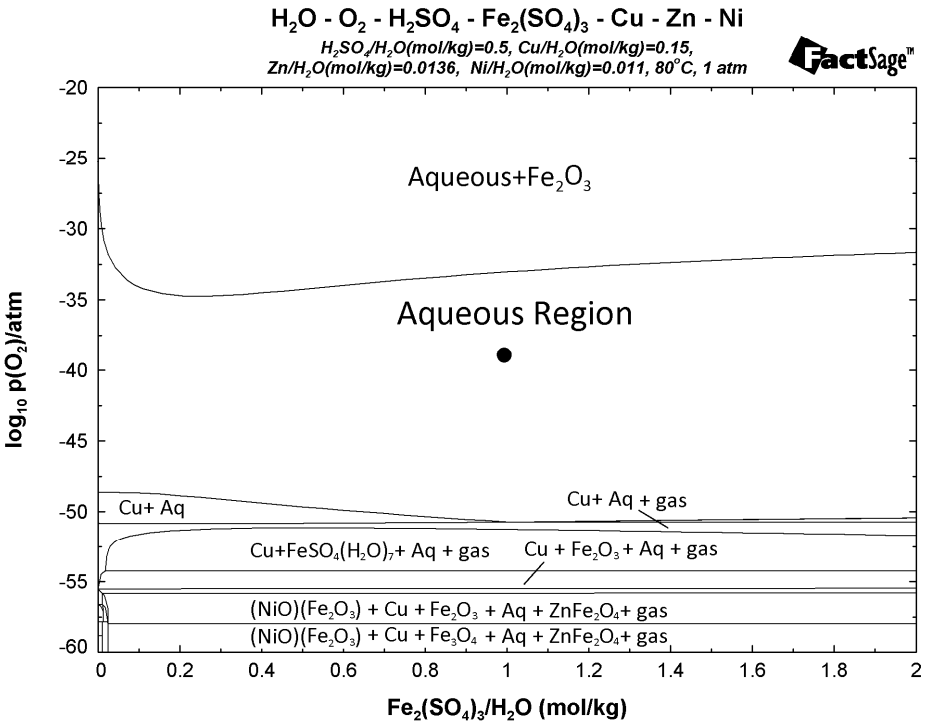

Fig. 5. Aqueous phase diagram – calculated partial pressure of O_2 vs molality of $Fe_2(SO_4)_3$ for the system H_2O-$Fe_2(SO_4)_3$-H_2SO_4-Cu-Zn-Ni under one of the present experimental conditions

Effect of liquid to solid phase ratio on the leaching

The weights of 20, 10 and 6.6 g of samples were leached in 200 ml of a solution containing 0.5 mol dm^{-3} $Fe_2(SO_4)_3$ + 0.5 mol dm^{-3} H_2SO_4 to determine the copper extraction yield from the PCB samples. Fig. 6 shows that the highest extraction (47.95 %) was achieved when the experiment was performed at L:S ratio of 20, at 333 K, with stirring rate 6.6 s^{-1} and 10 minutes of leaching.

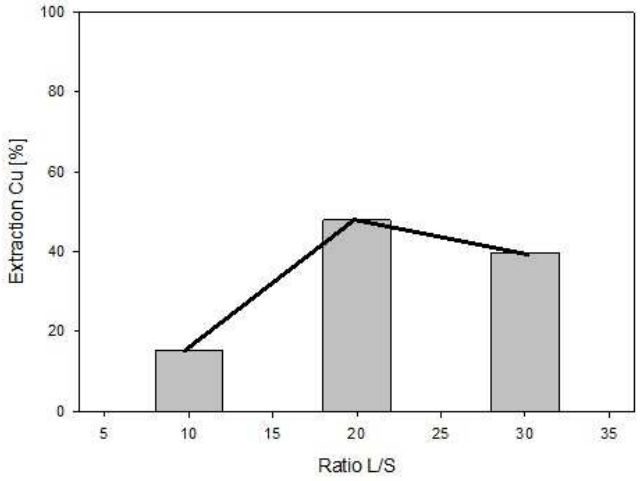

Fig. 6. Effect of liquid to solid ratio on copper extraction with 10 min. leaching

Effect of temperature

The leaching experiments were carried out at 313 K, 333 K, 353 K and 363 K and a liquid to solid ratio L/S 20 for the solution of 1 mol dm^{-3} $Fe_2(SO_4)_3$ + 0.5 mol dm^{-3} H_2SO_4 after 60 min of leaching. The positive effect on copper extraction of increasing leaching temperature is shown in Fig. 7. The highest Cu extraction (69.98 %) was achieved at 363 K after 15 min of leaching. No significant change was observed in Cu extraction after 30 minutes.

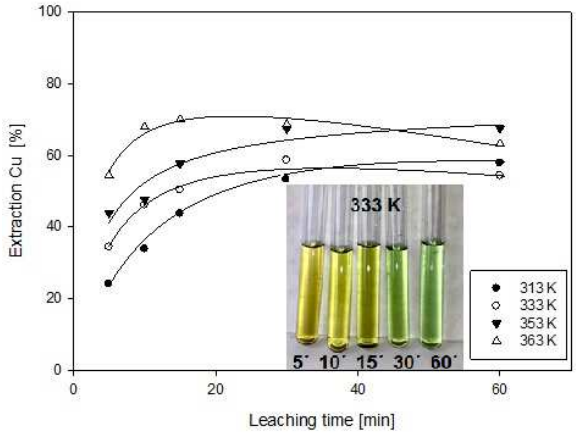

Fig. 7. Effect of temperature on copper extraction with time (1 mol $dm^{-3}Fe_2(SO_4)_3$ + 0.5 mol.dm^{-3} H_2SO_4, L/S 20, stirring rate 6.6 s^{-1})

The particle morphology of the treated sample, determined with a digital microscope (Dino-Lite ProAM413T), showed that the metallic parts were heterogeneously distributed throughout the sample (Fig.8a.). The sample was also studied with a digital microscope before and after leaching at 353 K and 60 min. The following figures show the morphological structures of the individual sample upon visual observation. It can be seen in Fig. 8 (a-b) that most of the metallic parts **X** found in the sample Fig.8a were dissolved after leaching sample **Y** in Fig. 9b.

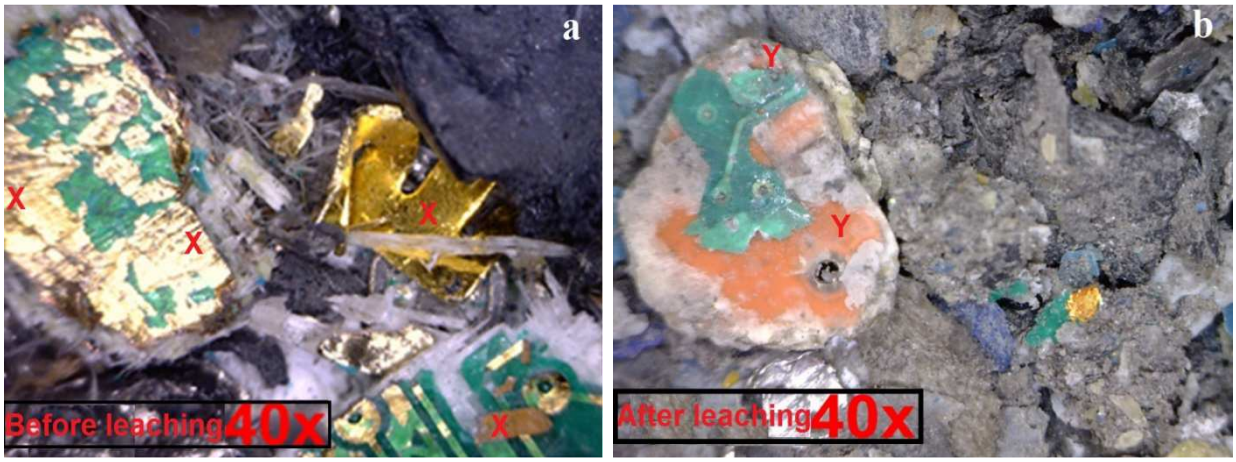

Fig. 8. Samples printed circuit boards a) before leaching, and b) after leaching at 353 K and 60 min (1 mol dm^{-3} $Fe_2(SO_4)_3$ + 0.5 mol.dm^{-3} H_2SO_4, L/S 10)

Effect of $Fe_2(SO_4)_3$ concentration

Fig. 9 shows the effect of leaching time on copper recovery with changing ferric sulfate concentrations ranging from 0.1 to 1 mol dm^{-3} $Fe_2(SO_4)_3$ at 0.5 mol dm^{-3} H_2SO_4 with L:S ratio of 20 at 313 K. The copper yield significantly increased with increasing concentration of ferric sulphate. The highest extraction of Cu (58.73 %) was achieved at 313 K after 30 min of leaching. Longer leaching durations did not give any more satisfactory result beyond 30 min.

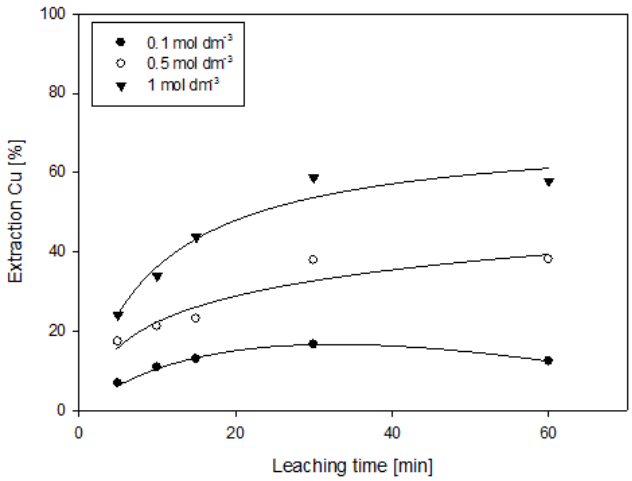

Fig. 9. Effect of $Fe_2(SO_4)_3$ concentration on copper extraction L/S 20, 6.6 $s^{-1}$and 313 K

Apparent Activation Energy "Ea" and Apparent Order of Reaction "n"

The apparent activation energy Ea was determined in the temperature interval of 313-363 K for the leaching solution of 1 mol.dm^{-3} $Fe_2(SO_4)_3$ + 0.5H_2SO_4 mol dm^{-3}. The apparent activation energy **Ea** was calculated experimentally by measuring the initial dissolution rate of copper at different temperatures **T** for the time interval of 0-300 s. The Arrhenius equation was used to determine the activation energy Eq. 2:

$$ln\, k = lnA - E_a/R\,.T \qquad (2)$$

where ***k*** is the rate constant, ***A*** is the frequency factor, ***R*** is the universal gas constant, and T is the temperature. The estimated **Ea** apparent activation energy for the sample was found to be 14.87 kJ mol^{-1} in the temperature interval from 313K to 363 K, and the frequency factor **A** was calculated as 0.2427 s^{-1}. It is generally believed that if the value of activation energy is higher than 40 kJ/mol, the process is chemically controlled, whereas values less than 20 kJ/mol suggest that the process is controlled by diffusion (Habashi, 1997).

The estimated Ea (14.87 kJ mol^{-1}) indicates that the leaching process is controlled by diffusion. The corresponding relationship between **ln k** and **1000/T** is shown in Fig. 10, which indicates that the mechanism for sample leaching in the temperature interval 313-363K does not change.

The apparent activation energy $\mathbf{E_a}$ and the apparent order of reaction **n** were determined using the linear regression method from Eq. 2 and Eq. 3, respectively (Cao et al., 2006; Kim and Lee, 2016).

The following concentration interval was used for determining the apparent order of reaction at temperature 313 K: from 0.1mol dm^{-3} to 1 mol dm^{-3} $Fe_2(SO_4)_3$.

The apparent order of reaction **n** with regard to the initial concentration of $Fe_2(SO_4)_3$ in the leaching solution was determined according to the following Eq. 3:

$$v_{Cu} = k.c_{Fe_2} \qquad (3)$$

or in logarithmic form Eq. 4:

$$lnv = lnk + n.lnc_{Fe_2} \qquad (4)$$

where **n** is the slope of the graph of $lnv_{Cu} = fc_{Fe_2}$, shown in Fig. 11. The value of n = 0.55 and $ln\, k$ = -7.104. The dissolution of Cu at the temperature of 313 K can be represented by the following Eq.5:

$$v = 8.21.10^{-4}c_{Fe_2} \qquad (5)$$

or in logarithmic form Eq. 6:

$$lnv = -7.104 + 0.55.lnc_{Fe_2} \quad (6)$$

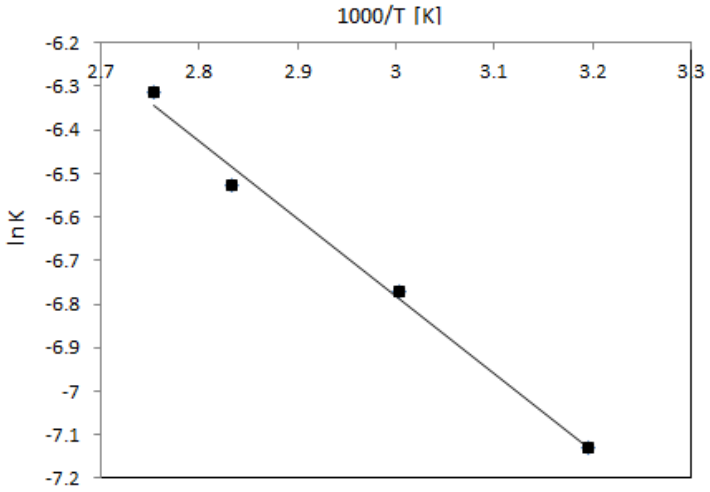

Fig. 10. Arrhenius plot for copper extraction from the waste sample: correlation coefficient R = -0.9957

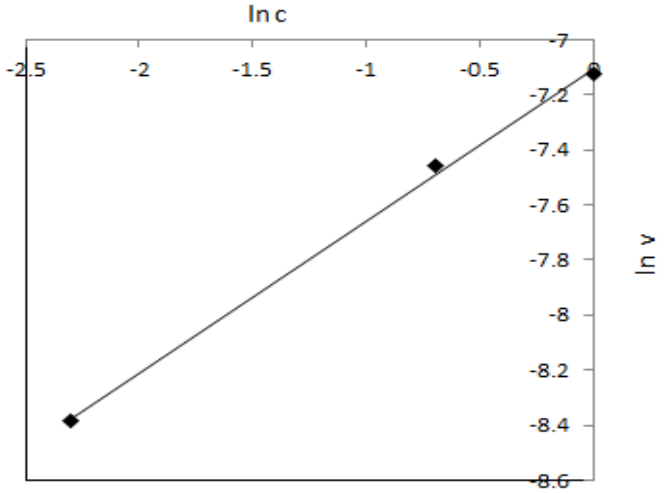

Fig 11. Logarithmic plot ln v versus ln C_{Fe_2} for waste sample: Correlation coefficient R = 0.99904

The result of the investigation was the finding that the best copper yields were achieved using 1 mol dm^{-3} $Fe_2(SO_4)_3$ + 0.5mol dm^{-3} H_2SO_4, at a temperature of 333K and liquid to solid phase ratio L:S 20. The conclusion and the ensuing recommendation was that the effect of milled mobile phones on Cu should be determined.

A cementation treatment has been proposed for the further treatment of the leached solution to precipitate out the copper as a saleable product in the presence of solid iron finings. The results of these experiments have been published elsewhere (Kovalcik, 2017). The proposed process flow sheet for the recovery of Cu from waste mobile phones is shown in Fig. 12

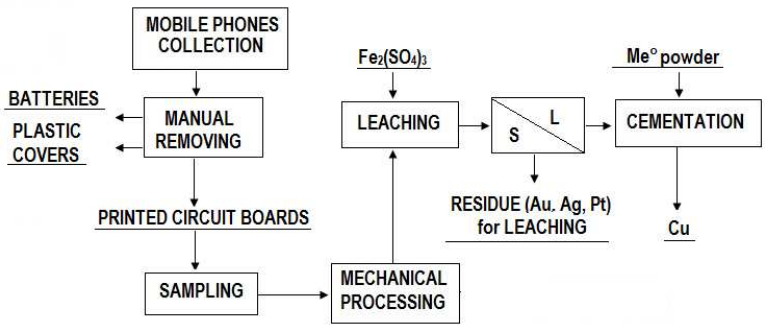

Fig.12. The proposed scheme of copper recovery from waste PCBs of mobile phones

Conclusions

Waste printed circuit boards from discarded mobile phones contain many interesting raw materials - base (copper 15%), precious (gold 400 g t), and rare metals. In the European Union, the biggest companies use pyrometallurgical process treatment methods based on smelting for metal recovery from electronic scrap on an industrial scale. The hydrometallurgy process of treatment printed circuit boards can achieve significantly lower environmental impacts than pyrometallurgy. From a life cycle perspective, the introduction of new technologies can also contribute to reducing greenhouse gases and, possibly, other environmental impacts.

The effects of temperature and concentration of ferric sulphate solution on the leaching rate of copper from milled discarded PCBs from button mobile phones were studied using the agitated leaching process in this research. The results show that the temperature has a significant effect on the leading rate of copper. According to the Arrhenius equation, the apparent activation energy value of the copper reaction for apparent activation energy value of copper reaction for the sample is calculated to be 14.87 kJ mol, under these conditions. On the basis of this value, it may be suggested that the process of leaching takes place in the diffusion region. The highest extraction Cu yield (69.98 %) was achieved at 363 K after 15 min of leaching when an L/S ratio of 20 and a solution of 1 mol dm^{-3} $Fe_2(SO_4)_3$ + 0.5 mol dm^{-3} were used. The apparent order of reaction with regard to the initial $Fe_2(SO_4)_3$ concentration was n = 0.55. Waste electronic materials such as discarded mobile phones are a secondary source of critical materials for the European Union. Hydrometallurgy could be one of the possible innovative ways to metals recovery from printed circuit boards of electronic waste materials.

Acknowledgement: *This work was supported by the Ministry for Education of the Slovak Republic under VEGA grant [1/0442/17] and VEGA grant [1/0631/17].*

References

Bale, C. W., Bélisle, E., Chartrand, P., Decterov, S. A., Eriksson, G., Gheribi, A. E., … Van Ende, M. A. (2016). FactSage thermochemical software and databases, 2010-2016. *Calphad: Computer Coupling of Phase Diagrams and Thermochemistry*, *54*, 35–53. https://doi.org/10.1016/j.calphad.2016.05.002

Behnamfard, A., Salarirad, M. M., & Veglio, F. (2013). Process development for recovery of copper and precious metals from waste printed circuit boards with emphasize on palladium and gold leaching and precipitation. *Waste Management*, *33*(11), 2354–2363. https://doi.org/10.1016/j.wasman.2013.07.017

Birloaga, I., De Michelis, I., Ferella, F., Buzatu, M., & Vegliò, F. (2013). Study on the influence of various factors in the hydrometallurgical processing of waste printed circuit boards for copper and gold recovery. *Waste Management*, *33*(4), 935–941. https://doi.org/10.1016/j.wasman.2013.01.003

Boliden. (2018). Retrieved from https://www.boliden.com/operations/smelters/boliden-ronnskar

Brown, T. J. (2018). *World mineral production 2012-2016,. British geological survey*. Retrieved from http://www.bgs.ac.uk/mineralsUK/statistics/worldStatistics.html

Camelino, S., Rao, J., Padilla, R. L., & Lucci, R. (2015). Initial Studies about Gold Leaching from Printed Circuit Boards (PCB's) of Waste Cell Phones. *Procedia Materials Science*, *9*, 105–112. https://doi.org/10.1016/j.mspro.2015.04.013

Cao, Y., Harjanto, S., Shibayama, A., Naitoh, I., Nanami, T., Kasahara, K., … Fujita, T. (2006). Kinetic Study on the Leaching of Pt, Pd and Rh from Automotive Catalyst Residue by Using Chloride Solutions. *Materials Transactions*, *47*(8), 2015–2024. https://doi.org/10.2320/matertrans.47.2015

Chi, T. D., Lee, J. C., Pandey, B. D., Yoo, K., & Jeong, J. (2011). Bioleaching of gold and copper from waste mobile phone PCBs by using a cyanogenic bacterium. In *Minerals Engineering* (pp. 1219–1222). https://doi.org/10.1016/j.mineng.2011.05.009

Cui, J., & Zhang, L. (2008). Metallurgical recovery of metals from electronic waste: A review. *Journal of Hazardous Materials*. https://doi.org/10.1016/j.jhazmat.2008.02.001

Dutta, D., Panda, R., Kumari, A., Goel, S., & Jha, M. K. (2018). Sustainable recycling process for metals recovery from used printed circuit boards (PCBs). *Sustainable Materials and Technologies*, *17*, e00066. https://doi.org/10.1016/j.susmat.2018.e00066

European Parliament, & The Council Of The European Union. (2012). Directive 2012/19/EU of the European Parliament and of the Council on waste electrical and electronic equipment (WEEE). *Official Journal of the European Union*. https://doi.org/10.3000/19770677.L_2012.197.eng

Ha, V. H., Lee, J. C., Huynh, T. H., Jeong, J., & Pandey, B. D. (2014). Optimizing the thiosulfate leaching of gold from printed circuit boards of discarded mobile phone. *Hydrometallurgy*, *149*, 118–126. https://doi.org/10.1016/j.hydromet.2014.07.007

Habashi, F. (1997). handbook of extractive metallurgy I.pdf. *Handbook of Extractive Metallurgy*, *Vol.2*.

Hagelüken, C. (2006). Recycling of electronic scrap at Umicore's integrated metals smelter and refinery. *Erzmetall*, *59*(3), 152–161.

Havlik, T. (2008). *Hydrometallurgy*. *Hydrometallurgy*. https://doi.org/10.1533/9781845694616

Havlik, T., Orac, D., Petranikova, M., & Miskufova, A. (2011). Hydrometallurgical treatment of used printed circuit boards after thermal treatment. *Waste Management*, *31*(7), 1542–1546. https://doi.org/10.1016/j.wasman.2011.02.012

Jing-ying, L., Xiu-li, X., & Wen-quan, L. (2012). Thiourea leaching gold and silver from the printed circuit boards of waste mobile phones. *Waste Management*, *32*(6), 1209–1212. https://doi.org/10.1016/j.wasman.2012.01.026

Kasper, A. C., Veit, H. M., García-Gabaldón, M., & Herranz, V. P. (2018). Electrochemical study of gold recovery from ammoniacal thiosulfate, simulating the PCBs leaching of mobile phones. *Electrochimica Acta*, *259*, 500–509. https://doi.org/10.1016/j.electacta.2017.10.161

Kim, E. Y., Kim, M. S., Lee, J. C., Jeong, J., & Pandey, B. D. (2011). Leaching kinetics of copper from waste printed circuit boards by electro-generated chlorine in HCl solution. *Hydrometallurgy*, *107*, 124–132. https://doi.org/10.1016/j.hydromet.2011.02.009

Kim, E. Y., Kim, M. S., Lee, J. C., & Pandey, B. D. (2011). Selective recovery of gold from waste mobile phone PCBs by hydrometallurgical process. *Journal of Hazardous Materials*, *198*, 206–215. https://doi.org/10.1016/j.jhazmat.2011.10.034

Kim, Y., & Lee, J. (2016). Leaching Kinetics of Zinc from Metal Oxide Varistors (MOVs) with Sulfuric Acid. *Metals*, *6*(8), 192. https://doi.org/10.3390/met6080192

Kovalcik, T. (2017). *Gold recovery from discarded mobile phones*. Technical university of Kosice.

Laubertova, M.; Sandorova, K. (2013). Hydrometallurgical recovery of copper and gold from spent mobile phones (pp. 171–180). Liptovsky Jan; Slovakia.

Laubertova, M.; Trpcevska, J.; Novicky, M. (2012). Designing technology for metal recovery from discarded mobile phones (pp. 124–131). Usti nad Labem: ICTKI.

Laubertova, M., Novicky, M., & Vindt, T. (2011). The possibilities of hydrometallurgical treatment of discarded mobile phones, 412–418. Retrieved from http://censo.sk/content/clanky/201105.pdf

Laubertová, M., Pirošková, J., & Dociová, S. (2017). The technology of lead production from waste. *World of Metallurgy - ERZMETALL*, *70*(1), 47–54.

Laubertova, M., Trpcevska, J., & Malindzakova, M. (2018). Logistics of the Electronic Waste Sampling Procedure: The Influence of Granularity on Determination of Copper Content in PCBs. *Polish Journal of Environmental Studies*, *27*(4), 1593–1599. https://doi.org/10.15244/pjoes/77049

Maurell-Lopez, S., Gül, S., Friedrich, B., Ayhan, M., & Eschen, M. (2011). Metallurgical fundamentals for an autothermic melting of WEEE in a top blown rotary converter. In *Proceedings - European Metallurgical Conference, EMC 2011* (pp. 1–15).

Mickova, V. et al. (2018). Sampling and digestion of waste mobile phones printed circuit boards for Cu, Pb, Ni, and Zn determination. *Chemical Papers*. https://doi.org/https://doi.org/10.1007/s11696-017-0353-y

Moskalyk, R. R., & Alfantazi, A. M. (2003). Review of copper pyrometallurgical practice: Today and tomorrow. *Minerals Engineering*. https://doi.org/10.1016/j.mineng.2003.08.002

Number of mobile phone users worldwide from 2013 to 2019 (in billions). (2018). Retrieved April 9, 2018, from https://www.statista.com/statistics/274774/forecast-of-mobile-phone-users-worldwide/

Palmieri, R., Bonifazi, G., & Serranti, S. (2014). Recycling-oriented characterization of plastic frames and printed circuit boards from mobile phones by electronic and chemical imaging. *Waste Management*, *34*(11), 2120–2130. https://doi.org/10.1016/j.wasman.2014.06.003

Rocchetti, L., Amato, A., & Beolchini, F. (2018). Printed circuit board recycling: A patent review. *Journal of Cleaner Production*. https://doi.org/10.1016/j.jclepro.2018.01.076

Roine, A. (2002). Outokumpu HSC Chemistry for Windows: Chemical Reaction and Equilibrium Software with Extensive Thermochemical Database. *User's Guide*.

Rudnik, E., KoŁczyk, K., & KutyŁa, D. (2015). Comparative studies on hydrometallurgical treatment of smelted low-grade electronic scraps for selective copper recovery. *Transactions of Nonferrous Metals Society of China (English Edition)*, *25*, 2763 − 2771. https://doi.org/10.1016/S1003-6326(15)63901-2

Sarath, P., Bonda, S., Mohanty, S., & Nayak, S. K. (2015). Mobile phone waste management and recycling: Views and trends. *Waste Management*. https://doi.org/10.1016/j.wasman.2015.09.013

Secondary copper production up 6% in first quarter of 2018. (2018). Retrieved from https://recyclinginternational.com/magazine/summer-issue-2018/pdf-viewer/

Trung, Z. H., Kukurugya, F., Takacova, Z., Orac, D., Laubertova, M., Miskufova, A., & Havlik, T. (2011). Acidic leaching both of zinc and iron from basic oxygen furnace sludge. *Journal of Hazardous Materials*, *192*, 1100–1107. https://doi.org/10.1016/j.jhazmat.2011.06.016

Waste Electrical & Electronic Equipment (WEEE). (2018). Retrieved January 15, 2018, from

http://ec.europa.eu/environment/waste/weee/index_en.htm

Xiu, F. R., Qi, Y., & Zhang, F. S. (2015). Leaching of Au, Ag, and Pd from waste printed circuit boards of mobile phone by iodide lixiviant after supercritical water pre-treatment. *Waste Management*, *41*, 134–141. https://doi.org/10.1016/j.wasman.2015.02.020

Yang, H., Liu, J., & Yang, J. (2011). Leaching copper from shredded particles of waste printed circuit boards. *Journal of Hazardous Materials*, *187*, 393–400. https://doi.org/10.1016/j.jhazmat.2011.01.051

Zazycki, M. A., Tanabe, E. H., Bertuol, D. A., & Dotto, G. L. (2017). Adsorption of valuable metals from leachates of mobile phone wastes using biopolymers and activated carbon. *Journal of Environmental Management*. https://doi.org/10.1016/j.jenvman.2016.11.078

Factors determining the construction and location of underground gas storage facilities

***Kornelia Osieczko*[1], *Andrzej Gazda*[2] *and* *Dušan Malindžák*[3]**

The growing demand for earth gas results in need for storing proper volumes of this fuel to ensure national energy security. Poland has its own earth gas reservoirs, but their exploitation cannot fully cover the constantly increasing demand. Most of the required volumes are covered by gas import, mainly from the Russian Federation. However, long-term agreements do not envisage seasonal variations, which causes that surplus volumes must be stored at underground storage facilities. Additionally, Poland's National Energy Policy imposes an obligation to store the reserves of this fuel. All of these factors determine the construction and development of underground gas storage facilities.

In recent years, a growing trend in building new and extending the existing gas storage facilities has been noticeable in the European Union. Most often, depleted gas and oil reservoirs, salt caverns and aquifers are used for that purpose. The most suitable locations of these types of storage facilities are areas near urban centres that are the final gas recipients. The construction of underground gas storage facilities is also related to the development of the gas transmission system. EU countries, including Poland, continue development of UGS facilities, aiming at diversification of gas supplies. It is also related to other activities, such as launching the LNG terminal in Świnoujście and searching for alternative gas suppliers.

Creating an efficient system of underground gas storage facilities should be focused on securing strategic reserves, balancing seasonal demand variability and optimising the transmission system throughout the country. In order to ensure the undisturbed function of the entire economy, countries maintain gas reserves in case of a failure or an interruption in the continuity of supplies. Additionally, continuous development allows using underground gas storage facilities commercially.

Keywords: *underground gas storage, location, geological structure, energy security*

Introduction

According to the BP Statistical Review of World Energy 2016, world demand for energy is rapidly growing. That growth is expected to stay around 34% in the period from 2015 to 2035, with an average yearly rate of 1.4% (PGI, 2017). Current forecasts indicate that fossil fuels should remain the major sources of energy until 2035. They are believed to constitute up to 80% of the world power supplies, covering 60% of the expected demand increase (Charun, 2004).

The demand for earth gas grows most rapidly when compared to other fossil fuels (IEA, 2014). This fuel is used in many branches of economy, in the industry, services sector, in households, as well as in the electric energy production sector (Mokrzycki, Szurlej, 2003).

Considering the world forecasts presented above, as well as earth gas exploitation in Poland, which covers 28.5% of the total usage, according to the data of 2015 (PGI, 2017), the efforts made to guarantee sufficient gas reserves in the following years seem understandable. Currently, the remaining gas volume is imported. The major earth gas supplier, not only for Poland but also for other European countries, is the Russian Federation.

Taking into account the need to ensure energy security of the country, reliability of gas supplies must be guaranteed through diversification of sources and become less dependent from a single major supplier. The document signed in 2009, "Poland's Energy Policy until 2030" envisaged the construction of the infrastructure allowing to reorganise gas import using the geographical situation of Poland with access to the Baltic Sea. This goal has been reached, and the LNG terminal in Świnoujście was launched in 2015. It has become a major gas hub in the north-east of Europe, performing transfer procedures and regasification of liquefied earth gas, offering the possibility to import gas from Norway or the USA (Egging, Holz, 2016). It is worth considering the various options for building natural gas storage facilities. Rehabilitation of abandoned mines makes it possible to implement new ways of use of closed mines and improve the economic and ecological situation in "mining cities" (Migaleva et al., 2018). An important element is also a way to obtain information from the stakeholders and take them into account when making decisions (Hąbek et al., 2019).

Considering the energy security of Poland, another important aspect can be distinguished, related with securing gas reserves based on extensive storage facilities, to allow to respond to the changes in demand/supply

[1] *Kornelia Osieczko,* Rzeszów University of Technology, Faculty of Management, Powstańców Warszawy 12, 35959 Rzeszów, Poland, *k.osieczko@prz.edu.pl*

[2] *Andrzej Gazda,* Rzeszów University of Technology, Faculty of Management, Powstańców Warszawy 12, 35959 Rzeszów, Poland, *agazda@prz.edu.pl*

[3] *Dušan Malindžák,* Technical University of Košice, Faculty BERG, Let ná 9, 04001 Košice, Slovakia, *dusan.malindzak@tuke.sk*

and fluctuation of prices. One of the instruments allowing to fulfil these assumptions, by encouraging competition on the gas market and improving the energy security of Poland, is increasing the working volumes of underground gas storage facilities (UGS). Additionally, the amendment to the Polish Energy Law of July 2005 contained a provision concerning the obligation to store imported gas. The legal aspect, as well as the internal policy, lead to searching solutions in this area (Kochanek, 2007). The purpose of this paper is to present the factors determining the construction and location of underground gas storage facilities, as well as to provide an outline of the principles of UGS functioning, using the example of the Strachocina USG.

Based on the forecast of the need to create natural gas underground gas reserves in Poland in 2035 and possible current locations for natural gas storage and the construction of new gas storage, it depends on a number of different economic, environmental, capacity, time, investment, policy, security. The problem can be defined as the role of multi-criteria assessment. The article proposes a methodology and a solution to how to use individual locations to increase the USG's need to cover the gradually rising level of natural gas reserves.

Methodology and theory background of solution

Deciding on serious strategic investments requires a scientific approach to decision making, decision making on a wide range of factors, and the various areas between which it is difficult to describe relationships. Such issues are addressed by multi-criterion decision-making methods as Weighted Method, AHP Method, Scoring Method, etc. (Malindžák et al., 2015). For the solution of the problem, a weighted sum method was applied.

In case we want to concentrate all factors or criteria into one decision – into one indicator, we use this method:

- Factors have a different character from quantification and casualness point of view,
- Factors are from different areas – business, manufacturing, distribution, etc.
- They have different significance related to the analysis objective.

Algorithm of such method follows:

a) Factor and criteria selection for the evaluation and decision F_1, F_2, ... F_n.
b) Evaluation of important factors contributing to a fulfillment of the main objective – assigning of factors' weights w_i. It is advised to select the factors and define the weights by an expert. Weights wi express factor's importance but at the same time, express the proportion of significance among the factors. From a practical point of view, it is advised to make the sum of weights equal to number 1. (It is related to a visual dividing of a "unit circle cake"). Figure 1 shows evaluation according to the Ratio-index method.

$$\sum_{i=1}^{n} w_i = 1$$

In case this is not valid, factors are normalised.

$$w_{ij} = \frac{w_i}{\sum_{i=1}^{n} w_i}, \quad i = 1, 2, \ldots n,$$

And the sum is $\sum_{i=1}^{n} w_{ii} = 1$.

Particular variants V_j are evaluated with the help of selected factors (HV_j – variant evaluation V_j). We evaluate particular factors F_i – (HF_{ij}) for each variant V_j. Factors are evaluated according to a pre-defined interval, so-called potency rate – K

$$HF_{ij} \in \langle 1, K \rangle$$

Potency rate value means the evaluation interval and defines the sensitivity of the method. The larger the amount of variants and factors is the larger interval, and higher potency rate becomes.

Variant evaluation

$$HV_j = \sum_{i=1}^{n} HF_{ij} * w_i$$

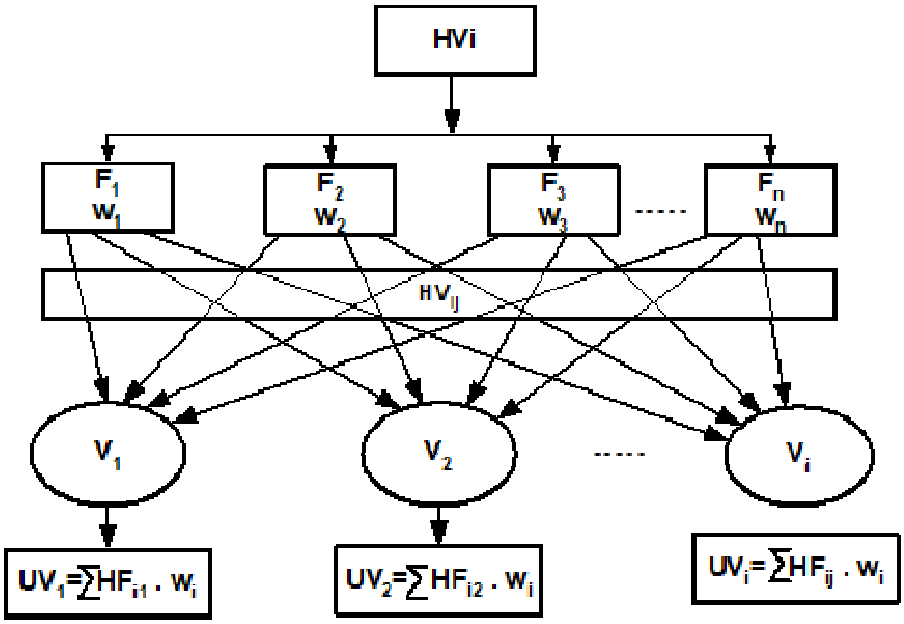

Fig. 1. Evaluation according to Ratio-index method

Factors are evaluated according to a pre-defined interval, so-called potency rate – K

$$HF_{ij} \in \langle 1, K \rangle$$

Potency rate value means an evaluation interval and defines the sensitivity of the method. The larger the amount of variants and factors is the larger interval, and higher potency rate becomes.

Variant evaluation

$$HV_j = \sum_{i=1}^{n} HF_{ij} * w_i$$

Analysis can be defined by minimalisation, meaning that the smaller evaluation HF_{ij} is the better, respectively vice versa by maximisation. The higher HF_{ij} is, the better and the same is valid for the weights w.

The solution then is

$$V_j(optim) = \min_j \langle HV_j \rangle$$

In the case of company analysis and evaluation, then we are talking about the evaluation of only one variant.

It is necessary to formulate both negative and positive factors in one form so they will become the same – either positive or negative. For example, in the case of evaluation of suppliers:

for example, F_1 – the amount of distribution per month (the bigger, the better)

F_2 – the time from the order till delivery (the smaller, the better)

In the case, for example, F_1 will be re-formulated – intervals between distribution (the smaller, the better) in case of a minimalisation task.

From a practical point of view, it is necessary to create the following evaluation table 1:

Tab. 1. Example evaluation table

Title of factor i	Factor I weight	Variant 1		Variant 2		...	Variant j	
F_1 F_2 F_3 F_4	w_1 w_2 w_3	HF_{11} HF_{12}	$HF_{11}.w_1$ $HF_{12}.w_2$.	HF_{21} HF_{22}	$HF_{21}.w_1$ $HF_{22}.w_2$.	...	HF_{j1} HF_{j2}	$HF_{j1}.w_1$ $HF_{j2}.w_2$
F_n	w_n	HF_{1n}	$HF_{1n}.w_n$	HF_{2n}	$HF_{2n}.w_n$		HF_{jn}	$HF_{jn}.w_n$
Total variant evaluation			HV1		HV2			HVj

Characteristics of usage and reasons behind earth gas storing

Earth gas belongs to the group of energy carriers with growing market participation due to economic and ecological considerations. It consists of a mixture of hydrocarbons (methane, ethane) and small portions of hydrogen, nitrogen, oxygen, hydrogen sulfide, helium and carbon disulfide. Gaseous fuels are easy in transfer, storage and distribution. Their scope of application includes the generation of thermal and electric energy as well as powering combustion engines. In comparison with other fuels, gas combustion processes are characterised by lower emission of contaminants. Earth gas is useful in municipal services and in households. Furthermore, in the chemical industry, it allows reducing the power consumption of various processes (PGNiG, 2017).

Poland has 292 earth gas reservoirs, including 207 exploited and 53 unexploited reservoirs. The exploitation of 32 gas reservoirs has been ceased. The volume of exploitable gas resources was 125.04 billion cubic metres in 2015. Most of the documented gas resources are reservoirs located in the Polish Lowlands (66.5%). The largest high-methane earth gas reservoirs in that area include Paproć, Załęcze, Kościan, Brońsko, Baranówko-Mostno-Buszewo, Radlin and Żuchlów. Around 29.3% of the resources are located in the Carpathian Foothills area. The largest earth gas reservoir in Poland is Przemyśl, with over 86 million cubic metres of this fuel. Other areas where earth gas can be found are Pilzno, Jasionka, Leżajsk, Żołynia, Jarosław, Dzików and Lubaczów. Figure 2 presents earth gas reservoirs locations in Poland.

Fig.2. Gas fields in Poland (PGNiG, 2018)

The 2015 data indicate that gas in the volume of 4,447.9 million cubic metres was extracted from domestic sources in Poland. The remaining part of the demand (11,174.48 million cubic metres) was covered by gas imported from Russia (9,549.1 million cubic metres), Germany (1,625.16 million cubic metres) and Czech Republic (0.22 million cubic metres) (PGI, 18.12.2017). In Poland, earth gas is distributed by pipelines. The largest volumes of this fuel are supplied by Russian Gazprom, through the Yamal-Europe pipeline. The flow capacity of the first leg is 32.3 billion cubic metres.

The documented Polish earth gas reservoirs remain under control of the *Polskie Górnictwo Naftowe iGazownictwo* S.A. (PGNiG). Their capacity reaches 98 billion cubic metres. Currently, PGNiG supplies gas to 6.5 million customers, including households, companies - combined heat and power plants, steel mills and nitrogen compounds plants. Within the last few years, the volume of gas extracted by PGNiG increased from approx. 3.6 billion cubic metres in 1998 to approx. 4.3 billion cubic metres in 2015. Extraction of high-methane gas recorded by the Sanok branch of the company reached 1.9 billion cubic metres, while the facility in Zielona Góra delivered 2.4 billion cubic metres.

The dynamic economic growth of Poland requires controlling gas storage facilities located in every region. Due to the lack of natural reservoirs in central and north Poland, further development of the national gas supply system should be based on the underground gas storage facilities (UGS), built not only in depleted reservoirs but also in aquifers and salt caverns (Filar, Kwilosz, 2008).

Previously, the primary function of underground gas storage facilities was to maintain commercial reserves. Their primary goal is to secure gas supply continuity in emergency situations, or in case of an unexpected

demand increase, and also to minimise the consequences of incidents threatening the national energy security. Long-term gas import agreements do not provide for seasonal consumption variations that are common in the European climatic zone. In summer months, surplus imported gas is stored at UGS facilities and covers peak demands during winter months, caused, among others, by increased gas consumption for heating. Additionally, underground gas storage facilities allow responding to increasing or decreasing blue fuel prices (Brzeziński and Wawrzynowicz, 2014).

The gas supply standard assumed in Poland is approx. 862 million cubic metres for 30 days of extra high earth gas consumption. Taking into account the expected increase in earth gas consumption in the power engineering sector, from 3.5% in 2013 to 30% in 2050, great emphasis is placed on ensuring the stability of the gas supply system and securing access to sufficient storage volumes (BiP, 2018). The total working capacity of UGS reached 2.5 billion cubic metres in 2014. Until 2021, that capacity should increase to 3.3 billion cubic metres, which would be 20% of the envisaged demand for gas during that period.

As far as the other EU member states are concerned, construction and development of underground gas storage facilities are related with energy policy priorities, the scale of gas consumption and the size of the existing gas transmission and distribution system, as well as the wealth of the country and its inhabitants. Table 2 presents the number of UGS facilities in individual countries, total working capacity and maximum deliverability in 2010 and 2015.

Table 2. Underground gas storage facilities (USG) in EU countries, 2010 and 2015 (Eurogas, 2014).

No.	Country	ISO 3166 sign	2010			2015		
			Number of UGS	Total working capacity [millions m3]	Maximum deliverability [millions m3/day]	Number of UGS	Total working capacity [millions m3]	Maximum deliverability [millions m3/day]
1.	Austria	AT	5	4,744	55	8	8,250	95
2.	Belgium	BE	1	600	25	2	1,085	57
3.	Bulgaria	BG	1	600	4	1	550	4
4.	Croatia	HR	0	0	0	1	553	6
5.	Czech Republic	CZ	8	3,127	52	8	3,517	59
6.	Denmark	DK	2	980	16	2	1,035	25
7.	France	FR	15	11,900	200	16	12,894	265
8.	Spain	ES	2	2,367	13	4	2,457	16
9.	Ireland	IE	1	230	3	1	230	3
10.	Latvia	LV	1	2,325	24	1	2,300	30
11.	Netherlands	NL	3	5,000	145	6	12,078	305
12.	Germany	DE	47	20,804	494	51	24,588	637
13.	Poland	PL	7	1,640	32	9	2,915	41
14.	Portugal	PT	1	175	2	6	333	8
15.	Romania	RO	8	3,110	28	7	3,050	28
16.	Slovakia	SK	6	2,770	34	2	3,156	46
17.	Slovenia	SL	0	0	0	1	2,300	30
18.	Sweden	SE	1	9	1	1	9	1
19.	Hungary	HU	5	4,340	55	5	6,330	74
20.	Great Britain	GB	6	4,480	86	8	4,528	154
21.	Italy	IT	10	14,336	152	13	16,696	332
∑			130	78,793	-	153	108,854	-

Underground gas storage facilities secure the operation of gas transmission systems in individual countries (Bergman, 2006; Hill, 2006). The data presented in Table 2 indicates a growing trend in launching new UGS facilities. From 2010 to 2015, 23 UGS facilities were built, which resulted in an increase in the working capacity by 30,061 million cubic metres. Poland was in the 11th place in this ranking in terms of working capacity. The largest number of USG facilities operated in Germany.

Gas storage capabilities characteristics

Building an appropriate network of USG facilities in Poland should secure the basic functions related with maintaining strategic reserves, balancing seasonal gas consumption variability and optimising the gas transmission system in terms of estimation of gas volume to be imported (Ciechanowska, 2016). In Poland, it is both possible to develop the existing storage infrastructure and build new facilities. Suitable geological structures

can be found and staff experienced in designing and building USG facilities is available. The development of underground gas storage facilities is followed by the necessity to extend the transmission pipelines.

Storing gas underground is much safer and more advantageous than constructing gas storages on the ground, which require a lot of space and are more vulnerable to acts of terrorism. Due to strict safety standards that must be met, the costs of construction and maintenance of that type of storage facilities is higher (Czapowski, 2006). The basic requirements for underground storage facilities are complete tightness and lack of any adverse reactions between gas and the surrounding rocks. Other desirable features include location in the vicinity of urban or industrial areas, closeness to existing gas pipelines and large capacity.

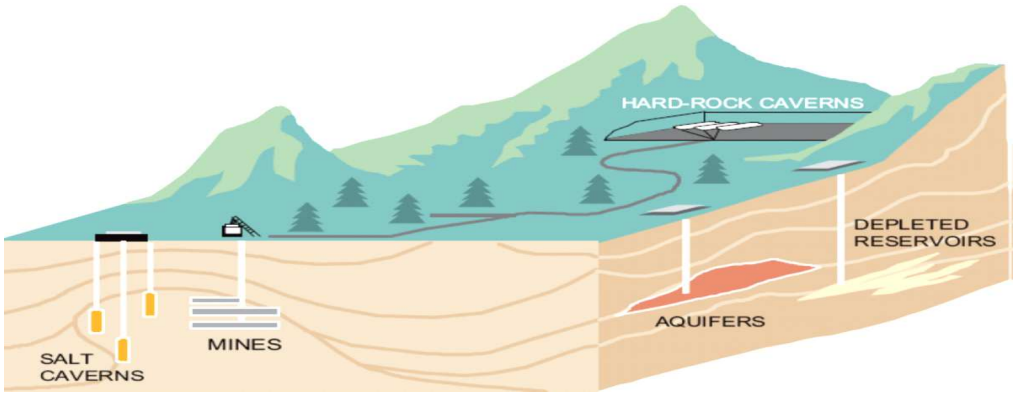

Fig.3. Gas storage using geological structures (AGH, 12 Feb 2017)

Hydrocarbons are stored underground in depleted gas and oil reservoirs, salt caverns and selected aquifers, and also in natural hard-rock caverns or old mines. Figure 3 presents all these types of structures.

Storage in selected aquifers is very expensive due to the protection of groundwater reservoirs. Additionally, selecting a suitable structure requires a lot of exploration and identification work. When a suitable structure is selected, it might not be properly tight (Schafer et al., 1993). Therefore, no structures of this type have been used in Poland so far. The advantages of storing gas in aquifers include high deliverability rate, the possibility of performing a number of cycles during the season and the fact that they are usually located close to final recipients. Mesozoic, Jurassic and Cretaceous aquifers within the anticlines: around Łódź, Warsaw and Szczecin, are also expensive in use but offer quite convenient storage conditions (Polit et al., 2010). Table 3 presents financial outlays and average construction time of UGS facilities depending on the type of structure.

Table 3. Cost and time of construction of different types of UGS

Type of UGS	Average financial outlays [euro/m3]	Average construction time [years]
Aquifers	0.7-1	10-12
Depleted reservoir	0.6-1	5-8
Salt cavern	0.8-1.2	5-10

A relatively cheap and most common form of storage of gaseous hydrocarbons (75% of all facilities in the world), is injecting gas into the porous spaces of depleted gas and oil reservoirs. This method is very advantageous due to the available storage capacity reaching hundreds of millions up to several billion cubic metres of gas. Depleted reservoirs are usually connected with pipelines, there are already existing wells, and their structure is known due to performed seismic and geophysical analyses as well as exploitation records. It is reflected in lower costs of construction of this type of storage facility.

The most suitable rocks in terms of using porous space are sedimentary rocks, especially sandstones, characterised by permeability that allows migration and formation of natural accumulation zones. There are 7 earth gas storage facilities of this type in Poland: Husów, Strachocina, Swarzów, Brzeźnica, Wierzchowice, Bonikowo and Daszewo. They are mostly situated in the Meso–Cenozoic gas reservoirs. Figure 4 presents the location of underground gas storage facilities in Poland. The UGS facilities located in depleted reservoirs are usually capable of performing only a single injection/extraction cycle during a year.

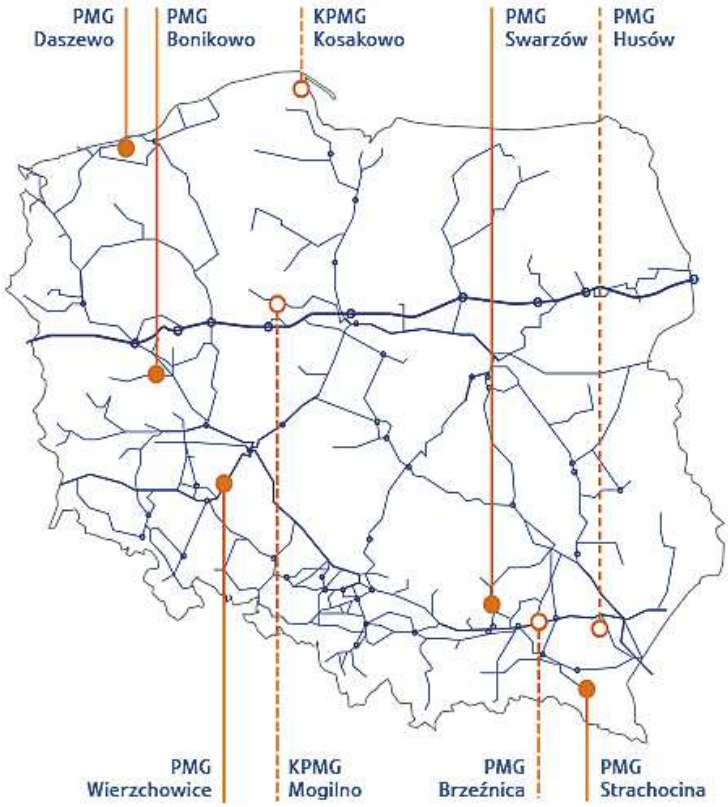

Fig.4. Gas storage facilities in Poland (PGNiG, 18 Dec 2012)

Caverns formed in halite deposits serve as underground storages of a special type. When compared with storage facilities in depleted oil and gas reservoirs, they are more expensive in construction but offer many advantages. This solution ensures complete and fast extraction of the injected medium and the structures can be used for waste disposal when they are no more used as gas storage facilities. These UGS facilities are characterised by very large injection and deliverability rate. They are also capable of being used in several injection/extraction cycles in a year, which enables balancing lower, for example, daily variations of earth gas demand and supply. The building of this type of storage facilities is related to high investment outlays and operating costs.

Favourable conditions for building salt cavern gas storage facilities are in bedded salt deposits with simple and homogeneous structure as well as Zechstein halite structures in salt domes. There are two underground salt cavern gas storage facilities in Poland: Mogilno and Kosakowo (Czapowski, 2006; Kochanek, 2007). Salt-bearing rocks provide good storage conditions due to constant temperature and low humidity. Salt is impermeable and very suitable for storing earth gas, liquefied gas and chemical substances (Evants et al., 2009). Gas can be stored in old salt mines and salt caverns, or in specially designed and built storage chambers (Kunstman et al., 2009; Siemek, Nagy, 2007). Germany has the largest number of cavern storage facilities in use (32 storage facilities in 266 caverns with a total capacity of 19.98 million cubic metres) (EID, 2017).

Operation of the Strachocina underground gas storage facility and development plan

The Strachocina underground gas storage facility is located in south-east Poland, in the Sanok and Brzozów communes area. The geological fold in that region contains flysch rocks of the Lower Cretaceous period (Stasiowski, Wagner-Staszewska, 2010). Until the second half of the 19th century, that fold was a subject of geological and drilling analyses, due to the occurrence of gas exhalations and oil outflows. The gas reservoir was discovered in 1928 when the first wells were drilled. A decision to transform the reservoir into underground gas storage was made in the 1990s.

Gas pipelines are installed in directional wells made by horizontal drilling. The currently used drilling technology allows reducing the costs of exploitation of power resources, improving the availability of the reservoir. The purpose of the horizontal wells at the Strachocina UGS is to reduce turbulences and increase gas storage efficiency (Pielech, 2017). The working capacity of that UGS is 360 million cubic metres.

Taking national energy security into account, infrastructure development is another important factor besides building underground storage facilities. Currently, the transmission system of the Strachocina UGS is extended

and modernised, along with the new Poland-Slovakia gas interconnector. 72 kilometres of gas pipeline Hermanowice-Strachocina shall be completed by 2018, including the execution of other related investment tasks. It is an important part of the implementation of the Central-European North-South Gas Corridor concept in Poland. The primary function of the new gas pipeline is the improvement of the technical conditions of gas transmission and improving the continuity and safety of gas supply to recipients. The planned investments in the national gas transmission system are presented in Figure 5.

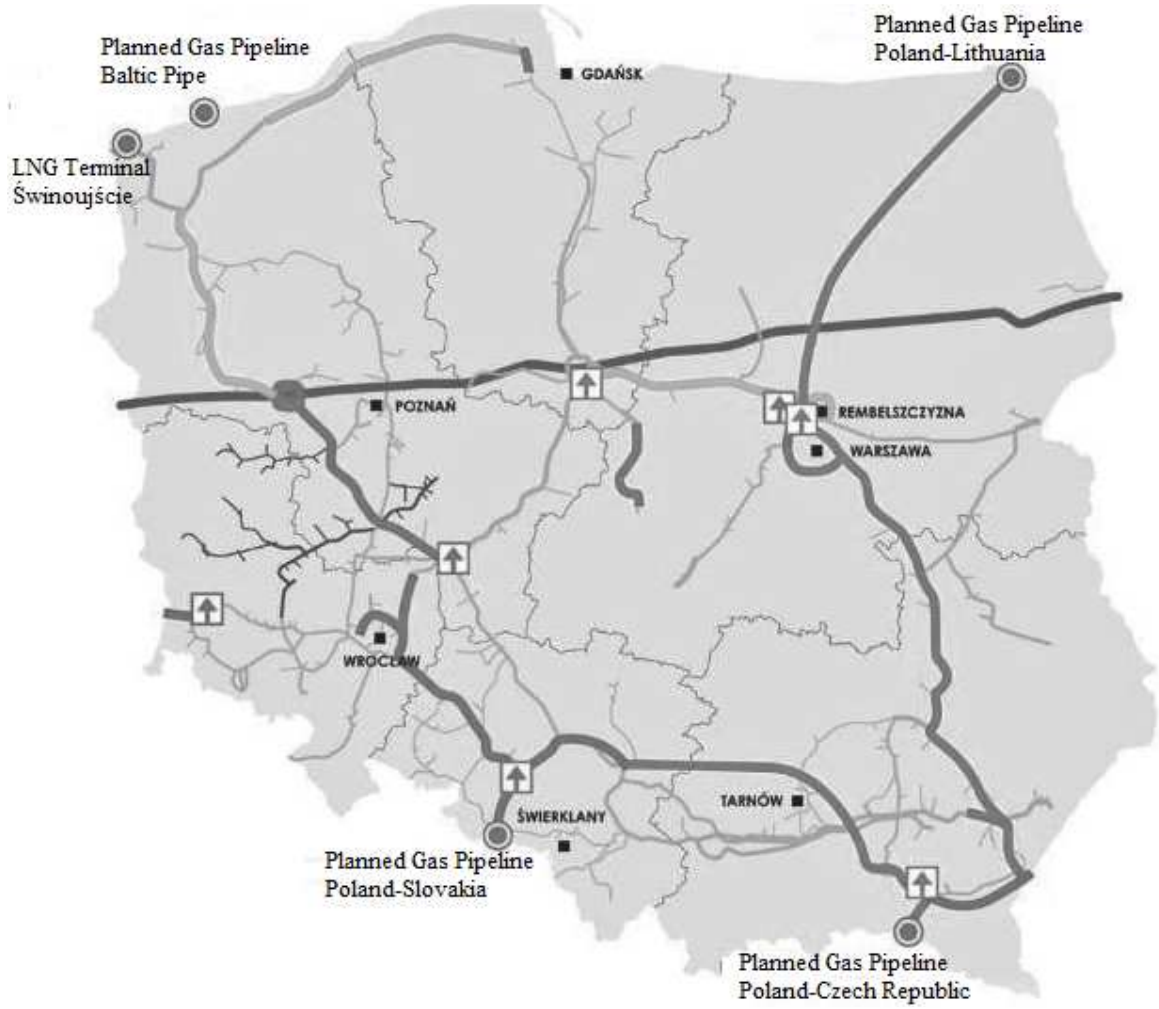

Fig. 5. Planned investments in the Polish gas transmission system until 2023 (Gaz-System, 2015)

Gas pipelines (for example, Poland-Lithuania, Poland-Czech Republic) are under development throughout Poland. It aims at building a well-functioning and uniform (in terms of operating parameters) main gas transmission network. Directions of physical gas supplies will be diversified, ensuring flexibility and continuity of supplies, and also creating conditions for the rapid growth of the national economy. It is envisaged that every client will have an option to buy gas from a selected source by 2023, getting better access to the global gas market through the LNG terminal in Świnoujście (Gaz-System, 2015).

Design of energy use capacity

For the case analysed, the authors selected exemplary criteria that can be taken into account when choosing gas storage facilities. The weights were assigned to individual criteria.

F1 - Economic - the cost of expanding the underground gas warehouse, $w_i = 0.3$;
F2 - Infrastructure - the distance from the agglomeration, $w_i = 0.15$;
F3 - Safety - the distance from other warehouses, $w_i = 0{,}2$;
F4 - Environmental – the distance from national parks, $w_i = 0{,}1$;
F5 - Technical – the injection capacity, $w_i = 0{,}25$.

For the criteria defined and the weights assigned to them, a list of variants for existing underground natural gas storages was developed. The development of options is an example of the development of a proposal, in what order underground storage facilities should be occupied or extended to cover the growing demand for natural gas consumption. The following table is an example of the order of selection of warehouses to be expanded; then it can be applied to potential new locations of underground gas storage facilities (Osieczko, Polaszczyk, 2018). The sum of the weights is 1. The scale of the assessment ranged from 1-5 points and was adjusted to the data concerning gas storage facilities located in Poland.

Table 4. Multicriteria model for the selection of underground gas storage facilities to be expanded

Title of factor i	weights	Variant 1		Variant 2		Variant 3		Variant 4		Variant 5		Variant 6		Variant 7		Variant 8		Variant 9	
		HF	HFw_i	HF	HFw_i	HF	HFw_i	HF	HFw_i	HF	HFw_i	HF	HFw_i	HF	HFw_i	HF	HFw_i	HF	HFw_i
F1	0,3	5	1,5	5	1,5	3	0,9	5	1,5	3	0,9	5	1,5	5	1,5	5	1,5	5	1,5
F2	0,15	2	0,3	5	0,75	5	0,75	4	0,6	*4*	0,6	5	0,75	2	0,3	*3*	0,45	2	0,3
F3	0,2	5	1	3	0,6	5	1	3	0,6	4	0,8	3	0,6	3	0,6	2	0,4	2	0,4
F4	0,1	5	0,5	4	0,4	5	0,5	5	0,5	5	0,5	5	0,5	5	0,5	5	0,5	5	0,5
F5	0,25	2	0,5	2	0,5	2	0,5	4	1	5	1,25	2	0,5	1	0,25	3	0,75	3	0,75
Total variant evaluation	1	3,8		3,75		3,65		4,2		4,05		3,85		3,15		3,6		3,45	

Variant 1 – Daszewo
Variant 2 – Bonikowo
Variant 3 – Kosakowo
Variant 4 – Wierzchowice
Variant 5 – Mogilno
Variant 6 – Brzeźnica
Variant 7 – Swarzów
Variant 8 – Husów
Variant 9 – Strachocina

The cost of expanding the warehouse:
5 - Depleted reservoir, Mines, 4- Aquifers, 3- Salt cavern.
Infrastructure - the distance from the agglomeration - (gas transmission infrastructure) - up to 50 km - 5, from 50 - 100 km - 4, from 100 - 200 km - 3, from 200-500 km - 2, over 500 km - 1. Adopted cities for agglomerations - Warsaw, Kraków, Katowice, Gdańsk, Wrocław, Łódź, Poznań.
Safety - the distance from other warehouses (nearest) - up to 50 km - 1, from 50 - 100 km - 2, from 100 - 150 km - 3, from 150 - 200 km - 4, over 200 km - 5.
Environmental - the distance from national parks - no national park in the area of 5 km - 1, from 5 - 10 km - 2, from 10 to 20 km - 3, from 30 to 50 km - 4, over 50 km - 5.
Technical - the injection capacity - up to 1 million m3/day - 1, from 1-2.5 million m3/day - 2, from 2.5 to 5 million m3/day - 3, from 5 -8.5 million m3/day - 4, above 8.5 million m3/day - 5.

Table 5. The proposal of the order of expansion of underground gas storages

No.	Variant number	Name	Total variant evaluation	Target capacity million m^3
1.	4	Wierzchowice	4,2	1200
2.	5	Mogilno	4,05	841
3.	6	Brzeźnica	3,85	100
4.	1	Daszewo	3,8	60
5.	2	Bonikowo	3,75	200
6.	3	Kosakowo	3,65	250
7.	8	Husów	3,6	500
8.	9	Strachocina	3,45	360
9.	7	Swarzów	3,15	90

Based on the information available on the pages of Polish Mining and Gas Extraction Company (Polskie Górnictwo Naftowe i Gazownictwo), a multi-criteria model for the development of existing gas storage facilities was developed. The results presented in Table 4 are an attempt to choose the order of expansion of warehouses in connection with the growing demand for natural gas in the coming years. The criteria should be adjusted accordingly to the requirements and expectations of underground gas storage facilities. Based on the criteria defined by the authors and the weights assigned to them, a certain sequence of extending existing warehouses was established along with the target capacity in a million cubic meters. The offer is presented in ***Table 5,*** along with the target capacity in a million cubic meters. The proposal is presented in Table 5.

The proposed use of the multicriteria model and determining the order of selecting individual objects is only an example that can be used to select new locations for underground gas storage. The authors, due to the lack of access to detailed information, chose the criteria allowing for the use of publicly available data. When selecting the location of gas storage, a number of factors related to technical aspects, construction costs, distance from main pipelines, expansion of the gas transmission installation, and distance from end users should be taken into account. It is also recommended to pay attention to safety-related aspects by considering topics related to the risk of explosion and fire.

Conclusion

Most EU countries rely on the import of earth gas. It is followed by the growing significance of underground gas storage facilities as the key part of the gas supply system. USG facilities ensure security against sudden supply interruptions and balance seasonal demand variations, optimising the operation of the gas supply system in a given country. As a strategic tool, underground gas storage facilities improve the energy security, but may also be operated as commercial undertakings, ensuring compensation of the financial outlays and providing profit from the fees charged for storing fuels for other countries.

Poland has proper geological structures, suitable for the development of underground gas storage facilities. Currently, Poland's energy policy is focused on ensuring energy independence of the country by the diversification of sources and directions of supplies. Certain projects aimed at the development and modernisation of the gas extraction and transmission infrastructure are being executed. Another essential factor is the development of underground gas storage facilities. A growing trend in the numbers and the capacity of UGS can be noticed in all EU countries.

Ensuring proper reserves of the blue fuel determines the energy security of a given country. Depleted gas and oil reservoirs, salt caverns and aquifers can be used as storages of fuel resources. Gas storage facilities should be situated over the entire area of the country, possibly closest to the recipients. Additionally, there is a need to extend the existing storage capacity, due to the obligation to maintain gas reserves in case of a failure or a sudden increase in consumption. The forecasts assume a fifty percent increase in gas consumption over the next few years. Therefore the analysis of the gas storage system indicated the necessity of further rapid development of the underground gas storage network, closely related to using gas as an energy carrier.

One of the elements facilitating the decision-making process may be an application of a multi-criteria model to the selection of a location and establishing the appropriate sequence of development of underground gas storage facilities. The selection of required criteria related to construction costs, depending on the type of warehouse, costs of infrastructure development, technical, environmental or security aspects and the allocation of appropriate weights, may facilitate decision making in the face of high investment expenditures and country security related to the growing natural gas demand. The proposed solution based on appropriate parameters important from the perspective of the strategic goals of the state may prove to be a helpful tool.

References

Bergman B.: Security of supply requires long term thinking, Fundamentals of the World Gas Industry, Petroleum Economist, London, 2006.

Biuletyn Informacji Publicznej, BIP, (2018. 01.07.). Available online http://bip.ms.gov.pl

Brzeziński T., Wawrzynowicz A.: Rozwój segmentu magazynowania poliw gazowych, zmiany otoczenia prawnego, zasady funkcjonowania oraz znaczenie segmentu dla rynku. Rynek Energii Nr 5 (114), pp. 3-15. 2014.

Charun H.: Podstawy gospodarki energetycznej, Wydawnictwo Politechniki Koszalińskiej, Koszalin, 2004.

Ciechanowska M.: Podziemne magazyny gazu elementem bezpieczeństwa energetycznego Polski. Nafta-Gaz, Rok LXXII, Nr 10/2016. pp. 833-840. 2016.

Czapkowski G.: Możliwości bezpiecznego podziemnego magazynowania węglowodorów (paliw) w strukturach geologicznych na obszarze Polski. Przegląd geologicznych, Vol. 54, nr 8. 2006.

Egging, R., Holz, F.: Risks in global gas markets: Investment, hedging and trade. Energy Policy Vol. 94, pp. 468-479. 2016.

EID Energie Informationsdienst: Unterlage Gasspeicherung in Deutschland. Erdöl Erdgas Kohle, 133, Heft 11, pp. 409-415. 2017.

Eurogas Statistical Reports 2010, 2015. (2017. 12.18.). Available online http://www.eurogas.org

Evants D., Stephenson M., Shaw R.: The present and future use of 'land' below grund. Land Use Policy, 26S. pp. 302-316. 2009.

Filar B., Kwilosz T.: Możliwości rozwoju podziemnych magazynów gazu w Polsce. Polityka Energetyczna t. 11, Zeszyt 2. pp. 33-39. ISSN 1429-6675. 2008.

Gaz-System: Gazociąg Hermanowice-Strachocina. Niespecjalistyczne omówienie aktualnego stanu projektu. Warszawa, 2015.

Hąbek P., Biały W., Livenskaya G.: *Stakeholder engagement in corporate social responsibility reporting. The case of mining companies*, Acta Montanistica Slovaca, Vol 23/1, 2019, pp. 25-34.

Hill A.: Single European gas market a distant possibility, Fundamentals of the World Gas Industry, Petroleum Economist, London, 2006.

IEA 2016: Gas Medium-Term Market Report– Market Analysis and Forecasts to 2021, International Energy Agency, 9 rue de la Fédération, Paris, 2016.

Kochanek E.: Podziemne magazynowanie paliw w strukturach geologicznych jako element bezpieczeństwa energetycznego Polski. Bezpieczeństwo Narodowe I-II/3-4, pp. 302-311. 2007.

Kunstman A., Poborska-Młynarska K., Urbańczyk K.: Geologiczne i górnicze aspekty budowy magazynowych kawern solnych. Przegląd Geologiczny 57, pp. 819-828. 2009.

Malindžák D.,Kačmary P.,Ostasz G.,Gazda A.,Zatwarnicka –Madura B.,Lorek M., *Design of logistic Systems*, Open Sience, New York, 2015.

Mingaleva Z., Zhulanov E., Shaidurova N., Molenda M., Gapenko A., Šoltésová M.: *The abandoned mines rehabilitation on the basis ofspeleotherapy: used forsustainable development of the territory(the case study of the single-industrytown of mining industry)*, Acta Montanistica Slovaca, Vol 23/3, 2018, pp. 312-324.

Mokrzycki E., Szurlej A.: Ekologiczne i energetyczne oraz ekonomiczne aspekty stosowania układów wykorzystujących gaz ziemny. Polityka Energetyczna t.6, pp. 199-211. 2003.

Osieczko K., Polaszczyk J., *Comparison of chosen aspects of Energy Security Index for the natural gas sector in Poland and Ukraine*, International Journal of Management and Economics 54(3) 2018, pp. 185-196.

Polskie Górnictwo Naftowe i Gazownictwo SA, PGNIG, (2017, 12.18.). Available online http://pgnig.pl

Państwowy Instytut Geologiczny – Państwowy Instytut Badawczy, PGI. (2017, 12.18.). Available online http://pgi.gov.pl

Pielech A.: Charakterystyka funkcjonowania podzimenych magazynów gazu w Polsce na przykładzie PMG Strachocina. Politechnika Rzeszowska, Wydział Zarządzania, Rzeszów, 2017.

Polit J., Moazurkowski M., Gałeg G.: Uwarunkowania strategii rozwoju podziemnych magazynów gazu ziemnego w Polsce. Nafta-Gaz nr 10, pp. 892-897. 2010.

Schafer P.S., Hower T., Ownes R.W.: Magaging water-drive gas reservoirs. GRI, Chicago. 1993.

Siemek S., Nagy S.: Podziemne magazyny gazu ziemnego w wyeksploatowanych kopalniach węgla. Wiertnictwo, Nafta, Gaz 24 (2). pp. 857-878. 2007.

Stasiowski B., Wagner-Staszewska T.: Rozbudowa podziemnego magazynu Strachocina, Nafta-Gaz nr 12, pp. 1109-1114. 2010.

Hydrodynamic and slope stability modelling of flood protection embankments and valley dams

***Gábor Nyiri*[1], *Balázs Zákányi*[2] *and* *Péter SzŤcs*[3]**

Hydrology conditions in recent years clearly demonstrate that flood protection is a priority task for Hungarian water management, and its importance cannot be questioned. This study examines three flood control embankments and two dams, including their subsoil characteristics. The examinations also contain the modelling of slope stability and seepage conditions. The seepage models were created with the Groundwater Modeling System 10 SEEP2D module, which uses the finite element method. As a part of the examination of the seepage models, we examine the free flows and the embankments' seepage conditions. Changing the modelling parameters also affects seepage conditions. Thus we examine the effects of the embankment's foot width and on the total flowrate and the seepage conditions. Our examination also includes a study about the effects of neglecting the subsoil in computations. For the slope stability examinations, both the Groundwater Modeling System UTEXAS module and the Soilvision SVSlope module are used, and their results are compared, showing significant differences. While the slope stability measurements were done in a dry state, we also examined the effects of pore water pressure on the embankments' stability. Modelling methods are useful and simple methods for the examination of seepage and slope stability of flood control embankments and can provide great help to flood protection professionals.

***Key words**: flood protection, slope stability, finite element modelling, dam seepage*

Introduction

Flood protection and drinking water supply are among the most urgent tasks of water management in Hungary (Ilyés et al., 2017; Palcsu et al., 2017). According to extreme weather conditions, floods along rivers or flash floods mean real risks to the civil society and to nature, not only in Hungary but all over the world (Francois et al., 2019). This is the reason why the proper operation of embankments is vital to have successful flood control. It is important to know how an embankment is behaving during a flood period. What kind of processing exists inside the embankments concerning water level and stability issues? To understand these physical processes, simulations methods can be used successfully in flood control processes (Xiaohui, 2017).

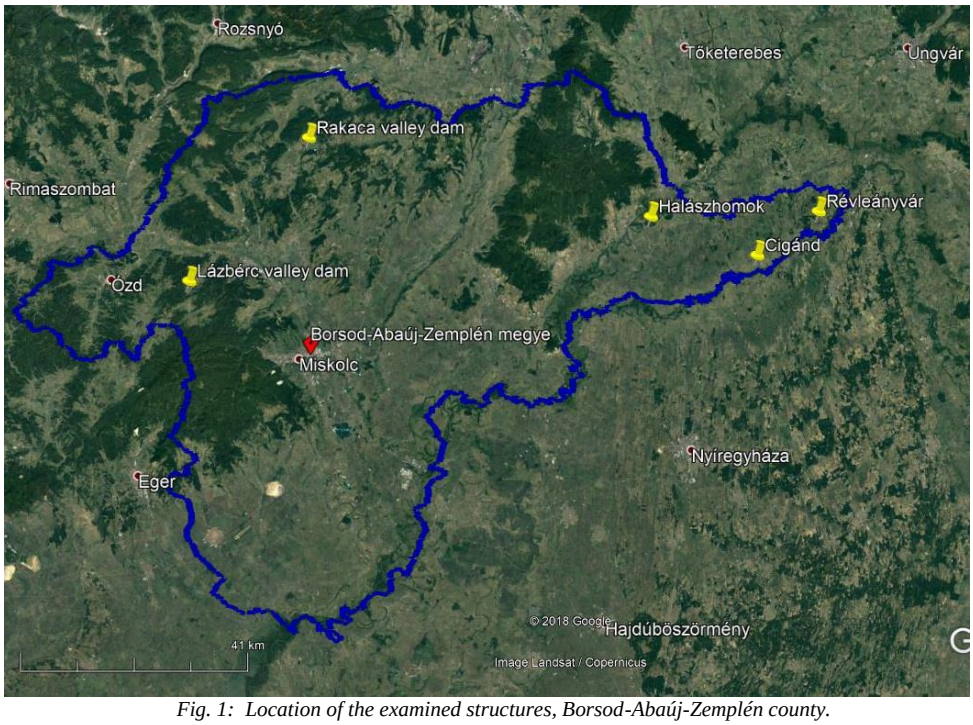

Fig. 1: Location of the examined structures, Borsod-Abaúj-Zemplén county.

[1] *Gábor Nyiri*, Institute of Environmental Management, University of Miskolc, 3515 Miskolc, Egyetemváros, Hungary, *hgnyg@uni-miskolc.hu*

[2] *Balázs Zákányi*, Institute of Environmental Management, University of Miskolc, 3515 Miskolc, Egyetemváros, Hungary, *hgzb@uni-miskolc.hu*

[3] *Péter SzŤcs*, Institute of Environmental Management, MTA-ME Geoengineering Research Group. University of Miskolc, 3515 Miskolc, Egyetemváros, Hungary, *hgszucs@uni-miskolc.hu*

Along the Tisza river in Hungary, the flood protection is mostly executed with the help of embankments. The increasing agricultural and settlement land use during the centuries made it necessary to develop a protection line covering the whole section of the Tisza river (Vágás, 2007). More precise knowledge of the related hydraulic relations of these protection lines is increasingly needed because huge damage can occur if the protection lines are destroyed. The purpose of valley dams is to control the even or changing runoff of the watercourse based on the needs of the users (Sternberg, 2006). They typically contain a structural element to control water leakage; thus, it is essential to be aware of these leakage conditions. In this study, we examined the seepage conditions of three flood protection embankments and two valley dams. These structures are situated in the north-east part of Hungary, in Borsod-Abaúj-Zemplén county (Figure 1). This work extends previous studies (Zákányi and SzŤcs, 2010, 2013) by taking subsoil into consideration. The obtained results can be generalized because simulation methods are very important in proper embankment design.

Flood protection in Hungary

In the Middle Ages, floods did not have a high damage factor. The environment of the rivers shows its natural status: wide floodplains, huge woody areas that decreased the flood water level. The improvement of agriculture brought the necessity for river regulation and floodplain draining. At the time of the regulation of the Tisza River, safety was secured by the height of the embankments practically by the end of the 19th century. The embankmentôs prescribed height was regulated to the largest formerly experienced flood with the addition of safety height (Nagy, 2014). However, the highest water level of rivers started to increase with the regulation of rivers, the development of the infrastructure and the growth of the agricultural lands (Vágási, 2007). Based on the eraôs protection philosophy, so-called bulbous structured embankments were made with the construction in several cycles (Figure 2). Nowadays, the length of the Hungarian flood protection embankments is more than 4,200 km (Nagy, 2003).

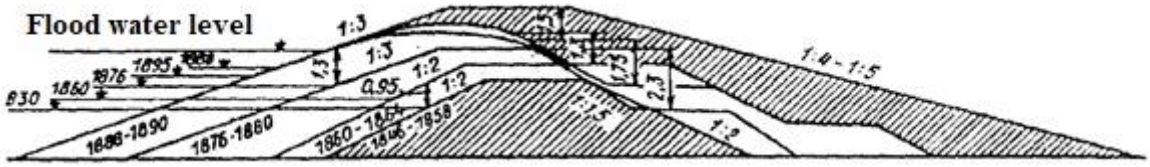

Fig. 2: The increase in the height of the Széchenyi Dam between Tiszadob and Polgár, 1845-1890 (Mihalik, 2000)

Besides the construction of embankments, we have to deal with another problem as well. The embankments are often built on unsuitable subsoil that contains permeable layers. The presence of these permeable layers increases the probability of the formation of sand boils (Nagy, 2008). The key element of flood protection is the stability of the flood protection dam. The failure and ruin of the embankment carry the possibility of catastrophe (Kádár and Nagy, 2017). Hungaryôs reservoirs, in addition to water supply, also provides flood protection because they delay the runoff of harmful excess water. The inland reservoirs are mostly bordered by valley dams, whose embankment was built from clay, which, in most cases, we cannot consider as an aquiclude. Therefore, the leakage through the dam has to be controlled, and leaking water has to be removed out from the embankment. The task of the interception drain is to block the dangerous seepage process and to decrease the dangerous pressure conditions in the embankment. Its material is mostly coarse-grained sand and sandy gravel. The advantage of its use is that it collects the leaking water in the water-side dam body and removes it from the dam, thus blocking the wetting of the dam across its whole cross-section. Nowadays, another problem for flood protection and drinking water reservoirs is extreme weather conditions. As we experienced in 2010, extreme floods formed in the Sajó and Bódva Rivers, and also in the Tisza River in the early 2000s (ZeleŕákovaÁ et al., 2018).

Site description and methodology

In Hungary, the valley of Tisza river is affected by floods mostly. During the 20th century, and after the 2000s, many floods were formed, and it caused several problems in flood protection, and the stability of the embankments. Considering this situation, we decided to deal with this area, especially the upper part of the Tisza river. During our investigation, we used the hydrodynamic and slope stability modelling, which is an important tool to know the hydraulic behaviour and its effects on slope stability. With the help of this tool, we can conclude the most frequent failures (hydraulic failure, seepage failure, piping) near the embankments, and dams (Shivakumar et al., 2015). We modelled three flood protection embankments near the Tisza River (near Cigánd, Révleányvár, and Halászhomok) and two valley dams (Lázbérc and Rakaca) during our investigation.

For the leaking model, the program applied was the SEEP2D module of Groundwater Modeling System 10.0, and for the examination of slope stability, the module of Groundwater Modeling System 10.0 UTEXAS and the module of Soilvision Slope were used. The Groundwater Modeling System (GMS) is a comprehensive graphical user environment for performing groundwater simulations. The entire GMS system consists of a graphical user interface (the GMS program) and a number of analysis codes (MODFLOW, MT3DMS, SEEP2D, etc.) (Aquaveo, 2019).

All of the programs apply the finite element method as the numerical method. The word ónumericalô stands, in this case, for approaching a solution (Völgyesi 2008). Numerical solutions approach the real situations in a way that they make sections of ongoing procedures in time and place (Kovács, 2004). In the finite element method, as opposed to the finite difference method, the given geometry can be precisely covered with arbitrarily shaped elements. Thus, the elements orient much better to the real range than when applying a different finite mesh (Durbin and Bond 1998; Zákányi and SzŤcs, 2010). The orientation of the elements to the original geometry helps to make the model accurate and to determine water flowing across the embankment more accurately.

SEEP2D is a two-dimensional steady-state finite element groundwater model, which is widely used in such calculations. Both saturated and unsaturated flow is simulated. SEEP2D is designed to be used on profile models (XZ models) such as cross-sections of earth dams or embankments. With the help of the SEEP2D module, we calculated the total flow rate, which is the flow rate into (out of) the problem domain (Aquaveo, 2019).

UTEXAS is a slope stability software package created by Dr Stephen G. Wright of the University of Texas at Austin. UTEXAS is used to analyze slope stability using the limit equilibrium method. The user provides the geometry and shear strength parameters for the slope in question and UTEXAS4 computes a factor of safety against slope failure. The factor of safety for a candidate failure surface is computed as the forces driving failure along the surface divided by the shear resistance of the soils along the surface. UTEXAS4 is a state-of-the-art slope stability code and has been widely used in industry for many years (Wright, 1999).

The hydrodynamical models show "steady state" at the same time because the SEEP2D module cannot handle the transient state. In the case of the valley dams, the water level of the reservoir has relatively small-scale fluctuation. Thus, the "steady-state" is presumed. And in the case of flood protection embankments, we can calculate with a permanently high flood level.

For the slope stability investigation, we used the Slope module of SoilVision software, which also calculate with the limit equilibrium method, and it also can calculate with the effect of leaking water.

Material characteristics of valley dams and flood protection embankments

We had to give several parameters during the examination of flood protection embankments and valley dams: for the leaking model, the parameters given were horizontal and vertical factors, for the modelling of slope stability they were cohesion and internal friction angle. Furthermore, effective porosity was necessary for the definition of given parameters. Some of the applied parameters were provided by the regional waterworks company, called ÉRV Zrt., while the rest were taken from a previous study (Zákányi and SzŤcs, 2013). The related data (not publicly available) of the geometry of the examined embankments was provided by ÉRV Zrt. and ÉVIZIG (the Water Management Directorate of Northern Hungary).

During the modelling, not all of the parameters requested by the program were available; unfortunately, sampling and lab examinations are possible only with the proper permission, and in the case of embankments only allowed in a justified case. For these reasons, we had to find data from another source. We used a Hungarian technical guideline (MI 10 269-1982) that contains parameter intervals, from which we chose a value to use in the computations.

In this paper, the construction and material characteristics of embankments are introduced based on the embankment of Cigánd. The shape of the embankments clearly shows the bulbous structure. Considering the subsoil, we can divide it into a permeable layer and a cover layer. The embankment was built with these two characteristic layers, in which a core and a surrounding shell can be found (Figure 3, Tables 1 and 2). The geometry of the dyke at the riverside was recorded by the information offered by ÉVIZIG (Zákányi and SzŤcs, 2013).

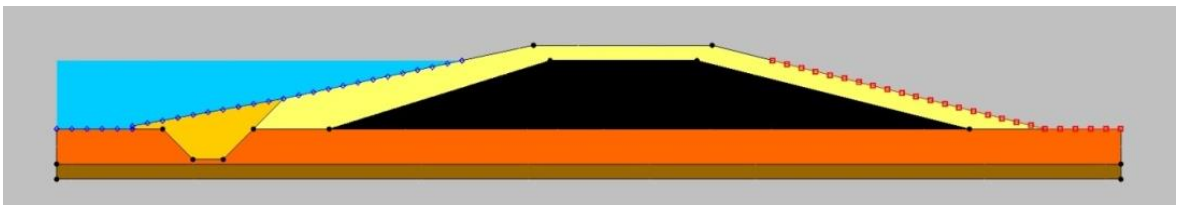

Fig. 3: Cross-section of the flood embankment around Cigánd

Table 1: Hydraulic conductivity values of the embankment of Cigánd

	k_h (horizontal) [m/d]	k_v (vertical) [m/d]
Inner core	0.00864	0.06
Shell	0.000864	0.000864
Impermeable foot	0.000432	0.000432
Cover layer	0.00086	0.00086
Water-bearing layer	0.43	0.43

Table 2: Shear strength parameters of the embankment of Cigánd

	Unit weight [kg/m^3]	Cohesion [kPa]	Friction angle [°]	Effective porosity [%]
Inner core	2100	35	15	35
Shell	2200	40	15	30
Impermeable foot	2200	40	15	30
Cover layer	2200	40	15	30
Water-bearing layer	2000	0	29	40

The conformation of the valley dam will be demonstrated in this paper by the reservoir dam of Lázbérc (Figure 4). The two dams investigated here are different in that an impermeable wall was not constructed under the Rakaca reservoir dam. The seepage parameters are shown in Tables 3 and 4. For the parameters of shear strength for the Lázbérc valley dam, in case of the watertight wall and bedrock, we assumed non-porous, grainy rock. When the ñhard rockò option is chosen among the types of material, the program does not ask for the cohesion, internal friction angle, or effective porosity. The bedrock is limestone, and the impermeable wall is concrete; thus, these parameters were not necessary for the program.

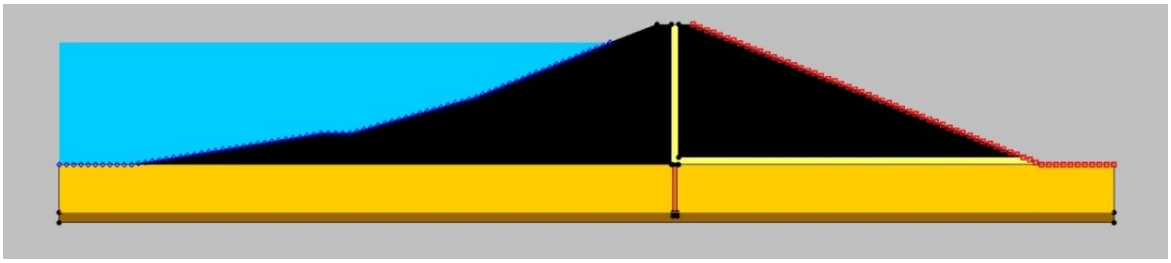

Fig. 4: The cross-section of the valley dam of Lázbérc

Table 3: Hydraulic conductivity values of the valley dam of Lázbérc

	Dam body	Drain	Subsoil	Watertight wall	Base rock
k [m/d]	0.00864	8.64	0.043	0.0000864	0.000864

Table 4: Shear strength parameters of the valley dam of Lázbérc

	Unit weight[kg/m^3]	Cohesion [kPa]	Friction angle [°]	Effective porosity [%]
Dam body	2000	40	15	30
Drain	2000	0	30	32
Subsoil	1800	10	25	25
Watertight wall	2500			
Base rock	2200			

Calculation results of hydrodynamic, and slope stability simulations

During the modelling, our examination covered leakage models and slope stability problems. The hydraulic modelling of the dam and its subsoil can be easily implemented with the help of GMS 10 program, and we have the opportunity to carry out a slope stability examination with the consideration of water seepage. After the water level and exit surface are provided, the program calculates the rate (the blue and red lines, respectively, in Figures 2ï 7), the rate of the flow velocity inside the dam and the pore water pressure and total flow rate, from which diagrams of the calculated rates can be easily made for visualisation. During the determination of the total

flow rate, the program calculated the flow rate related to a one-meter-long part of the embankment. For each embankment, we took the standard flood level as the basis, which is located one meter downwards from the shoulder, while for the valley dams, we took the maximal operational level into consideration. Using the SoilVision program Slope package and the GMS UTEXAS module, we examined the slope stability; one of the purposes for this was to compare the two programs. With the Slope module, we examined three stages. In one case we did dry condition modelling, in the other case we put the rate of pore water pressure calculated by the GMS as a discrete point into the Slope module and thus we took the water pressure into consideration. To consider the effect of water, we recorded the highest flow line calculated by the GMS in the Slope module and set it as water level. We compare the results of the different cases.

The GMS UTEXASô module considers the flow relation and the rate of water pressure calculated by the SEEP2D module, and thus calculates the critical slope failure surface with the Spencer method and its belonging security factor. All slope stability tests were done by the method of slices, followed by several types of calculation methods. The security factor and the place of critical slope failure surface were calculated by the Bishop, Spencer, Janbu and Morgenstern-Price methods, which all assume round slope failure surface.

Seepage conditions

Our aim during the application of GMS SEEP2D was the examination of the ongoing leak process of different geometrical and structural embankments. For the demonstration of flow conditions, the mesh of models are recorded with one-meter spacing, and on the riverside and protected side, the original ground level runs for a 10-meter-long stretch. The program defines the streamlines and calculates the total flow rate, velocity conditions, and the rates of pore water pressure. The models consider the standard flood water level.

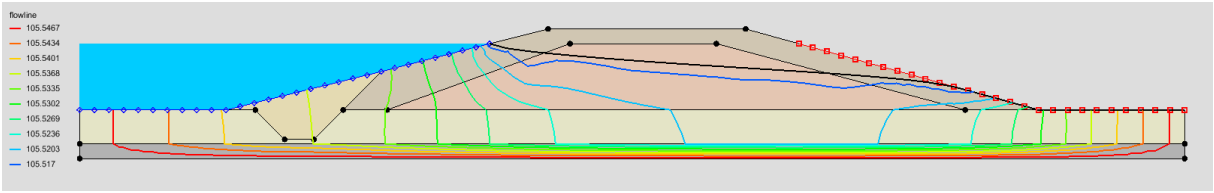

Fig. 5: Flowlines in the embankment around Cigánd

In Figure 5, we can see that the subsoil has an important role in the permeability of embankments because most of the flow lines can be seen in the water-bearing layer. The role of the subsoil can also be examined in the embankment of Révleányvár (Figure 6). We encountered thicker topsoil in the subsoil of the Halászhomok embankment, which prevents the seepage of water into the subsoil. In this case, most of the streamlines ran through the interior of the embankment.

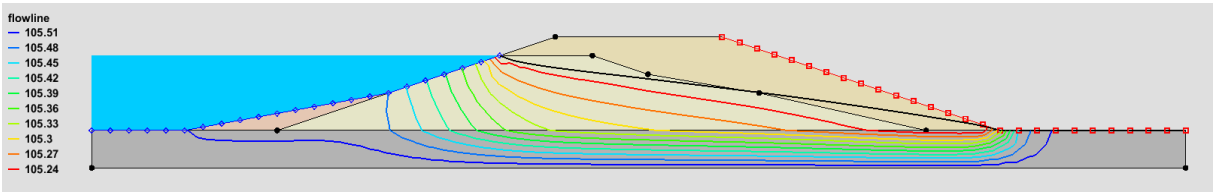

Fig. 6: Flowlines in the embankment around Révleányvár

In the case of the Lázbérc valley dam, the role of the drain inside the dam can be seen during the examination of the streamlines (Figure 7). The water leaking into the dam from the waterside accumulates in the vertical and horizontal sand layer and exits at the foot of the dam. Thus the dam does not get wet throughout its entire cross-section. The concrete wall under the dam blocks the water from leaking through the subsoil. The program allows us to demonstrate the water retention ability of the leaking control elements in dams. The calibration of the model also included on-site measurements from previous examinations. The flow rate of the outflowing water was determined from the collecting tube of the drain system.

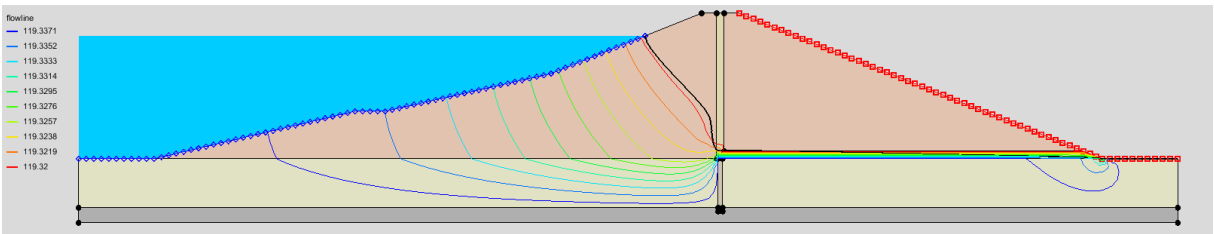

Fig. 7: Structural elements of the valley dam of Lázbérc and the computed streamlines

Looking at the cross-section of the Rakaca dam (Figure 8), we encounter very diverse subsoil. Inside the dam body, we can see that a 1-meter-wide drain system was built. The sandy and rocky drain system consists of a vertical drain, a right-angle bend, and a horizontal section (3% gradient). The water in the drain system is led off to the protected side by a 0.3-meter diameter concrete drain tube (not visible in the figure). The whole leakage system output flows into a container.

Examining the streamlines in Figure 7, it is visible that a layer can be found in the subsoil whose hydraulic conductivity is higher than that of the other materials, and the water flows through this layer towards the protected side. The role of the drain is also important because it collects most of the water flowing through the dam and collectively leads it away from the dam and the subsoil. Because a watertight concrete wall was not built into the subsoil, the streamlines penetrate the subsoil as well (Figure 8).

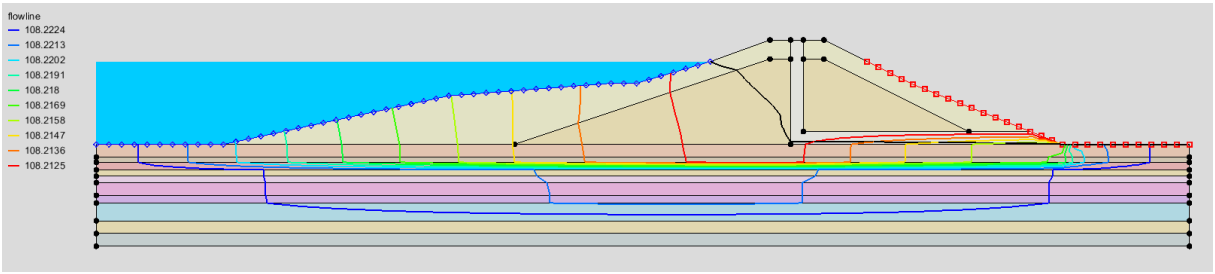

Fig. 8: Structural elements of the valley dam of Rakaca with the computed streamlines

We compared these results with a previous study in which the subsoil conditions were not considered. We made a comparison with the consideration of the total flow rate and outflowing length. From the comparison of total flow rate (Figures 9 and 10), we see that when the subsoil is taken into consideration, higher flow rates are obtained for the flood embankments and in the case of the Rakaca reservoir. The reason for this is that because of the hydraulic conductivity of the water-bearing layer of the subsoil, a high amount of water goes through the subsoil. In the case of the embankments, we have to be aware of the possible formation of sand boils. Because the pressure is high in the subsoil, we have to also count on the growth of pore water pressure, which negatively affects the stability of embankments, because the supporting force against water pressure decreases.

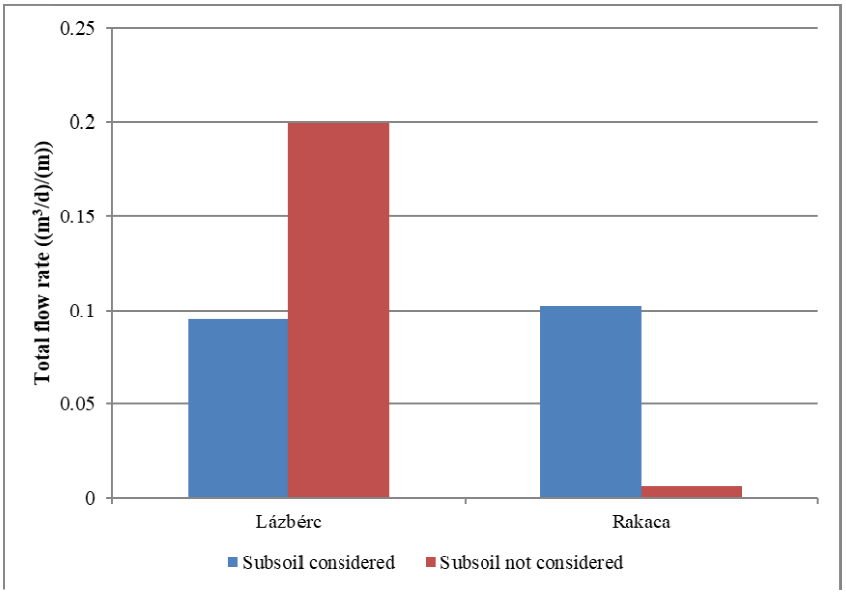

Fig. 9: Comparison of total flow rates for valley dams of two computational models

In the case of Lázbérc, we can see that we obtained a lower total flow rate value when the subsoil was considered. This can be explained by the presence of the watertight concrete wall. The concrete wall stops the water from leaking through the subsoil to the protected side and leads towards the water-bearing sand layer, thus protecting the dam and the subsoil from getting completely wet.

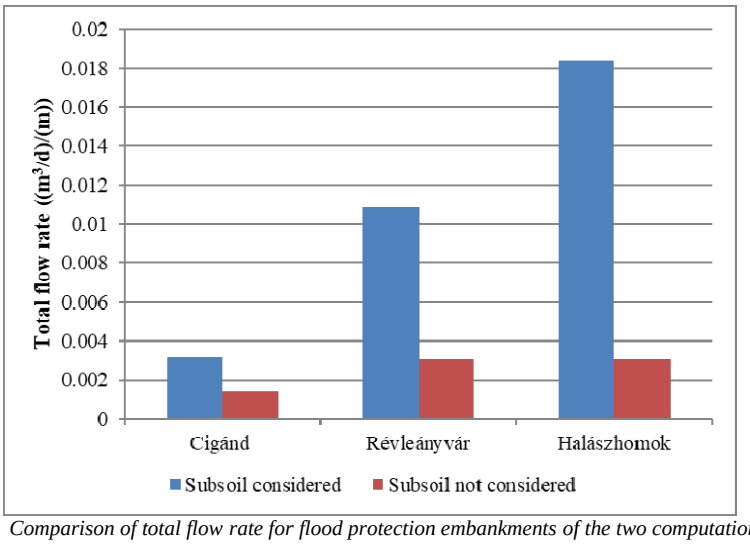

Fig. 10: Comparison of total flow rate for flood protection embankments of the two computational models

The outflow length value offers important information during the examination of embankments. Outflow length means the distance between the highest outflowing point and the foot of the embankment. This rate shows the predicted height of water outflows in the embankments and how wet the embankment has become. We only examined the flood protection embankments for outflow length, because at the dam's reservoir, the water exits through the permeable layers; thus, the outflow length is constant. We calculated the outflow length from the coordinates written by the program and the formula of triangles.

We can see that in case of the flood protection embankments in Révleányvár and Halászhomok, the outflow length occurred at lower levels; however, higher rates were found for the Cigánd embankment. In the Révleányvár and Halászhomok embankments, the subsoil conditions were proper for flow not only through the embankment but also in the subsoil. In the case of Cigánd a relatively watertight layer can be found under the embankment, which did not allow the high degree of infiltration to the subsoil; thus, most of the water flows through the embankment and less goes through the subsoil layer lying under the watertight layer, which has high hydraulic conductivity (Figure 11).

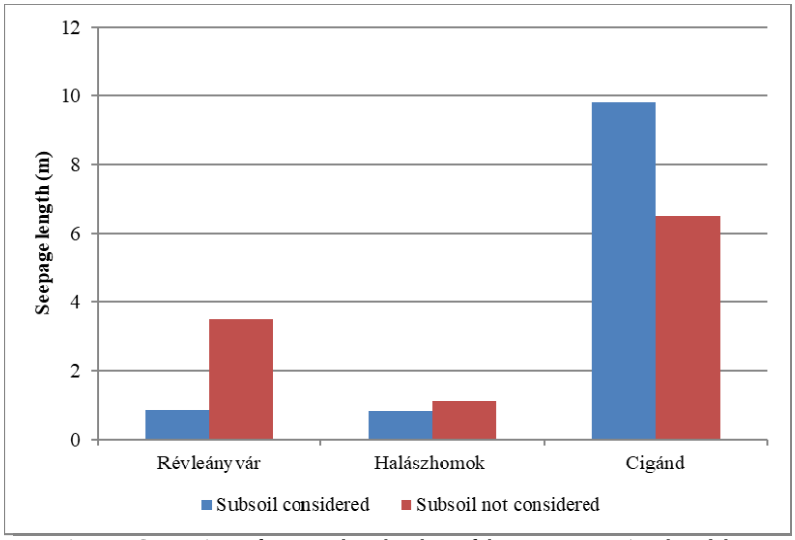

Fig .11: Comparison of seepage length values of the two computational models

Changes in modelling circumstances

During the modelling, we were curious about the effect of two chosen parameters connected to the geometry and mesh. During the modelling, the adoption of geometry was necessary. The aim of the examination was to see how much the width of the embankment foot influences the total flow rate in the model. The width of the embankment foot is defined as the distance between the meeting point of the subsoil and embankment and the edge of the model. Three cases were examined: 5 m, 10 m and 20 m foot width. For the Cigánd and Halászhomok embankments, changing the width of the embankment resulted in the total flow rate increases with

the width (Table 6). The degree of the increase in flow rate was not linear. The reason for this is that the exit face grows on the protected side with the foot's width; thus, more water can flow through the system.

Table 5: Change in total flow rate with different values of foot width of the embankment

Foot width of the embankment (m)	Cigánd (m^3/d/m)	Révleányvár (m^3/d/m)	Halászhomok (m^3/d/m)
5	0.0089	0.0107	0.0185
10	0.0113	0.0107	0.0187
20	0.0145	0.0107	0.0191

In the other examination, our aim was to find out how much the choice of mesh density influences the total flow rate and the streamlines. We set the meshôs density in the program by apportioning the embankmentôs side in a given spacing, and then the program was run based on the mesh. The choice of the spacing is influenced by the size of the given embankment. The differences in spacing between the embankments and valley dams are justified with this.

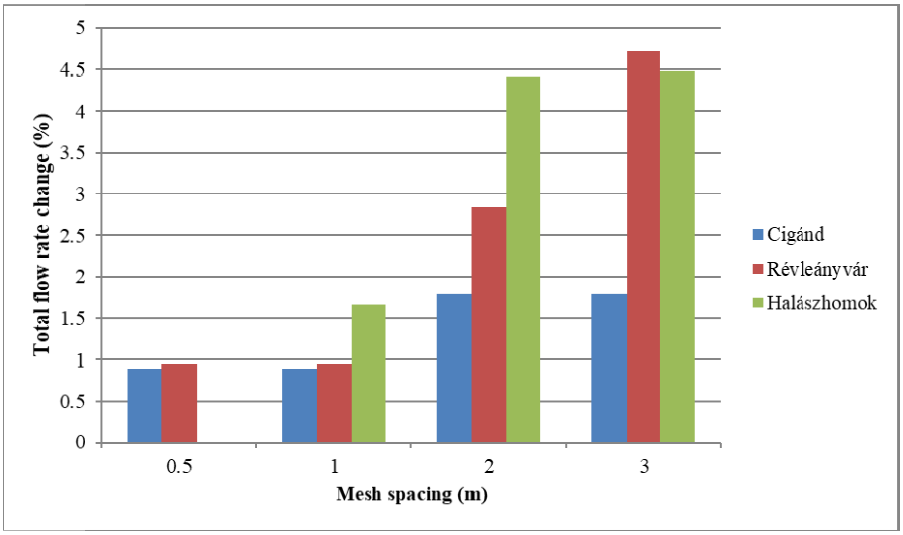

Fig. 12: Total change in flow rate for flood embankments with different mesh spacing

We can see from Figures 12 and 13 that the choice of the meshôs density plays an important role because there can be a 10ï12 % difference between the results obtained. Our experience was that the streamlines are influenced by the distribution of the mesh. We observed that the streamlines are shown in much more detail if the allocation of the meshôs division is denser. During modelling, it is necessary to choose the optimum setting, in which the streamlines and the total flow rate both give realistic rates.

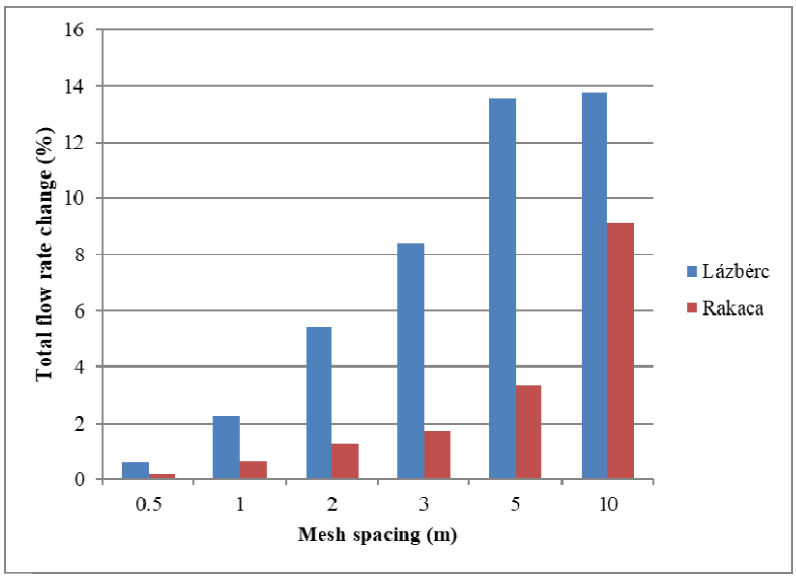

Fig. 13: The total flow rate change at the valley dams

Slope stability modelling

Slope stability examinations were carried out with two programs, the module Slope of SoilVision and with the UTEXAS module of Groundwater Modeling System 10. First, we did the modelling in the dry state with the Slope module. The program calculated the critical slope failure surface and the related safety factors with Bishop, Janbu, Spencer, and Morgenstern-Price methods. Our aim with this examination was to assess the safety of the given geometrical embankments knowing the assumed shear strength parameters.

Naturally, our aim was to define the effect of water on reducing stability using the leakage model. Results of the dry and wet states were compared with each other for all cases and in all slope stability calculation methods. We were also able to compare the two software programs, considering which is easier to use and what kind of differences will be computed by the two programs.

Slope stability without the consideration of pore water pressure

The modelling of dry state was necessary to define the stability reducing the effect of water. In this case, the system has no water in it, and the given parameters are only the volume weight, cohesion and the internal friction angle. The results are shown in Table 7.

Table 6: Factor of safety for dry condition calculated by SoilVision by different methods

	Cigánd	Révleányvár	Halászhomok	Lázbérc	Rakaca
Bishop	4.095	2.573	3.746	1.739	2.818
Janbu	3.879	2.482	3.413	1.623	2.666
Spencer	4.104	2.575	3.747	1.756	2.829
Morgenstern-Price	4.113	2.574	3.749	1.759	2.883

Slope stability with the consideration of pore water pressure

We examined the effect of water first with the GMS UTEXAS module (Figure 14). With the UTEXAS module, the program only calculates stability with the Spencer method. The UTEXAS slope stability safety module was provided with the leakage states calculated by the SEEP2D module from a previously given starting circle (the blue circle in Figure 14) using iteration.

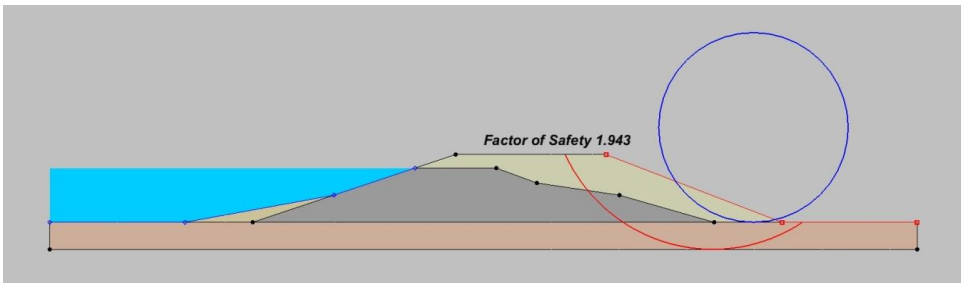

Fig. 14: The embankment around Révleányvár with the critical slip surface and the factor of safety

The effect of pore water pressure can be considered in two ways with the Slope module. One way is to record the pore water pressure rates calculated by the GMS SEEP2D module into the Slope module. These points are intersections of the mesh used by the SEEP2D. The other way is to build the leakage surface calculated by SEEP2D module into the Slope module. We did not give pressure values here, but the highest seepage surface.

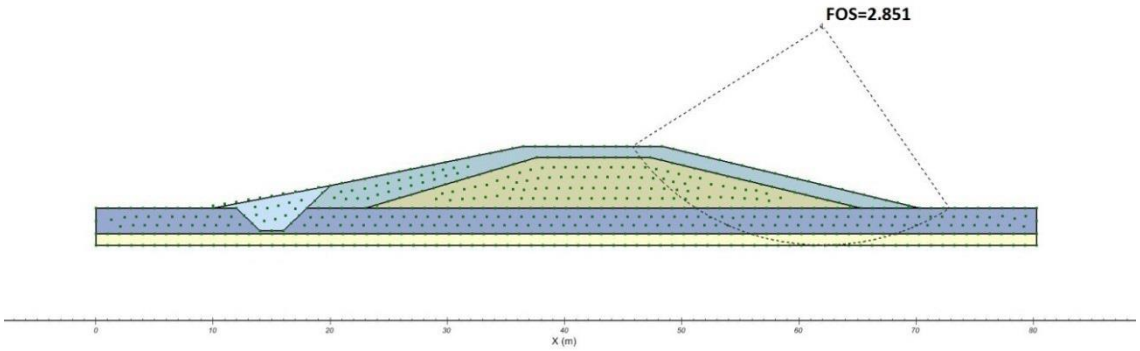

Fig. 15: The critical slip surface and the factor of safety, calculated by the SoilVision Slope module, at the embankment around Cigánd

We simulated the critical slip surfaces (Figure 15.) and compared the obtained safety factors with the safety factors referring to the dry state. The difference between the results for dry state and wet state is given in Tables 8 and 9.

Table 7: Changes in the factor of safety compared to a dry state, considering pore water pressure (discrete points)

	Cigánd (%)	**Révleányvár (%)**	**Halászhomok (%)**	**Lázbérc (%)**	**Rakaca (%)**
Bishop	43.6	21.9	36.9	10.2	12.3
Janbu	43.8	19.1	31.5	14.3	16.4
Spencer	43.6	22.0	36.8	10.1	12.8
Morgenstern-Price	43.6	22.0	36.8	10.1	14.5
Average	**43.6**	**21.3**	**35.5**	**11.2**	**14.0**

Table 8: Changes in the factor of safety compared to a dry state, considering the effect of water (highest seepage line)

	Cigánd (%)	**Révleányvár (%)**	**Halászhomok (%)**	**Lázbérc (%)**	**Rakaca (%)**
Bishop	24.1	16.4	17.6	10.2	0.8
Janbu	24.1	14.6	14.1	13.8	1.8
Spencer	24.2	16.4	17.6	10.1	1.4
Morgenstern-Price	24.2	16.4	17.6	10.3	2.8
Average	**24.1**	**16.0**	**16.7**	**11.1**	**1.7**

We can see from the table that the pore water pressure influences the safety factor. Using the Slope module, the highest difference was experienced in case of the embankment of Cigánd, which was caused by the shear strength parameters and the geometry of the embankment.

During our examination, we had the opportunity to compare the two programs used. We limited the comparison to the Spencer method because this method is found in both software. The differences are shown in Table 10, where we can see that the relative difference is quite small, so we can state that these two methods calculate a similar factor of safety values. Considering the data request, we can state that the using of GMS is easier, but the structure of the Slope module is more transparent. The GMS module can be a better solution if we have few data.

Table 9: Comparison of the factor of safety values calculated by GMS and SoilVision programs (Spencer method)

	GMS, UTEXAS	**SoilVision, Slope**	**Relative difference in factor of safety (%)**
Cigánd	2.971	2.555	14.00
Révleányvár	1.943	2.111	7.96
Halászhomok	2.815	2.738	2.81
Lázbérc	1.561	1.595	2.13
Rakaca	2.679	2.508	6.82

Conclusion

We modelled the seepage conditions of three flood protection embankments near the Tisza River and the Lázbérc and Rakaca reservoir dams, complemented with a slope stability test considering the subsoil. During our examination water level was correlated to the standard flood level in the case of embankments, while the correlation was to the maximal operational water level for the Lázbérc and Rakaca reservoir dams. During the modelling procedure, we assumed permanent, so-called steady-state conditions. The complexity is characteristic to the geometry of flood protection embankments, the parameters of embankment's materials we took over partially from previous works, and partially we derived them from the national technical directive.

For the valley dams, the characteristic cross-sections identify the constructional elements built in to control the leakage. In the case of embankments, it was noticeable that the position of streamlines depends greatly on the characteristics of subsoil, the thickness and the leakage factor. The various seepage effects of the drainage elements are visible at the valley dams. We prepared leakage models for several cases to explore the

effects of mesh density and the width of the embankment foot, which are important parameters in the modelling procedure. As mesh spacing increases, the increase in total flow rate can be seen, and with the decreasing of the mesh spacing, streamline contours are even more accurate. We compared the total flow rate results with those of a previous study in which the subsoil characteristics were not considered. We found that results for the total flow rate and the seepage conditions were highly influenced by the consideration of subsoil, which is confirmed by experiences in the field. Therefore, we can say that in the case of embankments, we get a better view of the seepage conditions, if we consider the subsoil. We used two programs in the slope stability investigation ï the UTEXAS module of Groundwater Modelling System version 10 and SoilVisionôs Slope module ï and carried out the examinations with multiple slope stability calculation methods. We examined two cases, a dry state and a wet state, to examine the effects of water pressure, and seepage on slope stability. We had the opportunity to compare the two programs in regard to their results and usage.

As a summary, we can say that useful results were obtained with the modelling procedures, which can provide great help for experts in the water industry. Flood protection works require continuous activity, and fast numerical computation methods cast light on potential upcoming failures and thus may help to mitigate or avoid catastrophes.

Acknowledgement: *The described article was carried out as part of the EFOP-3.6.1-16- 2016-00011 ñYounger and Renewing University ï Innovative Knowledge City ï institutional development of the University of Miskolc aiming at intelligent specialisationò project implemented in the framework of the Szechenyi 2020 program. The realization of this project is supported by the European Union, co-financed by the European Social Fund.*

References

Aquaveo, LLC (2019) GMS User Manual (v10.2.) The Groundwater Modeling System.

Durbin, T. J.; Bond, L. D. (1998). FEMFLOW3D A finite-element program for the simulation of three-dimensional aquifers. Version 1.0, U. S. Geological Survey, Open-File report 97-810.

François B., Schlef K. E., Wi S., Brown C. M. (2019): Design considerations for riverinefloods in a changing climateï A review. Journal of Hydrology Vol. 574, July 2019, https://doi.org/10.1016/j.jhydrol.2019.04.068, p. 557-573.

Ilyés, Cs., Turai, E., SzŤcs, P., Zsuga, J. (2017). Examination of the cyclic properties of 110-year-long precipitation time series. Acta Montanistica Slovaka 22(1) pp. 1-11.

Kádár, I; Nagy, L. (2017). Comparison of different standards based on computing the probability of failure of flood protection dikes. Periodica Polytechnica Civil Engineering, 61(1) pp. 146-153.

Kovács, B. (2004). Hidrodinamikai és transzportmodellezés I. ElsŖ kiadás, Miskolci Egyetem, MŤszaki Földtudományi Kar, Szegedi Tudományegyetem, Ásványtani, Geokémiai, és KŗzettaniTanszék, GÁMA-GEO Kft. (in Hungarian).

Mihalik, A. (2000). Szivárgást gátló árvízvédelmi töltések stabilitását biztosító vasalt földtámszerkezetek, MŤszaki szemle 9-10. pp. 26-33. (in Hungarian)

Nagy, L. (2003). Árvízvédelmi gátak szakadásai, MHT XXI. vándorgyŤlés (presentation). (in Hungarian).

Nagy, L. (2008). Hydraulic failure probability of a dike cross section. Periodica Polytechnica Civil Engineering. 55(2), pp. 83-89.

Nagy, L. (2014). Buzgárok az árvízvédelemben, Országos Vízügyi Fŗigazgatóság, (in Hungarian).

Palcsu, L., Kompár, L., Deák, J., SzŤcs, P., Papp, L. (2017). Estimation of the natural groundwater recharge using tritium-peak and tritium/helium-3 dating techniques in Hungary, Geochemical Journal, 51, pp. 439-448.

Shivakumar S. Athania, Shivamanth , C. H. Solanki and G. R. Dodagoudar (2015): Seepage and Stability Analyses of Earth Dam Using Finite Element Method. Aquatic Procedia Vol. 4 (2015), Elsevier, doi: 10.1016/j.aqpro.2015.02.110, p. 876 ï 883

Sternberg R. (2006): Damming the river: a changing perspectiveon altering nature. Renewable and Sustainable Energy Reviews 10 (2006), doi:10.1016/j.rser.2004.07.004, p. 165ï 197

Töltésállapot vizsgálata árvíz idején (Hungarian Technical Directive) MI 10 269-1982

Vágás, I. (2007). Második honfoglalásunk: A Tisza-völgy szabályozása, Hidrológiai közlöny, (in Hungarian) 87(3) pp. 30-38.

Völgyesi, I. (2008). Árvédelmi töltések szivárgáshidraulikai modellezése. Hidrológiai Közlöny, (in Hungarian) 88(1) pp. 32-35.

Wright, S. G. (1999). UTEXAS4 A computer program for slope stability calculations, Sinhoak Software, Austin, Texas

Xiaohui Tan, Xue Wang, Sara Khoshnevisan, Xiaoliang Hou, Fusheng Zha (2017): Seepage analysis of earth dams considering spatial variability of hydraulic parameters. Engineering Geology Volume 228, 13 October 2017, https://doi.org/10.1016/j.enggeo.2017.08.018, p. 260-269

Zákányi, B., SzŤcs P. (2010). Völgyzáró gát és árvízvédelmi töltések hidraulikai vizsgálata SEEP2D modullal. Hidrológiai közlöny, (in Hungarian) 90(4) pp. 54-62.

Zákányi, B., SzŤcs P. (2013). Hydraulic investigation of flood defences using analytic, and numerical methods, Acta Montanistica Slovaca, 18(3). pp. 188-197

Zeleŕákovaŕ M.; Dobos, E.; Kováļová, L.; Vágó, J.;Abu-Hashim, M.; Fijko, R.; Prucz, P. (2018). Flood vulnerability assessment of Bodva cross-border river basin, Acta Montanistica Slovaca, 23(1), pp. 53-61.

Economic Transformation of a Mining Territory Based on the Application of a Cluster Approach

***Zhanna Mingaleva*[1], *Evgeny Zhulanov*[1], *Natalia Shaidurova*[2] *and* *Natalia Vukovic*[3]**

The economic aspects of the transformation of the mining industry and spatial development in the city of Berezniki, Perm Region (Russia) are analyzed in the article. A quantitative assessment of inter-sectoral relations within the framework of the economy of a mining city is given. The results of economic and mathematical modelling of the creation of a territorial industrial cluster based on a mining enterprise are presented. The purpose of the study is to calculate changes in the economic development of a single-industry city and a municipal district when an industrial cluster is created on its territory with a mining enterprise as the core of a cluster (the flagship of the municipal economy). When applying the cluster approach, the emphasis was placed on the leading position of the mining enterprise in a specific territory, its role in the development of the economy of the single-industrial city and the municipality was assessed. The result of the study is a quantitative assessment of the effectiveness of creating an industrial cluster in the single-industrial city of the mining industry. It is proved that when forming a cluster around the existing mining enterprise, it is possible to obtain a high positive effect from the cluster for urban and municipal development.

Keywords: *Mining industry, sustainable development, economic and mathematical model, the cluster model*

Introduction

ñIndustrial cluster and enterprise agglomeration is industrial upgrading model of the high-end and most competitive advantage in the world todayò (*Le and Ning, 2015, p.1879*). One of the key policies in economic development to move towards becoming a country with global competitive potential is to promote cluster development. A ñclusterò is a powerful tool and mechanism for enhancing competitiveness and the development of an industrial economy in a country (*Fongsuwan, 2017*). This is fully consistent with the strategic objectives of the development of the territory with a predominance of extractive industries. This is especially important for territories with a single city-forming enterprise, on whose activities the well-being of entire large territories and cities depends. «Improvement of the economic activity of industrial companies determines conditions for the possible improvement of mining and metallurgical business activity and finds the sources of companiesô growth» (*Manová et al., 2018, p.132*).

Creating a more efficient economy is achieved on the basis of constant change. For the former socialist countries, «On example of such change is a transformation process from a centrally planned economy to market economy» (an example of such a change is the process of transition from a centrally planned economy to a market economy) (*Budaj et al., 2018, p.1*). In our study, we consider a transformation process as a process of changing the mechanism of interaction between enterprises of different sectoral affiliations operating within the limited framework of one mono-specialized territory - the mining area. Cluster association is the basis of this change and its result.

The theory of industrial clusters in the modern sense was developed from the works written by M. Porter. Porter M. determined that a cluster is a group of enterprises and related organizations involved in the same case with cooperative linking and addition (*Porter, 1998).* The expediency of creating a cluster is explained by the fact that "When considering success for the industry in developed or developing countries, it is apparent that successful industries do not come from a single company or entity alone. Instead, it comes from multiple ventures competing in clusters, resulting in sustainable economic growth (*Fongsuwan, 2017*).

One of the key factors for the success of this network development mechanism is the distribution of financial benefits for the business (*Martin and Sunley, 2002).* In turn, business in a cluster is often stimulated to increase efficiency, stimulate research and development, and increase business efficiency (*Porter, 2011).*

The activity of clusters leads to the creation of a more efficient regional economy, on the basis of obtaining by all enterprises in the region sustainable and high profits.

[1] *Zhanna Mingaleva, Evgeny Zhulanov,* Perm National Research Polytechnic University, Department of Economics and management in industrial production, 29 Komsomol'skii ave., Perm, 614990, Russia, *mingal1@pstu.ru, zeepstu@yandex.ru.*

[2] *Natalia Shaidurova,* Kalashnikov Izhevsk State Technical University (Votkinsky branch), Department of Economics and Organization of Production, 1 Shuvalov str., Votkinsk, 427433, Russia, *Shaydurovans@gmail.com*

[3] *Natalia Vukovic,* Ural Federal University named after the first President of Russia B. N. Yelts*in,* Graduate School of Economics and Management, 19, Mira str., Yekaterinburg, 620002, Russia, *shpak17121978@gmail.com*

Previous research also has proved, that by organizing cluster interaction and coordinating with industry member colleagues, smaller firms strengthen their competitive profile (*Lechner and Dowling, 2003*) and increase their chances of survival (*Hoang and Antoncic, 2003*).

The much positive impact on the development of the regional (municipal, urban) economy is enhanced if the industrial cluster is transformed into a technology park structure - i.e. in addition to purely industrial enterprises includes scientific centres and laboratories, educational institutions, business incubators, start-ups and other innovation infrastructure objects (*Pascu et al., 2013; Shaidurova, 2017; Mingaleva and Shaidurova, 2018*).

Numerous and diverse studies have explained many trends and issues of cluster development (Hervás-Oliver *et al., 2015; Trippl et al., 2014; Yu et al., 2015)*. The recommendations have been developed on the creation of industrial clusters (*Feser and Bergman, 2000*), their development (*Le and Ning, 2015).* A number of studies provide estimates of the role of clusters in national and world development (*Lindsay, 2005; Hsu et al., 2013*), in innovative development (*Lesnik and Mingalyova, 2013*), in creating research and development (Lechner and Dowling, 2003; *Ma Ding, 2014*) and a number of other economic processes (*Bengtsson and Sölvell, 2004; Zhu, 2003*). And these studies are not stopped but are supplemented with new data and take into account new trends and phenomena, including at the regional and municipal levels (*Mingaleva et al., 2017*).

The importance of industrial clusters for regional and municipal development is also noted in the most recent studies (*Kusa et al., 2019*). Thus, in the work of Sergey Anokhin, Joakim Wincent, Joakim Wincent, Vinit Parida, Natalya Chistyakova and Pejvak Oghazi the increasing role of industrial clusters for the development of the region is noted, since they are becoming significant positive predictors of innovation dynamics at present (*Anokhin et al., 2018*).

As for the creation of clusters in the mining industry or on the basis of a large extractive enterprise, at the present time, there are very few such studies. Basically, this is the study of such cluster development issues as the role and importance of the extractive industry as a whole for the national economy of specific countries (*Budaj et al., 2018).* In this case, the question of the feasibility of creating a cluster may be associated with the need to increase the competitiveness of the industry. Thus, it is particularly noted that in a number of countries "given the high level of mining costs and the cost of processing domestic ore raw materials, their mining is uneconomical" (*Budaj et al., 2018, p.3*). And the cluster could help.

The functioning of individual mining and extractive enterprises, including the environmental damage that these enterprises create, and environmental problems, are investigated (*Biaǧy 2014*; *Biaǧy & Mroczkowska, 2015)*. It is noted that in a number of countries, domestic resources of certain types of minerals (coal, shale, peat, etc.) are considered as a strategic resource base, reducing dependence on imports of primary fuel and energy raw materials, as well as ñreserves for unforeseen situations and as a source of employment opportunities"(*Budaj et al., 2018, p.3*). Also, a number of works are devoted to the creation of clusters in a low-carbon economy (*Zhang, 2016*).

Material and Methods

Method

The simplest and economically significant is the application of the cluster's methodology for cities with one or several city-forming enterprises. On the one hand, in such cities, there are a limited number of enterprises - the poles of economic growth, which simplifies the assessment and prioritization in determining the boundaries of clusters on the values of multipliers. On the other hand, it becomes easier to evaluate the synergistic effects obtained from the coordinated work of cluster members. By UNCTAD methodology the countries in which the share of mining and processing of raw materials in the gross domestic product (GDP) is more than 25% are classified as countries with the developed mining industry (*Budaj et al., 2018*). We extrapolated this methodology to the regional level and identified Berezniki as a city with a developed mining industry because the mining and chemical industries provide almost 90% of the industrial activity of the city. Based on the above, we consider the practical application of the author's developed methodology with reference to the industrial complex of the city of Berezniki, Perm Region of the Russian Federation, specialized in the mining of potash deposits and the production of mineral fertilizers.

The methodological approach to the selection of enterprises in a cluster takes into account that a cluster is a mutually dependent grouping that focuses on the real participation of all sectors (*Sölvell et al., 2003*). Therefore, we have included in the cluster all enterprises of different branches of production and material services operating in the city of Berezniki. In accordance with the methodology based on the available data of the Federal State Statistics Service of the Russian Federation according to the tables ñCosts - outputò in monetary terms for 2015 (*National Accounts, 2015, downloaded on 30. August 2018, available online:* www.gks.ru/wps/wcm) we identified possible options for building a technological chain of interconnection between the industrial enterprises located in the city Berezniki, Perm Region of the Russian Federation. Cluster vertical links unite business operators in ascending or descending technological lines, and horizontal links connect various auxiliary

industries designed to achieve common goals. ñThe businesses in the group are often stimulated to increase efficiency, promote research and development and improve business performanceò (*Porter, 2011).*

In the process of selecting industries and enterprises to build a technological chain in a cluster, we took into account the characteristics of the life cycle of technologies and their role in the viability of the cluster (*Dalum et al., 2005*) and the need to fill gaps and more precisely establish specialization in extended product chains (*Feser and Bergman, 2000*). We also took into account the impact of structural changes between sectors on the economic security of the territory where enterprises united in a cluster *(Mingaleva and Gataullina, 2012).*

An important feature of the cluster, which has been noted by many researchers, is its ability to coordinate supply chains (*Kristal et al., 2010).* And different industries and countries occupy different places in these chains. For example, studying the place and role of Chinese enterprises in global clusters showed that Chinese are ñmost of the cluster in the global value chain in the low middle value added production processing link..." (*Le and Ning, 2015, p.1879*). Le and Ning explain why most Chinese industrial clusters are still "at the lower end of the road in the development of industrial clusters" by this fact (*Le and Ning, 2015, p.1879*).

In our methodology, we used the results of the research of Ma Ding (*Ma Ding, 2014*), who investigated the collaboration in the supply chain and possible additional benefits from such collaboration. In particular, he wrote that the collaboration in the supply chain could work together in creating research and development.

Currently, science has already developed and applied methods for analyzing the efficiency of industrial clusters adapted to the requirements of the information economy and digitalization. For example, S. Papagiannidis, E.W.K. See-To, D.G. Assimakopoulos and Y. Yang, presented a methodology for big data analytics, which can be utilised as a decision support system for identifying industrial clusters in a specific geographic region (*Papagiannidis et al., 2018, p.355*). The proposed methodology was tested on the example of industrial clusters in the North East of England and showed good and accurate results with a large database.

The proposed methodological approach was used by us to develop the author's methodology for transforming the mechanism of interaction between enterprises operating within a specific territory in order to create an industrial cluster. The database consists of the data from the Federal State Statistics Service of the Russian Federation (ROSSTAT database). The main methods of applying statistical data for modelling the cluster we took from Hartigan 's work (*Hartigan, 1985*).

The database

The city Berezniki, Perm Region of the Russian Federation is an industrial city with most mining and processing companies in the chemical industry. Berezniki is characterized by an excessive concentration of industrial potential. There are many enterprises of heavy industry, its basic industries. The structure of industrial production of Berezniki is given in Table 1.

Tab. 1. The structure of industrial production of Berezniki city

The industry sector	The industry share in the fixed assets	The industry share in the industrial output of Berezniki
The chemical complex	87.3%	79.2%
The fuel and energy sector	8.2%	8.8%
The complex for the production of consumer goods	1.0%	6.7%
The mechanical engineering	1.6%	1.2%
Other industries	3.0%	4.1%

Source: own processing

Several enterprises that are official monopolists in Russia work in Berezniki. These are:

- "AVISMA" branch of PSC "VSMPO-AVISMA Corporation" (it produces the titanium sponge and titanium powders, metallic magnesium, magnesium alloys and products, chemical products, that are sold not only in Russia but throughout the world);
- ñAzotò branch of OJSC ñURALCHEMò (it produces the ammonium nitrate, carbamide and other nitrogenous fertilizers);
- PJSC Uralkali, which has in the city 2 Potash Production Mine Administration (BKPRU) ï BKPRU-1 and BKPRU-4 (it produces the potash fertilizers).

Berezniki is an important transportation hub: the main automobile road Perm-Solikamsk passes through the city, going further to the north of the Perm Territory. Also in Berezniki, there is water transport communication on the Kama River. At the present time, the railway is being restored, which was destroyed by a failure at the mine BKPRU-4 PJSC Uralkali.

All industrial enterprises located in the city Berezniki, Perm Region of the Russian Federation are united in 9 groups. The name of these groups, their conditions number for the econometric calculations and their correlation with Russian Classification of Economic Activities (OKVED) are given in Table 2. In our methodology, we take

into account conclusions about the limitations of the Standard Industrial Classification (SIC) codes, which are manifested in the digital economy (*Papagiannidis et al., 2018; Bako, 2016*).

Tab. 2. The clustering of enterprises in accordance with the Russian Classification of Economic Activities

The industry sector of enterprises	Identification by Russian Classification of Economic Activities (OKVED codes)	Reference numbers for the calculations
The production of potash fertilizers	Section C - "Manufacturing": 20.15.5 - Subgroup "Production of potash mineral or chemical fertilizers"	1
Fuel production	Section C - "Manufacturing": Class 20 ï ñManufacture of chemicals and chemical productsò	2
Manufacture of machinery and equipment	Section C - "Manufacturing": Class 28 - "Manufacture of machinery and equipment not included in other groups": Subclass 28.1 - "Manufacture of machinery and equipment for general use."	3
Electricity and heat supply services	Section D - "Provision of electric energy, gas and steam; air conditioningò: Subclass 35.30 ï ñProduction, transmission and distribution of steam and hot waterò; Subclass 35.1 - "Production, transmission and distribution of electricity."	4
Construction work	Section F ï ñConstructionò: Class 41 ï ñBuilding constructionò; Class 43 ï ñSpecialized construction worksò.	5
Wholesale trade services	Section G ï ñWholesale and retail tradeò: Class 46.1 ï ñTrade on a fee or contract basisò	6
Land transport services	Section H ï ñTransport and storageò: Class 49 ï ñActivity land and pipeline transportò	7
Services of water transport organizations	Section H ï ñTransport and storageò: Class 50 ï ñWater transport activitiesò.	8
Production of other goods and services	A cumulative group including multiple identification codes	9

Source: own processing

The territory of Berezniki can be divided into 3 industrial zones, where the main enterprises are concentrated. The map of Berezniki where these 3 industrial zones are indicated is shown in Figure 1.

Source: own processing

Fig.1. The main industrial zones of Berezniki

Figure 1 shows the following industrial zones formed by monopolistic enterprises in the mining and chemical industries:

- ñNorthern zoneò (the enterprises of ñAVISMAò branch of PSC ñVSMPO-AVISMA Corporationò);
- ñNortheast zoneò (the mines and enterprises of ñBKPRU-4 PJSC Uralkaliò)
- ñWestern zoneò (the mines and enterprises of ñBKPRU-1 PJSC Uralkaliò, ñOJSC Azotò, ñOJSC Berezniki Soda Plantò; ñJSC Berezniki Mechanical Plant" and other enterprises).

The ñNortheastò and ñWesternò zones were chosen as the basis for building the cluster model. Uralkali is the flagship enterprise in these zones.

The database consists of the data on the according to the tables ñCosts - outputò in monetary terms, the data on the industry sector of enterprises, the price data for major industrial products, the inflation data and other statistics.

In total, over 2000 enterprises and organizations of all sizes and forms of ownership were taken for calculations. These enterprises employ more than 40,000 workers.

The accounting and economic indicators of the main enterprises included in the technological chain of the proposed cluster are given in Table 3 (*Three **ñ**whales**ò**, 2017*).

Tab. 3. The accounting and economic indicators of the main enterprises of the city of Berezniki [rubles]

Place	*Name*	*Income*	*Profit (loss) before tax*	*Balance sheet*	*Non-current assets*	*Current assets*	*Capital and reserves*
3	PJSC Uralkali	131 311 916	80 911 970	630 367 555	522 332 297	108 035 258	168 086 315
26	LLC "Uralkali-Repair"	7 119 963	450 330	3 489 542	158 406	3 331 136	928 088
36	JSC "Bereznikovsky Soda Plant"	5 595 832	650 740	4 534 741	3 800 879	733 862	2 359 271
84	LLC "Soda-chlorate"	2 427 754	-633 816	4 089 511	3 560 425	529 086	612 511
156	CJSC "Bereznikovskaya network company"	1 384 436	-346 588	1 154 265	235 262	919 003	-497 345
160	Azottech LLC	1 347 591	81 723	271 399	106 852	164 547	192 137
180	LLC "Construction company "Himspetsstroy"	1 126 940	23 288	517 128	215 183	301 945	66 827
234	JSC Berezniki Mechanical Plant	803 913	5 017	1 714 527	472 550	1 241 977	32 346
246	LLC "AVISMA-Spetsremont"	751 364	32 880	376 592	2 526	374 066	40 472

Source: own processing

Table 3 shows the enterprises in the order of ranking places that they occupied in the TOP-300 of the largest enterprises of the Perm Krai (*TOP-300*). This rating is compiled in terms of revenue from the sale of goods, products, works and services.

Results

To solve the research task, under the transformation process, we understand the process of uniting enterprises of various industries that exist in a specific mining area in order to create a territorial (urban) multi-sectoral cluster. Determining the possibilities of organizing a regional cluster in Berezniki began with the choice of a market for end products, in which the flagship enterprise has an advantage in price or quality of goods. This will need to put pressure on the market at the expense of jointly organized shares of cluster members. The choice of the flagship enterprise is also important from the point of view of organizing the technological chain and network of interactions in the cluster. In accordance with the author's methodology, in the beginning, we calculated the coefficients of the total costs for each industry sector of enterprises. These coefficients obtained by the "Cost-output" model (*National Accounts, 2015, downloaded on 30. August 2018, available online:* www.gks.ru/wps/wcm) and characterizing the full standard of costs for the purchase of intermediate goods and services of the enterprises - suppliers, located in the ***i***-th lines of the table for the production of the monetary unit of the benefit of enterprises ï consumers indicated in the ***j***-th columns. The coefficients of the total costs present in Table 4.

Tab. 4. Coefficients of total material costs and the rate of value added by types of economic activity per monetary unit of finished goods

The numbers of industry sector	1	2	3	4	5	6	7	8	9
1	1,0135	0,0004	0,0006	0,0005	0,0124	0,0005	0,0020	0,0006	0,0000
2	0,0689	1,1519	0,0136	0,0356	0,0331	0,0261	0,0752	0,1744	0,0000
3	0,0557	0,0066	1,1647	0,0107	0,0216	0,0067	0,0134	0,0291	0,0000
4	0,0727	0,0333	0,0378	1,5542	0,0139	0,0193	0,0645	0,0192	0,0000
5	0,0182	0,0070	0,0060	0,0188	1,0288	0,0067	0,0186	0,0098	0,0000
6	0,0448	0,0413	0,0876	0,1866	0,0638	1,0391	0,0312	0,0408	0,0000
7	0,0627	0,1550	0,0541	0,0718	0,0416	0,2301	1,1949	0,1132	0,0000
8	0,0376	0,0023	0,0008	0,0008	0,0026	0,0019	0,0032	1,0234	0,0000
9	0,2554	0,6656	0,4719	0,4536	0,5205	0,5584	0,5439	0,5419	1,0000

Source: own processing

The calculation of aggregate value added norms are presented in Table 5.

Tab. 5. Calculation of aggregate value-added norms

The numbers of industry sector	The industry sector of enterprises	Aggregate value-added norm
1	The production of potash fertilizers	0,6224
2	Fuel production	0,2198
3	Manufacture of machinery and equipment	0,3985
4	Electricity and heat supply services	0,2830
5	Construction work	0,4043
6	Wholesale trade services	0,3349
7	Land transport services	0,3311
8	Services of water transport organizations	0,3394
9	Production of other goods and services	0,5100

Source: own processing

Based on the data obtained, it becomes possible to determine the multipliers of the total value-added. Hence the multiplier is (Eq. 1):

$$m = \frac{\sum_{j=1}^{M} v_j \cdot \Delta X_j}{\Delta Y_j}, \quad (1)$$

where v_j ï unit value added per unit of product *j*;

ΔX_j ï the increase in gross output of the good *j* after increasing Y_j per unit - ΔY_j.

Consider the calculation of this multiplier on the example of the production of potash fertilizers of JSC ñUralkaliò, based on the increase in the volume of final products by one monetary unit of Eq. 1:

$$m = \frac{\sum_{j=1}^{M} v_j \cdot \Delta X_j}{\Delta Y_j} = \frac{0{,}0182 \cdot 0{,}4043 \cdot 1 + 0{,}0448 \cdot 0{,}3349 \cdot 1 + 0{,}0627 \cdot 0{,}3311 \cdot 1 + 0{,}0376 \cdot 0{,}3394}{1} + \frac{0{,}2554 \cdot 0{,}5100 \cdot 1}{1} = 0{,}88$$

The resulting multiplier indicates that an increase in sales of the final product of an enterprise producing potash fertilizers by one monetary unit provides an increase in value-added along the technological chain of production of the city of Berezniki by 0.88 monetary units. Similar multipliers were calculated for other types of economic activity. The final results of the calculations are presented in table 6.

Tab. 6. Calculation of aggregate value-added multipliers

The numbers of industry sector	The industry sector of enterprises	Aggregate value-added multiplier
1	The production of potash fertilizers	0,88
2	Fuel production	0,68
3	Manufacture of machinery and equipment	0,77
4	Electricity and heat supply services	0,78
5	Construction work	0,75
6	Wholesale trade services	0,73
7	Land transport services	0,73
8	Services of water transport organizations	0,74

Source: own processing

The resulting multiplier shows how many monetary units will increase the value-added for the considered technologically interrelated enterprises (sub-sectors or markets) with an increase in sales of final products j per unit. As can be seen from Table 6, the largest multiplier is observed in the production of potash fertilizers (1). Therefore, this type of production is the pole of economic growth in the city and the basis for the formation of a cluster that combines all the above-mentioned activities.

The determination of the capabilities and competitive advantages, which opened for business in the process of clusters organization is the next element of the methodological approach and research method. They become apparent only in the detailed calculation of economic projects related to the production and sale of cluster products. It is necessary to create a table of competitive advantage assessment, which compares these parameters for enterprises before and after joining the cluster in comparison with those competitors who are supposed to be pushed in the market. This table is formed along the technological chain of goods production from the final product to the initial intermediate resource. It should be noted that this table can be formed for products of specific enterprises that form a small cluster, and for sub-sectors or markets that are part of a large system of the territorial cluster.

The assessment of economic and competitive advantages of creating a cluster is presented in Table 7.

Tab. 7. Assessment of economic and competitive advantages of creating a cluster

Products	*Data of the leading competitor*			*Results of the functioning of the enterprises / sub-sectors / markets capable of forming a cluster*			*Change of results of functioning of the enterprises / sub-sectors / markets after cluster creation*		
	Price	*Quality*	*Sales volume*	*Price*	*Quality*	*Sales volume*	*Price*	*Quality*	*Sales volume*
Product 1 (final)	$P_{c,1}$	$S_{c,1}$	$Q_{c,1}$	$P_{l,1}$	$S_{l,1}$	$Q_{l,1}$	$\Delta P_1 = (P_{c,1} - P_{l,1})$, *if* $\Delta P_1 < 0$	$\Delta S_1 = (S_{c,1} - S_{l,1})$, *if* $\Delta S_1 > 0$	$Q_{c,1}$, *if* $\Delta S_1 > 0$ *and* $\Delta P_1 < 0$
Product 2 (intermediate)	$P_{c,2}$	$S_{c,2}$	$Q_{c,2}$	$P_{l,2}$	$S_{l,2}$	$Q_{l,2}$	$\Delta P_2 = (P_{c,2} - P_{l,2})$, *if* $\Delta P_2 < 0$	$\Delta S_1 = (S_{c,1} - S_{l,1})$, *if* $\Delta S_1 > 0$	$Q_{c,2}$, *if* $\Delta S_2 > 0$ *and* $\Delta P_2 < 0$
Product 3 (intermediate)	$P_{c,3}$	$S_{c,3}$	$Q_{c,3}$	$P_{l,3}$	$S_{l,3}$	$Q_{l,3}$	$\Delta P_3 = (P_{c,3} - P_{l,3})$, *if* $\Delta P_3 < 0$	$\Delta S_1 = (S_{c,1} - S_{l,1})$, *if* $\Delta S_1 > 0$	$Q_{c,3}$, *if* $\Delta S_3 > 0$ *and* $\Delta P_3 < 0$
é	*é*	*é*	*é*	*é*	*é*	*é*	*é*		*é*
Product n (intermediate)	$P_{c,n}$	$S_{c,n}$	$Q_{c,n}$	$P_{l,n}$	$S_{l,n}$	$Q_{l,n}$	$\Delta P_n = (P_{c,n} - P_{l,n})$, *if* $\Delta P_n < 0$	$\Delta S_1 = (S_{c,1} - S_{l,1})$, *if* $\Delta S_1 > 0$	$Q_{c,n}$, *if* $\Delta S_n > 0$ *and* $\Delta P_n < 0$

Source: own processing

Note:

$P_{c,i}$, $P_{l,i}$, $P_{k,i}$ ï prices of the *i*-th product of the leading competitor, the potential member of the cluster, respectively, before and after its organization;

$S_{c,i}$, $S_{l,i}$, $S_{k,i}$ ï an integral indicator of the quality of the *i*-th product of the leading competitor, the potential member of the cluster, respectively, before and after its organization;

$Q_{c,i}$, $Q_{l,i}$, $Q_{k,i}$ ï an integral indicator of the quality of the *i*-th product of the leading competitor, the potential member of the cluster, respectively, before and after its organization;

n - the number of types of goods planned for production within the cluster;

1.01 - the coefficient correcting value of the indicator on the small size for ensuring the enterprise of competitive advantage.

The integral quality index is proposed to be calculated by the formula characterizing the sum of dimensionless quantities calculated by the consumer characteristics of the *i*-th product (Eq. 2):

$$S_i = \sum_{j=1}^{M} \frac{s_j - s_{min}}{s_{max} - s_{min}}, \quad (2)$$

where s_j ï numeric value of consumer characteristic *j* for the product *i*;

s_{max} and s_{min} ï the maximum and minimum value of the consumer characteristic *j*, observed in the market.

If the value of the consumer characteristic has an inverse connection with demand, the values $1/s_j$, $1/s_{max}$ and $1/s_{min}$ are used in the calculation. If the parameter does not have a quantitative value, but only a qualitative one, then if the product has a qualitative characteristic j, its value is equal to 1 and to 0 in the opposite case. The maximum value of the quality indicator is equal to the number of consumer characteristics.

Next, we analyzed the international market of potash fertilizers. Based on the analysis, it can be noted that it is characterized by price differentiation depending on the region of sales and the length of transport routes. On this basis, for the purposes of the analysis being conducted, its geographically limited part should be emphasized on which there is a "leading" competitor whose products have the advantages in price or quality of goods. The Chinese market for potash fertilizers can be considered as such a market. On it, the Berezniki company OJSC Uralkalii (URK) confronts the OJSC Belarusian Potash Company (BPC).

Characteristics of prices, production capacity and sales volumes in the Chinese market of both companies are presented in Table 8. The data in Table 6 is given from official sources of companies OJSC Uralkalii (***ñ****Uralkali****ò*** *leaves the world's largest mineral fertilizer markets, downloaded on 11. January 2019, available online:* https://www.vedomosti.ru/business/articles/2018/12/03/788258-uralkalii) and OJSC Belarusian Potash Company (*Belarusian Potash Company Signs New Contract With China, downloaded on 11. January 2019, available online:* https://www.vedomosti.ru/business/articles/2018/09/17/781074-belorusskaya-kaliinaya).

Tab. 8. Characteristics of the prices, production capacity and sales volume of potash fertilizers of competing companies in the Chinese market in 2017

The legal name of the company	Prices set before 2019 [USD per ton]	Sales volume, [million tons of fertilizers]
OJSC Belarusian Potash Company	290	2
OJSC Uralkalii	300	7,5

Source: own processing

To fill the data in Table 8, it is necessary to calculate the quality level indicator. Consider its calculation on the example of potash fertilizers. To this end, we choose the following main consumer characteristics of the product with the permissible level of their values indicated in brackets: mass fraction of K2O (3-63%), mass fraction of H20 (0.1-1%), mass fraction of fractions (1-4 mm), dynamic strength (80-100%), friability (5-100%). Using formula (2), we define the quality level of the products of the Belarusian Potash Company (*The products of Belaruskali, downloaded on 11. January 2019, available online:* https://kali.by/products/khloristyy-kaliy):

$$S_{1,BPC} = \sum_{j=1}^{M} \frac{s_j - s_{min}}{s_{max} - s_{min}} = \frac{60-3}{63-3} + \frac{\frac{1}{0,5} - \frac{1}{0,1}}{1 - \frac{1}{0,1}} + \frac{4-1}{4-1} + \frac{85-80}{100-80} + \frac{100-5}{100-5} = 4,09$$

A similar calculation of the quality indicator for the characteristics of potash fertilizers of OJSC Uralkali (*Product Catalog* ***ñ****Uralkali****ò****, downloaded on 11. January 2019, available online: http://pda.uralkali.com /upload/content/products/Products_catalogue_ru.pdf*) indicates that it is at about the same level:

$$S_{1,URK} = \sum_{j=1}^{M} \frac{s_j - s_{min}}{s_{max} - s_{min}} = \frac{60-3}{63-3} + \frac{1 - \frac{1}{0,1}}{1 - \frac{1}{0,1}} + \frac{4-1}{4-1} + \frac{80-80}{100-80} + \frac{100-5}{100-5} = 4$$

The next intermediate product is diesel fuel. In Belorussia, one litre of this fuel cost 0.78 USD per litre in 2017 (How much does fuel cost in Belarus? *downloaded on 11. January 2019, available online:* https://www.blr.cc/benzin), and in Russia, it was equal to 0.67 USD. The quality of diesel fuel can be assessed by its characteristics: viscosity, density, surface tension, fractional composition and pressure of saturated fuel vapours. To simplify the calculation, in view of the identity of the production technology, we take its value at level 5 by the number of consumer characteristics. It can be noted that competitors have no advantages in this technological chain of production, and there is no need for any coordination actions of fuel producers with the exception of logistics.

The next intermediate product used in the technological chain of potash production is engineering products. Since it is diverse in purpose, consumer qualities and cost, it should focus on the equipment, the introduction of which in the potash industry will provide it with a competitive advantage. In accordance with the annual report of Uralkali, 8% of the cost of potash fertilizers is the cost of repairing mining tunnelling machines and other technological equipment, which is USD 41.92 million (Integrated report of "Uralkali", *downloaded on 11. January 2019, available online: https://www.uralkali.com/upload/iblock/0dc/uralkali_ar2017_rus.pdf).* In this regard, at JSC Berezniki Mechanical Plant (hereinafter BMZ), within the cluster, repair works of equipment of JSC Uralkali can be arranged at a lower price due to the proximity of the location of the repair production and its raw material base. The required capital investments in its organization are approximately equal to 61 million

USD. However, according to the accounting statements of BMZ, the net profit will be enough to invest only 8 million USD. Hence the need to use the funds of cluster enterprises arises that can benefit from such innovation.

Thus, the selected production and numerical parameters should be recorded in Table 9:

Tab. 9. Assessing the economic and competitive advantages of creating a cluster

Products	Data of the leading competitor			Results of the functioning of enterprises / sub-sectors / markets capable of forming a cluster			Change of results of functioning of enterprises / sub-sectors / markets after the creation of a cluster		
	Price	Quality	Sales volume	Price	Quality	Sales volume	Price	Quality	Sales volume
Potash fertilizers	$290 /ton	4,09	2 million tons	$300 /ton	4	7,5 million tons	$289,9 /ton	4	2 million tons
Fuel	$0,78 per litre	5	36212, 6 thousand litres	$0,67 per litre	5	163543,8 thousand litres	$0,67 per litre	5	43611,68 thousand litres
Repair of mining equipment	-	-	$21,72, million	-	-	4$1,92, million	-	-	$21,72, million

Source: own processing

It should be noted that since energy supply, heat supply, and transportation services belong to natural monopolistic activities, and there is no competition for them in the city of Berezniki, it does not make sense to analyze the possibility of increasing their competitiveness.

Construction and wholesale services in the city of Berezniki are represented by numerous firms competing with each other. Therefore, the coordination of their activities does not make sense, since the "narrow" places for the cluster are eliminated in the process of competition.

As can be seen from Table 8, in order to provide the necessary competitive advantage in the sale of final goods, it is necessary to reduce the price of potash fertilizers by 10.1 USD ((300-290)*1.01). This will push the competitor out of the market and increase sales by 2 million tons. To this end, analyzing the possibility of reducing costs along the technological chain of production, you can see that reducing repair costs by at least 20.2 million USD (10.1 Ã2 million tons) will allow acquiring the desired competitive advantage.

Discussion

Using the author's methodology for calculating the economic efficiency of the newly created cluster, high positive values were obtained from the creation of a cluster around an enterprise for the extraction of potassium salts and the production of potash fertilizers. For the final confirmation of this possibility, it is required to calculate the indicators

The forecast horizon of indicators was 5 years, based on the depreciation period of the equipment in which it is proposed to invest.

Additional profits of enterprises from the organization of the cluster is determined as follows:

1) for JSC ñUralkaliò:

$$Pr_{URK,1} = (Pr1_{i,i} \cdot Q_{c,i} - SN_{pr,i}) \cdot (1 - N_{in}) = (289{,}9 \cdot 0{,}3952 \cdot 2 - 0) \cdot (1 - 0{,}2) = \$183{,}31\ mln$$

where 289,9 ï price per ton of potash fertilizer with a competitive advantage, USD / ton;

0.3952 - coefficient characterizing the profitability of sales;

2 - the volume of additional sales of potash fertilizers as a result of displacing a competitor from the Chinese market;

0.2 is the coefficient characterizing the tax rate on profits in the Russian Federation.

2) for diesel manufacturers:

$$Pr_{DOT,2} = (Pr_{DOT,2} \cdot Q_{c,2} - SN_{pr,DOT}) \cdot (1 - N_{in}) = (v_j \cdot \Delta X_j - SN_{pr,DOT}) \cdot (1 - N_{in}) = (v_j \cdot b_{i,j} \cdot \Delta Y_j - SN_{pr,DOT}) \cdot (1 - N_{in}) = (0{,}2198 \cdot 0{,}0689 \cdot 289{,}9 \cdot 2 - 0) \cdot (1 - 0{,}2) = \$7{,}02\ mln$$

where 0.2198 ï the coefficient characterizing the rate of value-added in the price of diesel fuel,

0.0689 - the ratio of the full cost of the use of diesel fuel in the production of one ton of potash.

It should be noted that the increase in profits from the additional sales of diesel fuel is formed by increasing the amount of fuel consumed as a result of the growth in the output of final products. Hence, the sales volume of diesel fuel, indicated in table 6, was calculated according to the technological production chain as follows:

$$Q_{c.2} = Q_{c.1} \cdot \frac{Q_{l.2}}{Q_{l.1}} = 2 \cdot \frac{163543{,}8}{7{,}5} = \ 43611{,}68\ tous.l.$$

3) for the JSC "Berezniki Mechanical Plant" profit will be:

As can be seen in Table 7, the annual profit is taken into account at the same level, based on the preservation of competitive advantage. Depreciation charges are formed only at the enterprise BMZ, as it is the only enterprise that makes investments. In the process of discounting cash flows, the discount rate (Yon) was taken into account, based on the bank interest rate on the US dollar at 2.5%. The net present value was determined by the traditional formula:

$$NPV = \sum_{t=1}^{T} \frac{CF_t}{(1+i)^{t-1}}, \tag{3}$$

Where CF_t is the cash flow of the enterprise l for the year *t*, mln. USD,
i - the interest rate on the US dollar,
T - forecast horizon, years.

The results of the simulation of cash flow from the creation of a mining cluster in the city of Berezniki presented in Table 10.

Tab.10. Simulation of cash flows from the creation of a mining cluster in the city of Berezniki [million USD]

Indicator	Forecast horizon, years				
	1	2	3	4	5
Additional capital investment	61	0	0	0	0
- investments of JSC Uralkali	0	0	0	0	0
- investments of diesel fuel manufacturers	0	0	0	0	0
- investments of JSC "Berezniki Mechanical Plant"	61	0	0	0	0
Additional profit	195,715	195,715	195,715	195,715	195,715
- profit of JSC Uralkali	183,31	183,31	183,31	183,31	183,31
- profit of diesel fuel manufacturers	7,02	7,02	7,02	7,02	7,02
- profit of JSC "Berezniki Mechanical Plant"	5,385	5,385	5,385	5,385	5,385
Additional depreciation	12,2	12,2	12,2	12,2	12,2
- increase in depreciation of JSC Uralkali	0	0	0	0	0
- increase in depreciation of diesel fuel manufacturers	0	0	0	0	0
- increase in depreciation of JSC "Berezniki Mechanical Plant"	12,2	12,2	12,2	12,2	12,2
Cash flows (ч F_t):	146,915	207,915	207,915	207,915	207,915
- JSC Uralkali	183,31	183,31	183,31	183,31	183,31
- diesel fuel manufacturers	7,02	7,02	7,02	7,02	7,02
- JSC "Berezniki Mechanical Plant"	-43,415	17,585	17,585	17,585	17,585
Discount coefficient $(1/(1+i)^{t-1})$	1	0,9756	0,9518	0,9286	0,9060
Net discounted cash flow	146,915	202,84	197,896	193,07	188,361
- JSC Uralkali	183,31	178,839	174,477	170,222	166,07
- diesel fuel manufacturers	7,02	6,848	6,681	6,518	6,359
- JSC "Berezniki Mechanical Plant"	-43,415	17,156	16,737	16,329	15,931
Cumulative net present value (NPV)	146,915	349,759	547,655	740,725	929,086
The rate of compensation of negative cash flow	22,18				
Compensation of losses to companies with negative cash flow	42,220				
- JSC Uralkali	40,663				
- diesel fuel manufacturers	1,557				
- JSC "Berezniki Mechanical Plant"					

Source: own processing

Analyzing Table 10, we can conclude that since NPV> 0, then cluster organization is beneficial for its participants. However, in the first year, enterprise BMZ has significant investment costs. As a result, it can refuse them. To prevent this from happening, formula (4) was used to calculate the rate of compensation for its losses - 22.18.

$$m = \frac{\sum_{j=1}^{n} |F_{l.t}|}{\sum_{j=1}^{n} Pr_{l.i}}, \tag{4}$$

On this basis, in the same table, a part of the profit of each enterprise was determined, which it will receive as a result of the work of the cluster and which it will need to invest in the composition of the JSC Berezniki Mechanical Plant. These investments will pay off in the first year. Their return by JSC Berezniki

Mechanical Plant can be stipulated for a five-year period during which this enterprise will be able to painlessly compensate investments from the accumulated depreciation fund.

Conclusion

From the research results, we can draw the following conclusions.

Cluster organization of activity has a positive impact on competitive advantages and sustainable development of all enterprises of the city and municipality.

Our studies were limited to one mining area (Berezniki industrial centre), and the results were obtained for a sample of enterprises in the city of Berezniki and the Berezniki municipal district. Whether this model and the results are true for other mining areas is something that should be considered in future studies.

Another direction of future research is to identify the relationship between the industrial cluster and innovation. To carry out this study will require a more detailed analysis of data on specific industrial networks, on the dynamics of intercluster connections within and between regions.

Also, as further research, it is planned to expand the proposed industrial cluster model to the technopark model, complementing it with scientific and educational organizations, innovation infrastructure organizations, and technology park support infrastructure.

Acknowledgements: *The work is carried out based on the task on fulfilment of government contractual work in the field of scientific activities as a part of base portion of the state task of the Ministry of Education and Science of the Russian Federation to Perm National Research Polytechnic University (the topic ¯ 26.6884.2017/8.9 ñSustainable development of urban areas and the improvement of the human environmentò).*

References

Anokhin, S., Wincent, J., Parida, V., Chistyakova, N. and Oghazi, P. (2018). Industrial clusters, flagship enterprises and regional innovation, Entrepreneurship & Regional Development, 31(1-2), 104-118.

Bako, B. and Bozek, P. (2016) Trends in simulation and planning of manufacturing companies. International Conference on Manufacturing Engineering and Materials (ICMEM), Procedia Engineering, 149, 571-575.

Belarusian Potash Company Signs New Contract With China, available online: https://www.vedomosti.ru/business/articles/2018/09/17/781074-belorusskaya-kaliinaya, downloaded on 26. December 2018.

Bengtsson, M. and Sölvell, Ö. (2004). Climate of competition, clusters and innovative performance Scandinavian Journal of Management, 20(3), 225-244.

Biağy W. (2014). Post-mining areas reclamation ï case study. 14th SGEM GeoConference on Science and Technologies In Geology, Exploration and Mining, SGEM2014 Conference Proceedings, June 17-26, 2014, Vol. III, BUĞGARIA ISBN 978-619-7105-09-4/ISSN 1314-2704. s. 443-450.

Biağy W., Mroczkowska P. (2015). Influence of coal waste heaps on water environment in upper silesian borderland areas ï case study. 15th SGEM GeoConference on Science and Technologies In Geology, Exploration and Mining, SGEM2015 Conference Proceedings, June 18-24, 2015, Vol. III, BUĞGARIA ISBN 978-619-7105-33-9/ISSN 1314-2704. s. 675-682.

Budaj, P., Klencová, J., DaŕkováÁ, A. and Piteková, J. (2018). Economic aspects of the mining industry in the Slovak Republic. Acta Montanistica Slovaca, 23(1), 1-9.

Dalum, B., Pedersen, C.Ø.R. and Villumsen, G. (2005). Technological life-cycles: Lessons from a cluster facing disruption. European Urban and Regional Studies, 12(3), 229-246.

Feser, E.J. and Bergman, E.M. (2000). National industry cluster templates: A framework for applied regional cluster analysis. Regional Studies, 34, 1ï 19.

Fongsuwan, W., Chamsuk, W., Tawinunt, K., and Josu, T. (2017). Cluster and R&D Affecting the Competitive Advantage of the Mould and Die Sector in the Thai Automotive Industry. Management and Production Engineering Review, 8(4), 3ï 12.

Hartigan, J.A. (1985). Statistical theory in clustering. Journal of Classification, 2(1). 63ï 76.

Hervás-Oliver, J.L., González, G., Caja, P. and Sempere-Ripoll, F. (2015). Clusters and industrial districts: Where is the literature going? Identifying emerging sub-fields of research. European Planning Studies 23: 1827ï 1872

Hoang, H. and Antoncic, B. (2003). Network-based research in entrepreneurship: A critical review. Journal of Business Venturing, 18(2), 165-187.

How much does fuel cost in Belarus? https://www.blr.cc/benzin/.

Hsu, M.-Sh., Lai, Yu.-L. and Lin, F.-J. (2013). Effects of Industry Clusters on Company Competitiveness: Special Economic Zones in Taiwan, Review of Pacific Basin Financial Markets and Policies, 16(3),

Integrated report of ñUralkaliò, https://www.uralkali.com/upload/iblock/0dc/uralkali_ar2017_rus.pdf

Kristal, M. M., Huang, X. and Roth, A.V. (2010). The effect of an ambidextrous supply chain strategy on combinative competitive capabilities and business performance. Journal of Operations Management, 28, 415ï 429,

Kusa, R., Marques, D.P. and Navarrete, B.R. (2019). External cooperation and entrepreneurial orientation in industrial clusters, Entrepreneurship & Regional Development, 31(1-2), 119-132.

Le, Z. and Ning Z. (2015). The Development and Research of China Industrial Cluster Based on Supply Chain: A Case of Beijing-Tianjin-Hebei Tourism Destination. The Open Cybernetics & Systemics Journal, 9, 1879-1884.

Lechner, C. and Dowling, M. (2003) Firm Networks: External relationships as Sources for the Growth and Competitiveness of Enterpreneurial Firms. Enterpreneurship & Regional Development, 1-26.

Lesnik, A. and Mingalyova, Z. (2013). The development of innovation activities clusters in Russia and in the Czech Republic. Economy of Region, 3, 190-197.

Lindsay, V.J. (2005). The Development of International Industry Clusters: A Complexity Theory Approach. Journal of International Entrepreneurship, 3 (1), 71ï 97.

Ma Ding (2014). Supply Chain Collaboration toward Eco-innovation: an SEM Analysis of the Inner Mechanism, IEEE,129ï 134.

Manová, E., Ļulková, K., Lukáļ, J., Simonidesová J. and Kudlová, Z. (2018). Position of the chosen industrial companies in connection to the mining. Acta Montanistica Slovaca, 23(2), 132-140.

Martin, R. and Sunley, P. (2002). Deconstructing Clusters: Chaotic Concept or Policy Panacea. Working Papers wp244, Centre for Business Research, University of Cambridge.

Mingaleva, Z. and Gataullina, A. (2012). Structural modernization of economy and aspects of economic security of territory. *Middle East Journal of Scientific Research*, 12 (11): 1535-1540.

Mingaleva, Zh., Shaidurova, N. and Prajová, V. (2018). The role of technoparks in technological upgrading of the economy (using the example of agricultural production). Management Systems in Production Engineering, 26 (4), 241-245.

Mingaleva, Z., Sheresheva, M., Oborin, M. and Gvarliani, T. (2017). Networking of small cities to gain sustainability. Entrepreneurship and Sustainability Issues, 5(1), 140-156.

National Accounts, 2018. www.gks.ru/wps/wcm

Papagiannidis, S., See-To, E.W.K., Assimakopoulos, D.G. and Yang, Y. (2018). Identifying industrial clusters with a novel big-data methodology: Are SIC codes (not) fit for purpose in the Internet age? Computers and Operations Research, 98, 355-366.

Pascu, G., Bayon, J. and Gheorghiu, T.O. (2013) Strategies of regeneration of former mining sites in Romania. CESB 2013 PRAGUE - Central Europe Towards Sustainable Building 2013: Sustainable Building and Refurbishment for Next Generations, pp. 257-260.

Porter, M.E. (1998). Clusters and the New Economics of Competition. Harvard Business Review, 76 (6), 77ï 90.

Porter, M.E. (2011). Competitive advantage of nations: creating and sustaining superior performance. Free Press.

Product Catalog ñUralkaliò. http://pda.uralkali.com/upload/content/ products/Products_catalogue_ru.pdf

Products of Belaruskali https://kali.by/products/khloristyy-kaliy

Sölvell Ö., Lindqvist G. and Ketels C. (2003). The Cluster Initiative Greenbook. Stokholm.

Shaidurova, N.S. (2017). Technopark as an element of the conducting infrastructure of high-tech products.In the collection: The Russian economy: a look into the future, in 2 parts, pp.336-343.

Three ñwhalesò. Top 300 largest enterprises of the Perm region. 2017. https://www.business-class.su/news/2017/10/23/cifry-fakty-tendencii-top-300-krupneyshih-predpriyatiy-permskogo-kraya

Trippl, M., Grillitsch, M., Isaksen A. and Sinozic T. Perspectives on Cluster Evolution: Critical Review and Future Research Issues. WP 2014/12.

ñUralkaliò leaves the world's largest mineral fertilizer markets. https://www.vedomosti.ru/business/articles/2018/12/03/788258-uralkalii

Yu, H-y., Jiang, M-h. and Qin, C-y. (2015). Review: Application of Complexity Theory in Industrial Cluster Evolution. In: Proceeding of 22 International Conference on Management Science and Engineering, 19-=21 October 2015, Dubai, pp. 1951-1959.

Zhu, Y. (2003). On the innovative advantage of industrial clusters. China Soft Science, 7, 107-112.

Analysis of notice boards (panels) as general information media in the outdoor mining tourism

***Karol Weis*[1], *Pavel Hronček*[2], *Dana Tometzová*[3], *Bohuslava Gregorová*[4], *Martin Přibil*[5], *Miloš Jesenský*[6] *and* *Vladimír Čech*[7]**

Despite the fact that computer technologies, digitization, and social networks are used and preferred almost in all spheres of life, information boards installed as part of educational trails have an irreplaceable role in tourism. The aim of the presented study is to point out the importance of information boards in mining tourism. The first part of the study analyses the theoretical and methodological aspects and procedures of notice boards, their content classification and suitable use in situ. Methodologically correctly constructed illustrated notice boards are a suitable and often irreplaceable visual tool of old mining sites or mining trails.

The second part of the article is dedicated to a case study of preparing, making and promoting the installation of illustrated notice boards using the example of the mining educational trail in Vyhne (Central Slovakia) which was open in 2016 under the name "In the Footsteps of Mining Activities". The stationary boards installed along the trail serve their function and are actively used in mining tourism.

The third part of the study analyzes the instructions for creating external notice boards from the perspective of the recommended limits (time intervals) needed for the identification of directions and for reading and understanding pictograms, illustration and texts. The aim of the questionnaire survey carried out on a group of respondents was to verify the previously published and recommended rules for compiling the content and range of the information published on boards or to modify them according to the specific conditions defined by a particular topic and area. The research results show that the text must be well-arranged and brief, graphically interesting containing appropriate topics.

Keywords: *notice boards, design of boards, basic characteristics, mining site, mining tourist trail, mining tourism, mining trail Vyhne*

Introduction

Despite the age of the internet and new technologies we live in, these modern tools cannot be used as across-the-board information media in mining tourism.

The problem does not lie in their affordability but rather in signal reception, especially in historical mining locations. The reception issue is not only connected with the uninhabited areas, i.e. remote mountains and narrow valleys, but also with the mountain, foothill or valley settlements connected with mining activities. Therefore, many organizations (self-government, civic associations, and mining associations) still prefer the "traditional" way of informing tourists in situ, i.e. stationary boards.

Over the last decade, these forms and means of informing tourist about the Slovak mining history have been used heavily. As for the expert public, they are generally called educational in-situ (in nature) installations. They are a proven and currently widely spread form of promotional and educational activities for the general public, including young people, and for the specialized groups of visitors or experts and scientists. Such stationary installations are subsequently grouped for form educational trails, educational sites and educational points.

They are associated not only with the possibility of expanding knowledge and gaining new useful information connected with visual demonstrations, often with a creative part but also with a stay in nature and landscape.

In the mining tourism, stationary panels (boards) are used to mark solitary mining elements (galleries, shafts, technical equipment, places of major events, etc.), mining sites, as well as marked mining trails and routes.

[1] *Karol Weis,* Department of Geography and Geology, Faculty of natural Sciences, Matej Bel University, Tajovského 40, 974 01 Banská Bystrica, Slovakia, *e-mail: karol.weis@umb.sk*

[2] *Pavel Hronček,* Department of Geo and Mining Tourism, Faculty of Mining, Ecology, Process Control and Geotechnology, Institute of Earth Resources, Technical University of Košice, Letná 9, 042 00 Košice, Slovakia, *e-mail: pavel.hroncek@tuke.sk*

[3] *Dana Tometzová,* Department of Management of Earth Resources, Institute of Earth Resources, Faculty of Mining, Ecology, Process Control and Geotechnology, Technical University of Košice, Park Komenského 19, 042 00 Košice, Slovakia, *email: dana.tometzova@tuke.sk*

[4] *Bohuslava Gregorová,* Department of Geography and Geology, Faculty of natural Sciences, Matej Bel University, Tajovského 40, 974 01 Banská Bystrica, Slovakia, e-mail: *bohuslava.gregorová@umb.sk*

[5] *Martin Přibil,* Museum of Industry, National Technical Museum, Kostelni 42, 170 78 Prague 7, Czech Republic, *e-mail: martin.pribil@ntm.cz*

[6] *Miloš Jesenský,* Museum of Kysuce in Čadca, Moyzesova 50, 022 01 Čadca, Slovakia, e-mail: *jesensky@kysuckemuzeum.sk*

[7] *Vladimír Čech,* Department of Geography and Applied Geoinformatics, Faculty of Humanities and Natural Sciences, University of Presov in Presov, 17 novembra 1, 081 16 Prešov, Slovakia, e-mail: *vladimir.cech@unipo.sk*

State of the art

External notice boards as part of marked routes - mining trails

Several authors have dealt with the topic of nature trails in the Czech Republic (former Czechoslovakia). The first who developed the methodology of the educational trails was Čeřovský (Čeřovský, 1976, 1978a, 1978b). Currently, the issue of nature trails is largely addressed by Bizubová (1984, 1994, 1995, 2001), Bizubová et al. (1998, 1999), Suchá (1990), Bizubová & Minka (Bizubová & Minka 2001) and others. Mazúrek (1988) and Bizubová (1995) were devoted to the primary intended use of educational trails.

The nature trail can be defined as an educational tourist route marked by means of information panels, or in some other form. A route of different length and thematic focus leads to the areas of remarkable nature, landscape, history and culture. On the route, there are some important objects and evidence of mining activities selected. These are described through information panels, leaflets, guidebooks and tourist guides providing information on the origin and development of individual elements of the natural or cultural landscape. They show the landscape comprehensively in all its relations.

Educational trails can be classified according to different classification criteria *(Čeřovský, 1976, 1978a, 1978b)**:***

1 Based on how information is delivered:
a) Trails without a guide;
b) Trails with a guide;
c) Combined trails.

2 Based on a route length:
a) Short trails of up to 5 km;
b) Medium-length rails of approx. 5 - 15 km;
c) Long trails of approx. 15 km

3 Based on their thematic focus, we recognise:
a) Multi-thematic trails (specialization - science, culture and history, forestry);
b) Monothematic trails (mining nature trails included).

4 Based on the route duration, there are:
a) Half-day (up to about 5 km);
b) Half to all-day (approx. 5 - 15 km);
c) All-day and multi-day (approx. 15 km) routes.

5 Based on the location of a route in relation to a protected area, we recognise:
a) Trails in a protected area;
b) Trails in a wild unprotected area.

6 Based on a route shape, there can be:
a) Linear trails;
b) Loop trails.

7 Based on route passing options, there are:
a) Point-to-point trails;
b) Out-and-back trails.

8 Based on the type of transport means used, we recognise:
a) Walking paths;
b) Cycling paths;
c) Other.

The first nature trails were created in the early 20th century in Canada and the USA. In Europe, the first nature trail was opened in Germany, followed by trails in Great Britain, the Netherlands, Austria, Sweden, Hungary and the former Czechoslovak Republic. The first unofficial educational trail focused on forestry was opened in Slovakia in 1926 in the current Štiavnické vrchy (Štiavnické Mountains) PLA (Protected Landscape Area) (Burkovský and Kollár, 1989). The opening of the first official nature trail in former Czechoslovakia (the

area of the today's Slovakia and the Czech Republic) dates back to 1956 (Čeřovský, 1976), according to Bizubová (Bizubová 1998) to 1960. The path was located in the Pieniny National Park, in the area between Červený kláštor and the Lesnický Brook.

As regards the mining trails in Slovakia, they are experiencing a great comeback. In the last decade, there were, for example, the following mining trails opened:

In 2019

- Educational mining trail Nová Baňa (Nová Baňa and surroundings, Žarnovica District) focused on the history of precious metal mining in Nová Baňa; the 15 information boards placed on the trail can be divided into two historical and thematic areas. The 4.3 km-long route A of 210 m difference in elevation leads along with the places showing the evidence of the Middle Ages surface and underground mining activities, passes through more physically demanding forest terrain in the area of Mýtny Vrch (Mýtny Hill) and the Gupňa Hill in the southern part of the deposit. Route B is less difficult to walk and leads mostly through the urban area of the town Nová Baňa called Vŕšky. It is 5.6 km long, and its altitude difference is 130 m. It mainly shows the 16th to 19th-century mining works, including the local ore processing facilities and mining water system.

In 2018

- The educational trail in Kvetnica (Poprad District) and its 5 information boards are focused on the presentation of mining history and old mining works in the surroundings of Kvetnica and Spiš.

In 2017

- Educational mining trail Rákoš (Rákoš and surroundings, Rožňava District) focused on the history of mining in Gemer; there are 5 information boards on the trail.
- Mining educational trail in Gelnica focused on the local mining history in Turzov; 6 information boards installed.
- Pezinok mining trail (Pezinok and its surroundings, Pezinok District); the 6,750 m-long educational trail with 156 m difference in elevation has 11 stops and takes about 2.5 hours to walk. It passes through the areas of pyrite and antimony ore mining and marginally touches upon the gold mining

In 2016

- The Poráč mining educational trail (Poráč and surroundings, Spišská Nová Ves District) consists of three separate interconnected loop trails. One may learn from the information boards along the route and from the trail guide book.

In 2015

- Educational Trail Staré mesto – Glanzenberg (Banská Štiavnica Glanzenberg hill, Staré mesto/ Old Town); a less physically demanding route passing through a part of Banská Štiavnica with typical mining settlements and areas of opencast ore mining and archaeological excavations. It takes about 2 hours to walk this nature trail of 200 m difference in elevation, along which 23 information boards are placed.

In 2014

- Mining nature trail in Vyhne (Handel, Vyhne and surroundings, Žiar nad Hronom District), about 3.7 km long, medium difficulty and smaller elevation difference. On the route, you can see the remains of mining activities and their impact on the landscape, reconstructed mining mouths, water galleries and the upper part of Vyhne. The footpath named "Tracing the history of the mining activities in Vyhne" has 10 information boards in total.
- Educational mining trail in Ľubietová (Ľubietová and its surroundings, B. Bystrica District) leads to a significant historical copper ore deposit in Ľubietová, Podlipa. It is installed along forest roads and footpaths, heap fields near the mouth of old mining galleries and pingen. It starts on the square in Ľubietová, passes through the old mining cuttings to the small retention pond in Podlipa and continues along the mining fields. Each of the 13 stops, along with a total of 4 routes, are thematically differentiated and follow the geological and mining activity of the copper-ore deposit in Podlipa.
- The Mining Trail of Staré Hory (the village of Staré Hory and its surroundings, Banská Bystrica District) with 10 information boards on the route has a length of 3.5 km. It leads through difficult terrain with an elevation difference of 130 m.

In 2013

- Internet educational trail „We travel in time"- Banská Hodruša (Banská Hodruša and its surroundings, Žarnovica District), has length 3.1 km and 16 stops. Each stop is numbered and marked with a brown oak column with a QR code table. A trail guide book is also available.
- Educational mining trail Spišská Nová Ves - Novoveská Huta (Novoveská Huta, Spišská Nová Ves District). The educational mining trail has a total length of 18 km with 8 notice boards.

- Modra mining nature trail (Modra, Harmónia recreation zone of town Modra, Pezinok District). The footpath has a length of about 3 km, the elevation difference of the route is 170 meters.

In 2012

- Educational Iron trail in Čučma (Čučma and its surroundings, Rožňava District) - on the route of the trail there are 9 information boards.
- Nature trail Hnilčík (Gelnica District) is built around the village. It presents the rich mining history of the region through seven information boards.

In 2010

- Educational mining trail in Nováky (town of Nováky and its surroundings, Prievidza District). The educational trail has 15 stops with information boards.

In 2009

- Turecká educational trail (around the village of Rudná, Rožňava District) with mining and forestry themes. It has a length of 8.2 km. The trail consists of 26 educational boards and two relaxation zones.
- The tourist-educational mining trail in Handlová (Prievidza District) is about 9.5 km long with 13 information boards and two rest zones
- and another example is an educational trail called "Through the history of mining" in Hnilčík (Hnilčík, Spišská Nová Ves District).

Basic rules for the design of externally mounted panels - boards resulting from the practice

How the (educational) information element - the board will be perceived by visitors of mining tourism will be significantly influenced by their attractiveness, colour, graphic design. A mining tourist differs from a tourist in a wide landscape focused on natural beauty or diverse social phenomena in the landscape by his specificity and interest in the narrow specialized historical activity and its relics in the landscape. These are often educated groups of tourists, not only laymen but also experts in mining research. Therefore, the rules for the design of externally mounted notice boards cannot strictly be based on generally used methodical procedures applied in tourism, but are adapted to the requirements of mining tourism clients. That is why their content interpretation is more professional, often technical terms are used, and the texts on the panels are longer. Form of design - graphic design is more complicated, often using professional schemes and maps.

However, the design of notice boards for mining tourism must be based on a number of important rules for their content and graphic design and their production and placement in the landscape.

Before we start building these installations, we have to realize that with their text and graphics (as well as used material and in situ localization) they have to fulfil several functions (Schneider et al., 2008):

The first and basic function is to give directions to a visitor in the terrain. Each board should contain the name of the visualized site (point) and must have a serial number (with the name of the specific stop) in the case of nature trails and routes. It should include a tourist map (for educational trails it is necessary to place such a map on the first or welcome board of the trail). Notice boards should also include information on how many kilometres or how much time remains until the end of the route; that means to the destination from where the tourist started the route, or to the place from which the visitor can hike further.

Another important function is to provide quality and interesting text and image information not only about a special visualized mining element, object or phenomenon and its specifics, but it should also provide basic information about the surroundings and possibly wider territorial and landscape relations.

The notice board should arouse interest or enthusiasm in the presented issue among mining tourists (mainly from the general public).

As intended for clients, especially pupils and students, as well as the general public, it should encourage appropriate behaviour in nature, but also encourage them to visit other (similar) places in the area.

Even before the actual design of information boards and after realizing their basic functions based on practice, the creator must also sort and adopt the generally applicable rules for their design (Jelínek et al., 2009), which are:

- Easy to read text - suitable style, font size at least 8 mm, sufficient colour contrast of font and background, when placing the board in a place exposed to the light, it is advisable to use light text colours on a dark background.

-Brief and well-structured text - clear title of the board, summarize long text into short words and sentences, used up to 50 words per paragraph, if the board contains more text, it is advisable to divide it into more parts with highlighted headings. Stylize the text so that each board topic provides information separately.

- Always maintain the appropriate ratio of text and graphics, with the image part prevailing. The text should be 20 to 35% of the board area.

-Maintaining clarity, which in the case of information boards with mining focus often requires appropriate avoidance of technical terms (possibly explaining them by text or scheme). If the boards are also in a foreign language, it should not have a longer version than the language of the country in which it is installed.

- An important feature is a timeliness. As far as historical topics are concerned, the text must be designed in such a way that it remains up to date (credibility) even after several years (during the lifetime of a board).

Only after acquiring all the above functions of notice boards in the mining tourism and observing the main best-practice rules, it is possible to proceed with the methodological part of board preparation. This does include not only their content and graphics but also their actual production as installations designed for mining tourism. Obviously, the rules of external information boards design for mining tourism have their specifics.

Methodological rules for designing mining tourism information boards

Several types of information boards are commonly used to mark mining educational installations in the landscape, which we generally call signs. ***The sign*** is a tool - an area or a spatial mark which communicates with a participant of mining tourism.

The sign is a form of impersonal communication with a visitor that must meet three requirements which can be expressed by a communication triangle (Ludwig, 2003). When one of the three inextricably interconnected vertices of the triangle represents the method used to prepare the installation, then the other represents the visitor (reader) themselves, and the third vertex represents the topic of individual introduced phenomena (*Fig. 1*).

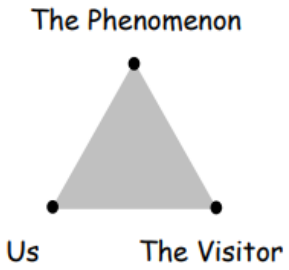

Fig. 1: Communication triangle schematically depicting impersonal communication between a visitor and a board (sign, panel), referring to a topic displayed on a board

It is undisputed that the use of information signs in the landscape in mining tourism has both advantages and disadvantages (Gross et al., 2006). In order to be of benefit to the visitor, the signs must be user-friendly as visitors themselves ultimately choose what they will or will not read and will select the range of sing information they will take in. Signs should be used for educational purposes; that means they must provide visitors with information and indirect content interpretation. However, they must be economical not only in terms of content but also in terms of technology and material. In case of improper processing, production or use in situ, they also have negatives that need to be eliminated. Signs cannot be invisible, and they cannot blend with the landscape (*Fig. 2*). Despite the quality of the sign, it cannot answer all the questions (such as a guide). They cannot be text-based because visitors ignore such signs. However, in mining tourism, these signs are often used because many tourists visiting mining sites have a specific - positive relationship to mining, and they accept the boards processed in this way.

The purpose of trail signing determines the total content and form of the sign itself (Ludwig, 2003). There are four basic groups of signs based on their purpose:

• directional signs which provide to give direction to the tourist and facilitate his movement in the area, on the site or along the mining educational trail,

• regulatory signs regulate behaviour in the area, on the site or on the mine sidewalk, introduces various rules of behaviour, but also possible sanctions;

• informational signs bring information about other points of interest in the surroundings about danger etc.

and the last type are

• interpretative signs, which are most important for the presence of a mining tourist because they make available information about mining phenomena on the site.

Fig. 2: Organized group of mining tourists on Mining trail Ľubietová (photo by P. Hronček)

Notice, educational or interpretative signs - boards, panels

The task of the information panel is to give the visitor interesting facts, uniqueness or various specifics about the place where they are installed. They provide information on the natural and socio-economic elements of the landscape, including man, his culture, technology and history, settlements and cultural monuments.

Their main goal is not only to educate or explain, but also to lead visitors to discover new connections, relationships or ties and meanings. They cannot, or should not, contain heterogeneous information. They should be simple and clear, therefore, first of all, the title of the topic should be included, if they are part of a nature trail they should include its name, stop number, accompanied by the trail logo and small picture and graphic material. This should create a kind of "header" of the board. The textual information (i.e., the interpretation itself) should be brief, interesting and understandable. The form is often used through an engaging story. The textual part of the presentation must be accompanied by photographs, maps, diagrams and drawings. The golden rule for the graphical part of information boards is that they should not only form the visual part of the topic described in the text but also complement, disseminate and provide new information. Therefore, they must be self-supporting and self-reading, meaning they must have a concise, interesting and self-supporting description.

The graphic design of the information board should be not only engaging but also simple and logical. For educational installations where there are several boards on the route, they must have a single design, which the visitor will understand at the beginning of the route at the introductory board. Also, their form and material should fit into the environment and show the presented topic.

In general, we can state that the information board is effective if its "communication" with the visitor is not only quick but also interesting or even dramatic. That way, it can provide the visitor with the information about what they can see, experience or learn on the route.

According to research conducted on visitors of indoor expositions (Ham, 2013), the majority of them concentrates on one panel for less than 6 seconds (Medek et al., 2016). However, according to our field measurements, this is not relevant neither applicable for mining tourism. Attendance of mining facilities in the landscape is significantly limited by seasonal and weather conditions. During the summer season and on sunny days, the visitors usually spend more time reading individual panels. Our findings show that, on average, a visitor can spend as much as 5 minutes studying a single mining tourism information board. However, the specificity in the case of mining installations in the landscape is that tourists coming to these sites have a particular interest in the mining heritage.

When reading information boards, we have to realize one thing - the visitor reads the boards not as linear as a book, but non-linearly, like a newspaper (Medek et al., 2016). Text-based compilation of explanatory boards often uses 3-30-3 rule of visitor-board interaction, which in 2005 introduces the Rocky Mountain Region Centre for Design & Interpretation (US Forest Service, 2005). M. Gross, R. Zimmerman and J. Buchholz (2006) dealt with this rule in detail. To the rule dedicated attention also Czech authors J. Woitsch and K. Pauknerová (2014) or M. Medek et al. (2016). The rule, which is the result of research in other geopolitical conditions, is often transmitted without critical reassessment to our central European environment, where nature trails have a different form, boards have more detailed content and also tourist motivations to visit are different.

3-30-3 time rule - board reading rule, or rule of visitor-board interaction, is interpreted as follows:

3 seconds - most visitors only look at the board for 3 seconds. This is where the visual familiarisation with the board takes place, and this piece of information usually includes an eye-catching title, a large image, or both.

30 seconds - as long as the board caught their attention in the first three-second phase, its viewing last about 30 seconds. The main information is usually longer described in 1-2 paragraphs.

3 minutes – the board which will grab the attention of visitors thematically and graphically will be viewed up to 3 minutes (in detail).

Based on our field research, we came to the conclusion that this rule is more likely to be applied to generally focused boards (nature trails) with various topics, where the boards are more graphically compiled with lay descriptions. These kinds of nature trails are mainly intended for children or a wide spectrum of tourists. The thematic notice boards, that means mining installations in a landscape, are high-level expert-content or medium-level expert-content notice boards placed on trails visited by a small group of tourists (mining tourists) who, unlike other tourists, spend more time reading and studying the text and content of individual boards. We can observe this situation especially during student field trips (secondary schools and universities), also during professional events and seminars, events aimed at popularization of mining heritage, etc. We have also seen a higher interest in explanatory boards by many individual visits to these facilities. As mentioned above, it is on average more than 3 minutes, often up to 5 minutes, when reading the content of the board with an understanding and perception of its graphic schemes and links to the surrounding landscape.

Czech authors (Medek et al., 2016) divide the visitor's interaction with the board; in other words the visitor's interest in the board content and reading it in phases, based on 3-30-3 rule. The phases of a visitor's time interaction with the board can be characterized as follows:

- Engagement - arousing the visitor's interest in board content for about 3 seconds,
- Detection - getting to know the contents of the board within about 30 seconds,
- Start – reading the information board in about 3 minutes,
- Interest - the visitor gains interest (does not have to), creates his own conclusions and decides how to continue along the route (*Fig. 3*).

It is important to emphasize that in each of the phases, the visitor decides whether to continue reading the board. The tourist decides individually depending on the textual and graphic composition of boards. Our research on the mining trails in Slovakia confirmed that abovementioned factors influencing the visitor effort to read the board until the end or to finish the visitor interaction with the board prematurely.

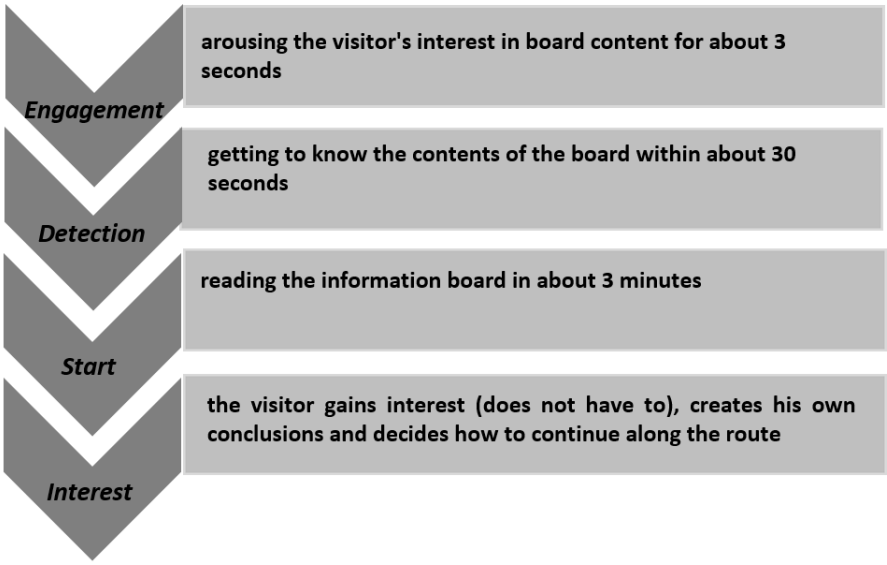

Fig. 3: The phases and time range of the visitor's interaction with the notice board (edited by Medek et al., 2016, s. 51)

Based on various guidelines (Ludwig et all., 2003; US Forest Service, 2005; Anonymous, 2008; Jelínek, Kozubková, Kostečka, 2009; Anonymous, 2008) or methodological works by M. Gross, R. Zimmerman and J. Buchholz (Gross et al., 2006), J. Woitsch and K. Pauknerová (Woitsch & Pauknerová, 2014) or M. Medek with a team (Medek et al., 2016) we can present basic methodological characteristics regarding content and form (font or colour), which is necessary to follow when creating notice boards.

The methodology of the used questionnaire survey

Questionnaire survey is a method aimed at mass and quick identification of facts, opinions, attitudes, preferences, values, motives, needs, interests, etc. For the purposes of the present study, a public opinion survey was carried out based on the general methodology of questionnaire creation, according to E. Taylor-Powell

(Taylor-Powell 1998), Š. Švec (Švec 1998), N. Bradburn, S. Sudman and B. Wansink (Bradburn at al. 2004), P. Gavora and coauthors (Gavora et al. 2010) and M. Bačíková (Bačíková 2018).

We conducted our research through a unique form with questions answered by respondents. In order to achieve the stated goals of the research and easy statistical processing of responses, it was necessary to follow basic methodical procedures during its creation. When preparing, it is necessary to pay attention to whom the questionnaire is intended and what we need to find out with it. The validity of the questionnaire survey depends on the quality of the questionnaire, the accuracy and clarity/transparency of the questions with respect to the target group of respondents.

For our survey connected to mining nature trail boards, we have selected a questionnaire with closed-ended questions (pre-offered answers from which respondents could choose). This method is much more advanced, more convincing and more accurate in achieving research objectives (Weis et al., 2016). This means that by the use of open-ended questions we can easier identify what individual respondents think, but we are unable to evaluate and validate its conclusions through results in relation to specific objectives set in advance as in the case of closed-ended questions.

We prepared the questionnaire using a closed-ended form of questions. Selective questions, with multiple choices designed to meet the research objective on the basis of the answers, were used. Subsequently, the questionnaire was assigned to the respondents, and finally, we did a statistical evaluation. A specific example was question no. 15, which is an open-ended question without any answer option offered. The aim of the question was to obtain an independent evaluation of the educational trail attractiveness by the respondent with the respondent's suggestions for any changes or additions to the educational trail as an experience-oriented type of information medium. The results of statistical analyses were used in the formulation of the research conclusions.

Fig. 4: Example of notice board, central board on the main square in Smolník (on the left), information board no. 8 as a part of Educational mining trail in Nováky (on the right) (photo K.Weis)

Fig. 5: Information board on the mining site Korňa oil spring in Korňa (on the left) and the information board of Nature trail in Ľubietová (on the right) (photo P. Hronček)

Results

Modern notice boards on the example of the Vyhne nature trail

The Vyhne nature trail

Educational mining trail „Tracing the history of the mining activities in Vyhne" (Žiar nad Hronom District), was opened on October 11, 2014, in the Handel locality. Its length along the less demanding route is 3.7 km and has a total of 9 stops with explanatory boards. The tenth board is introductory. The trail is self-service, out-and-back and its route takes about 1.5 to 2 hours. It is freely available all year round according to suitable tourist equipment *(Figs. 4, 5, 6)*.

- Welcome board

Welcome boards can also be called starting-point boards as they are usually placed at nature trail starting points. They must contain the name of the nature trail with the logo, the name of the founder, administrator, author(s), the implementation company, eventual project partners. The introductory board must necessarily correspond with the graphics of the other boards.

The welcome board of the trail in question (like all others), a co-author of the scientific text and graphic design of which is K. Weis, who is, at the same time, the author of this scientific study, follows the basic rules of mining nature trail design listed in the introductory part of the study.

It is based on the 3-30-3 rule, which is apparent from its content and graphics. The other methodological rules are also well traceable.

The introductory board shows the name of the nature trail, the authors of the texts, a brief introductory description in Slovak and English. For easy reading, the text is arranged in columns. In the central part of the board, there is a brief description of each stop to which the photo is attached. In addition to the precise identification of stops in the map at the bottom of the board, there is also a trail profile. In the right corner is a map showing the wider geographical space of the nature trail and its accessibility. In the middle top of the introductory board, there are rules of behaviour and movement on the educational path.

Tourist's rules of the Vyhne educational trail:

1. Stay on the signed path at all times;
2. Keep quiet and remain disciplined;
3. Do not destroy the forest and do not frighten animals away;
4. Do not damage educational trail notice boards,
5. Do not damage or pollute the environment and do not set fire;
6. Pay attention to your personal safety;
7. Do not enter open mining works.

There is also a brief description of the individual boards, their photos and the exact location on the map included:

- Board no. 1: St. Anthony of Padua Adit – At the entrance to the trail is parking available. The route leads from the adit of St. Anthony of Padua almost along the contour, towards the village Vyhne. Along the route, you can see the remains of mining activities - heaps, spoil banks and surface mining pit.
- Board no. 2: Old St. Anthony of Padua Adit - Originally the second mouth of the St. Anthony of Padua, called the Old Adit of St. Anthony of Padua. It is located on the site of the first mining administration house - the Lower Handelhaus.
- Board no. 3: Stamp-mill no. 5 and water adit Gabriel - Here are the remains of Stamp-mill no. 5, where the ore exported from the mine was treated. The water used to drive the processing plants was the water supplied by a water gallery, which runs above the remains of the building. The route continues to the observatory rock with a cross, from where the ascent is more physically demanding and then continues along the ridge to the Šprochova Valley.
- Board no. 4: Joseph Adit and Šprochová Valley - The Joseph Adit is located on the floor of the Šprochová Valley. By descending the valley, there are visible remains from the beginning of mining activity in Vyhnianska Valley. At the level of the state road, the trail turns right and continues to the opposite hill, where it continues along with the level of Upper láf railway track.
- Board no. 5: The Luke Adit and Upper láf - This adit is located at the level of the Upper láf - railway track, on which the ore was transported to stamp-mill and processing facilities.
- Board no. 6: Holy Trinity Shaft- A place where the mining tower of the Holy Trinity Shaft and the Central Ore Processing Plant stood.

- Board no. 7: Central processing plant and Anna Antónia Adit - from the Anna Antónia Adit we cross the stone ditch and continue along the route of the collecting water ditch.
- Board no. 8: The Katharine Adit and collecting ditches - At the level of the original collecting ditches, it continues to the state road and then back to Vyhne.
- Board no. 9: John's Cross-Cut to Holy Trinity Shaft - This cross-cut served as an access adit under the Holy Trinity Shaft. Above it is a knocker, as it used to be in the past.

Fig. 6: Organised field trip for university students along the signed nature trail (photo B. Gregorová)

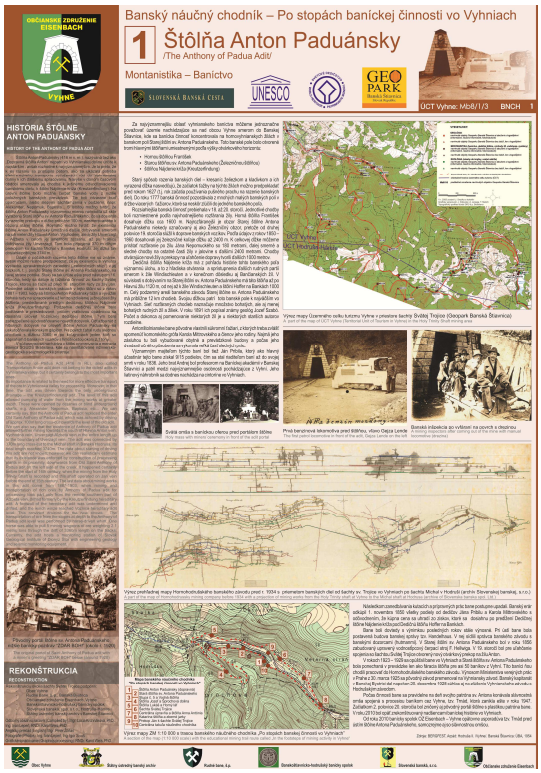

Fig. 7: The example of the board in Vyhne village. Autor of the board is K. Weis (photo K. Weis)

All information boards of the nature trail in Vyhne meet the basic methodological rules for the design of boards for mining nature trails. We started from the methodological bases as we described them in the part of the Study Material and methods.

Results of the questionnaire survey

The questionnaire consisted of 15 questions (*Fig. 8*), answered by respondents in writing. A total of 1,400 respondents participated in the survey during years 2018 and 2019, and the questionnaire survey was conducted on the following educational and mining Trails:

- Mining nature trail in Vyhne (*Fig. 7*),
- Educational mining hiking trail in Nováky,
- Educational trail on the iron road in Čučma,
- Educational mining trail in Ľubietová,
- Mining educational trail Nová Baňa.

Students who attended the survey were from different years of study from the Department of Geography and Geology (Faculty of Natural Sciences, Matej Bel University in Banská Bystrica) and from the Institute of Geo and Mining Tourism, Faculty of BERG, Technical University of Košice.

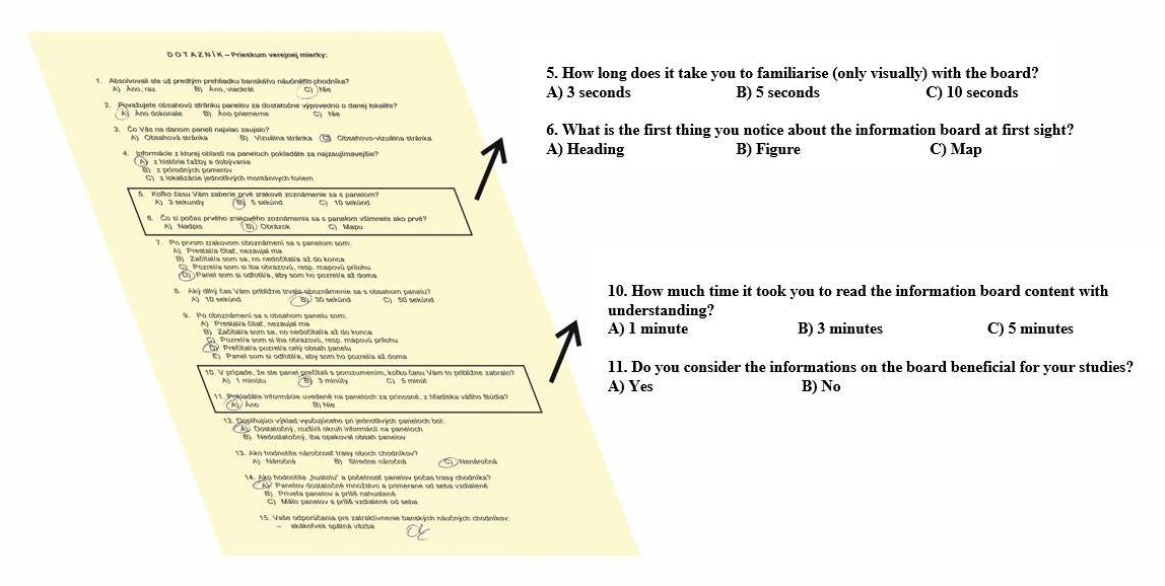

5. How long does it take you to familiarise (only visually) with the board?
A) 3 seconds **B) 5 seconds** **C) 10 seconds**

6. What is the first thing you notice about the information board at first sight?
A) Heading **B) Figure** **C) Map**

10. How much time it took you to read the information board content with understanding?
A) 1 minute **B) 3 minutes** **C) 5 minutes**

11. Do you consider the informations on the board beneficial for your studies?
A) Yes **B) No**

Fig. 8: Questionnaire used in the survey with a detailed view of selected questions

The basic evaluation of the survey responses is summarized in Fig 9. When compiling a database file, several correlations, more or less significant, were observed, but mostly only for certain pairs of questions.

Given that nearly half of the participants were students of study programmes with related or marginally related fields, the most surprising fact is that 43% of respondents (aged 18 to 23) have never taken a route of any mining nature trail and 26.7% report that they have experienced such an educational trail just once. Perhaps this is also the reason for relatively high correlation between such answers and, what seems surprising, the square of A's answers and the cube of C's answers (question No. 2: Does, in your opinion, the content of the boards provide sufficient information on the site?... A) Yes, absolutely or question no. 3: What did you like most about the board? … C) Its content and visual). This probably implies that although respondents do not know the topic, they are able to get enthusiastic about it, but they are particularly interested in the content-visual aspect of the information boards.

Considering time needed to first visual familiarisation with the issue (question no. 5), it can be stated that the information boards, due to their diversity and territorial differences, have a suitable composition and visually mastered graphics, as almost 59% of respondents claim 5 seconds was enough, and of course, they were mostly interested in graphics, i.e. picture attachments (45.8%) and maps (30.6%). It took only 30 seconds for most respondents (47.4%) to get acquainted with the whole board and read the whole board with an understanding of either 3 minutes (50.4%) or up to 5 minutes (39.8%). The above demonstrates that, in general, there was too much textual information used to design boards. The information was, however, often drawn from archival collections and other documents without any objectively acceptable degree of its compression and generalization. Such an interpretation corresponds to the relatively high level of criticism of technical approach and the extent of the information sought, which are most often oral comments of respondents. The reason for this may be the fact that there is still a tendency in Slovakia to produce relatively specialized or narrowly specialized (technical) texts on educational trails corresponding to relatively specialized topics, but without trying to reach other interest groups, not to mention other age categories. We strongly recommend paying more attention to this fact. The degree of acceptance of the scope and expertise of textual information was also reflected in the willingness, or reluctance to pay attention to the text and boards. Therefore, it is not surprising that up to 37% of respondents started reading the text but did not finish it. 38.8% of respondents either viewed more or less just picture attachments, or 14.6% respondents just took a picture of a board to see it at home (?), see question no. 7. question no. 9 brought very similar results, where up to 29.4% of respondents said they had read the entire board

(this does not correspond to the answer to question no. 7), but 25.8% only looked at the map attachments, and 25.7% started reading the text, without finishing it. Only 6.6% say they took a picture of the board to look at it at home ... The trend of taking pictures of information boards by mobile phones is understandable since there is a gradual degradation of common forms of communication between young people in general, and they are replacing them with "social networks" or other forms of digital communication. However, it is highly unlikely that this form of "education" will take on a wider meaning now and in our conditions. Rather, we assume that this type of response was more of an excuse for the respondents, as reflected in the low revealed interest in textual information (17.7%, question 3 (A) and partial correlation with the answers to question 7). (A) and 9 (A), expressed as a percentage of 9.57% and 12.6%.

The answers to questions no. 11 and 12 provided a positive finding, i.e. whether the respondents consider the information presented in the boards useful for their study, or their study programme (question 11) and whether the teacher's interpretation was/was not sufficient and widened the range of information obtained (question 12). Up to 83.1% of respondents answered the question no. 11 with 'Yes' and up to 84.4% responded with the same answer to question no. 12. In addition to the positive outcome in terms of boards content and teacher quality, it is also possible to state the ability of respondents to assess the content of the board and the complementary interpretation of the subject matter of their own study (which should be obvious). However, they are not willing to spend the necessary energy and time to read. This trend is consistent with the decreasing ability of our young generation to understand written text, and they rely on 'complementary' ideal experiential forms of education. As teachers, we will have to adapt to this trend as it is now commonplace in several developed countries. Nevertheless, the inconsistency of educational standards at different stages of the education process in Slovakia and the declared efforts to optimize or make more attractive forms of education remain.

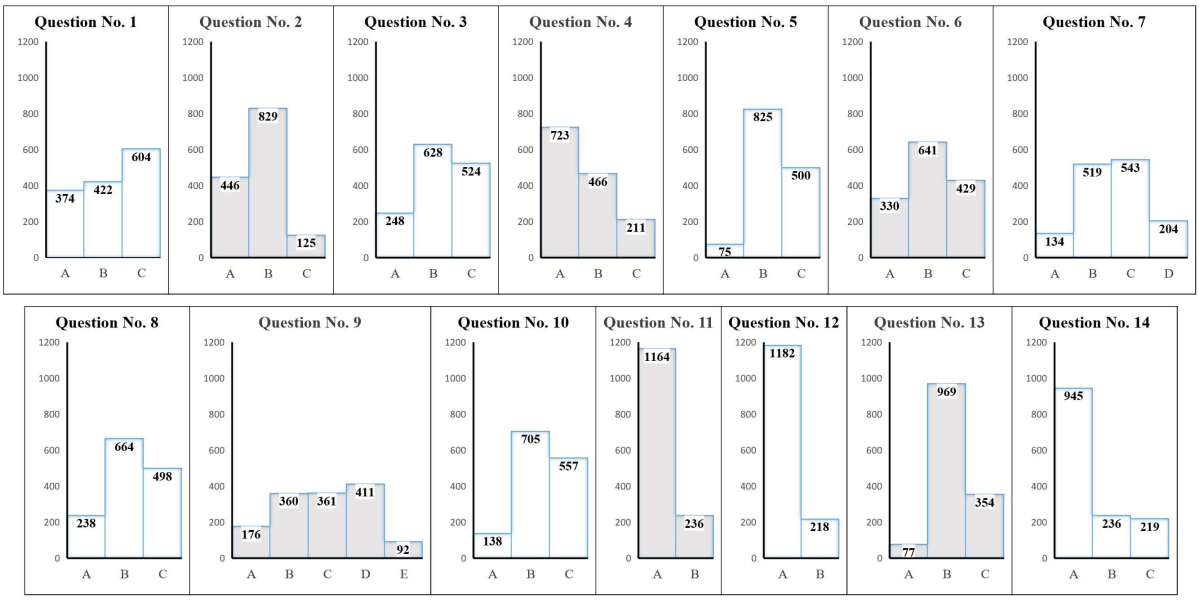

Fig. 9: Basic processing of questionnaire survey results

Evaluation of respondents' answers to open-ended question no. 15 brought interesting results. Of the total of 1,400 respondents, only 267 respondents used the opportunity to answer this question, which is surprising, but the unwillingness to respond was partly correlated with the occurrence of answer C to question no. 1 and significantly with answer C to question no. 2. A significant correlation has also been shown with answers A to questions no. 7 and 9, suggesting that this group of non-responders is not professionally close to the mining theme, has no experience with this specific kind of objects and technical monuments, and has not shown any significant familiarisation with the presented issue.

Most frequent were proposals for any type of nature trail upgrade with live attractions, or the possibility to experience something real, to be involved in some activities (this type of answers occurred up to 195 times). The second most common suggestion was to add multilingual texts for the main content, or at least for descriptions of images and other graphics add-ons (maps, archival sources, tables, etc.). Given that only 23 foreigners participated in the research, even though they were foreign language-speaking respondents with varying degrees of understanding of the Slovak text, this result was very surprising. One of the possibilities of interpretation is a general effort to standardize the content of information boards with expectations and experience from abroad (?), Or it is more likely to try to understand the issue also from a foreign language text and to test it at the same time.

Most answers in the questionnaire (up to 96%) suggested adding texts either only in the world languages or in the languages of neighbouring countries of the Slovak Republic with the exception of the Czech language (there is a high degree of similarity and understanding of the spoken word as well as written text).

The second-largest group of proposals were requests to make the nature trail more attractive by adding either originals or replicas (best functional) of the former technological facilities used in mining and metallurgy. The third-largest group were only different types of comments with a predominantly positive perception of a particular nature trail (the ratio of positive responses to negative was 71/29 out of a total of 74 such responses).

Given that all nature trails on which the survey has been carried out operate as self-guided trails without any hired guide and mostly in rural areas, it is not possible to assume any change in the way of operation in the near future. The existence and use of functional models is tied to closed areas with paid entry. Only in this way can the protection and maintenance of such objects be ensured. This fact is valid not only for Slovakia, but it is universal.

Discussion

For the information boards preparation and design, with emphasis on mining themes, we recommend following subsequent methodological principles.

Based on our analysis of the latest world and domestic (Czech and Slovak) literature and almost three years of our own research, we came to the conclusions that we recommend to observe following methodological principles when preparing and creating external (text-pictorial) information boards presenting mining themes (for mining tourism):

- The main text should not exceed 1 standard page (i.e. 1800 characters, including space character - approx. 350 words), as it takes the average person to read the page with understanding within one minute. For narrowly specialized topics in specific cases, it could be up to 1.5 pages.
- Ideally, the main text should be readable from a distance of 1, max. 2 meters, which in practice, however, cannot usually be observed. Only headings and subheadings are readable from this distance. Typically 60-72 points are used for the title, 44-48 points for the subheading. Typically, 24-30 point fonts are commonly used for the main interpretative text, 20 points in exceptional cases, but the font is less readable. The 18-point size is used for callouts.
- It is better to design additional text as extended captions for images (up to 500 characters). Despite their small size, they are usually read-only by specialists in the field, and they do not bother ordinary tourists.
- The used font size must correspond to the size of the board, and legibility must be guaranteed even in poor weather conditions.
- The font used must be easy to read. Use a serif font that is not only easy to read, but also makes you feel calm. It is inappropriate to use, for example, graphical forms of writing or imitations of handwriting.
- The text needs to be clearly divided into several parts with sub-headings. To emphasize a certain part of the text, it is advisable to use a soft background colour.
- The line length is optimal between 8 and 15 words. Paragraph alignment and text justification are necessary for information boards. Narrow text blocks are easier to read; they are clear and more dynamic.
- Pictographic material should be used to represent phenomena or objects (themes) that are not visible in the landscape, or that look different (images from the past), or have already disappeared.
- It is advisable to avoid too complicated visual (graphical) information (arrows, lines, ornaments, diagrams, etc.).
- Images and maps must be self-reading (descriptions below the images and maps, maps should have a basic legend, scale indicator, and north arrow or compass rose). These pictorial elements should complement the main text appropriately, transparently and extensively.
- The introductory board shall include the location of the mining trail in the wider landscape, taking into account well-known and accessible tourist points. There must be a clear map of the route and description of trail stops on the board. Included must be not only a description of the route length but also its difficulty (it is suitable to depict the route length and profile graphically). It is also advisable to remind visitors of rules or restrictions (prohibitions) or to specify the visitors' regulations.
- The board at each stop should include a schematic map of the entire site or the nature trail to know which way the route leads, for giving more accurate directions to visitors. This schematic map must be graphically identical to the initial map but must indicate the current location of the visitor.
- The colours of the images, fonts and overall graphics used must be tested directly in the terrain in order to be legible during cloudy days or strong sunlight.

- The use of different types of materials for the production of boards (such as wood, metal, foil or other modern materials) must be tested in practice. So their quality can withstand unfavourable weather conditions (colour fading caused by sunlight, damages caused by frost and freezing or rotting caused by moisture, etc.). An important factor in material selection is their appropriate integration with the natural landscape and their appropriate placement.
- Boards should not be placed in areas where they are distracting, often extremely unesthetic. We should care that they will sensitively blend in with the environment (especially their material, colour design, location).

We also need to consider the way of their implementation - installation, since the information boards can be vertical or inclined (lectern) or horizontal. Sometimes they are mounted on the surface level of the nature trail. These factors are important for their readability.

- The placement of the boards (of nature trail route) must reflect the specific needs of local communities and must comply with the legal requirements of the company (land ownership, etc.).
- Routes of nature trails should start in places where there is good transport accessibility not only for individual tourists but also for organized groups.
- When preparing board content, producing and installing boards “in-situ” one must always take into account the subsequent maintenance, sustainability and update of the content at reasonable costs. Protection against vandalism is significant as well.
- When creating boards for mining tourism, it is important to follow the phases step by step considering the time range of the visitor's interaction with the notice board. We modified the results of this interaction, according to Medek and co-workers (Medek et al. 2016, p. 51) based on the results of the questionnaire survey.

Conclusion

The final methodological recommendations for the design of a modern notice (interpretative, educational) board in mining tourism are:

- Create a simple profile (graphics) of a board;
- Keep the text well-arranged, not only in the middle part of the board but also in its corners;
- Create a strong focus of interest, particularly in the form of images;
- Choose graphics so that the visitor's attention is not lost;
- The text must not be as wide as to cover the entire board space;
- Individual boards on the trail must be linked (not thematically, but they must be consistent one to another);
- The task of the board must be to produce a short but visually interesting interpretation;
- If photos from the board's location are used, it is advisable that the visitor could see the object in situ;
- Use self-reading maps, graphs, sketches, historical drawings and sources;
- For modern trails, it is necessary to use QR codes.

The information boards created in this way placed along with an increasing number of modern mining nature trails, which will be equipped with traditional stationary panels, will have great potential to attract more and more mining tourists not only individuals but also organized groups of cognitive mining tourism.

Acknowledgement: *The present study was prepared as part of the project VEGA: Environmental aspects of mining localities settings in Slovakia in the Middle Ages and the beginning of Modern history. No.: 1/0236/18.*
The article was created with the support of the project APVV-18-0185 "Land-use changes of Slovak cultural landscape and prediction of its further development" financed by the Slovak Research and Development Agency.

References

Anonymous. (2008). Outdoor Interpretive Signage. *Tourism Development*, How-to Guide. Province of Nova Scotia.

Anonymous. (2008). Trails Management Manual. Standards and Guidelines for Planning, Design, Construction, and Maintenance of the Trails and Track Systems. *Maricopa County Parks and Recreation Department*.

Bačíková, M. (2018) Dotazník. In Bačíková, M., Janovská, A.: Základy metodológie pedagogicko-psychologického výskumu. *Sprievodca pre študentov učiteľstva*. Košice : Univerzita Pavla Jozefa Šafárika v Košiciach, pp. 65 – 84.

Bizubová, M. (1984). Náučné chodníky na Slovensku. PVVŠ, roč. XXXV, č. 10, s. 391-393.

Bizubová, M. (1994). Náučné chodníky, cesty a lokality na Slovensku. *Geografia*, roč. 2. č. 1. s. 15-18.

Bizubová, M. (1995). Úloha náučných chodníkov v prírodovednom vzdelávaní na základných školách. „*Zborník z národnej konferencie „Stratégia environmentálnej výchovy a vzdelávania na školách*", Bratislava,

Bizubová, M. (1998). Formovanie ekologického vedomia prostredníctvom náučných chodníkov. *Zborník z 1. jubilejnej konferencie „Trvalo udržateľný rozvoj krajiny a ochrana životného prostredia"*, Zvolen, s. 55-61.

Bizubová, M. (2001). Geografické informácie v systéme náučných chodníkov a ich didaktické využitie. Geografické štúdie Nr. 8 – *Premeny Slovenska v regionálnom a didaktickom kontexte*. Fakulta prírodných vied Banská Bystrica, s. 269-272.

Bizubová, M., Ružek, I., Makýš, O. (1998). Náučné chodníky Slovenska. I. časť. Bratislava: Strom života. 104 s.

Bizubová, M., Ružek, I., Makýš, O. (1999). Náučné chodníky Slovenska. II. časť. Bratislava: Strom života, 140 s.

Bizubová & Minka (2001). Aktívny cestovný ruch cez prizmu náučných poznávacích trás v regiónoch SR. Sborník přednášek. I. medzinárodní konference „Aktívni cestovní ruch - strategický faktor rozvoje regionu". Newport Univerzity Ostrava 24.-26.5.1999. Ostrava, s.15 - 22.

Bradburn, N., Sudman, S., Wansink, B. (2004) Asking questions: The definitive guide to questionnaire design. For market research, political polls, and social and health questionnaires. San Francisco, CA, US : Jossey-Bass, 426 p.

Burkovský, J. & Kollár, Š., (1989). Príležitostný náučný chodník z roku 1926. In *Chránené územia Slovenska*, z. 13, pp. 80 – 81.

Čeřovský, J. (1976). Poznávame prírodné bohatstvo socialistickej vlasti – Sprievodca výstavou o náučných chodníkoch. Správa CHKO Malá Fatra, s. 40.

Čeřovský, J. (1978a). Vyhlídky, zákruty a cíle našich naučných stezek. Památky a příroda, roč. III, č. 7, s. 425-433.

Čeřovský, J. (1978b). Chráněné krajinné oblasti a kultúrně výchovná činnosť. Památky a příroda, roč. III, č. 8, s. 449-455.

Gavora, P., Koldeová, L., Dvorská, D., Pekárová, J. & Moravčík, M. (2010). Elektronická učebnica pedagogického výskumu. Bratislava : Univerzita Komenského. Online: http://www.e-metodologia.fedu.uniba.sk

Gross, M., Zimmerman, R., Buchholz, J. (2006). Signs, trails, and wayside exhibits: connecting people and places (3). UW-SP Foundation press, Inc.

Ham, S. H. (2013). Interpretation – Making a Difference on Purpose. Golden: Fulcrum http://www.fs.usda.gov/Internet/FSE_DOCUMENTS/stelprdb5167249.pdf

Jelínek, M., Kozubková, J. and Kostečka, P. (2009). Realizace návštěvnické infrastruktury. Praha: AOPK ČR. Králiková, K. and Burkovský, J. (2008). Náučné zariadenia v prírode. In *Enviromagazín*, 2008, Nr. 3.

Ludwig, T. (2003). Basic Interpretive Skills. The Course Manual. Werleshausen: Bildungswerk Interpretation.

Mazúrek, J. (1988). Didaktické využitie náučných chodníkov a lokalít pre geologicko – geografické exkurzie na príklade CHKO Štiavnické vrchy. In *Acta facultatis pedagogacae Banská Bystrica* – Prírodné vedy IX., SPN, Bratislava, s. 161-194.

Medek, M., Činčera, J., Gregorová, J., Pořízová, K. Lisková, M. (2016). Naučné stezky: zpracování a hodnocení nepřímých interpretačních programů. Brno: Masarykova univerzita.

Schneider, J., Fialová, J. and Vyskot, I. (2008). Krajinná rekreologie I. Brno, MZLU v Brně.

US Forest Service (2005). Interpretive Media Design Guidelines [online].

Suchá, B. (1990). Sprievodca – náučné chodníky Slovenska. Ústredie štátnej ochrany prírody L. Mikuláš, s. 134.

Švec, Š. (1998) Metodológia vied o výchove: Kvantitatívno-scientické a kvalitatívno-humanitné prístupy v edukačnom výskume. Bratislava : Iris, 303 p. http://www.fs.usda.gov/Internet/FSE_DOCUMENTS/stelprdb5167249.pdf

Taylor-Powell, E. (1998) Questionnaire Design: Asking questions with a purpose. The Texas University, 46 p.

Weis, K., Bednárik, P., Masný, M. (2016). Geographically-montanistic research of mining site Smolník and its mining works virtual reconstruction. In *Geographical information* : Nitra, University of Konštantín Filozof. - Vol. 20, No. 2 (2016).

Woitsch, J. and Pauknerová, K. (2014). Metodika pro prezentaci sídelního a krajinného prostoru a kulturního dědictví prostřednictvím tvorby naučných stezek. Plzeň: Západočeská univerzita v Plzni.